

ABSTRACT

Pollen development is critical for plant reproduction. Numerous nuclear mutations affect the function of pollen resulting in male sterility. The *myb26* mutant is one such male sterile mutant allele, which results in anther indehiscence. Five putative MYB26 interactive proteins were previously identified from screening an *Arabidopsis* stamen yeast-2-hybrid library with MYB26 as bait. These proteins include Y2H128, Y2H320, Y2560, Y2H620 and Y2H970. Transient expression of these proteins, except Y2H128 were studied *in planta* by infiltration of *Nicotiana benthamiana* leaves and all were found to be expressed in the nucleus and co-localised with MYB26. Förster Resonance Energy Transfer (FRET) was used to confirm the positive interaction between MYB26 and the Y2H320 protein.

Analysis of the expression and possible function of the putative interactors was examined using SALK knockout T-DNA insertion mutants, RNAi and over-expression lines. SALK knockout lines of four *Y2H* genes were fully fertile and produced viable pollen despite no expression of the corresponding genes in the insertional mutants of *Y2H320* and *Y2H560*. Independent silencing by RNAi of the other two genes, *Y2H970* and *Y2H128*, also resulted in no alteration in plant phenotype. Transgenic plants over-expressing the *Y2H* genes also showed no differences in secondary thickening of anthers in endothecium compared to the wild type (*Ler*). Using a *Prom320::GUS* transgene, GUS expression was observed in the anthers, nectaries and stigmatic tissues; this pattern of *Y2H320* expression corresponds to that seen for *MYB26*, confirming that interaction *in planta* is possible.

The research also involved an analysis of additional four *Arabidopsis* male sterile mutants in the M2 and M4 generations. The phenotypes of these mutants were similar to that of the *myb26* mutant, where viable pollen was evident, but anther dehiscence did not occur. These novel mutants were not rescued by Jasmonic Acid (JA) treatment. Allelism/complementation analyses indicated that the two mutants *c20* and *mss* are alleles of *myb26*, whilst *msak* and *c12* are novel mutations at different loci. Gene mapping of the *MSAK* gene indicated that it is located on chromosome 1. Further higher resolution genetic mapping with Simple Sequence Length Polymorphism (SSLP) molecular markers identified a closer linked marker (12.57 cM to *MSAK*), suggesting that the gene is located ~3.2 Mb from the start of chromosome 1. A possible candidate for *MSAK* gene located within the region 3.4-3.5 Mb is the transcription factor Transducin/WD40 repeat-like protein (*At1g10580*; located at 3.49 Mb), which is involved in pollen development. Further investigation of additional candidate genes for *MSAK* in the region of ~3.0-4.0 Mb of chromosome 1 that are related to male gametophyte, pollen development or belong to MYB superfamily identified a number of genes, one likely candidate is *At1g10770* (located at ~3.59 Mb). Previous reports indicated that reduction of *At1g10770* transcript resulted in pollen tube growth retardation, partial male sterility and reduced seed set.

CHAPTER 1: INTRODUCTION

1.1 ARABIDOPSIS THALIANA AS A MODEL PLANT

Arabidopsis thaliana is widely used as a model plant for plant science research (Meyerowitz, 2001) and extensively used in studies based on evolution, genetics, population genetics and plant development.

One important trait that makes *Arabidopsis* an ideal model plant is its small genome size (125 Megabase pairs) and the fact that it was the first plant genome to be sequenced (*Arabidopsis* Genome Initiative, 2000). It has only five chromosomes, 33,602 genes, of which 27,416 are protein-coding, more than 50% of protein-coding genes annotated and 125 million base pairs of DNA (Bennett *et al.*, 2003). Table 1.1 summarizes the important features of the *Arabidopsis thaliana* genome.

Arabidopsis has a short life cycle (six weeks from seed germination to seed maturation); plant height at maturity is around 20-25 cm and it produces small white flowers. It belongs to the family Brassicaceae. Plants of this family are known as crucifers due to their uniform flower structure that resembles a cross and are also characterized by a fruit (silique), which is 5-20 mm long with 20-30 seeds. *Arabidopsis* can be efficiently transformed with *Agrobacterium* by floral dipping, allowing introduction of genetic material (Clough and Bent, 1998). The consensus of research focus on *Arabidopsis* has led to the development of extensive genomic resources, including stock centres that supply seeds from landraces exhibiting natural variation, mutants reverse genetic and insertion lines, databases of sequences, clones and mutants. These tools are proving

invaluable for research on *Arabidopsis* and are thus facilitating in-depth molecular understanding of the biology of plants. *Arabidopsis thaliana* is similar to many other plant species, therefore, analysing the structure and function of *Arabidopsis* genes is paving the way to providing detailed understanding of the molecular development of other plant species, yielding data that is proving valuable for application to crop species.

Table1.1 Important features of the *Arabidopsis thaliana* genome.

Genes	33,602
Genome size	125 Mbp
Protein coding genes	27,416
Pseudogenes	4,827
ncRNAs	1,359
Haploid genome size	125,000,000
Bases	249,689,164
Entries	183,987

*Taken from (<http://www.arabidopsis.org/>).

1.2 ANTHOR AND POLLEN DEVELOPMENT

The development and release of functional pollen is critical for plant reproduction and selective breeding. When two inbred lines with certain desirable traits are crossed, the first generation offspring (F1 hybrids) often exhibit heterosis or hybrid vigour. This is typically apparent as improvements in growth and yield traits compared to the both parents, in such characteristics as size, growth rate, fertility and yield of a hybrid organism over those of its parents. Hybrid vigour is often determined by non-mutually exclusive mechanisms resulting in superiority of a hybrid over its parents (Lippman and Zamir, 2007). This process has been utilised extensively in agriculture, however, there is still no clear understanding of the mechanisms that are involved. Stokes *et al.* (2007) used the *Arabidopsis* male sterile mutant *ms1* as a female parent to create a range of *Arabidopsis* hybrids that demonstrated positive and negative heterosis. Thus,

providing a tool to study a process that is crucial to the agriculture industry.

The use of hybrids has proven to be an effective strategy for increasing crop yield, for example yield increases of 15-20% are seen in hybrid rice (Cheng *et al.*, 2007). However, the emasculation process, required to avoid self-fertilisation during the generation of hybrids, can be challenging and time consuming. Male sterile lines are often favoured in commercial hybrid seed production (Wilson and Zhang, 2009). Therefore, a better understanding of the processes of pollen development may provide effective mechanisms for the efficient generation of hybrids. Pollen development is also considered to be a useful system for research into the differentiation of cells, polar growth, cellular signalling and other biological processes in plants (McCormick, 1993).

1.2.1 Pollen development in *Arabidopsis*

The male reproductive organ of a flowering plant is the stamen, which consists of an anther and filament. Pollen development takes place in the anther, while the filament transmits water and nutrients to the anther. The filament also holds the anther in a suitable position, which aids pollen dispersal during dehiscence (Scott *et al.*, 2004).

The major events associated with *Arabidopsis* anther development have been described, including the generation of specific cell layers within the anther, meiosis of pollen mother cells and pollen maturation with associated wall development (Sanders *et al.*, 1999; Wilson and Zhang, 2009; Table 1.2). The development of the *Arabidopsis* anther has been divided in to

two distinct phases, which are microsporogenesis (stages 1 to 7), and microgametogenesis (stages 8 to 14) (Table 1.2) (Figure 1.1). During the early stages of the anther development, a program of events is initiated, which defines the future breakpoint of the anther and culminates in the breaking of stomium and pollen release (Figure 1.2).

Anther development begins when the stamen primordia in the third whorl of the floral meristem emerge (Goldberg *et al.*, 1993). Cells in the stamen primordia undergo specification and differentiate to produce the different cell types, which generate the anther and filament. Generally, anthers have four lobes, each with four distinct somatic cell layers, epidermis, endothecium, middle layer and tapetum. The Primary sporogenous cells (Ps) undergo division to generate the meiocytes, whereas the Primary parital cells (Pp) divide periclinally to form an endothelial cell subjacent to Secondary parietal cells (Sp) (Figure 1.3). Then, the Sp cells divide to form a middle layer cell adjacent to the endothecium, and a tapetal cell next to the sporogenous cells (Scott *et al.*, 2004). The tapetum comprises the inner maternal cell layer of the anther and provides nutrients and enzymes for pollen development. It is also vital for formation of the pollen wall and pollen coat (Yang *et al.*, 2007).

Pollen develops inside the anther and archesporial cells in the anther lobes differentiate into pollen mother cells (PMC) and undergo meiosis (Figure 1.1). During meiosis, these cells form tetrads of haploid microspores and the second phase of anther development occurs which give rise to microspores. Callose is deposited around the tetrads, this then breaks down and the

microspores are released into the locule. The microspores then go through two mitotic divisions to form mature pollen, comprising two cells, one is larger, the vegetative, while the smaller one is the generative cell. When the microspores are released into the anther locule, the development of male gametophyte begins (Figure 1.2).

Pollen wall formation occurs as two distinct layers; the outer exine, which is synthesized by the tapetum (Quilichini *et al.*, 2010), is composed of sporopollenin and generates the strength of the wall, and the inner intine (made from cellulose, protein and pectin) (Scott *et al.*, 2004). When mature pollen grains have formed, the filaments begin rapid elongation, the anthers enlarge and expand, and the anther enters into the dehiscence program, resulting in flower opening and release of mature pollen.

During dehiscence, the anther wall breaks at a specific site along the anther length between two adjacent locules, the septum. Prior to dehiscence, the stomium and septum cells differentiate from precursor cells between the anther locules and subsequently these cells undergo a timed cell degeneration program (Sanders *et al.*, 1999).

Table 1.2 Major events in *Arabidopsis* anther development. Anther development stages have been taken from Sanders *et al.* (1999). Flower development stages **(A)** have been taken from Smyth *et al.* (1990) and Bowman *et al.* (1991). Pollen development stages **(B)** have been taken from Regan and Moffatt (1990).

Anther stage	Major events of anther development	Flower stage (A)	Pollen stage (B)
1	Six rounded stamen primordia emerge.	5	
2	Oval shaped; Archesporial cells arise in four corners of the anther primordia.		
3	Sporogenous layers generated by mitotic division. The 2 parietal layers and sporogenous cells are generated.	7	
4	Four-lobed anther pattern with two developing stomium regions. Vascular region initiated.	8	
5	Four defined locules recognized. All anther cell types present and pollen mother cells emerge.	9	3
6	Pollen mother cells enter meiosis. Middle layer is damaged and degenerates and the anther increases in size.		4
7	Meiosis completed. Tetrads of microspores free within each locule.		
8	Callose wall surrounding tetrads degenerates and individual microspores released.	10	5
9	Anther growth and expansion continues.		6-7
10	Tapetum degeneration commencing, pollen mitosis ongoing.	11-12	
11	Tapetum degenerates, pollen mitosis. Secondary thickening occurs in endothecium and connective cells. Septum cell degeneration initiated.		
12	Anther becomes bilocular after degeneration and damage of septum.	10	
13	Dehiscence and pollen release.		13-14
14	Senescence of stamen. Shrinkage of cells and anther structure.	15-16	
15	Stamen falls off senescing flower.	17	

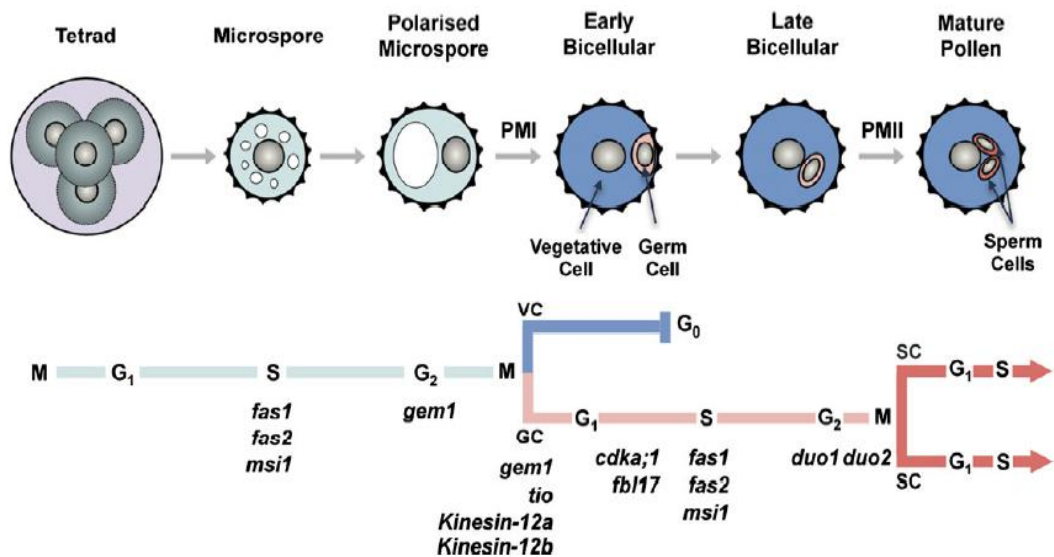


Figure 1.1 Overview of the distinct morphological stages of male gametophyte development in *Arabidopsis*. A coloured-coded timeline of the cell cycle progression of the cell cycle of each cell type is shown. Microsporocytes undergo meiotic division giving rise to a tetrad of four haploid microspores during microsporogenesis. The microspores that are released undergo an asymmetric division known as Pollen Mitosis I (PMI) during microgametogenesis, producing a bicellular pollen grain with a small germ cell enclosed within the cytoplasm of the large vegetative cell. The germ cell goes through a further mitotic division known as Pollen Mitosis II (PMII) resulting in two sperm cells. The vegetative cell exits the cell cycle. The resulting sperm cells then continue to go through the cell cycle to reach G₂ preceding karyogamy and double fertilization. VC = vegetative cell; GC = germ cell; SC = sperm cell. Taken from Borg *et al.* (2009).

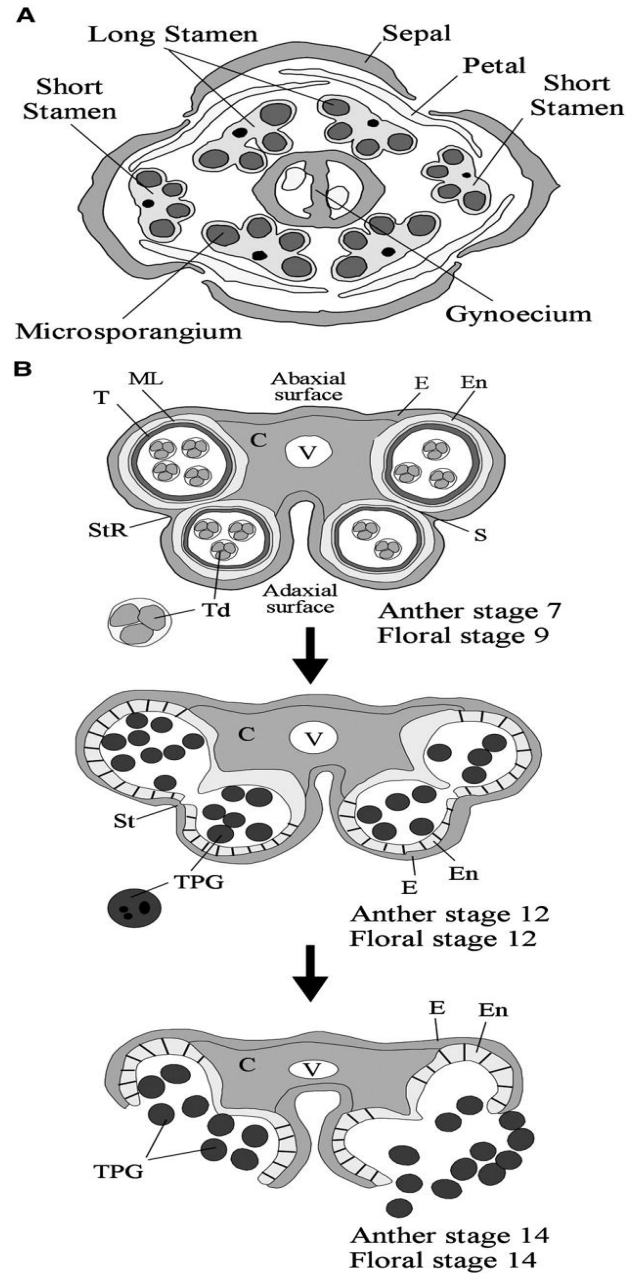


Figure 1.2 Anther development.

(A) *Arabidopsis* floral bud showing the number, position, and orientation of the floral organs. Taken from Hill and Lord (1989).

(B) *Arabidopsis* anthers at different stages. Taken from Sanders *et al.*, (1999). Floral stages are as described by Smyth *et al.* (1990); anther stages are as described by Sanders *et al.* (1999). C, connective; E, epidermis; En, endothecium; ML, middle layer; S, septum; St, stomium; StR, stomium region; T, tapetum; Td, tetrads; TPG, tricellular pollen grains; V, vascular bundle.

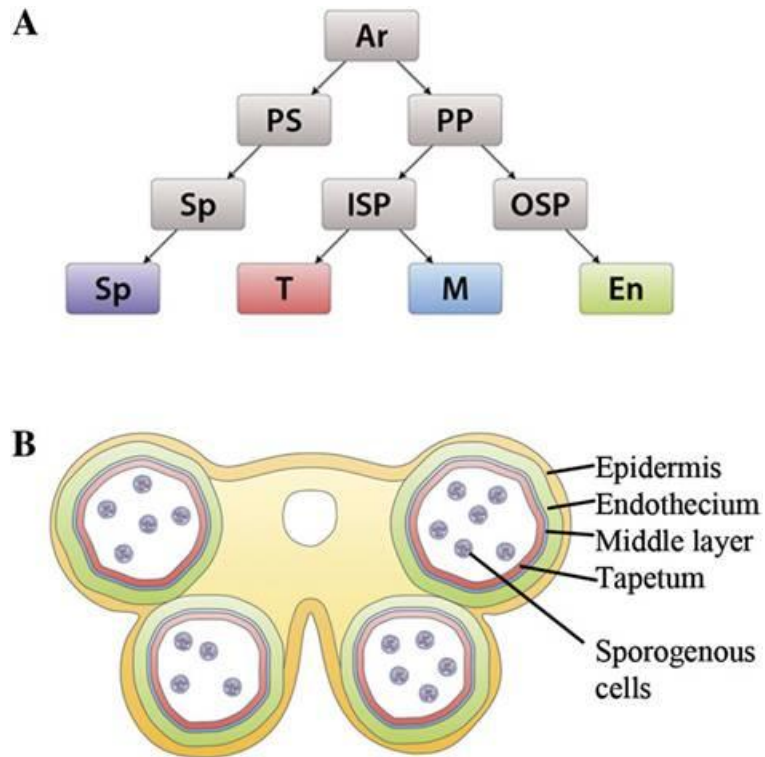


Figure 1.3 Anther structure.

- A) Diagram of the cell layers of *Arabidopsis* anther. Ar: Archesporial cells; PP: Primary parietal cells; PS: Primary Sporogenous cells; Sp: sporogenous layer; ISP: Inner Secondary Parietal layer; OSP: Outer Secondary Parietal layer; T: Tapetum; M: Middle layer; En: Endothecium.
- B) Archesporial cell division to form final anther cell layers. Taken from Wilson *et al.* (2011).

The septum separating the locules degenerates by enzymatic lysis, forming a bilocular anther, leaving the stomium as the site for anther wall breakage to release pollen. Several hydrolytic enzymes and proteins linked to cell wall loosening are thought to be involved in the septum degeneration, including polygalacturonases (PGs), β -1,4-glucanases, (Cosgrove, 2000). PGs are hydrolase and loosening enzymes involved in the degradation of pectin and disintegration of the cell wall. During

anther and pollen development, many tissue types, including pollen mother cells, microspores, tapetum and septum, undergo cell-wall modification (Neelam and Sexton, 1995). Thus, PGs may play multiple roles in pollen and/or anther development (Huang *et al.*, 2009). It has been suggested that one group of related PGs tend to be expressed in flowers and flower buds (Kim *et al.*, 2005). A number of these have been characterized in *Arabidopsis* and linked to changes in pollen wall development; *QUARTET1* (*QRT1*), *QUARTET2* (*QRT2*) (Rhee and Somerville 1998) and *QUARTET3* (*QRT3*) (Rhee *et al.*, 2003) are required for degradation of the pollen mother cell wall as microspores are released from their tetrads. Three endo-PGs have also been identified as involved in anther dehiscence, silique dehiscence and floral abscission; *ARABIDOPSIS DEHISCENCE ZONE POLYGALACTURONASE1* (*ADPG1*) and (*ADPG2*) are both required for anther dehiscence (Ogawa *et al.*, 2009). After the septum degeneration, the stomium subsequently splits due to stresses associated with pollen swelling and dehydration of anthers to release the pollen (Wilson *et al.*, 2011) (Section 1.4) and the pollen is released. A brief description of the mutants acting during pollen development and release in *Arabidopsis* is shown in Figure 1.4.

The gene regulatory network controlling anther development and pollen release has been extensively studied in *Arabidopsis* (Scott *et al.*, 2004; Ma, 2005; Feng and Dickinson, 2007; Borg *et al.*, 2009). This network has been shown to be conserved in crop species, including rice (Wilson and Zhang, 2009), maize (Ma *et al.*, 2008) and barley (Murray *et al.*, 2003; Fernández Gómez and Wilson, 2014).

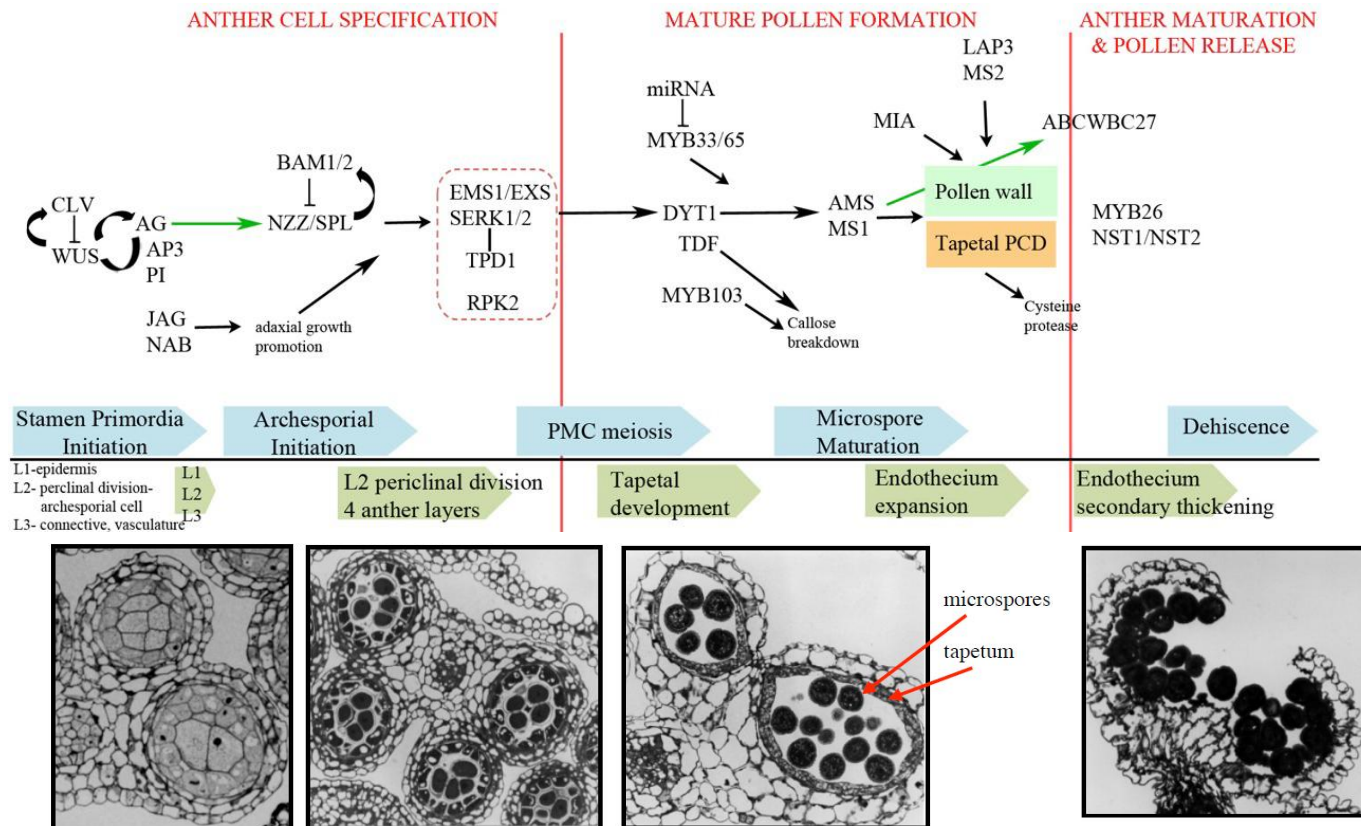


Figure 1.4 Description of the *Arabidopsis* pollen development and release network map identifying when different mutants are acting in the pathway. Taken from prof. Zoe A Wilson Lab.

1.3 MALE STERILITY IN HIGHER PLANTS

Male sterility is the failure of a plant to produce functional anthers, pollen or male gametes, or it can be a failure in the release of functional pollen (Wilson *et al.*, 2011). Male sterility can arise as cytoplasmic male sterility (CMS), nuclear (genetic) male sterility and genetic-cytoplasmic male sterility (Jain, 1959). CMS is maternally inherited, while genetic-cytoplasmic male sterility involves genes from the nucleus as well as from the cytoplasm. Nuclear male sterility follows Mendelian inheritance patterns. In crop breeding programmes where hybrid seeds are desired, male sterility becomes important as it enables cross-fertilisation and overcomes the need for manual emasculation, which is a time- and labour-intensive process. Male sterility occurs naturally or it can be induced by mutations in nuclear or cytoplasmic genes, however, a system of fertility restoration is also required for deployment in agriculture to ensure that the “hybrid” crop is subsequently fully fertile.

CMS systems have been identified in a number of species. These are due to mutations in the mitochondrial genomes, which are masked by nuclear “restorer” genes. These restorers provide a mechanism for recovering fertility and, hence, CMS systems have been effectively deployed in many strategies for agricultural hybrid seed production. There are a number of different types of CMS systems with distinct genetic features, both within and among different species, but key features that appear to be shared are (i) CMS is associated with chimeric

mitochondrial ORFs, and (ii) fertility restoration is often associated with genes encoding pentatricopeptide repeat (PPR) proteins (Chase and Babay-Laughnan, 2004).

However, access to CMS systems is very limited and species specific. Therefore, inducing male sterility by genetic engineering offers an alternative option. Genetic engineering has been increasingly becoming more important in the world for growing crops. However, such approaches require a detailed understanding of the molecular development of pollen formation. Characterising male sterile mutants for pollen and anther dehiscence has proved a successful approach to identify genes involved in pollen formation, which provides access to novel information for controlling fertility (Xu *et al.*, 2010; Ariizumi and Toriyama, 2011; Chen *et al.*, 2011; Ma *et al.*, 2012).

Numerous male sterile mutants have been described in *Arabidopsis* (Sakata and Higashitani, 2008) (Table 1.3). These involve mutations in nuclear genes that are fundamental to pollen formation. A detailed study by Sanders *et al.* (1999) revealed that *Arabidopsis thaliana* male sterile mutants were due to defects in anther morphology, microspore production, differentiation of anther cell types, pollen function and anther dehiscence. High temperature stress and heat shock also causes defects in pollen development in *Arabidopsis* due, at least in part, to the degradation of the anther wall, abnormal tapetal Program Cell Death (PCD) and cell cycle arrest (Kim *et al.*, 2001; Vacca *et al.*, 2007; Sakata and Higashitani, 2008).

Table1.3 Male sterile mutants genes identified in *Arabidopsis*.

Mutants	Functions and Major events	References
<i>defective in anther dehiscence 1 (dad1)</i>	Essential for <i>Arabidopsis</i> male fertility and fails to dehiscence.	Ishiguro <i>et al.</i> (2001)
<i>extra sporogenous cells1 (exs1)</i>	Tapetum and middle cell layers formation. Vascular region initiated. Meicytes are formed.	Zhao <i>et al.</i> (2000)
<i>excess microsporocyte 1 (ems1)</i>		Yang <i>et al.</i> (2003) Canales <i>et al.</i> (2002)
<i>tapetum determinant 1 (tpd1)</i>	Expressed within the microsporocyte and may mediate interaction between sporocytes developing in the absence of <i>tpd1</i> .	Yang <i>et al.</i> (2003)
<i>male meiocyte death 1 (mmd1)</i>	Gene is important for successful progression through meiosis; middle layer is compressed and degenerates and the anther increase in size.	Yang <i>et al.</i> (2003)
<i>dysfunctional tapetum 1 (dvt1)</i>	Tapetum degeneration and defective pollen wall formation.	Zhang <i>et al.</i> (2006)
<i>male sterility 35 (ms35)</i>	Responsible for male sterile phenotype. Fails to dehiscence.	Yang <i>et al.</i> (2007)
<i>male sterility 1 (ms1)</i>	Gene is vital for tapetal development and microspore maturation. Tapetum degeneration initiated.	Wilson <i>et al.</i> (2001)
<i>male sterility 2 (ms2)</i>	Gene is important for pollen wall formation and pollen absent.	Aarts <i>et al.</i> (1997)
<i>male sterility 3 (ms3)</i>	Arrest of pollen development.	Chaudhury (1993)
<i>bacel core mutant (bcp1)</i>	Is a male specific gene responsible for pollen development and is active in tapetum and microspores.	Tehseen <i>et al.</i> (2010)
<i>myb46</i>	Transcription factor regulates the gene expression of secondary wall associated cellulose synthases in <i>Arabidopsis</i> .	Kim <i>et al.</i> (2013)
<i>myb108, myb24 and myb21</i>	Regulate jasmonate-mediated stamen maturation in <i>Arabidopsis</i> . Exhibit defects in pollen maturation, anther dehiscence and filament elongation.	Mandaokar and Browse, (2008) Song <i>et al.</i> (2011)
Double mutants (<i>myb65, myb33</i>)	Important during the earlier stages of tapetal development.	Millar and Gubler ,(2005)
<i>myb80, myb103</i>	Required for Pollen and tapetal development.	Phan <i>et al.</i> (2011)
<i>myb63 and myb58</i>	Transcriptional activators of the lignin biosynthetic during secondary wall in <i>Arabidopsis</i> .	Zhou <i>et al.</i> (2009) Zhong and Ye, (2012)
<i>myb83</i>	Caused a lack of secondary walls in vessels.	McCarthy <i>et al.</i> (2009)

1.4 ANTHER DEHISCENCE

Dehiscence is the final action of the anther that results in the release of pollen grains for pollination, fertilization and subsequent seed formation (Goldberg *et al.*, 1993). This process is precisely coordinated to ensure the synchronized differentiation of pollen, floral development and flower opening (Sanders *et al.*, 2000). Pollenless mutants are due to defects in early anther developmental process, whereas dehiscence mutants are frequently associated with the development and functioning of the stomium region. Dehiscence mutants arise either due to 'non-dehiscence', where as a consequence of an abnormal cell death program or other factors during anther development, the anther is unable to release the viable pollen, or due to 'delayed dehiscence' where pollen is released late when stigmatic papillae are no longer receptive for pollination.

The process of anther dehiscence begins with the degeneration of the middle layer and tapetum (Scott *et al.*, 2004), the endothecium layer becomes expanded and fibrous bands (secondary wall thickenings) are deposited in the endothecium and connective cells. Secondary thickening in the endothecium is critical for dehiscence, as shown by the male sterile mutant *myb26* (Dawson *et al.*, 1993). In addition, two other NAC-domain transcription factors, NAC SECONDARY WALL THICKENING PROMOTING FACTOR1 (NST1) and (NST2) have been shown to act redundantly in the regulation of anther secondary thickening (Mitsuda *et al.*, 2005). It is thought that these act downstream of *MYB26* and are required for induction of secondary thickening associated gene expression (Yang *et al.*, 2007) (Section 1.7). The septum separating the locules

degenerates by enzymatic lysis, leaving the stomium as the site for anther wall breakage to release pollen (Section 1.2.1). The stomium subsequently splits due to stresses associated with pollen swelling and dehydration of the anther to release pollen (Wilson *et al.*, 2011).

Before dehiscence, the anther epidermal and endothecium cells become turgid, which generates the inwardly directed force in the anther wall, causing the weakened stomium to rupture. The desiccation of the epidermis and endothecium then causes differential shrinkage of thickened and non-thickened parts of the cell wall resulting in an outwardly bending force. This force leads to the retraction of the anther wall and the stomium is fully opened thereby permitting pollen release (Nelson *et al.*, 2012).

A number of dehiscence mutants have been described. Kim *et al.* (2010) reported that the *Arabidopsis* gene *REDUCED MALE FERTILITY (RMF)* regulates tapetum and middle layer degeneration during anther development. *RMF* expression is detected in anthers and especially in pollen grains. Over-expression of the *RMF* gene alters the plant phenotype and disturbs pollen maturity.

Anthers in the *non-dehiscence1* mutant undergo an abnormal striking cell-death programme, which results in endothecium degeneration and indirectly causes failure of stomium region breakage, although in this mutant the pollen appears normal (Sanders *et al.*, 1999).

Jung *et al.* (2008) postulates that the *Arabidopsis* histidine-containing phosphotransfer Factor 4 protein (AHP4) is a mediator in a multistep phosphorelay pathway for cytokinin hormone

signalling, which negatively regulates thickening of the secondary cell wall of the anther endothecium. Over-expression of *AHP4* gene in *Arabidopsis* reduced fertility due to lack of secondary wall thickening of the endothecium and inhibited the expression of *IRXs*, the xylem genes, suggesting that *AHP4* gene negatively regulates secondary thickening in the anther endothecium.

Homeodomain proteins are an important group of transcription factors in plants. They are characterized by a 180-bp DNA 'homeobox' sequence (Gehring *et al.*, 1994). Plant homeobox genes are a large family of transcription factors that play an important role in growth and development processes. The *Arabidopsis thaliana* genome encodes 89 homeodomain proteins; out of which 47 are members of the HD-ZIP subfamily (Li *et al.*, 2007); HDG3 (At2g32370) is a member of class IV HD-ZIP subfamily that is specifically expressed in flowers and anthers. Over-expression of *HDG3* (or *OExHDG3*) gene causes a failure of dehiscence due to a lack of endothecium secondary thickening (Li *et al.*, 2007). Analysis of gene expression in the *OExHDG3* line indicated that three positive transcriptional regulators of endothecium secondary thickening, *MYB26*, *NST1* and *NST2*, were down-regulated (Li *et al.*, 2007). These three genes are essential for anther dehiscence (Steiner-Lange *et al.*, 2003; Mitsuda *et al.*, 2005; Zhong and Ye, 2007), suggesting that *HDG3* plays a negative role in the regulation of anther dehiscence by directly or indirectly controlling the expression of *MYB26*, *NST1* and *NST2* in *Arabidopsis thaliana*.

1.5 PHYTOHORMONES AND ANTHHER DEHISCENCE

1.5.1 JASMONIC ACID (JA)

JA acts as a critical signal for dehiscence and several mutants in JA biosynthetic enzymes result in male sterility, many of which can be rescued by application of JA (Park *et al.*, 2002; Sanders *et al.*, 2000; van Malek *et al.*, 2002). JA along with its methyl ester (MeJA) were the first members of the jasmonate signalling family discovered that play a key role in the regulation of metabolic, developmental and defensive processes in plants (Shan *et al.*, 2007). The JA pathway is linked with pathogen defence by induction of the expression of proteinase inhibitors, as a part of a defence response against insects (Farmer and Ryan, 1990). These were shown to be active inducers of antimicrobial phytoalexins (Gundlach *et al.*, 1992) and subsequent mutant studies have indicated their importance in plant defence, making them of great interest for agriculture. Pathogen and insect resistance is compromised in mutants unable to synthesise or respond to JA. Mutants that have been identified with altered responses to pathogens due to impaired JA biosynthesis and responses, also exhibit impaired male sterile phenotypes due to defects in anther and pollen maturation (Schaller *et al.*, 2004), demonstrating the importance of JA to correct development of stamen.

1.5.1.1 SYNTHESIS AND SIGNAL TRANSDUCTION

Jasmonic acid (JA) is a lipid – derived signalling compound that is widely distributed throughout the plant kingdom. Jasmonates are synthesized from oxylipins (oxygenated polyunsaturated

fatty acids) by the octadecanoid pathway and are characterized by a pentacyclic ring structure (Schaller *et al.*, 2004). Mutants have been characterised from this pathway that have defects in pollen development and release (Figure 1.5). The first step of JA biosynthesis is the conversion of the cellular lipid phospholipid linoleic acid to free linolenic acid (LA). This is catalysed by a lipolytic enzyme encoded by the *DEFECTIVE IN ANTHOR DEHISCENCE (DAD1)* gene (Figure 1.5), then oxygenated by LIPOXYGENASE (LOX) and converted to 13-hydroperoxylinolenic acid (HPL) by ALLENE OXIDE SYNTHASE (AOS) and ALLENE OXIDE CYCLASE (AOC). 12-OXO-PHYTODIENOIC ACID REDUCTASE (*OPR3/DDE1*) reduces HPL in three β -oxidation steps resulting in the final JA molecule. JA can then be methylated by JASMONIC ACID CARBOXYL METHYL TRANSFERASE (Ishiguro *et al.*, 2001; Schaller *et al.*, 2004; Shan *et al.*, 2007). The initial steps of synthesis, involving the LOX, AOS and AOC enzymes, occur within the chloroplast. The next steps occur after transport into the peroxisome where synthesis continues up to the final β -oxidation steps. After that, JA is released into the cytosol, where it can be modified (Schaller *et al.*, 2004).

CORONATINE INSENSITIVE 1 (COI1), a 66 kDa protein containing a leucine-rich repeat domain and N-terminal F-box motif (Xie *et al.*, 1998), has been identified as the receptor of bioactive JA (Katsir *et al.*, 2008). The *coi1* mutant is jasmonate insensitive, male sterile and susceptible to pathogen invasion, which has shed some light on the signal transduction pathway. Using a co-immunoprecipitation assay, Xu *et al.*, (2001) demonstrated in *planta* interactions between COI1, CUL1 and SKP1-like proteins,

ASK1 or ASK2, to assemble the SCF^{COI1} complex. This complex acts to polyubiquitinate JA response gene repressors, such as the JAZ genes (Thines *et al.*, 2007), targeting them for proteasomal degradation (Figure 1.6). During JA-responsive signal transduction, the *coi1* mutant fails to respond to JA. As a result, in cells containing low JA levels, JAZs restrain the activity of TFs that positively regulate early JA-responsive genes (Figure 1.6). This aspect of the model is based upon the key finding that *Arabidopsis* JAZ3 interacts directly with MYC2, a basic helix-loop-helix TF that serves a well-established role in JA signalling (Katsir *et al.*, 2008). JAZ genes themselves are rapidly induced in response to JA treatment and environmental stress conditions that stimulate JA production. Based on the function of JAZs as negative regulators, JA-induced JAZ expression appears to constitute a negative feedback loop in which newly synthesized JAZs desensitize the strength of the response by obstructing TF activity (Katsir *et al.*, 2008). Expression of JAZ genes in response to increased endogenous JA content is consistent with the idea that early JA-response genes are expressed upon hormone-induced release of TFs from JAZ control (Katsir *et al.*, 2008). Studies using the protein synthesis inhibitor cycloheximide further suggest that JAZ gene expression is activated upon COI1-dependent turnover of labile repressors, presumably JAZs (Katsir *et al.*, 2008) (Figure 1.6). JAZ proteins are not degraded in the presence of these signals.

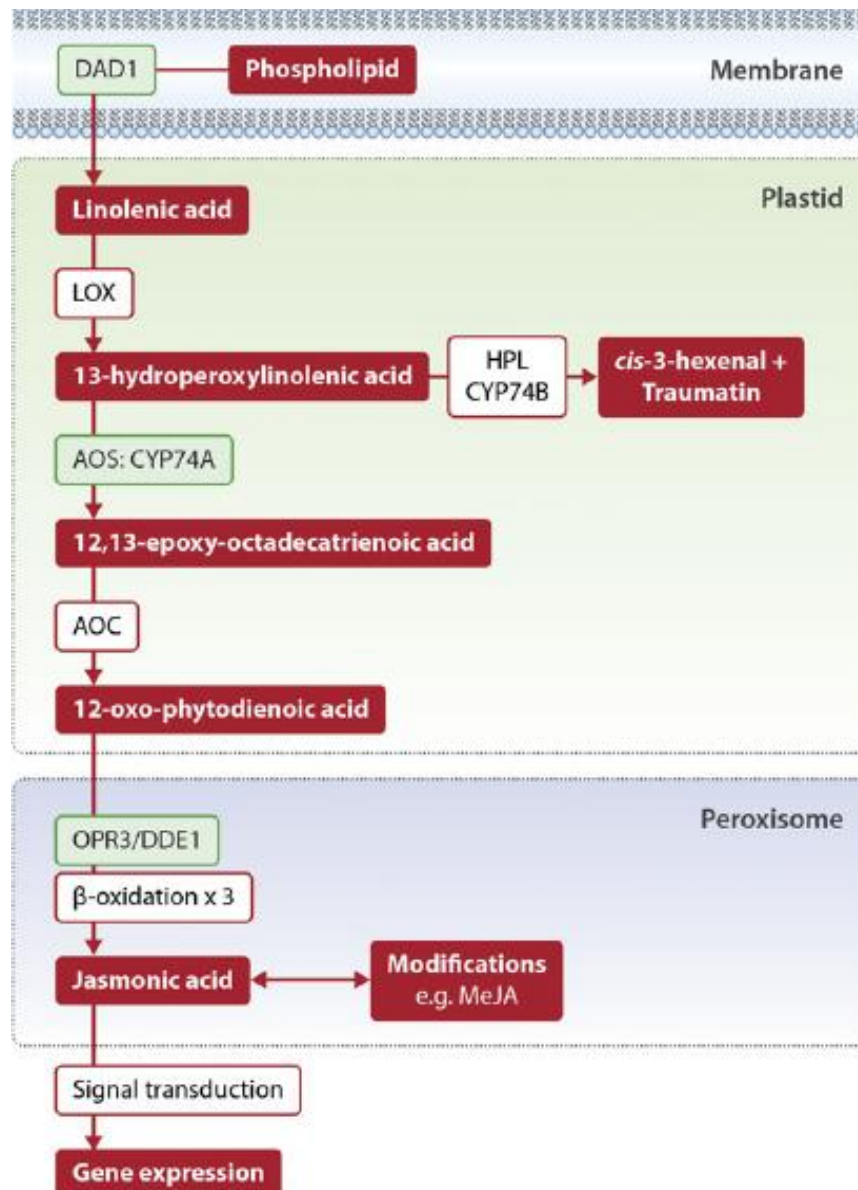


Figure 1.5 Jasmonic acid (JA) biosynthesis pathways. Linolic acid (18:3) is released from membrane phospholipid by DAD1 (which is a lipolytic enzyme) and is converted to an allene oxide (12, 13-epoxy-octadecatrienoic acid) by a lipoxygenase (LOX) and allene oxide synthase (AOS), which is a member of the cytochrome P450 enzyme family (CYP74A). To generate Jasmonic acid, one cyclization, one reduction and three rounds of β -oxidation steps are required. Also, another pathway can occur where 13-hydroperoxylinolenic acid is converted to cis-3-hexenal and Traumatol through HPL (CYP74B). The mutants that have been characterized in this pathway are highlighted in green. Taken from Wilson *et al.* (2011).

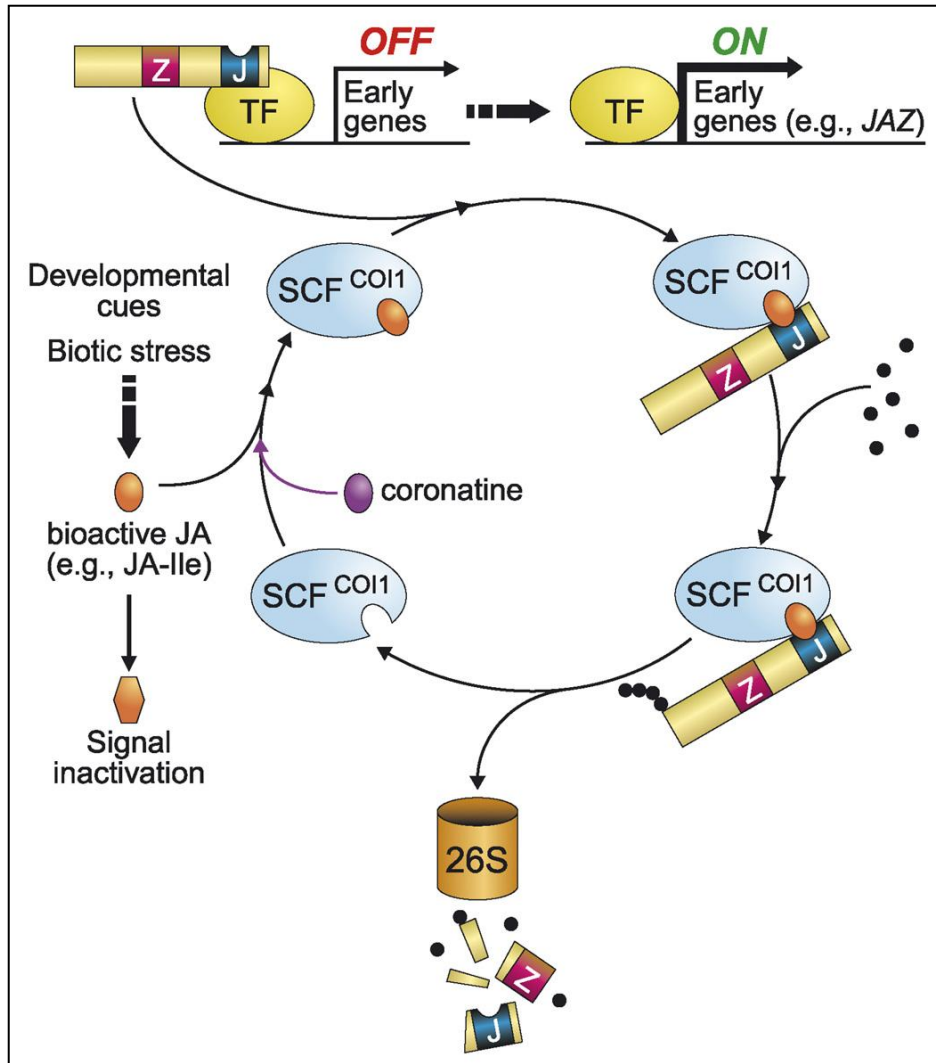


Figure 1.6 Model of JA signal transduction. Taken from Katsir *et al.* (2008). JA-responsive genes are repressed (*OFF*) by JAZ proteins (denoted with their ZIM and Jas motifs). The transition from the repressed to the active (*ON*) state of gene expression is initiated by developmental or environmental cues (e.g., biotic stress) that increase the accumulation of bioactive JAs (orange oval). *COI1* is an F-box protein that determines the substrate specificity of the SCF-type E₃ ubiquitin ligase, SCF^{COI1} (blue oval). Bioactive JAs, such as JA-Ile, are proposed to bind to the LRR domain of COI1. Interaction of JAZs with ligand-bound COI1 leads to the formation of a COI1-ligand-JAZ ternary complex in which JAZs are polyubiquitinated (filled black circles) and subsequently degraded by the 26S proteasome (26S). Signalling is attenuated by metabolism of bioactive JAs to inactive forms of the hormone (orange hexagon), as well as by JA-induced *de novo* JAZ synthesis. Some plant pathogenic strains of *Pseudomonas syringae* produce a virulence factor called coronatine (purple oval). The model predicts that *coi1* mutants fail to respond to JA and coronatine because JAZ proteins are not degraded in the presence of these signals.

1.5.1.2 ROLE OF JA IN ANTHER DEVELOPMENT

All mutants in the biosynthetic pathway downstream of JA have been characterised for their affect on male fertility (Sanders *et al.*, 2000). All display defects in timing of tissue elongation and delayed dehiscence, as well as susceptibility to pathogen attack. Mutants in the JA biosynthetic pathway can be rescued by exogenous application of JA (Ishiguro *et al.*, 2001). A male sterile mutant *dad1* was identified in *Arabidopsis thaliana* by Ishiguro *et al.* (2001), which was defective in biosynthesis of Jasmonic acid. Anther dehiscence failed, in addition to flower opening, a lack of maturation of pollen grains and delayed development in flower buds. All defects of *dad1* were rescued by application of linoleic acid, which is the initial step of JA biosynthesis (Figure 1.5). *DAD1* encodes for PHOSPHOLIPASE A1 (PLA1) that catalyses the first step of the octadecanoid pathway releasing phospholipids. When over-expressed, an excess amount of DAD1 protein is targeted to chloroplasts resulting in hydrolysis of the membrane phospholipids, causing destruction of the chloroplasts (Ishiguro *et al.*, 2001). The mutant is unable to dehisce and produces inviable pollen (Ishiguro *et al.*, 2001). The observations that *dad1* anther locules remain filled with liquid, as also occurs in the *dde1* and *coi1* mutants, combined with *DAD1 promoter::GUS* expression, suggests that the *dad1* mutation blocks water transport to vascular tissues from the endothecium, connective tissue, and the locules. Ishiguro *et al.* (2001) subsequently proposed that JA regulates expression of the sucrose transporter *SUC1*, and other genes associated with water transport in the anther and that this regulated water levels

within the anther and floral tissues, thus synchronising flower and anther opening (Figure 1.7).

Other *Arabidopsis* mutants that are disrupted in the JA biosynthesis pathway, such as *dde1/opr3*, *coi1* and *aos/dde2-2* also result in delayed dehiscence (Sanders *et al.*, 2000; Park *et al.*, 2002; van Malek *et al.*, 2002). *DDE1* encodes the enzyme OPR that catalyses the conversion of OPDA to OPC, which was identified by Sanders *et al.*, (2000) by the *delayed dehiscence 1(dde1)* mutant that fails to dehisce in time to allow successful fertilization due to delayed stomium breakdown. In wild type plants, prior to the initiation of dehiscence the *DDE1* mRNA accumulates in the pistil, petals and stamen filaments. During the dehiscence program, *DDE1* mRNA becomes restricted to the vascular region of the anther (Sanders *et al.*, 2000). Exogenous application of JA rescues the *dde1* phenotype and is effective in anthers at stages 10 and 11, when the stomium differentiates (Table 1.2), suggesting that JA concentration has a role in the timing of anther dehiscence (Cecchetti *et al.*, 2013) (Figure 1.7).

In yeast and in *planta*, two R2R3-MYB transcription factors, MYB21 and MYB24, were found to interact with JAZ1, JAZ8, and JAZ11 (Song *et al.*, 2011). The *myb21 myb24* double mutant exhibited defects in pollen maturation, anther dehiscence and filament elongation leading to male sterility (Song *et al.*, 2011). The R2R3-MYB transcription factors MYB21 and MYB24 appear to function as direct targets of JAZs to regulate male fertility since the transgenic expression of *MYB21* in the *coi1-1* mutant was able to partially rescue male fertility, but was unable to recover JA-regulated root growth inhibition and plant defence (Song *et*

al., 2011); pathogen and insect resistance is compromised in mutants unable to synthesis or respond to JA.

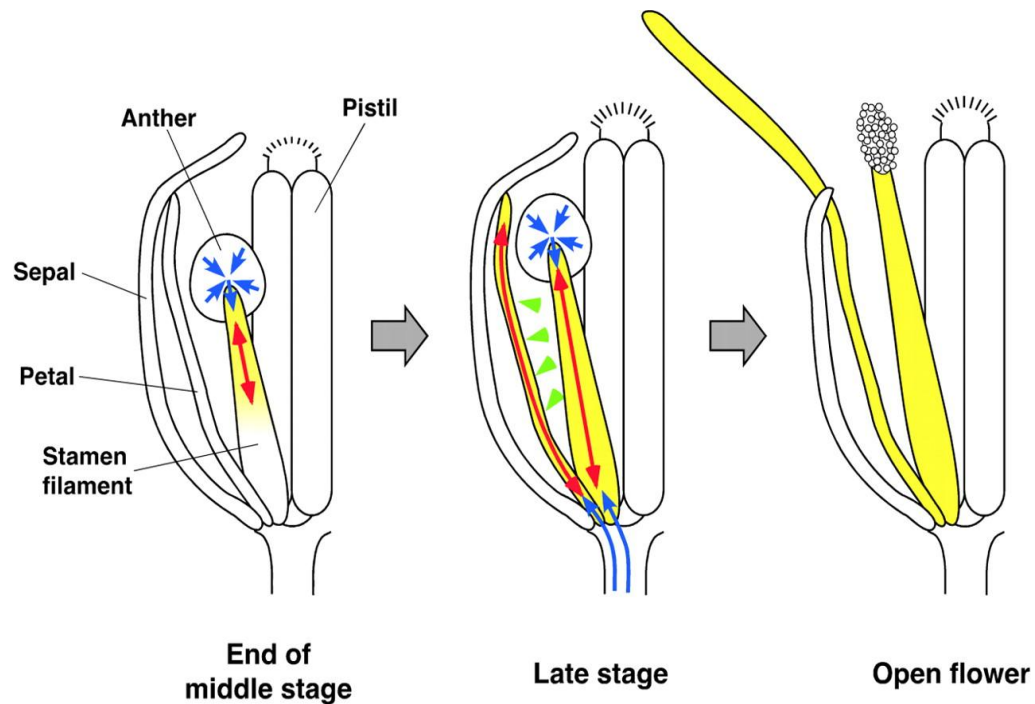


Figure 1.7 Proposed model of the synchronous regulation of pollen maturation, anther dehiscence and flower opening by JA.

The yellow-coloured regions represent organs that actively take up water and elongate in response to JA. Transmission of JA (green arrowheads); organ elongation (red arrows); water transport (blue arrows). Taken from Ishiguro *et al.* (2001).

1.5.2 AUXIN

The first auxin isolated was indole-3-acetic acid (IAA), which was characterised by its ability to induce cell expansion (Paciorek and Friml, 2006). Auxins appear to be ubiquitous signalling molecules with a broad range of developmental effects such as embryo and fruit development, organogenesis, vascular tissue differentiation, root patterning, elongation, apical hook formation, fertility, also rapid morphological effects such a plasma membrane depolarization and apoplast acidification (Paciorek and Friml, 2006). Auxins have become valuable tools for agriculture with synthetic auxins, e.g. 2,4-D used as

herbicides and the native auxin used to induce lateral root growth without the inhibition of root elongation that occurs with IAA (Woodward and Bartel, 2005).

1.5.2.1 AUXIN SYNTHESIS AND SIGNAL TRANSDUCTION

The majority of IAA synthesis occurs in young actively separating cells in the aerial part of the plant (Ljung *et al.*, 2005). There have been several biosynthesis pathways proposed for auxin (Ljung *et al.*, 2005; Mashiguchia *et al.*, 2011) (Figure 1.8). Previous study has indicated that IAA is synthesized *in planta* via tryptophan (Trp) dependent and independent pathways (Ljung *et al.*, 2005). *YUCCA* (*YUC*) gene expression, encoding for a flavin monooxygenase, has been shown to be rate limiting for auxin biosynthesis. Several genes encoding for flavin monooxygenases, with a high degree of similarity to *YUC* and overlapping roles have been identified (Cheng *et al.*, 2006). Trp is converted to indole-3-acetaldoxime (IAOx) via the cytochrome enzymes CYP79B2 and CYP79B3. However, the *cyp79b2 cyp79b3* double mutants are only partially IAA deficient, demonstrating a possible alternative pathway for the biosynthesis of IAA (Zhao *et al.*, 2002). IAOx is subsequently converted to indole-3-acetonitrile (IAN) which is then converted to IAA in a step catalysed by nitrilases of the NIT gene family (Ljung *et al.*, 2005) (Figure 1.8).

The majority of IAA found in plant tissue is in a conjugated form, which is inactive IAA that can be hydrolysed to release active hormone. This allows the plant to respond quicker to a stimulus than relying upon *de novo* synthesis of IAA. Conjugation occurs

between the carboxyl group of IAA and sugars or amino acids, with different conjugations possibly indicating different roles for bound IAA (Paciorek and Friml, 2006). The developmental signals provided by IAA are highly dependent upon cellular IAA levels that in the main part are determined by directional intercellular transport of IAA. This transport causes gradients at both the tissue and cellular levels (Paciorek and Friml, 2006). The main IAA transporters that have been identified are the AUXIN INFLUX CARRIER PROTEIN 1 (AUX1) (Bennett *et al.*, 1996) and the PIN-FORMED (PIN) family of auxin efflux proteins (Galweiler *et al.*, 1998). PIN proteins are thought to form multicomponent complexes that maintain a polar flow of IAA due to polar, subcellular plasma membrane localisation (Wisniewska *et al.*, 2006). These form an auxin transport network that mediates local IAA distribution and triggers different cellular responses in various developmental contexts (Paciorek and Friml, 2006).

SMALL AUXIN-UP RNAs (SAURs), GH3-related transcripts and *AUXIN/INDOLE-3-ACETIC ACID (Aux/IAA)* family members are rapidly and transiently induced by auxin (Woodward and Bartel, 2005). The transduction pathway by which this occurs remained elusive until Dharmasiri *et al.* (2005) demonstrated that IAA is bound directly by the F-box protein TIR1, which allows TIR1 to bind AUX/IAA proteins, as part of the SCF^{TIR1} complex, targeting the AUX/IAA proteins for proteasomal degradation by polyubiquitination. AUX/IAA degradation removes repression of auxin-response factors (ARFs) and allows ARFs to bind to the auxin response element (AuxRE) TGTCTC found in many primary auxin-response gene promoters (Ulmasov *et al.*, 1997).

Activation/repression studies using the *DR5::β-glucuronidase* (*GUS*) auxin reporter construct in carrot protoplasts indicated that ARFs 1, 2, 3, 4 and 9 act as repressors of transcription in response to auxins, while ARFs 5, 6, 7 and 8 act as activators of transcription in response to auxins (Tiwari *et al.*, 2003). So, different ARFs can have different responses to the initial IAA signal. Of the main gene families activated *GH3* and *AUX/IAAs* are induced as part of a dampening mechanism. *GH3* family proteins are associated with conjugation of IAA and other signals (Woodward and Bartel, 2005) while the repressive role of *AUX/IAA* has already been described. *SAURs* have been identified in a wide range of plant species but their exact biological function is still unknown (Jain *et al.*, 2006). Some studies have also suggested a possible role in the calcium and calmodulin auxin transduction pathway (Hagen and Guilfoyle, 2002). Beside these three primary gene families, genome wide profiling studies have demonstrated a large number of auxin-induced genes (Himanen *et al.*, 2004). Additional auxin responses, such as auxin-dependent changes in membrane K^+ are also seen, including activation of H^+ pumping, MAP kinase, phospholipase A and inhibition of the endocytic cycling of plasma membrane proteins (Paciorek *et al.*, 2005).

Prior to the discovery of the TIR1 nuclear transduction pathway, the only protein shown to bind auxin was AUXIN BINDING PROTEIN1 (ABP1), a protein localized to the endoplasmic reticulum and the plasma membrane (Henderson *et al.*, 1997). It has been suggested that ABP1 may be involved in a TIR1 independent pathway that mediates the more rapid responses to auxin (Kepinski and Leyser, 2005).

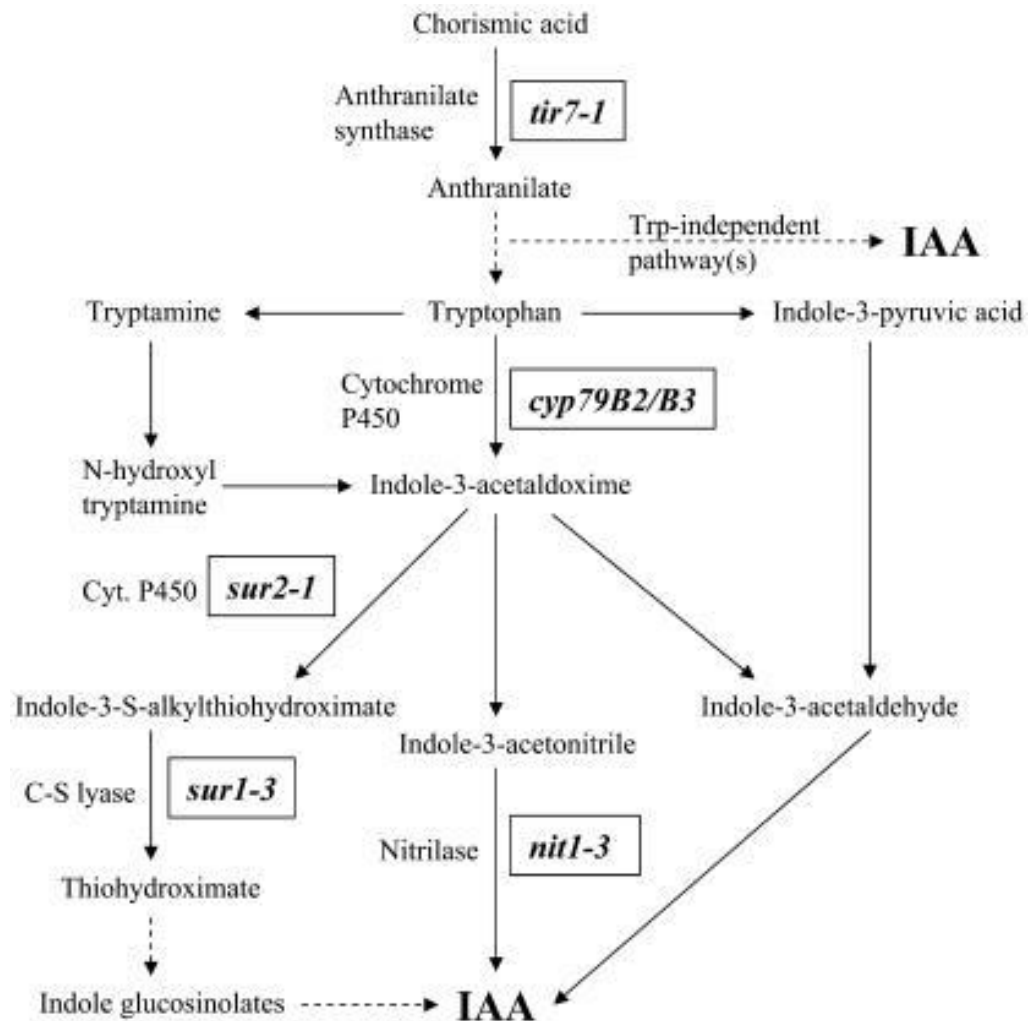


Figure 1.8 IAA Biosynthesis. Taken from Ljung *et al.* (2005).

The proposed pathway for IAA biosynthesis. Solid Arrows indicate Trp-dependant pathway. Dashed arrow indicates Trp-independent pathway. IAA, indole-3-acetic acid; Trp, Tryptophan.

1.5.2.2 ROLE OF AUXIN IN ANTHER DEVELOPMENT

The hormone auxin is involved in pollen development and anther dehiscence (Wilson *et al.*, 2011). Auxin has been shown to be synthesized in anthers and to play a major role in coordinating anther dehiscence, pollen maturation and pre-anthesis filament elongation (Cecchetti *et al.*, 2008). The first demonstration of the role of auxin in flower development was by characterization

of the *pinoid1* mutant (Galweiler *et al.*, 1998) that has pin shaped inflorescences and failed flower formation. The loss of polar auxin transport due to the loss of the PLN1 transporter prevents the inflorescence meristem from forming floral meristems (Cheng and Zhao, 2007). The *pinoid* mutant (Bennett *et al.*, 1995) shares the inability to form floral primordia. *PINOID* encodes a protein kinase associated with *PIN* expression and cellular localization (Frimi *et al.*, 2004).

The auxin biosynthesis genes *YUC1*, *YUC2*, *YUC4* and *YUC6* have been demonstrated to have a direct role in regulating floral development. The double mutants *yuc2 yuc6* is sterile due to abnormal late anther development and pollen formation, while the double mutant *yuc1 yuc4* has gross floral morphological abnormalities and shows a lack of determinacy, suggesting a role for auxin in regulating meristematic cell proliferation (Cheng *et al.*, 2006). The *yuc1 yuc2 yuc4 yuc6* quadruple mutants resembles the *pin* mutant inflorescence phenotype (Cheng *et al.*, 2006). Floral development in mutants varies greatly from flower to flower in both the auxin biosynthesis and transport most likely due to a breakdown of normal auxin distribution leading to variable and transient local auxin concentration that differ from one floral initial to another (Cheng *et al.*, 2007).

Aloni *et al.* (2006) used the *DR5::GUS* as a reporter of free auxin and an auxin polyclonal antibody to report conjugated auxin to suggest a role for auxins in floral development. The youngest buds contained the highest concentration of conjugated IAA, which becomes depleted during floral maturation suggesting a more complex mechanism than sole reliance upon the YUC proteins for IAA synthesis. The highest

concentration of free IAA is located in the stamen between floral stages 10 and 12 (Feng *et al.*, 2006). These high levels seem to retard development within neighbouring organs as removal of the anthers results in early expansion of the petals and change in IAA levels in nectaries. It seems that as a repressor of petal expansion, IAA may be acting antagonistically to the role of JA that promotes petal expansion latter in floral development (Aloni *et al.*, 2006). Free auxin appears to accumulate in the tapetum and subsequently accumulates within the pollen, with auxin flow within the anther filament important for pollen mitosis to occur (Feng *et al.*, 2006). Free IAA also accumulates in the style just below the stigma in time for pollen germination (Aloni *et al.*, 2006). Auxin has also been shown to have an effect on anther dehiscence and endothecium secondary thickening, in part via repression of *MYB26* gene expression (Cecchetti *et al.*, 2013) (Section 1.7).

1.5.3 OTHER PHYTOHORMONES THAT IMPACT ON FLORAL DEVELOPMENT

1.5.3.1 ETHYLENE

Ethylene is a gaseous hormone that plays a role in regulating the development of plant growth (Bleecker and Kende, 2000). Ethylene is proposed to play a role in anther dehiscence in tobacco and *Petunia* in a manner related to JA regulation of anther dehiscence in *Arabidopsis* (Rieu *et al.*, 2003). Altering the level of ethylene has been observed to retard anther dehiscence. The effects of ethylene during the final events of dehiscence, stomium cell degeneration and dehydration have been observed in tobacco (Rieu *et al.*, 2003; Wilson *et al.*, 2011).

It has been hypothesised that the promoter of *ETHYLENE RESPONSE FACTOR 1 (ERF1)* acts as an integrator of JA and ethylene signals for defence responses (Brown *et al.*, 2003). The GCC box required for *ERF1* to bind the *PLANT DEFENSIN 1.2 (PDF1.2)* promoter has also been identified as a JA-responsive element (Brown *et al.*, 2003). *ETHYLENE INSENSITIVE 3-LIKE1 (EIL1)* gene has been identified as the ethylene-regulated transcription factor that initiates transcription of *ERF1*, but the JA regulated transcription factor that binds the *ERF1* promoter has not been identified (Guo and Ecker, 2004). Ethylene has been identified as a negative regulator of floral transition (Achard *et al.*, 2007), which has a negative effect upon cell elongation possibly due to alterations to hydroxyproline-rich glycoproteins crosslinking of wall structural proteins. This is a system of cellular regulation with potentially important functions in cell maturation and toughening of cell walls, which are involved in the initial stages of plant defence (Bradley *et al.*, 1992; Sommer-Knudsen *et al.*, 1998; De Cnodder *et al.*, 2005).

1.5.3.2 GIBBERELLINS

Gibberic Acid (GA) mutants are defective in stamen development with defects in male fertility (Chhun *et al.*, 2007; Hu *et al.*, 2008; Rieu *et al.*, 2008). In *Arabidopsis*, GA is important for pollen development, as well as for filament elongation (Cheng *et al.*, 2004). GA has been shown to play a key role in tapetum development (Hu *et al.*, 2008). It is also required for stamen and petal development, and is important for the elongation of the pollen tube in *Arabidopsis* (Singh *et al.*, 2002).

The gibberellic acid (GA) receptor, *GIBBERELLIN INSENSITIVE DWARF 1 (GID1)*, was the first gene identified in rice (Ueguchi-Tanaka *et al.*, 2005). The GID1 protein binds GA and binds to DELLA proteins targeting them for proteasomal degradation via the SCF^{SLY1} complex. In *Arabidopsis*, there are three *GID1* homologues, *GID1a*, *GID1b* and *GID1c*, which are partially redundant (Griffiths *et al.*, 2006). Single knockouts of the three genes fail to produce a phenotype; the *gid1a gid1b* double mutant is male sterile as the stamen filament fails to elongate and it has a dwarf phenotype (Griffiths *et al.*, 2006). Whereas the triple mutant *gid1a gid1b gid1c* produces no flowers, neither the stigma nor the anther filaments extend; the triple mutant is also a severe dwarf (Griffiths *et al.*, 2006). GA-deficient mutants have an effect on flower and pollen development and these mutants tend to be male sterile because of defects in pollen development as well as filament elongation (Fleet and Sun, 2005). The *DELLA* genes *REPRESSOR OF GA1-3 (RGA)*, *RGA-LIKE 1(RGL1)* and *RGL2* act together to repress GA-dependent petal and pollen development, as well as the elongation of the anther filament (Cheng *et al.*, 2004). Furthermore, in *Arabidopsis*, GA has been shown to induce expression of floral meristem identity genes such as *LEAFY (LFY)* (Blazquez *et al.*, 1998), *APETELA3 (AP3)*, *PISTILLATA (PI)* and *AGAMOUS*, which control the formation of petal and stamen primordia (Yu *et al.*, 2004).

The reduction in fertility of *Arabidopsis* plants with reduced GA levels cannot be explained purely by a mechanical barrier to pollination (Plackett *et al.*, 2012; Plackett *et al.*, 2011), with the precise level of GA appearing critical to floral organ growth and

pollen development (Plackett *et al.*, 2014). Anther size was also reduced under GA treatment, suggesting that disrupted anther development could underlie the fertility effects of GA (Plackett *et al.*, 2014). In *Arabidopsis*, GA treatment has been shown to reduce the frequency of silique set (Plackett *et al.*, 2012).

1.6 MYB GENE FAMILY

The MYB protein family is a large group of proteins present in all eukaryotes, which function as transcription factors (Stracke *et al.*, 2001). The MYB family proteins are classified based upon a motif of three imperfect repeats. The R2R3-type MYB protein encoded genes have been classified into 22 subgroups (Kranz *et al.*, 1998), which have been phylogenetically clustered based on sequence homology (Stracke *et al.*, 2001; Figure 1.9). The general structure of the MYB domain in R2R3 MYBs is two helix-turn-helix domains, which form two helices separated by a loop that acts as transcription factors and as a sequence-specific DNA binding domain. In the mammalian three repeat MYBs, the R2 and R3 repeats recognise different sequences, while the R3 repeat can form the helix-turn-helix structure in solution. The R2 appears to depend on sequence-specific DNA binding to adopt and stabilise this conformation (Solano *et al.*, 1995). There are several cases of functional conservation of genes that cluster together based on sequence similarity (Figure 1.9). Examples of the roles of the R2R3 MYBs are diverse and include four LIPS (FLP) and MYB88, which negatively regulate cell division in stomatal cells (Lai *et al.*, 2005). WEREWOLF (WER) that acts in the epidermis to determine cell fate via an interaction with the three repeat MYB protein CAPRICE (CPC) (Tominaga *et al.*, 2007) and MYB21 and MYB24, implicated in JA signalling within

the anthers (Mandoaker *et al.*, 2006) (Section 1.5.1.2).

The R2R3 MYB proteins in *Arabidopsis* are involved in controlling primary and secondary metabolism (AtMYB11/PEG1, AtMYB12/PFG2 and AtMYB111/PFG3 in flavonoid biosynthesis), in regulating plant developmental processes (AtMYB37/RAX1, AtMYB38/RAX2/B1T1 and AtMYB84/RAX3/subgroup), in axillary meristem formation, in anther development (AtMYB21, AtMYB24, AtMYB57) and in regulating cell fate and identity (AtMYB0 and AtMYB23 in controlling trichome initiation in shoots and AtMYB66 in controlling root hair patterning) (Dubos *et al.*, 2010).

A number of *MYB* transcription factors have been linked to pollen development; for example the *AtMYB103* gene regulates tapetum and trichome development in *Arabidopsis thaliana* (Li *et al.*, 2007). The *AtMYB32* and *AtMYB4* genes have been implicated in pollen wall formation, with the *myb32* mutant exhibiting deformed pollen grains that lacked cytoplasm (Preston *et al.*, 2004). Expression of *AtMYB32* is observed in many tissues, especially in anther tapetum, stigma and lateral root primordia. This deformation of pollen was observed in both *AtMYB32* and *AtMYB4* mutants (Preston *et al.*, 2004). These workers concluded that the change in the levels of *AtMYB32* and *AtMYB4* expression influenced pollen development through affecting pollen wall composition via the phenylpropanoid pathway and flavonoid levels. A *FLOWER FLAVONOID TRANSPORTER (FFT)* in *Arabidopsis* (*AtDTX35*) is highly transcribed in floral tissues (anthers, stigma, nectarines and siliques) and mutant analysis has also shown that absence of this transcription factor affects pollen development and anther dehiscence (Thompson *et al.*, 2010).

Another prominent role of R2R3 MYBs is in the regulation of secondary thickening that is carried out by at least 11 *MYBs* (Oh *et al.*, 2003), including the distantly related *MYB46* and *MYB63* (Figure 1.9). *MYB26* has been implicated as a key regulator of secondary thickening in the anther endothecium that is critical for anther dehiscence (Yang *et al.*, 2007) (Section 1.4 and 1.7). This indicates a large diversity of function even among those *MYBs* that regulate similar processes. Relatively few studies have examined secondary cell wall R2R3 MYB function in grasses, which may have diverged from dicots in terms of secondary cell wall regulatory mechanisms, as they have in cell wall composition and patterning. Understanding cell wall regulation is especially important for improving lignocellulosic bioenergy crops, such as switchgrass (Zhao and Bartley, 2014).

1.7 *MYB26/MS35* ASSOCIATION WITH ANther DEHISCENCE

Male sterile mutants, either due to a lack of viable pollen formation or due to lack of dehiscence mechanisms, are potentially valuable in plants where hybrid production is desired. Defects in dehiscence of viable pollen have a further advantage since they produce pollen that could be collected and subsequently used for hybrid production. As this is the case with *Arabidopsis thaliana AtMYB26*, it is potentially an important tool for manipulating male fertility in higher plants (Steiner-Lange *et al.*, 2003; Wilson *et al.*, 2011).

The *male sterility35 (myb26/ms35)* recessive mutant was first identified as generated by x-ray mutagenesis of *Ler* seeds (Dawson *et al.*, 1999). The *MYB26* gene mapped to the upper

arm of chromosome three, and the *myb26* mutant is the result of a deletion 1288 bp upstream of the translational start of *MYB26*, which results in the down regulation of *MYB26* expression and dehiscence failure (Steiner-Lange *et al.*, 2003) (Figure 1.10).

The *ms35* mutant of the *MYB26* gene fails to deposit secondary thickening and thereby prevents pollen dehiscence (Figure 1.11). When the mutant pollen was released mechanically from the anther, self-fertilisation was possible indicating pollen viability. PCR analysis of the *myb26* mutant suggested the *ms35* mutation was due to a major chromosomal rearrangement; database analysis of the *MYB26* region identified four additional stable mutant alleles all affected within the first of three exons, one with a transposon tag, two with stop codons and one with disruption to the coding region. All three of which were due to imperfect excision of the transposon tag.

The disruption of the DNA binding domain of this R2R3-type *MYB* transcription factor, resulted in the prevention of the secondary wall thickening of the endothecium in the *myb26* mutant (Steiner-Lange *et al.*, 2003). The ability to regulate secondary cell wall thickening in a conserved manner also has a significant commercial application for the wood and paper industry (Yang *et al.*, 2007). Therefore, a further study in relation to woody plant species would also be valuable in understanding the process of wood formation. Wood is the most abundant biomass produced by plants and it is an important raw material for traditional forest products, paper making and pulping. Also, the secondary cell walls of mature plants form the greater portion of lignocellulosic biomass used in bio-fuel production (Harris and DeBolt, 2010).

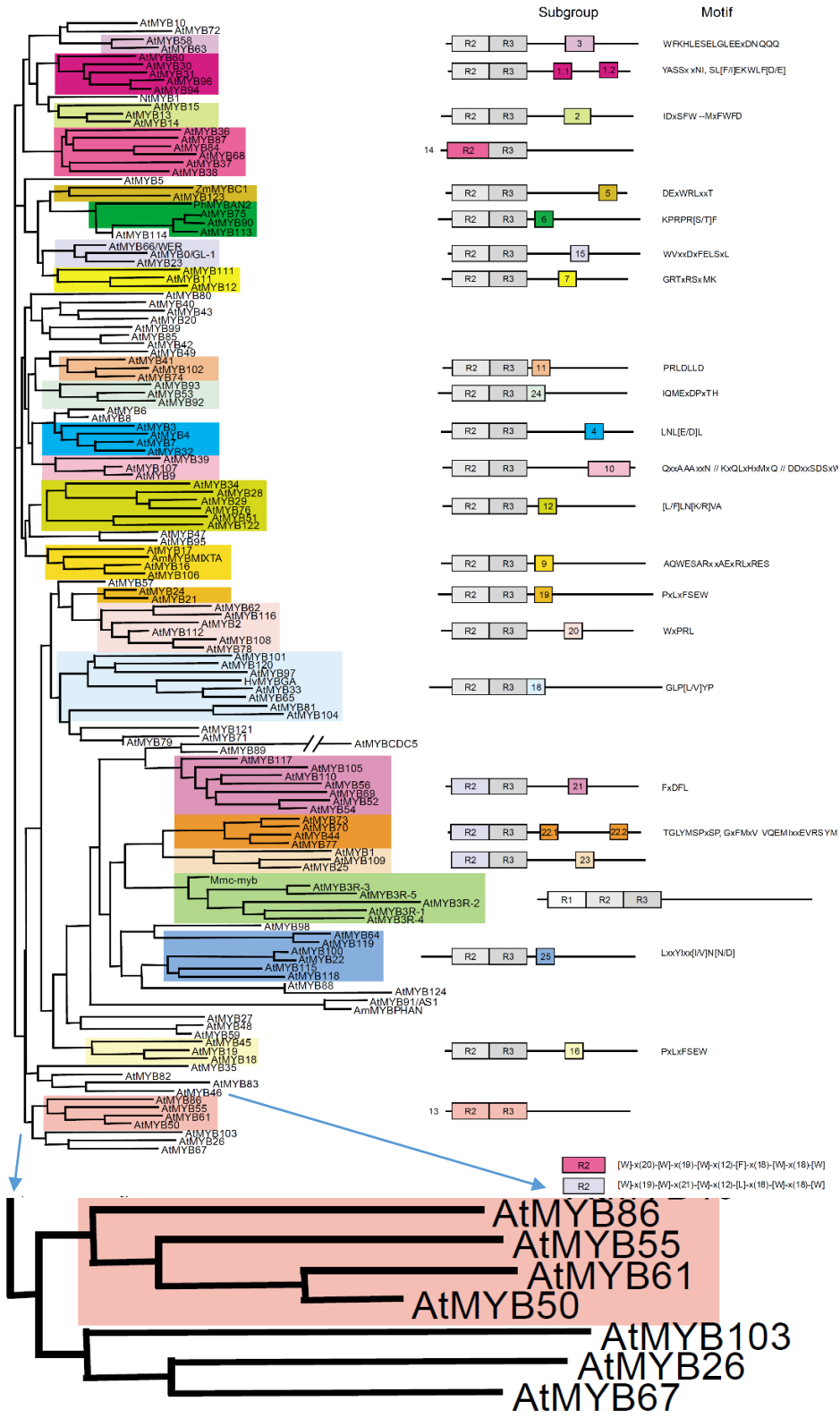


Figure 1.9 *Arabidopsis* MYB Proteins subgroups in *Arabidopsis*. Taken from Stracke *et al.* (2001). Proteins are grouped by similarities in protein sequence 3' to the MYB repeats indicated by coloured boxes. MYB26 cluster is enlarged below.

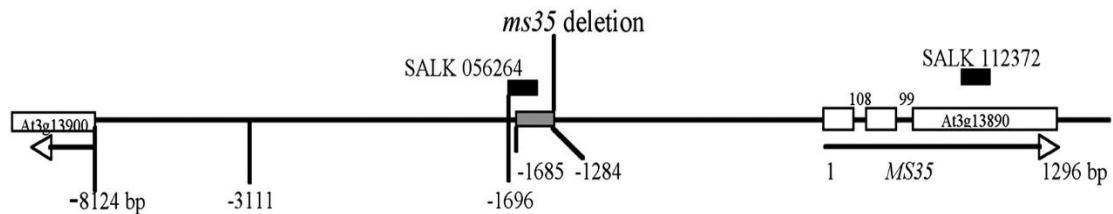


Figure 1.10 Structure of the *At3g13890* (*MS35* or *MYB26*) gene. Map of the *Arabidopsis At3g13890* region, showing the *ms35* deletion and positions of SALK knockout lines. Arrows indicate open reading frames. Taken from Yang *et al.* (2007).

1.8 SECONDARY CELL WALL THICKENING

It is clear that *MYB26* is involved in regulating anther secondary thickening (Yang *et al.*, 2007); the *myb26* mutant lacks endothecium secondary thickening and qRT-PCR results show that genes such as *MYB46*, *MYB85* and *HOMEBOX PROTEIN KNOTTED-1-LIKE 7 (KNAT7)* that are regulators of secondary thickening (Zhong *et al.*, 2006; Zhong and Ye, 2007), are down-regulated in the *myb26* mutant (Yang *et al.*, 2007).

As microspores mature, secondary wall thickening occurs in the endothecium and connective tissues of the anther, leading to the deposition of cellulose, hemicelluloses and lignin in the endothecium cells (Figure 1.11). In *Arabidopsis*, the endothecium is first established in the anther during stage 5. When the anther reaches stages 6-10, it goes through expansion leading to the development of secondary cell wall thickening in stage 11 (Sanders *et al.*, 1999). The secondary thickening of the cell wall is an important requirement of various plant developmental processes including the transport of water, support and where mechanical forces are required. This is necessary for the dehiscence of the anthers since cell wall thickening in the endothecium cells produces the physical forces

necessary for the dehiscence process (Dawson *et al.*, 1999; Nelson *et al.*, 2012).

The secondary cell wall deposition occurs once cell growth and expansion has stopped, and involves coordinated regulation of a number of complex metabolic pathways (Knox, 2008). The secondary cell wall is composed predominantly of cellulose, lignin and xylan (Knox, 2008). In mature plants, the cellulose accounts for approximately 40% of the dry weight of the secondary walls (Delmer and Amor, 1995). Xylans are abundant in secondary cell walls (Knox, 2008). The three major secondary wall components are systematically regulated, cellulose, lignin and xylan (Zhong *et al.*, 2007a, b).

Overexpression of *MYB26* resulted in patches of ectopic lignified secondary thickening in aboveground tissues (Zhong *et al.*, 2006; Mitsuda *et al.*, 2007; Yang *et al.*, 2007). This ectopic secondary thickening occurred in various tissues, in floral tissues it resembled the xylem and endothecium thickening (Figure 1.11), whilst in the epidermis it formed net-like thickening. This was also seen when *MYB26* was over expressed in tobacco (Yang *et al.*, 2007). *MYB26*, therefore, appears able to induce and regulate secondary thickening in a cell-specific manner in the anther.

Native *MYB26* expression is localized in inflorescences, with a high level of expression during pollen mitosis I (PMI), and low level expression prior to PMI and during PMII (Yang *et al.*, 2007). Expression of *ProMYB26::GUS* was seen in floral tissues, in the anthers and filaments of the flowers, a strong signal was also detected in the style and nectaries of the flowers (Yang *et al.*,

2007) (Figure 1.12). Weaker expression was observed through to open flowers in the tapetum and endothecium (Figure 1.12). Over-expression of *MYB26* under the *CaMV35S* promoter resulted in thickening of epidermal tissues, and in ectopic secondary thickening in various tissues including leaf, stem and floral organs (Figure 1.12) (Yang *et al.*, 2007b).

MYB26 has been shown to act upstream of the *NAC* transcription factors, *NAC SECONDARY WALL THICKENING PROMOTING FACTOR1 (NST1)* and *(NST2)*, and miss-expression of *MYB26* in *Arabidopsis* causes ectopic lignification, particularly in epidermal tissues, and increased expression of *NST1* and *NST2* (Yang *et al.*, 2007). Mutations in *MYB26* result in plants that are male sterile, despite having viable pollen. During normal development, shearing forces are developed by the differential contraction of the thickened and unthickened parts of the cell walls in the endothecium during anther desiccation (Keijzer, 1987; Bonner and Dickinson, 1989). In *myb26* mutant plants, the lack of secondary thickening in the endothecium means that the mechanical force required for pollen release cannot be generated, thus viable pollen remains trapped within the tissues of the anther (Dawson *et al.*, 1999; Steiner-Lange *et al.*, 2003).

Chimeric expression of repressors derived from *NST1 (At2g46770)* and *NST2 (At3g61910)* resulted in failure of anther dehiscence as a result of the loss of secondary wall thickening in the anther endothecium (Mitsuda *et al.*, 2007). The expression of *NST1* was seen in various tissues, which undergo secondary wall synthesis, whilst *NST2* expression was only localized to the anther (Mitsuda *et al.*, 2005). The *nst1 nst2* double mutant was observed to have an anther indehiscent phenotype as a result of

the lack of secondary thickening in the endothecium, a phenotype that is equivalent to that of the *myb26* mutant (Mitsuda *et al.*, 2005).

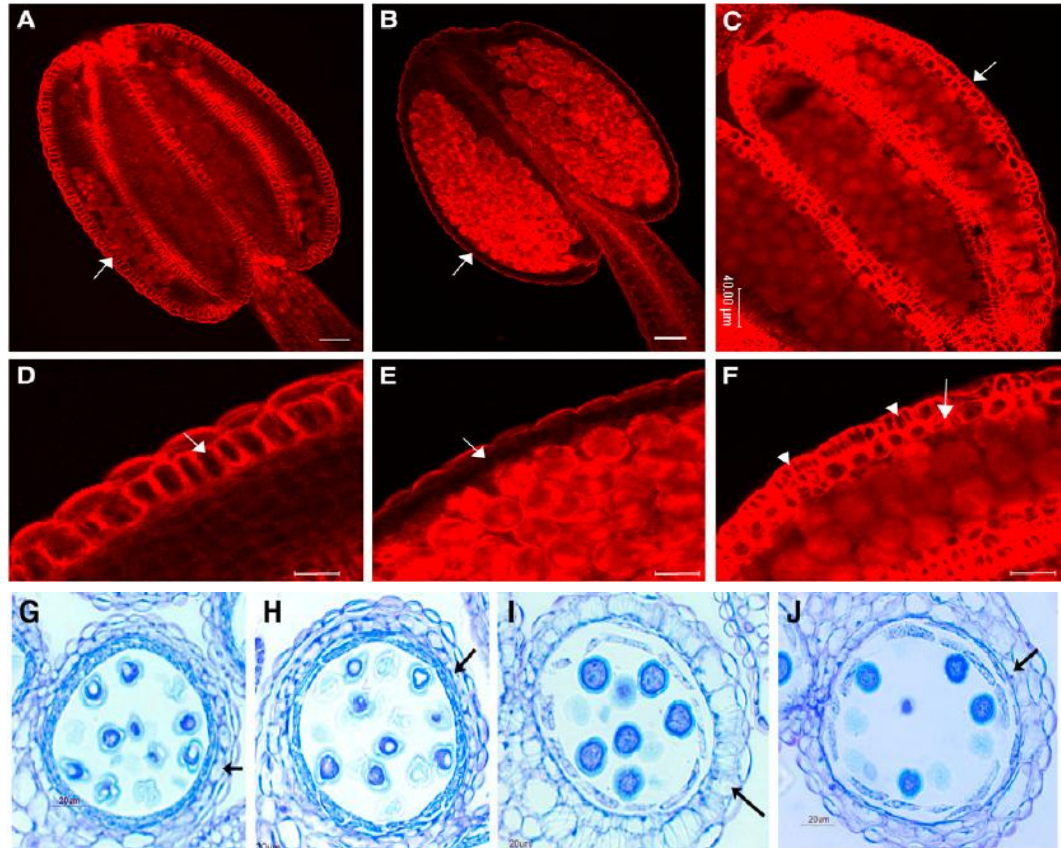


Figure 1.11 Phenotypic characterization of MYB26 and over-expression of MYB26 in *Arabidopsis*. Taken from Yang *et al.* (2007).

(A) to (F) Anther from open flowers stained with acridine orange/ethidium bromide and visualized by confocal microscopy. (A) Ler wild type partially dehiscent anther displaying thickening in the endothecium (arrow). (B) Indehiscent *myb26* mutant anther from mature open flower, the endothecium thickening is absent (arrow). (C) Mature anther from open flowers of MYB26 overexpression line. (D) Close up of (A). (E) Close up of (B). (F) Close up of (C). (G) to (J) Sections through wild type anthers (G and I) and *myb26* mutant anthers (H and J). (G) Endothecium cells begin to expand during pollen mitosis I in Wild type (arrow). (H) Minimal endothecium expansion in *myb26* mutant (arrow). (I) In the Wild type, endothecium expansion continues and secondary thickening is visible during Pollen Mitosis II (arrow). (J) In the *myb26* mutant, the endothecium fails to fully expand and no secondary thickening occurs (arrow). Bars=40 μ m except in (G) to (J) where bars=20 μ m.

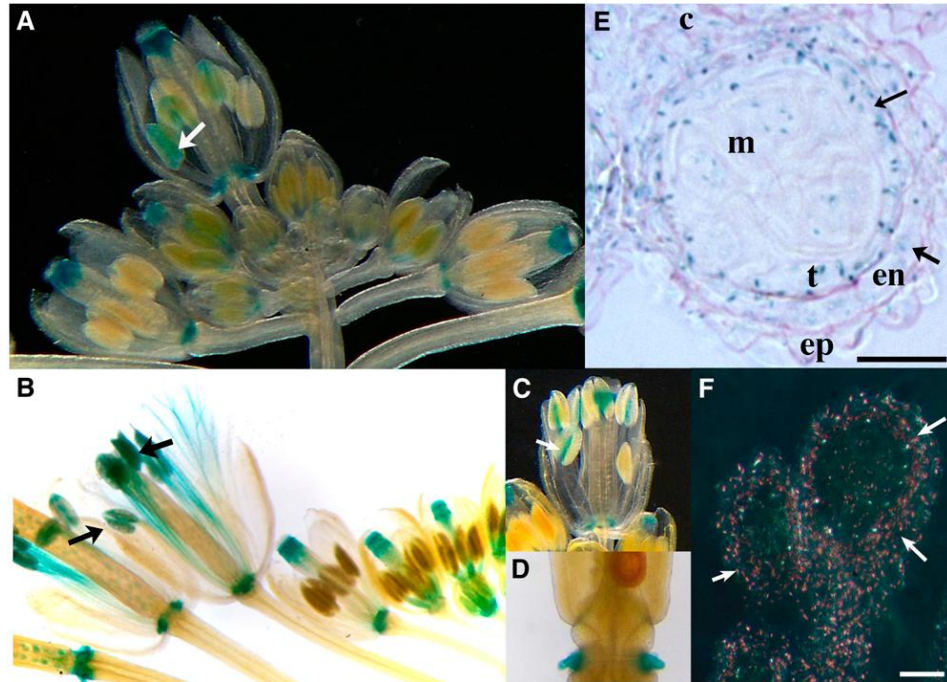


Figure 1.12 *ProMYB26:GUS* Fusion Expression in *Arabidopsis*.

(A) and (B) GUS expression in inflorescences anthers, filaments, nectaries and stylar tissues (arrows indicate expression in anther tissue). (C) Close up dark-field image of buds before opening. Showing expression in anthers (arrow). (D) Immature silique showing GUS expression in nectaries. (E) and (F) sections through anther at Pollen Mitosis I stage. GUS expression in the anther, particularly in the endothecium, tapetum and connective tissues (arrows). (F) Dark-field image. c, connective tissue; en, endothecium; ep, epidermis; m, microspores; t, tapetum. Bars= 40 μ m. Taken from Yang *et al.* (2007b).

1.9 GENE EXPRESSION NETWORK FOR SECONDARY THICKENING

The lack of anther lignification in the *myb26* mutant lines suggests that *MYB26* plays a role in regulation of anther endothecium thickenings and regulation of the phenylpropanoid pathway (Figure 1.13). The general phenylpropanoid pathway transforms phenylalanine into 4-coumarate: coenzyme A (also called p-coumarate: coenzyme A, p-coumarate: CoA, p for para position), which can enter the two major downstream pathways,

monolignol and flavonoid biosynthesis. Enzymes in the general phenylpropanoid pathway include phenylalanine ammonia-lyase (PAL) (Olsen *et al.*, 2008; Ritter and Schulz, 2004), cinnamic acid 4-hydroxylase (C4H) (Achnine *et al.*, 2004), and 4-coumarate: coenzyme A ligase (4CL) (Harding *et al.*, 2002). Genes encoding enzymes in the phenylpropanoid pathway and lignin biosynthetic pathway are likely to be co-ordinately regulated. The potential for MYB transcription factors to regulate the expression of phenylpropanoid pathways genes has been demonstrated with *AmMYB308* (from *Antirrhinum majus*), *AmMYB330*, *PtMYB4* (from *Pinus taeda*) and *AtMYBPAP1* (Rogers and Campbell, 2004). It has been reported that lignin biosynthesis in xylem can be modulated by *NtLIM1* (from *Nicotiana tabacum*) (Kawaoka *et al.*, 2000) and *AtIRX4* (*IRREGULAR XYLEM 4*) (Jones *et al.*, 2001). Secondary cell wall formation is also being intensively studied since they are important putative sources of renewable energy, by fermentation to produce ethanol, or simply burned to produce steam for generators and recovered as electricity (Carroll and Somerville, 2009). Nevertheless some cell wall components, for example lignins, are less desirable since they have to be removed in the production of cellulosic ethanol.

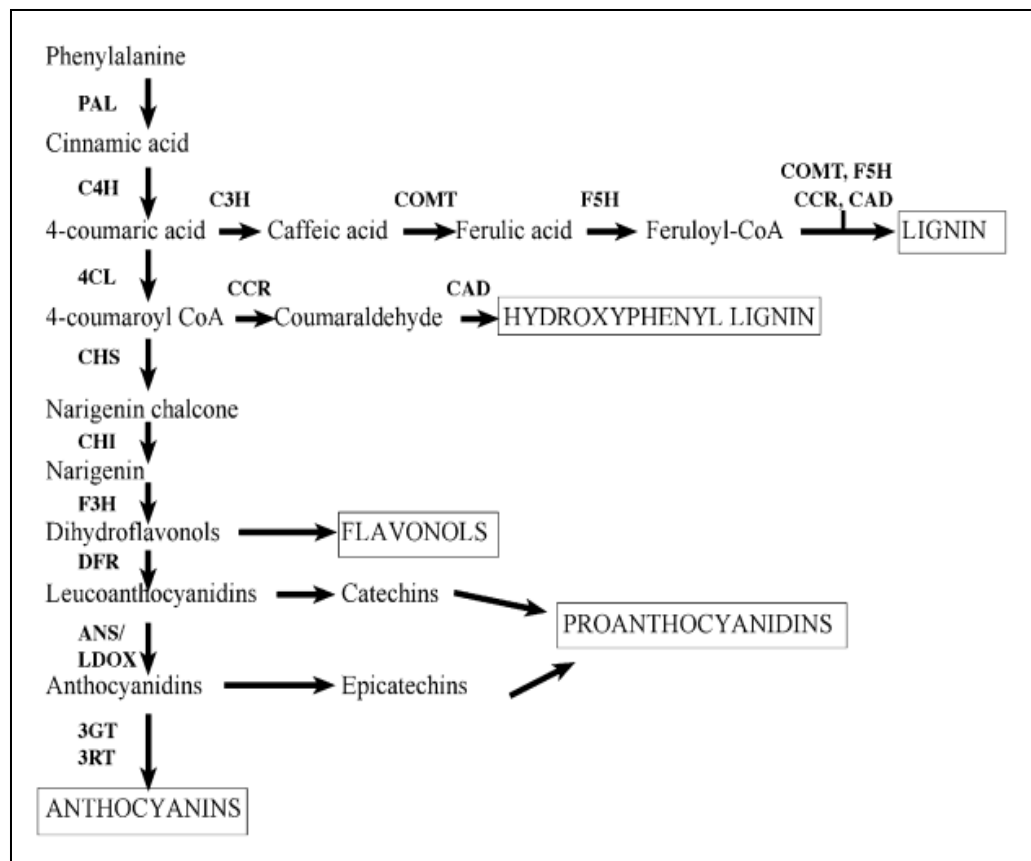


Figure 1.13 Simplified scheme of phenylpropanoid synthesis in *Arabidopsis*.

ANS/LDOX, anthocyanidin synthase; CAD, cinnamyl alcohol dehydrogenase; CCR, cinnamyl-CoA reductase; C3H, 4- coumarate-3-hydroxylase; C4H, cinnamate 4-hydroxylase; CHI, chalcone isomerase; CHS, chalcone synthase; 4CL, 4- coumarate-CoA ligase; COMT, caffeic acid O-methyltransferase; DFR, dihydroflavonol 4-reductase; F3H, flavonoid 3-hydroxylase; F5H, ferulate 5-hydroxylase; 3GT, anthocyanidin 3-glucosyltransferase; PAL, phenylalanine ammonia-lyase; 3RT, anthocyanidin-3-glucoside rhamnosyl transferase. Taken from Yang *et al.* (2007).

However, the three major secondary wall components, cellulose, lignin and xylan, seem to be systematically regulated. The double mutant *irx10irx10-L* with defects in xylan biosynthesis shows a large reduction of xylan as well as cellulose (Brown *et al.*, 2009). Mutations in genes encoding subunits of the cellulose synthase complex have also indicated that both cellulose and lignin synthesis are affected (Taylor *et al.*, 2003). In the lignin

biosynthesis mutant *irx4*, cellulose content is also reduced by 10-20% (Patten *et al.*, 2005).

To date, studies have suggested that the control of secondary wall formation in interfascicular fibres and secondary xylem involves *NAC SECONDARY WALL THICKENING PROMOTING FACTOR1* (*NST1*, *At2g46770*) and *SECONDARY WALL ASSOCIATED NAC DOMAIN PROTEIN1* (*SND1*, *At1g32770*, also called *NST3*) (Mitsuda *et al.*, 2007). *NST1* and *SND1* function redundantly in the regulation of secondary thickening in fibers (Mitsuda *et al.*, 2007) and siliques (Mitsuda and Ohme-Takagi, 2008). *NST1* and *SND1* are expressed in various lignified tissues. Dominant repression of *NST1* or *SND1* and the double knockout caused a severe reduction in the secondary thickening of fibres while overexpression of either gene induces ectopic secondary thickening in various aboveground tissues (Mitsuda *et al.*, 2007). Little is known about secondary thickening in the anther endothecium, except for two NAC domain transcription factors, *NST1* and *NST2*, which act redundantly to regulate secondary thickening in anther walls and are required for anther dehiscence (Mitsuda *et al.*, 2005). The double mutant *nst1 nst2* has an anther-indehiscent phenotype due to lack of secondary thickening in the endothecium, which is similar to the *myb26* mutant (Mitsuda *et al.*, 2005).

1.10 AIMS AND OBJECTIVES OF THE PROJECT

The aim of this project was to investigate the process of anther dehiscence by characterising and confirming the proteins that interact with MYB26, alongside characterization of novel dehiscence mutants. This included characterisation of five putative MYB26 interactive proteins that were previously identified from screening an *Arabidopsis* stamen yeast 2-hybrid (Y2H) library with MYB26 protein as bait (Section 3.1.2; Table 3.2).

To achieve the goals of this work the following specific objectives were undertaken:

- i) Confirmation of the interaction of the different candidate Y2H proteins and the MYB26 protein. To confirm co-localisation of transiently expressed proteins in *Nicotiana benthamiana* and protein-protein interactions (Bhat *et al.*, 2006), Förster Resonance Energy Transfer (FRET) was carried out (Chapter 3).
- ii) Analysis of the expression and possible function of the putative MYB26-interacting proteins using SALK insertional lines mutants and over-expression lines (involving genotypic, phenotypic and expression analysis of these mutants) (Chapter 4).
- iii) Analysis of novel male sterile mutants that have defects in anther dehiscence to determine their effect on pollen generation and anther development. This included phenotyping, backcrossing of these male sterile mutants with the wild type parental plants, checking for allelism to the *myb26* mutant and then mapping of a novel gene involved in anther dehiscence (Chapter 5).

CHAPTER 2: MATERIALS AND METHODS

2.1 ARABIDOPSIS PLANT MATERIALS AND GROWTH CONDITIONS

Plants materials, the *ms35/myb26* mutant for irregular secondary thickening of the anther endothecium, SALK lines for the genes of interest and overexpression lines, *Arabidopsis thaliana* ecotype of the wild type Landsberg (*Ler*) and Columbia (*Col*) as a background (control) were obtained from Prof. Zoe A. Wilson's Lab (School of Biosciences, University of Nottingham, Loughborough, UK) or from NASC (Nottingham *Arabidopsis* Stock Centre, University of Nottingham, Loughborough, UK).

For growing the plants in the glasshouse, seeds were sown in 9 cm plastic pots in Levington M3 compost containing the systemic insecticide Intercept 5GR (21g in 75 L; Scotts Company, UK). The latter was added and mixed with water before sowing the seeds. Plant materials were grown in the glasshouse under conditions of 22/20°C ± 2°C day/night temperatures with a 16 h photoperiod under light intensity of 111 μmol s⁻¹m light⁻² warm white fluorescence. Mature seeds were harvested after the plants were dried and then seeds were stored in moisture-porous paper bags at room temperature for further use.

2.2 NICOTIANA BENTHAMIANA PLANT MATERIAL

For transient assays, *N. benthamiana* seeds (University of Nottingham) were grown at 22°C+/-2°C in 25 cm pots for 5-6 weeks and then infiltrated (Kapila *et al.*, 1997) with appropriate gene constructs to check the protein expression (Section 2.7).

2.3 ARABIDOPSIS THALIANA SALK T-DNA KNOCKOUT (KO) LINES

Arabidopsis thaliana T-DNA insertion “knockout” (KO) lines were obtained from Nottingham *Arabidopsis* Stock Centre (NASC) (Table 2.1) in *Arabidopsis* ecotype Columbia (*Col*) background. Gene information for these lines along with insertion positions was obtained from NASC Ensembl website (<http://atensembl.arabidopsis.info/index.html>) to locate the insertion site of the T-DNA insert and determine the expression patterns. The KO lines were genotyped and phenotyped to identify homozygous sterile plants (Section 4.3.2).

Table 2.1 Description of T-DNA insertion lines and their gene-specific primers used for genotyping and RT-PCR analysis.

Gene	SALK knockout line	NASC ID	Insert position	Genotyping primers	Primers for RT-PCR
<i>At5g25560</i> (<i>CHY</i>) zinc finger protein	008223	N508223	Chr 5 (8,897,871-8,901,709)	SALK_008223R SALK_008223F SALK-LBb1	At5g25560R At5g25560F
<i>At1g47128</i> (<i>RD21</i>) cysteine proteinase	090550	N590551	Chr 1 (17,282,825-17,285,670)	SALK_090551R SALK_090551F SALK-LBb1	At1g47128R At1g47128F
<i>At1g08320</i> (<i>bZIP</i>) transcription factor	091349	N591349	Chr 1 (2,621,904-2,627,848)	SALK_091349R SALK_091349F SALK-LBb1	At1g08320R At1g08320F
<i>At3g62970</i> Zinc finger (<i>C3HC4 RING finger</i>) protein	106671	N606671	Chr 3 (23,270,633-23,272,923)	SALK_106671R SALK_106671F SALK-LBb1	At3g62970R At3g62970F

*Primers (APPENDIX II)

2.4 SEED STERILISATION FOR TRANSGENIC PLANT SELECTION

Seed sterilisation was carried out in a sterile flow hood. Seeds were washed three times with sterile distilled water and re-suspended in 100% (v/v) ethanol and dried on sterile filter paper

under the hood. After drying, the seeds were plated onto MS medium (4.33 g/l MS, 0.5% (w/v) sucrose pH 5-6, 0.8% (w/v) agar) (Murashige and Skoog, 1962) (APPENDIX II) in 9 cm Petri dishes. Then, plates were incubated at 4°C for four days before being transferred to a growth room at ~23°C in white light intensity of 111 µmol.

2.5 PHENOTYPIC ANALYSIS

Transgenic plants were analysed for their general phenotypes focusing on reproductive organ development and were observed for the presence of extended siliques-containing seeds. All plants were compared to *Ler* or *Col* wild types depending on the appropriate mutant background. Particular attention was paid to pollen development and secondary thickening processes (Section 2.6).

2.6 MICROSCOPIC ANALYSIS

2.6.1 ALEXANDER STAINING

Alexander's stain (Alexander, 1969) (APPENDIX I) was used to test for pollen viability; it contains malachite green, which stains pollen cellulose walls and pollen cytoplasm and distinguishes between viable (red-purple) and non-viable (green-blue) pollen grains. Anthers were excised from buds and flowers, placed onto glass slides with a drop of Alexander's stain and a cover slip. Anthers were, then, viewed using a Zeiss microscope at X20 magnification to detect the viable and non-viable pollen and determine percentage of viability.

2.6.2 LIGNIN STAINING USING PHLORO-GLUCINOL

The primary stem close to the rosette are hand-sectioned, placed onto a microscope slide with one drop of 1% (w/v) phloroglucinol (dissolved in 70% (v/v) ethanol) for 1 min and subsequently one drop of HCl >25% (v/v) to stain lignin red. Sections were, then, covered with a cover slip and observed using a light microscope (Nikon).

2.6.3 ACRIDINE ORANGE STAIN FOR LIGNIN

Whole inflorescences were placed in 1x PBS containing 2% (v/v) Tween-20 overnight at 4°C, then rinsed in 1x PBS lacking Tween-20. They were then, stained in Acridine Orange 0.01% (w/v) for 1 h, washed twice with 1x PBS for 5 min, then, stained in Ethidium Bromide 0.00005% (w/v) for 1 h and washed twice with 1x PBS for 5 min (according to Yang *et al.*, 2007). Anthers, in 1x PBS, were excised from the buds and flowers, placed on glass slides and observed using a Leica confocal microscope SP2 with appropriate settings (Table 2.2). Ethidium bromide stains lignified cell wall with red fluorescence (514 nm excitation), acridine orange stains non-lignified cell wall with green fluorescence (488 nm excitation).

Table 2.2 Excitation and emission settings of Leica confocal microscopic analysis.

Dye	Excitation	Emission collected
Ethidium bromide	514 nm	570- 620
Acridine orange	488nm	510-530

2.6.4 HISTOCHEMICAL GLUCURONIDASE (GUS) ASSAY OF TRANSFORMED TISSUES

Histochemical analysis of *GUS* gene expression was performed based on the method of Jefferson *et al.*, (1987). Inflorescences and extended siliques were collected and placed in GUS staining solution (0.5 mg/ml X-Gluc (5-bromo-4-chloro-3-indolyl- β -glucuronic acid), 0.1% (v/v) X-100 Triton, 0.5 mM potassium ferricyanide $K_3Fe(CN)_6$, 0.5 mM potassium ferrocyanide $K_4Fe(CN)_6$ in 50 mM phosphate buffer (pH 7.0) and incubated for 24 to 48 h at 37°C. The inflorescences were clarified by an ethanol gradient 95%, 75%, 50%, 20% and 10% (v/v) for 1 h each, to remove chlorophyll. Then, the GUS expression was detected using a Leica microscope.

2.7 PROTEIN METHODS

2.7.1 PROTEIN EXTRACTION FOR WESTERN BLOTTING

Leaves (0.5 g) from *Nicotiana benthamiana* that had been previously infiltrated with expression constructs (Section 2.2) were ground into a very fine powder in liquid N_2 using a mortar and pestle. Then, 5 ml extraction buffer/mg of plant tissue (10% glycerol, 25 mM Tris-HCl, pH 7.5, 1 mM EDTA, pH 8.0, 150 mM NaCl, 10 mM DTT, 0.15% NP-40, 2% polyvinylpyrrolidone (PVPP), and 1X plant protease inhibitor cocktail (Sigma) (Devarshi *et al.*, 2013) were added.

2.7.2 SEPARATION AND VISUALIZATION OF RECOMBINANT FUSION PROTEINS BY SODIUM DODECYL SULFATE-POLYACRYLAMIDE GEL ELECTROPHORESIS (SDS-PAGE)

Protein samples in 1x SDS loading buffer (25 mM Tris-HCl pH 6.8, 10% (v/v) glycerol, 2% (w/v) SDS, 5% (v/v) β -mercaptoethanol, 0.001% (w/v) bromophenol blue) were heated to 100°C for 5 min and separated according to their size using SDS-PAGE. A pre-stained protein marker (New England Biolabs) was run alongside the samples. SDS-PAGE gels consisted of an upper stacking gel and lower separating gel. The stacking gel (132 mM Tris-HCl pH 6.8, 4% (w/v) acrylamide, 0.1% (w/v) SDS, 0.05% (w/v) APS, 0.15% (v/v) TEMED) was used for loading and concentrating the protein samples. A 10% (w/v) SDS-PAGE separating gel (0.38 M Tris-HCl pH 8.8, 10% (w/v) acrylamide, 0.1% (w/v) SDS, 0.05% (w/v) APS, 0.07% TEMED) was used for fractionating the proteins according to their molecular weight. The gels were loaded into a Mini-PROTEAN II cassette (Bio-Rad) filled with SDS running buffer (25 mM Tris-HCl pH 8.5, 190 mM glycine, 1% (w/v) SDS). Proteins were first electrophoresed at 80V until they reached the end of the stacking gel, after which the voltage was increased to 150V for 1 h.

2.7.3 WESTERN BLOTTING AND IMMUNO LABELLING

Nitocellulose-C membrane (Amersham) was activated by soaking in water for 1 min before use. After SDS-PAGE, proteins were transferred onto the Nitocellulose-C membrane by electro-

transfer at 150V for 1 h. The membrane was, then, blocked in 5% (w/v) non-fat dried milk dissolved in TBS-T (15 mM Tris-HCl pH 7.6, 150 mM NaCl, 0.1% (v/v) Tween 20) with gentle agitation, to reduce non-specific binding. Then, primary antibodies (raised against GFP, Abcam, Table 2.3) diluted in TBS-T containing 3% (w/v) non-fat dried milk, were added to the membrane and incubated at 4°C for 1 h. The membrane was then, washed several times with TBS-T for 20 min before incubation at 4°C for 45 min with secondary antibodies (Sigma). Following the incubation, the membranes were washed five times with TBS-T for 25 min.

Table 2.3 Primary and Secondary antibodies used in this study. All dilutions were made in TBST (15mM Tris-HCl pH7.6, 150 mM NaCl, 0.1% (v/v) Tween 20).

Antibody	Source	Dilution	Manufacturer
Primary Anti-GFP antibody	rabbit polyclonal (Catalog Number ab6556)*	1:5000	Abcam
Secondary antibody	Anti-Rabbit IgG (whole molecule) HRP conjugate antibody(Catalog Number A8102)	1:1000	Sigma

*This antibody is an affinity purified rabbit anti-GFP antibody purified on an affinity chromatography column made with highly purified recombinant GFP.

2.7.4 IMMUNODETECTION

Immunodetection was carried out using Immobilon (Millipore) and chemiluminescence detection in accordance with the manufacturer's instructions. The membrane (Section 2.7.3), washed to remove any unbound anti IgG secondary antibody, was incubated in 1:1 Luminol reagent and peroxide solution for 5 min at room temperature. Excess substrate was drained and the membrane was covered in cling film and placed in an X-ray

cassette overnight. The membrane was, then, exposed to X-ray film (Kodak) in the dark room and the film developed using developer and fixer solutions consecutively.

2.8 BACTERIAL TRANSFORMATION

2.8.1 CHEMICAL TRANSFORMATION

One 50 μ l aliquot of chemically competent cells was thawed on ice, then, 1-50 ng of the appropriate plasmid was added and mixed by gentle agitation of the tube. The competent cells were further incubated on ice for 30 min, then; the cells were heat-shocked at 42°C for 30 sec and transferred back on ice for 1 min. Then, 250 μ l of liquid LB media (without antibiotics) was added and the cells were grown in 37°C shaking incubator with shaking at 200 rpm for 1 h. Then, 50 μ l aliquot of the bacteria was spread on a plate of LB medium with appropriate antibiotic selection (Table 2.4) and left at 37°C overnight and the resulting colonies were screened by PCR (Section 2.9.9).

2.8.2 ELECTROPORATION

Electroporation was used to transform *Agrobacterium tumefaciens* competent cells (MP90 or GV3101 strain) (Table 2.10) (Wen-Jun and Forde, 1998). An aliquot (50 μ l) of electrochemically competent cells was thawed on ice, then, 100-200 ng of the appropriate plasmid was added. The bacteria were then transferred to prechilled electroporation cuvettes of 1-2 mm gap size. Electroporation was performed in an electroporator (MicroPulsar, BioRad) at 2.5 kV. One ml of LB medium was added directly to the cuvette immediately after the pulse and, then cells were transferred into a fresh 1.5 ml microfuge tube. The transformation was incubated at 28°C with shaking at 200

rpm for 3 h. Then, 20 μ l and 50 μ l aliquot of cells were spread onto two LB agar plates containing 25 μ g/ml rifampicin selection and the other selective antibiotic appropriate to the transformed plasmid (Table 2.4). The plates were incubated at 28°C for 2-3 days and colonies were screened by PCR (Section 2.9.9).

Table 2.4 Antibiotic stock solutions (Stored at -20°C).

Antibiotic	Solvent	Stock conc.	Working conc.
Kanamycin (Kan)	H ₂ O	50 mg/ml	50 μ g/ml
Spectinomycin (Spect)	H ₂ O	50 mg/ml	50 μ g/ml
Ampicillin (Amp)	H ₂ O	100 mg/ml	100 μ g/ml
Gentamycin (Gent)	H ₂ O	15 mg/ml	15 μ g/ml
Rifampicin (Rif)	DMSO	25 mg/ml	50 μ g/ml
Tetracycline (Tet)	Ethanol	10 mg/ml	5-10 μ g/ml

2.9 MOLECULAR METHODS

2.9.1 DNA EXTRACTION

Genomic DNA extraction was performed using Extract-N-Amp plant kits (Sigma) from young *Arabidopsis* leaves. Leaf tissues (0.5-0.7 cm long) were excised from the plants, ground in liquid nitrogen, collected into 2 ml collection tubes and incubated at 95°C in 50 μ l of extraction buffer for 10 min. An equal volume of dilution solution was added to the extract to neutralize inhibitory substances prior to PCR. The mixture was, then, vortexed and incubated at 90°C for 10 min. After centrifugation (8400 xg for 5 min), the supernatant was collected and stored at -20°C until used.

2.9.2 RNA EXTRACTION AND ANALYSIS

RNA was extracted from *Arabidopsis* tissues using the RNeasy Mini kit (Qiagen), from different stages of buds and open flowers, and other tissues to test gene expression levels in the plants. Plant material was collected in 2 ml collection tubes and

frozen immediately in liquid nitrogen. The material was then ground to a fine powder, without allowing the materials to thaw. Then, 450 μ l RLT (GITC-containing) lysis buffer was added and vortexed thoroughly. Samples were then incubated at 56°C for 3 min, centrifuged (14,000 xg for 3 min), and the supernatant transferred to a new tube and this step repeated. Then, 225 μ l of ethanol (100%) was added and mixed well by gentle pipetting. The mixture was transferred to an RNeasy mini spin column and centrifuged at full speed (10,000 xg) for 20 sec and the flow-through discarded. Then, 350 μ l of RW1 was added to remove contaminants and centrifuged for 20 sec at full speed (10,000 xg) and the flow-through discarded. Then, 80 μ l of DNase solution was added to the centre of each column, then columns were incubated at room temperature for 15-20 min. Each column was washed twice with 500 μ l RPE buffer. Then, columns were centrifuged at full speed for 2 min to dry the column and ensure that no ethanol was carried over during RNA elution. The RNeasy spin column was, then, placed in a fresh 1.5 ml collection tube. RNase-free water (50 μ l) was added to the spin column membrane and centrifuged at 10,000 xg for 1 min. RNA quantity was measured on a NanoDrop fluorospectrometer (ND-1000 Spectrophotometer, NanoDrop Technologies Inc., USA). RNA extracts were stored at -80°C until required.

2.9.3 cDNA SYNTHESIS FOR RT-PCR

SuperScript™ III Reverse Transcriptase (Invitrogen) was used for performing first-strand cDNA synthesis. Total RNA (2.5-5.0 μ g) was mixed with 1 μ l of oligo(dT)₂₀ (50 μ M) primer and 1 μ l (10 mM) dNTP mix and RNAase-free sterile water added to 13 μ l. The mixture was incubated at 65°C for 5 min and transferred

immediately onto ice for 1 min. The contents were collected by brief centrifugation, then, the following components were added: 4 μ l of 5x first strand buffer, 1 μ l (0.1 M) DTT, 1 μ l RNaseOUT™ (40 U/ μ l, Invitrogen) and 1 μ l SuperScript™ III Reverse Transcriptase (200 U/ μ l). Contents were mixed by gentle pipetting (to avoid RNA shearing) and incubated at 50°C for 60 min; the reaction was halted by incubation at 75°C for 10 min. Recovered cDNA was stored at -20°C until required.

2.9.4 PCR GENOTYPING OF SALK INSERTION LINES

PCR amplification from genomic DNA was carried out using the Extract-N-Amp plant PCR reaction mix in a volume of 10 μ l. Genomic DNA from T-DNA KO lines and wild type (ecotype Columbia) control plants were genotyped using forward and reverse gene-specific primers and SALK-LBb1 primer (Tables 2.1, 2.5 and 2.6).

Table 2.5 PCR reaction mixture for SALK line genotyping analysis

Reaction	Volume (μl)
Distilled water (dH ₂ O)	1.5
Sigma Taq mix (red)	5.0
LBb1 primer* (10 μ M)	0.5
Forward primer* (10 μ M)	0.5
Reverse Primer* (10 μ M)	0.5
Template DNA (100 ng/ μ l)	2.0
Total volume	10.0

*Primers (APPENDIX II)

Table 2.6 PCR cycling for genotyping analysis

Step	Temperature	Time	No. cycle
Initial Denaturation	94°C	4min	1
Denaturation	94°C	30sec	35
Annealing	58°C	30sec	
Extension	72°C	1 min	
Final Extension	72°C	5 min	1

2.9.5 DETECTION OF QUANTITY AND QUALITY OF cDNA

Quantity and quality of cDNA was tested by nanodrop analysis and RT-PCR amplification of house-keeping genes. The *ACTIN7* gene was selected as it is expressed constitutively across vegetative and floral tissues; RT-PCR was conducted with ACT7F and ACT7R primers (APPENDIX II) alongside RT-PCR using gene-specific primers (APPENDIX II) (Table 2.6 and 2.7). Comparisons between samples, by analysis of the band intensity for the house-keeping gene, was used to confirm that initial template inputs were equivalent between samples after cDNA synthesis (Section 2.9.3).

Table 2.7 RT-PCR Reaction mixture.

Reaction	Volume (μ l)
Distilled water (dH ₂ O)	7.75
Taq (5U/ μ l)	0.25
dNTPs (25 mM)	0.5
PCR Buffer (x10)	0.5
*Forward primer (10 μ M)	0.25
*Reverse primer (10 μ M)	0.25
Template cDNA (50-100 ng/ μ l)	0.5
Total volume	10.0

*Primers (APPENDIX II).

2.9.6 QUANTITATIVE (REAL-TIME) REVERSE TRANSCRIPTASE PCR (QRT-PCR)

QRT-PCR was used for quantitative gene expression analysis, since it is very sensitive and accurate and also allows analysis of genes of interest, which are expressed at a very low level. The fluorescent dye, SYBR® Green I (provided in the Maxima SYBR Green qPCR Master Mixes Fisher Scientific Inc., USA), was employed to detect and quantify gene expression. The dye exhibits minimal fluorescence in the unbound state; the

fluorescence is detectable when bound non-specifically to Double-stranded DNA. As PCR products accumulate during amplification, the fluorescence from SYBR® Green increases, making it possible for the detection of product accumulation in real-time. QRT-PCR was performed using the LightCycler®480 System (Roche, USA). LightCycler® 480 Software, Version 1.5 was used to operate the machine and analyse the data. All reagents were provided in the Maxima SYBR Green qPCR Master mix, Fisher Scientific Inc., USA, except primers and templates. The experimental reaction comprised 12.5 µl 2X master mix (provided in the kit), 0.2 µl + 2.0 µl dH₂O each forward and reverse primers (10 µM) (APPENDIX II), 4.5 µl SYBR Green qPCR Master Mix 2x, The experimental reaction comprised 12.5 µl 2X master mix, 0.25 µl upstream primer (10 µM), 0.25µl downstream primer (10 µM), 0.375 µl reference dye (2 µM), 0.5 µl cDNA template (Section 2.9.3) and nuclease-free water to adjust the final volume to 25 µl. All samples were run at least in duplicate.

cDNA sample was amplified with ACTIN7 primers and primers for genes of interest (APPENDIX II) in separate tubes, following the programme shown in (Table 2.8). *ACTIN* expression was used to normalize amplification between experimental samples. Relative expression levels were determined in comparison to *ACTIN7* expression by analysis. Following amplification, a Melt curve was generated in order to assess the specificity of the amplified PCR product. The DNA was first denatured by holding the temperature at 95°C for 5 seconds and then re-annealed by lowering the temperature to 65°C for 1 minute. The fluorescence signal was then monitored continuously as the temperature was

increased in small increments. As the DNA denatures ('melts'), the fluorescence decreases. All primers were designed to have equivalent melting temperatures.

Table 2.8 The standard program for running real time PCR on the LightCycle.

Cycles	Duration of cycle	Temperature
1	10 min	95°C
45	30 Sec	95°C
	30 Sec	58°C
	1 min	72°C
1	5 sec	95°C
	1 min	65°C

2.9.7 GATEWAY BP AND LR RECOMBINATION

Gateway™ cloning technology (Invitrogen, USA) was employed to prepare gene constructs. Amplicons generated by PCR were cloned into pENTR201-pENTER™/D-TOPO vectors (APPENDIX III) in a BP recombination reaction to create entry clones. The LR reaction was carried out to transfer the sequence of interest (entry clones) to the destination vectors (Table 2.9, APPENDIX III). The LR reaction involved a recombination reaction between *attI* and *attR* sites. To carry out the LR reaction, 50-150 ng of entry clone plasmid DNA, 100-150 ng of plasmid DNA of the appropriate destination vector, 1 µl of 5x LR Clonase plus buffer (1.5 µl TE pH 8.0, 1 µl of LR Clonase enzyme directly from the freezer) were added into a 1.5 ml tube and then mixed by pipetting. The mixture was incubated at 25°C overnight. Then, 0.5 µl proteinase K was added to the reaction mix and incubated at 37°C for 10 min to terminate the reaction. To perform heat shock transformation, 50 µl of Library Efficiency® chemically

competent *E. coli* strain DH5a cells (Invitrogen™, cat. No. 18263-012, Table 2.10) were taken directly from -80°C and added to the LR reaction. The reaction mixture was left on ice for 30 min, then, heat shocked in a water bath at 42°C for 1.5 min, then, transferred to ice immediately for 3 min. A total of 250 µl of S.O.C (APPENDIX II) medium was added to the reaction mixture and incubated on a shaking incubator at 37°C for 2 h. The bacterial culture was then plated onto LB plates containing 50µg/ml spectinomycin as the selective agent (Table 2.4). The plates were incubated at 37°C overnight and the clones analysed by PCR using specific primers for the genes of interest (APPENDIX II).

Table 2.9 Plasmid vectors used for Gateway cloning system.

Plasmid name	Description	Features	Source
pDONR™201	Donor vector	kanamycin resistance recombination cloning	Invitrogen
pGWB433	Destination vector	attR1-attR2-GUS- no pro, C-GUSs, spectinomycin resistance	Dr. Ranjan Swarup
pGWB402Ω	Destination vector	P2x35sΩ-attR1-attR2-Tnos,spectinomycin resistance	Dr. Ranjan Swarup
pK7GW1GW2(II)	Destination vector	attR1-attR2- hpRNA expression (35S pro) spectinomycin resistant gene.	
pUB-GFP	Destination vector	Contains Ubiquitin C promoter spectinomycin resistance	
pUB-RFP	Destination vector	Contains Ubiquitin N promoter spectinomycin resistance	

Table 2.10 Bacterial genotypes and growth media.

Strain	Genotype	Purpose	Growth medium
<i>Escherichia coli</i> (DH5a)	F ⁻ Φ 80/ <i>lacZ</i> Δ M15 Δ (<i>lacZYA-argF</i>) U169 <i>recA1 endA1</i> <i>hsdR17</i> (r _k ⁻ , m _k ⁺) <i>phoA supE44 thi-1</i> <i>gyrA96 relA1</i> λ ⁻	Amplification/ Cloning	(LB) liquid/agar Laural Broth (APPENDIX I)
<i>Escherichia coli</i> (BL21 A1)	F ⁻ <i>ompT hsdSB</i> (rB ⁻ , mB ⁻) <i>gal dcm</i> <i>araB::T7RNAP-tetA</i>	Amplification/ Cloning	(LB) liquid/agar Laural Broth (APPENDIX I)
<i>Agrobacterium tumefaciens</i> MP90	C58 background, pMP90(pTiBo542 Δ T- DNA) plasmid, rifampicin R, kanamycin R, Nopaline	Floral dip transformation	(LB) liquid/agar Laural Broth (APPENDIX I)
<i>Agrobacterium tumefaciens</i> (GV3101)	C58 background, free plasmid, rifampicin R, nopaline	Transient assays in tobacco and <i>Arabidopsis</i>	(LB) liquid/agar Laural Broth (APPENDIX I)

2.9.8 RESTRICTION ENZYME DIGESTION

Restriction enzyme digestion was carried out in 50 μ l reactions by adding 6 μ l of the required enzyme, 5 μ l of 10x BSA, 5 μ l of 10x specific buffer and 2.1 μ g of DNA. Incubation was carried out following the instruction supplied by the manufacturer for each enzyme (New England BioLabs, UK).

2.9.9 COLONY PCR ANALYSIS OF CLONES

Colony PCR was carried out to confirm cloning using a vector specific primer (typically the CaMV35S forward primer and a gene specific primer as a reverse primer (APPENDIX II). Colonies were also used to inoculate LB medium (APPENDIX I) containing the appropriate selection antibiotic (Table 2.4) then grown at 37°C overnight for plasmid miniprep analysis (Section 2.9.10).

2.9.10 PLASMID DNA PURIFICATION

Plasmids were extracted using the Qiagen QIAprep Spin Miniprep spin kit. For the extraction, 5 ml of liquid LB medium (APPENDIX I) were inoculated with bacteria containing the plasmid of interest and incubated overnight. The culture was centrifuged at 500 xg for 10 min. The pelleted bacterial cells were re-suspended in 250 μ l of buffer P1 and transferred to microfuge tubes. Then, 250 μ l of buffer P2 was added and gently mixed by inverting the tube 4-6 times for less than 5 min. Then, 350 μ l of buffer N3 was added and inverted gently 4-6 times. The mixture was then centrifuged for 10 min at 10,000 xg . A QIAprep spin column was placed in a 2 ml collection tube and the supernatant was applied to the QIAprep column by pipetting. The column was centrifuged for 30-60 sec. The flow-through was discarded and the QIA prep spin column was washed by adding 0.5 ml of PB buffer and centrifugation for 30-60 sec. The flow-through was discarded and QIAprep spin column washed by adding 0.75 ml of PE buffer and centrifuged for 30-60 sec. The flow-through was discarded and the QIAprep spin column was centrifuged for an additional 1 min to 1.5 ml microfuge tube and 30 μ l of water sterile for 1 min, and centrifuged for 1 min at 10,000 xg (or 13,000 rpm). The concentration of DNA from the plasmid extraction was measured using a NanoDrop ND-1000 Spectrophotometer (NanoDrop Technologies, Rockland, USA) and the plasmid DNA stored at -20°C until required.

2.9.11 SEQUENCING OF CONSTRUCTS

All constructs were validated by sequencing (APPENDIX III). Sequencing reactions were performed using 100-200 ng template DNA and BigDye Terminator v1.1 Cycle Sequencing kit (Applied Biosynthesis, USA). Samples were sent to the Genomics facility, (Queen's Medical Centre, University of Nottingham, UK) and analysed using CLUSTAL multiple sequence alignment by Kalign (2.0) (<http://www.ebi.ac.uk/Tools/msa/kalign/>).

2.9.12 ARABIDOPSIS TRANSFORMATION

Agrobacterium tumefaciens competent cells (C58 strain) were transformed with plasmid DNA by electroporation (2.2kV; MicroPulser, BioRad) and screened on solid LB medium with selective antibiotics (Table 2.4) for the plasmid used (Table 2.10). Positive colonies were PCR-screened and propagated firstly in 5 ml, then, in 100-200 ml LB medium with antibiotic at 28°C for 3-4 days, or until an OD₆₀₀ of 0.7-1.0 was reached (Spectrophotometer from Cecil, UK). The cells were pelleted by centrifugation at 3500 xg for 10 min and then re-suspended in 5% (w/v) fresh sucrose (Fisher scientific, UK) aqueous solution to OD₆₀₀=0.8. Silwet L-77 (0.02% (v/v) Michigan State University, USA) was added to the suspension just prior to dipping. Plants with numerous buds and few siliques were used for floral dipping (Clough and Bent, 1998). After dipping, plants were placed in a tray on the side and covered with a plastic bag for three days to maintain high humidity. After three days, the bags were opened and plants were grown until the siliques were brown and dry. Seeds were subsequently screened on MS medium (APPENDIX I) with selective antibiotics.

2.9.13 AGAROSE GEL ELECTROPHORESIS

PCR products were checked by agarose gel (1.5%-4% w/v) electrophoresis (100v, 1 h); gels with different percentages of agarose were used depending on the expected product size, and stained with 0.15 µg/ml ethidium bromide in 0.5 x TBE buffer (APPENDIX I). 4µl of Hyper Ladder I or II was run alongside as a size marker. After the electrophoresis, the gels were visualized under UV light and photographed using a digital imaging system.

2.9.14 DNA PURIFICATION FROM THE AGAROSE GEL

For DNA purification from the agarose gel, DNA products were size separated by electrophoresis (Section 2.9.13) and cut from the gel, whilst minimizing UV exposure. The gel pieces were loaded into dialysis tubing (Sigma D9777) that had been previously prepared by boiling and stored in 0.5x TBE (APPENDIX I) buffer at 4°C. The tube was washed with 0.5x TBE buffer both inside and outside and the pieces of gel were introduced and bubbles were removed and the tube clipped. The dialysis tube was then placed into an electrophoresis tank (100 volts for 1.5 h) in 0.5x TBE orientated so that the membrane was in line with the electrodes and the run was reversed for 30 sec. The dialysis tubing contains the DNA dissolved in 0.5x TBE buffer was mixed well by pipette and washed from outside with 0.5x TBE and placed into an Eppendorf tube. An equal volume of butanol (100% v/v) was added and mixed well and centrifuging for 3 min (12,000 xg). Two layers could be seen following centrifugation, the top layer was removed and discarded, additional butanol (100% v/v) was added to the samples and

shaken briefly, then, the supernatant was discarded. This step was repeated until 60µl of the DNA solution remained, it was then transferred into a new tube. Isolated DNA was, then, precipitated with 0.1x (3 M) sodium acetate and 2.5 x 100% ethanol and stored at -20°C for overnight. Samples were centrifuged at 12,000 *xg* for 15 min and washed in 200 µl of 70% (v/v) ethanol, and stored at -20°C for 30 min, centrifuged again (15 min, 12,000 *xg*) and dried for 10 min. Samples were re-suspended in distilled water depending on the expected concentration.

2.9.15 PRIMER DESIGN

Primer3 software (<http://frodo.wi.mit.edu/primer3>) was used for primer design. Each pair of primers was tested using MacVector software and BLAST analysis to confirm specificity. Primers were synthesised by MWG Eurofins (Ebersberg, Germany).

CHAPTER 3: CONFIRMATION OF THE PROTEIN-PROTEIN INTERACTION WITH MYB26

3.1 INTRODUCTION

Transcription factors have been frequently shown to work as complexes with other proteins; this is particularly true for MYB and basic helix-loop-helix (bHLH) factors that act as repressors and activators by forming homo- or heterodimers to regulate specific cellular processes (Feller *et al.*, 2011; Pireyre and Burow, 2015). There are several techniques that can be used to investigate protein-protein interactions. These techniques can involve *in planta* expression and analysis of interactions, or expression in ectopic systems (Table 3.1).

Studying the genetic and physical interactions between two molecules is important for understanding cell function and survival. Frequently, similar interactions occur for classes of proteins indicating a conserved mode of function. For example, common cooperative actions are shown for MYBs and bHLH (basic helix-loop-helix) proteins, particularly, in the case of the phenylpropanoid and flavonoid biosynthetic pathways (Du *et al.*, 2009). Two MYB factors AtMYB5 and Transparent Testa 2 (TT2) redundantly interact with Transparent Testa Glabra 1 (TTG1) and the basic helix-loop-helix (bHLH) Transparent Testa 8 (TT8) to control the expression of a core enzyme in proanthocyanidin biosynthesis in the *Arabidopsis* seed coat (Baudry *et al.*, 2004). This enzyme is thought to be conserved across the plant kingdom, as the regulation of phenylpropanoid biosynthesis by MYBs associated with bHLH proteins is shown not only in *Arabidopsis*, but also in *Fragaria* (strawberry) (Aharoni *et al.*,

2001), *Gentiana triflora* (gentian) (Nakatsuka *et al.*, 2008), and *Zea mays* (Goff *et al.*, 1992). Protein-protein interactions appear highly tissue or cell-specific, but in some pathways, the physical interaction between MYBs and bHLHs has not been experimentally confirmed (Nakatsuka *et al.*, 2008; Penfield *et al.*, 2001; Zhang *et al.*, 2003).

Table 3.1 Different approaches commonly used to confirm protein-protein interactions.

Approach	Description
Pull downs	<i>E.coli</i> co-expression of the proteins, native protein isolation then purification using an antibody to one protein and then a western using an antibody to the other protein to confirm that other protein is present and has been co-purified (http://www.promega.com/tbs/tm249.html)
Bimolecular fluorescence complementation (BiFC)	Two fusion proteins are generated with truncated fluorescent proteins. Fluorescence should be observed if the proteins interact resulting in the reconstruction of the split protein. This can be analysed by transient expression in plant cells (onion epidermis /protoplasts or <i>N benthamiana</i> leaves (Bhat <i>et al.</i> , 2006)
Förster Resonance Energy Transfer (FRET)	Different fluorochromes can be attached to the proteins. These can be co-expressed in plant material. One fluorescent tag is attached and the other tested for activation by transfer of energy (Bhat <i>et al.</i> , 2006)

3.1.1 DETECTION OF PROTEIN INTERACTION USING YEAST TWO-HYBRID SYSTEM

A powerful tool for investigating protein-protein interactions is the yeast two-hybrid (Y2H) system (Figure 3.1) (Lalonde *et al.*, 2008; Suter *et al.*, 2008). This functions by splitting the yeast GAL4 transcriptional regulator into two domains, the DNA-binding domain (DB; Figure 3.1, blue zigzag line) and the activation domain (AD; Figure 3.1, green arrow), which are independently fused to two proteins that may interact (the bait and prey proteins). Interactions between the two proteins bring the two domains together and result in transcriptional activation

of the reporter genes, usually *Ade2*, *His3* or *LacZ*. Protein-protein interactions can be found practically in every cellular event and serve to determine gene regulation and also cellular activities. Given that MYB factors frequently function in duplexes, or larger complexes, it is possible that MYB26 may act by interacting with other proteins. Therefore, a yeast 2-hybrid (Y2H) screen using an *Arabidopsis* stamen library was previously conducted to identify potential interacting proteins.

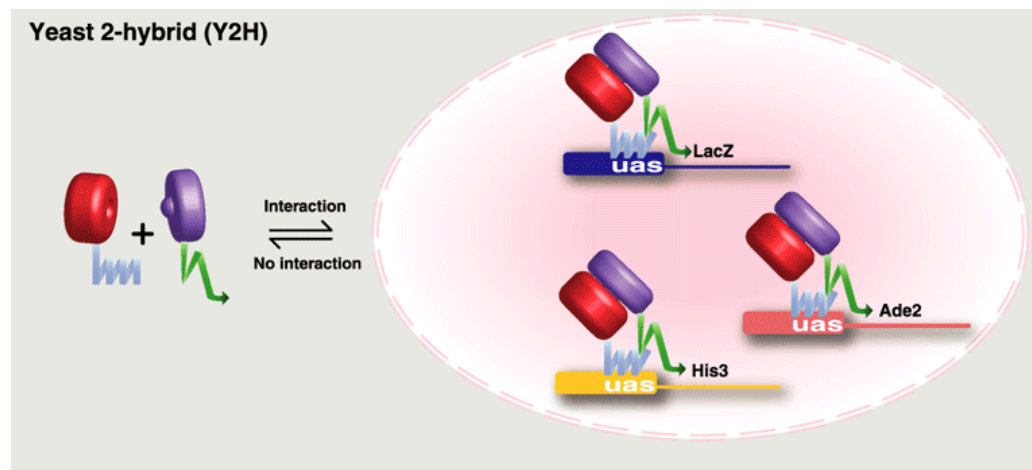


Figure 3.1 The yeast two-hybrid system. Taken from Lalonde *et al.* (2008).

The GAL4 transcription factor is split into the DNA-binding domain (DBD, blue zigzag line) and the activation domain (AD, green arrow), which are fused to the bait and prey proteins, respectively. Interactions between the two proteins lead to activation of transcription of the reporter gene, commonly *Ade2*, *His3* and *LacZ* (Lalonde *et al.*, 2008). UAS=upstream activation sequence.

Five putative MYB26 interactive proteins (Y2H560, Y2H128, Y2H320, Y2H620 and Y2H970) were previously identified from screening a stamen Y2H library, using the full length MYB26 protein as bait (Yang and Wilson, unpublished data). Y2H560 and Y2H970 are members of the zinc finger (C3HC4-type ring finger) family (Table 3.2). There are no reports of zinc finger associations with MYBs, nevertheless, this may be a genuine

interaction that is involved in the turnover of the MYB26 protein, rather than in complex formation for activation/repression of target genes. Y2H620 is a member of the basic helix-loop-helix (bHLH) family (Table 3.2) and there are multiple reports of association between bHLH protein and MYBs (Du *et al.*, 2009). Y2H320 is a member of the basic Leucine Zipper transcription factor (bZIP) family (Table 3.2). This family regulates diverse biological processes including pathogen defense, stress and light signaling, and flower development (Jakoby *et al.*, 2002). The Y2H320 and TGA factors show sequence similarity to the bZIP family (Jakoby *et al.*, 2002). TGA transcription factors were shown to interact with NONEXPRESSOR OF PATHOGENESIS-RELATED GENES (*NPR1*) (Fobert and Després 2005; Mueller *et al.*, 2008) and to the floral glutaredoxins ROXY1 and ROXY2 (Murmu *et al.*, 2010). bZIP proteins are thought to be recruited early in plant evolution, compared to the R2R3-MYB family proteins and, therefore, are involved in the regulation of diverse biological processes, including light and stress signaling, seed maturation and flower development (Jakoby *et al.*, 2002).

Many transcription factors and secondary wall synthetic genes of *Arabidopsis*, that are associated with anther secondary thickening, have been identified (Brown *et al.*, 2005; Ye *et al.*, 2006; Zhong *et al.*, 2008). The interactions of the putative MYB26 interactor proteins, e.g., Y2H320, Y2H970 and Y2H620, that were identified from the previous yeast 2-hybrid (Y2H) screen, were, therefore, tested using Förster Resonance Energy Transfer (FRET).

Table 3.2 Description of the genes identified by yeast 2-hybrid screening of a stamen library with MYB26.

Gene ID	Y2H code	Gene description*
<i>At5g25560</i>	Y2H560	Family protein Zinc finger (C3C4-type RING finger).
<i>At1g08320</i>	Y2H320	bZIP family transcription factor.
<i>At3g62970</i>	Y2H970	Protein binding/Zinc ion binding, similar to zinc finger (C3HC4-type RING finger) family protein.
<i>At3g47620</i>	Y2H620	bHLH-type transcription factors, encodes a transcription factor that regulates seed germination which shows elevated expression level just prior to germination.
<i>At1g47128</i>	Y2H128	Cysteine proteinase precursor-like protein/dehydration stress-responsive gene.

*Description taken from TAIR (<http://www.arabidopsis.org>)

3.1.2 ANALYSIS OF PROTEIN INTERACTION USING FÖRSTER RESONANCE ENERGY TRANSFER (FRET) ANALYSIS

Although yeast 2-hybrid analysis gives a good indication of possible protein-protein interactions, it has been shown to be prone to identifying false positives, thus, further independent methods to confirm protein-protein interactions are required. A number of different techniques can be used to confirm such interactions including Förster resonance energy transfer (FRET) (Figure 3.2). The assay has previously been used to confirm interactions between a donor fluorescent (e.g., GFP) molecule and an acceptor neighbouring chromophore (e.g., RFP) (Immink *et al.*, 2002).

FRET analysis of MYB26 and the putative interacting proteins was conducted in a transient system by co-transformation of tobacco leaves using fusion constructs of MYB26-GFP and Y2H-

RFP-protein, to express the different proteins. Co-transformation results in cells containing the MYB26 protein (e.g., bait) fused to GFP and the different Y2H proteins (e.g., prey) individually fused to RFP. If the bait-prey proteins interact, excitation of GFP will induce FRET between the two chromophores, thus, emission of RFP (Bhat *et al.*, 2006; Immink *et al.*, 2002).

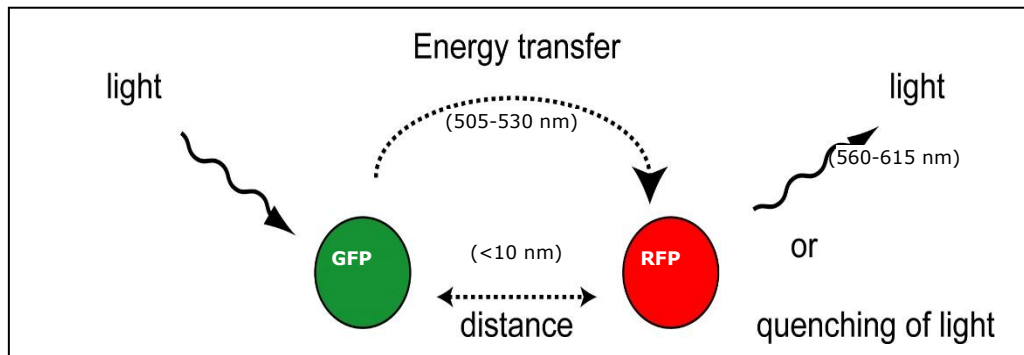


Figure 3.2 Förster resonance energy transfer (FRET). Resonance energy transfer will occur between the donor fluorophore (GFP) and the acceptor fluorophore (RFP) (http://www.molecularbeacons.org/toto/Marras_energy_transfer.html).

3.2 MATERIALS AND METHODS

3.2.1 CLONING AND TRANSIENT EXPRESSION OF MYB26 AND EACH OF Y2H320, Y2H620 or Y2H970 GENES IN TOBACCO

Using Gateway cloning technology (Section 2.9.7), all genes were cloned into entry vector pENTR201 (Invitrogen) and then via the LR reaction into destination vector pUBC-GFP for *MYB26* gene (APPENDIX III) to create the fusion protein MYB26-GFP. The other three genes, e.g., *Y2H620*, *Y2H970* and *Y2H320*, were cloned into the destination pUBN-RFP by the LR reaction to create RFP-Y2H620, RFP-Y2H970 and RFP-Y2H320 fusion

proteins. The LR reaction was transformed into *E.coli* DH5a (Section 2.9.7) and selected overnight on spectinomycin (50 µg/ml) (Section 2.8.1). Positive clones were detected by PCR using appropriate vector and gene-specific primers (Table 3.3) (APPENDIX II). Plasmid DNA was extracted from the expression clones (Section 2.9.10), then transformed into competent *Agrobacterium* cells (GV3101) (Section 2.9.12) for transient expression. *Nicotiana benthamiana* seeds were grown at 22°C ± 2°C in pots (Section 2.2). Transient assays were conducted in *N. benthamiana* (University of Nottingham) leaves from plants that had been grown for 5-6 weeks (Kapila *et al.*, 1997).

Table 3.3 Primer names and sequences along with amplicon size (bp) and annealing temperatures (T_m) used during PCR to confirm occurrence of genetic transformation in a number of transiently co-transformed tobacco plants with pUBC-MYB26-GFP and pUBN-RFP-Y2H constructs.

Contract name	Primer name	Primer sequence (5' - 3')	Size (bp)	T _m (°C)
pUBC-MYB26-GFP	MYB26-F	ATGGGTCATCACTCATGCTG	1240	57
	GFP_PGWB5_R	AAGTCGTGCTGCTTCATGTG		57
pUBN-RFP-Y2H320	RFP-F	ATGAGGCTGAAGCTGAAGGA	1646	60
	At1g08320_R	CATTTGTTGCATTCCGTCAA		60
pUBN-RFP-Y2H620	RFP-F	ATGAGGCTGAAGCTGAAGGA	1670	60
	At3g47620_R	AATGGAAGGAAACGTCCAAA		59
pUBN-RFP-Y2H970	RFP-F	ATGAGGCTGAAGCTGAAGGA	1064	60
	At3g62970_R	GGATCTTGTGGCGTTGAGAT		60

3.2.2 CO-LOCALISATION OF FUSION PROTEINS AND FRET

The abaxial side of 6-week-old leaves of *N. benthamiana* plants (Section 2.2) were infiltrated (co-transformed) with the *Agrobacterium* (GV3101) strain (Table 2.10) carrying pUBC-MYB26-GFP and independently each of pUBN-RFP-Y2H320, pUBN-RFP-Y2H620 or pUBN-RFP-Y2H970 construct. The transformed *Agrobacterium* were checked for the correct expression constructs (APPENDIX III) by PCR using gene- and

vector-specific primer pairs. Expression of *GFP* and *RFP* genes and subcellular localisation of the two encoded proteins were confirmed by sequential scanning of infiltrated *N. benthamiana* leaves using Sp2 confocal microscope (Leica). FRET analysis was conducted following the methods of Bhat *et al.* (2006) and Zhong *et al.* (2008) after co-transformation of MYB26-GFP and each of the RFP-Y2H constructs into *N. benthamiana* cells. The samples were initially observed by confocal microscopy with the donor channel set to maximum (99%) for the 458 nm laser. The acceptor channel, for the 514 nm laser, and the PMT voltage, for RFP, were also adjusted to below detector saturation. The acceptor and donor channel settings were saved as defaults and all other settings were examined under exactly the same conditions.

3.3 RESULTS

3.3.1 TRANSIENT TRANSFORMATION OF *MYB26* AND *Y2H* GENE CONSTRUCTS IN *N. BENTHAMIANA*

The entry clone of *MYB26* and the *Y2H* clones pDONR201 were transferred by LR cloning (Section 2.9.7) into the destination vectors containing the *UBQ10* promoter followed by the Gateway cassette, thereby creating pUBC-Dest (with pUBC-GFP fluorescence tag, mGFP) and pUBN-RFP (with fluorescence tag mRFP) (Grefen *et al.*, 2010) vectors (Table 2.9). After antibiotic screening, positive colonies in *E. coli* were analysed by PCR using primer GFP_PGWB5_R, for pUBC-MYB26-GFP, and RFP-F, for pUBN-RFP-Y2H, with gene-specific forward primers of *MYB26* and reverse primers of each of the three *Y2H* genes, respectively

(Table 3.3) (APPENDIX II) (Figure 3.3). pUBC-MYB26-GFP and pUBN-RFP-Y2H970, pUBN-RFP-Y2H320 and pUBN-RFP-Y2H620 plasmid DNAs were purified (Section 2.9.10) and transformed into *Agrobacterium* strain GV3101. *Agrobacterium* carrying expression constructs were checked by PCR using a vector- and a gene-specific primers pair (Figure 3.4). The plasmid DNA constructs were also sequenced to confirm that the gene of interest harbored the appropriate N-terminal (RFP) or C-terminal (GFP) tag (APPENDIX III). Positive clones were transformed into *N. benthamiana* plants (Section 2.2) by infiltration of the abaxial side of the leaves (Figure 3.5).

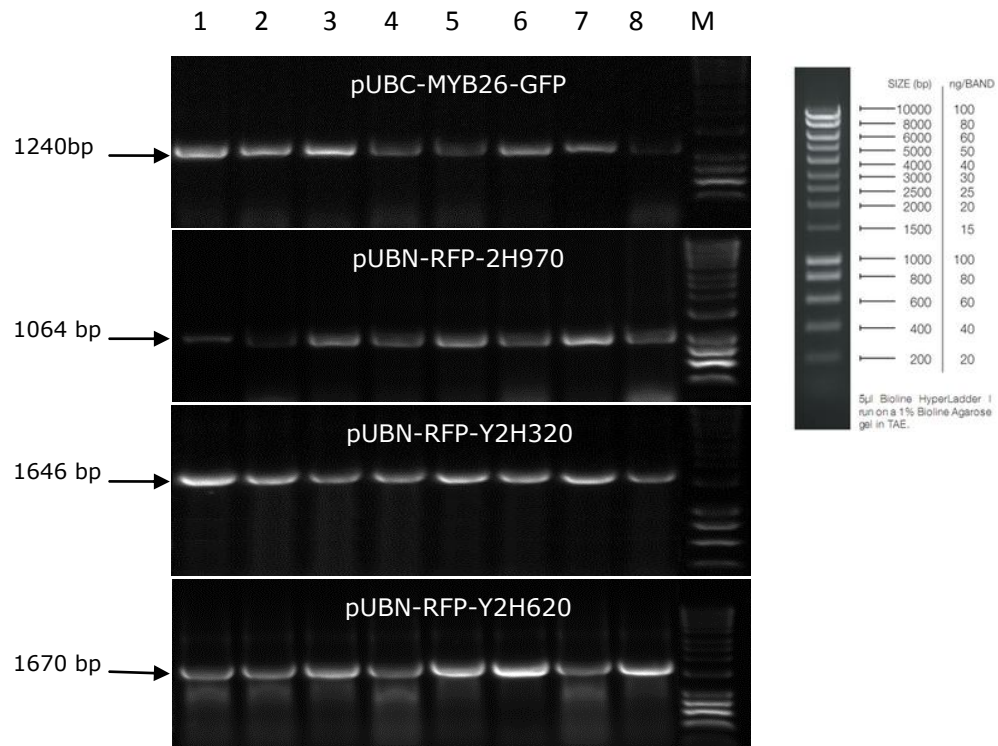


Figure 3.3 PCR screening of putative *E. coli* DH5α transformants after LR cloning of *MYB26* gene into the pUBC-GFP destination vector (e.g., pUBC-MYB26-GFP) and genes of the three putative *MYB26* interacting proteins into pUBN-RFP destination vector (e.g., pUBN-RFP-Y2H). PCR was done using appropriate vector primer and gene-specific primers of *MYB26*, *At3g62970*, *At1g08320* or *At3g47620* gene (Table 3.3 and APPENDIX II). DNA was separated on a 0.8% (w/v) agarose gel. Lanes 1-8=individual putative colonies. Hyper ladder I (Bio-line.com) was used as DNA standard (M).

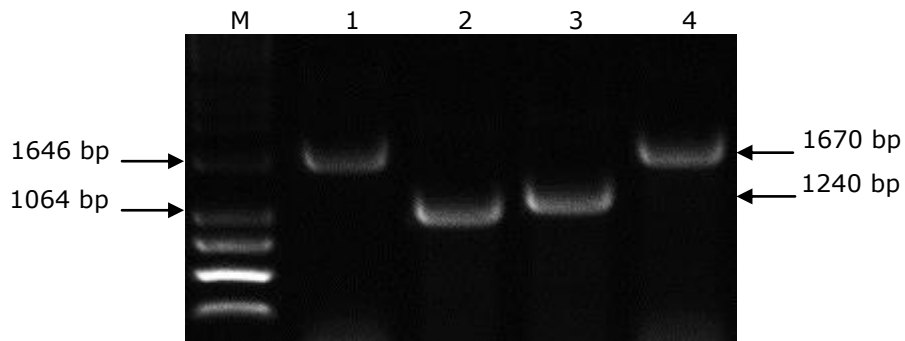


Figure 3.4 PCR of putative positive *Agrobacterium* colonies carrying plasmid constructs pUBN-RFP-Y2H320 (1), pUBN-RFP-Y2H970 (2), pUBC-MYB26-GFP (3) and pUBN-RFP-Y2H620 (4) in GV3101 *Agrobacterium* cells. PCR was done using appropriate vector primers of GFP_PGWB5_R (for pUBC-MYB26-GFP) and RFP-F (for pUBN-RFP-Y2H) with gene-specific forward primer of MYB26 gene and reverse primers of *At3g62970*, *At1g08320* or *At3g47620* gene (Table 3.3 and APPENDIX II). DNA was separated on a 0.8% (w/v) agarose gel with the Hyper ladder I (Bio-line.com) used as DNA standard (M).

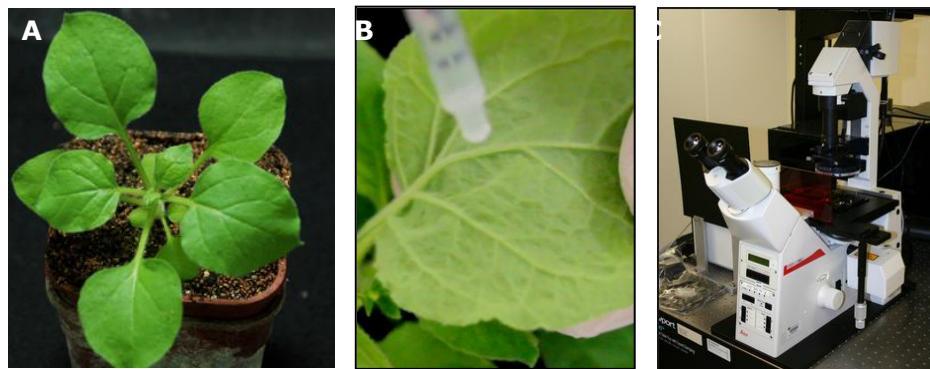


Figure 3.5 Infiltration transformation of *N. benthamiana* leaves. (A) leaf-stage after 5-6 weeks growth, (B) abaxial side of the leaf was used for infiltrated with pUBC-MYB26-GFP and pUBN-RFP-Y2H gene constructs, (C) Leica SP2 confocal microscope. Leaves were observed by confocal microscopy (Leica SP2) 3 days after infiltration to confirm gene expression localization and to be used for FRET analysis.

3.3.2 CO-LOCALISATION OF MYB26 AND THE Y2H PROTEINS

An aliquot of each RFP-Y2H construct and MYB26-GFP construct (Section 3.2.1) from an overnight culture was used to separately

inoculate (1:10 dilution) fresh LB medium and this was grown until an OD₆₀₀ of 0.2-0.3 was obtained. The RFP-Y2H and MYB26-GFP constructs were, then, infiltrated on their own and also in combination with pUBC-MYB26-GFP into tobacco leaves, and subsequently imaged by confocal microscopy using a Leica SP2 microscope to confirm the co-localization of the two proteins. Tobacco cell leaves were incubated in a glasshouse for 3 days prior to imaging. Each MYB26-GFP, RFP-Y2H320, RFP-Y2H620 and RFP-Y2H970 fluorescence was observed separately in the nucleus (Figure 3.6). Nuclear localisation was also observed for RFP-Y2H320, RFP-Y2H620 and RFP-Y2H970 fusion proteins, which co-expressed with MYB26-GFP fusion protein in tobacco leaves (Figures 3.7-3.9). MYB26-GFP fusion protein, therefore, could be seen to co-localise with each of RFP-Y2H320, RFP-Y2H620 or RFP-Y2H970 fusion protein in the nucleus.

Y2H320 is a bZIP transcription factor, whose transient expression in tobacco leaf cells demonstrated its co-localisation with MYB26 in the nucleus (Figure 3.7). FRET analysis was used to determine whether Y2H320, Y2H620 or Y2H970 proteins, on one hand, and MYB26 protein, on the other hand, interact in living plant cells by the detection of fusion tags. Table 3.4 summarizes the data of the constructs used for the subcellular localisation of the proteins by transient expression of the two fusion tags fused to different Y2H proteins.

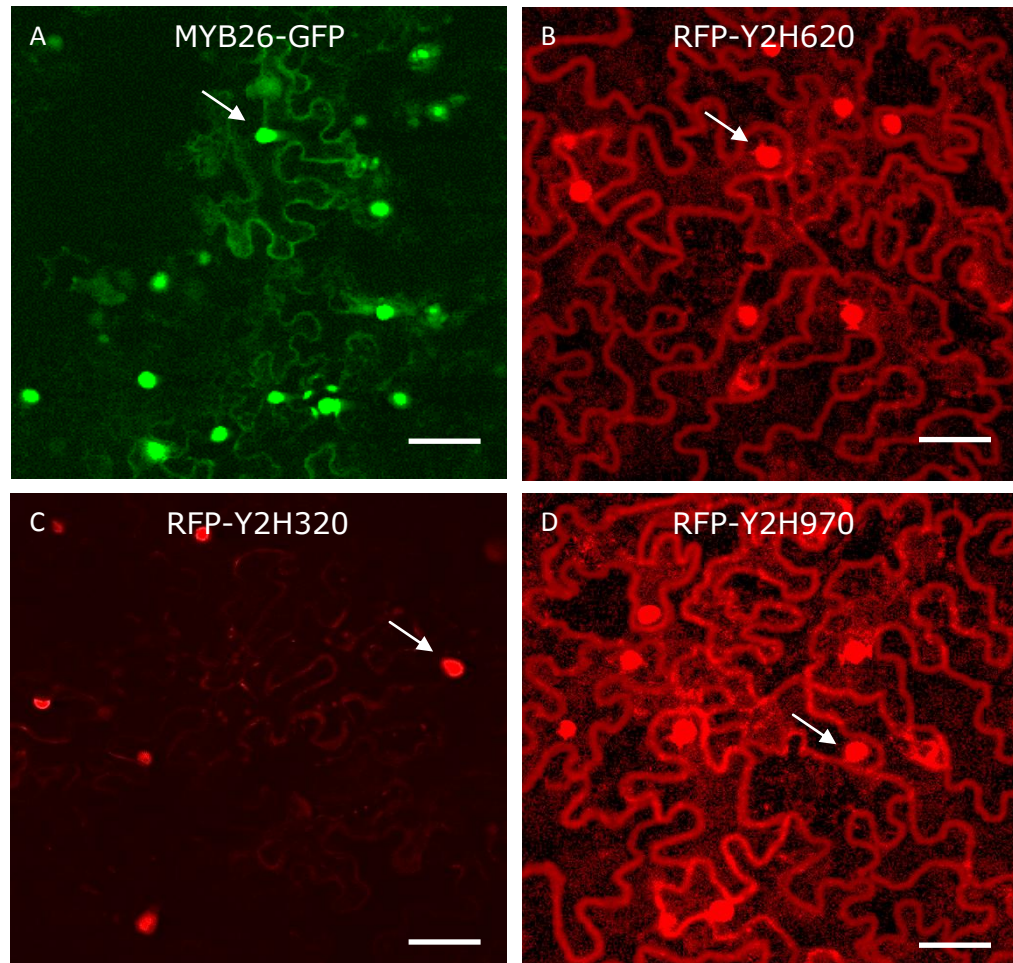


Figure 3.6 Nuclear localised expression of MYB26 and putative MYB26-interacting fusion proteins with fluorescent tags (GFP and RFP) after infiltration and transient expression of fusion constructs in *N. benthamiana* leaf tissues. Images were taken using sequential scan confocal microscopy. (A) Nuclear-localised MYB26-GFP fusion protein (B) Nuclear-localised RFP-Y2H620 fusion protein (C) Nuclear-localised RFP-Y2H320 fusion protein, and (D) Nuclear-localised RFP-Y2H970 fusion protein. Arrows indicate nuclear expression. Green fluorescent protein imaged with excitation at 488 nm and emission collected at 505-530 nm. Red fluorescent protein imaged with excitation at 543 nm and emission collected at 560-615 nm. Scale bar = 50.46 μm .

FRET measurements were performed on tobacco cells co-expressing MYB26-GFP fusion protein and each of the RFP-Y2H fusion proteins. FRET between MYB26-GFP and each of the three RFP-Y2H fusion proteins was measured in a number of 11-13 independent transformation events (Table 3.5) with each of the three *Y2H* genes using the following formula:

$$R = R_0 \sqrt[6]{\frac{1 - E}{E}}$$

The distance “R” indicates the efficacy of using FRET as a tool for probing molecular interactions and was calculated as provided that the value of R_0 is constant (5.1 nm). The efficiency “E” was calculated by the FRET application wizard according to manufacturer’s instruction (Leica) application software (Table 3.5).

Table 3.4 Constructs and localization of MYB26 and the three putative Y2H interacting proteins in transient expression experiments through the detection of fusion tags (e.g., mGFP and mRFP).

Construct	Subcellular localisation	Fusion tag
pUBC-MYB26-GFP	Nucleus	mGFP
pUBN-RFP-Y2H320	Nucleus	mRFP
pUBN-RFP-Y2H620	Nucleus	mRFP
pUBN-RFP-Y2H970	Nucleus	mRFP

Table 3.5 Individual measurements for the region of interest (ROI) of FRET efficiencies (E) between MYB26-GFP and each of the three RFP-Y2H fusion proteins.

Y2H	ROI													Mean E	R (nm)
	1	2	3	4	5	6	7	8	9	10	11	12	13		
320	0.31	0.31	0.3	0.32	0.32	0.31	0.33	0.31	0.31	0.32	0.31	-	-	0.3136364	5.81
620	0.01	0.01	0.01	0.01	0.01	0.01	0.01	0.01	0.01	0.01	0.01	0.01	0.01	0.01	10.97
970	0.02	0.03	0.04	0.03	0.04	0.04	0.02	0.03	0.02	0.04	0.03	0.04	-	0.031667	9.05

R=distance between the two fusion tags (e.g., mGFP and mRFP).

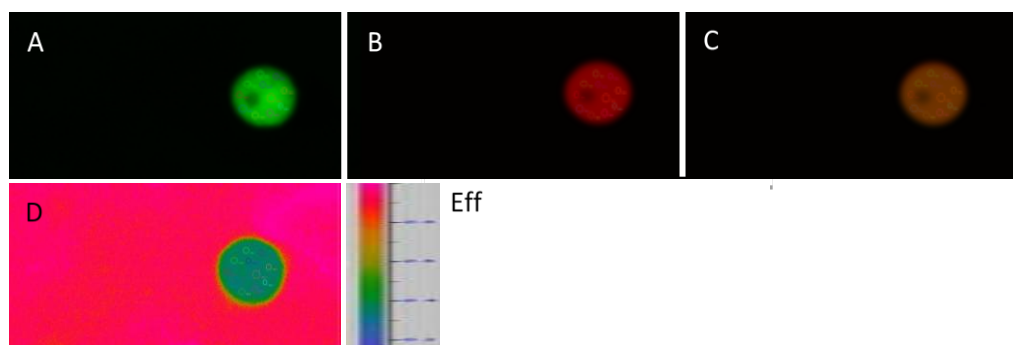


Figure 3.7 FRET analysis between MYB26-GFP and RFP-Y2H320 fusion proteins. (A) Donor MYB26-GFP emission under donor (GFP) excitation. (B) Acceptor RFP-Y2H320 emission under donor (GFP) excitation. (C) MYB26-GFP and RFP-Y2H320 merge. (D) FRET calculated by the FRET application wizard according to manufacturer's instruction (Leica); Eff= scale bar indicating FRET efficiency.

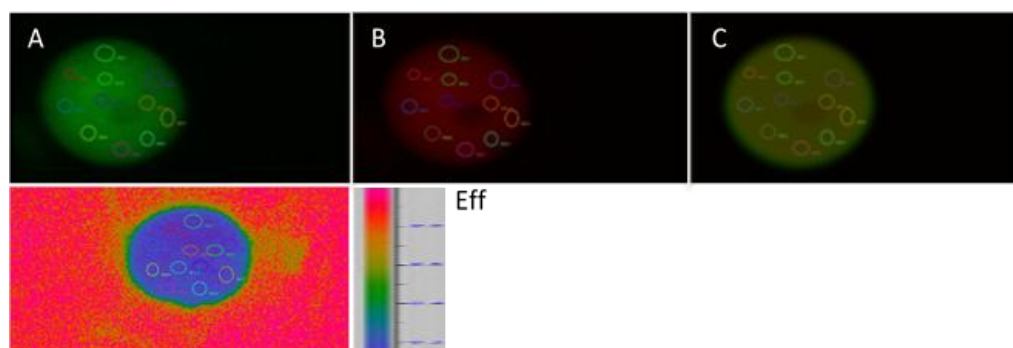


Figure 3.8 FRET analysis between MYB26-GFP and Y2H620-RFP fusion proteins. (A) Donor MYB26-GFP emission under donor (GFP) excitation. (B) Acceptor RFP-Y2H620 emission under donor (GFP) excitation. (C) MYB26-GFP and RFP-Y2H620 merge. (D) FRET calculated by the FRET application wizard according to manufacturer's instruction (Leica); Eff= scale bar indicating FRET efficiency.

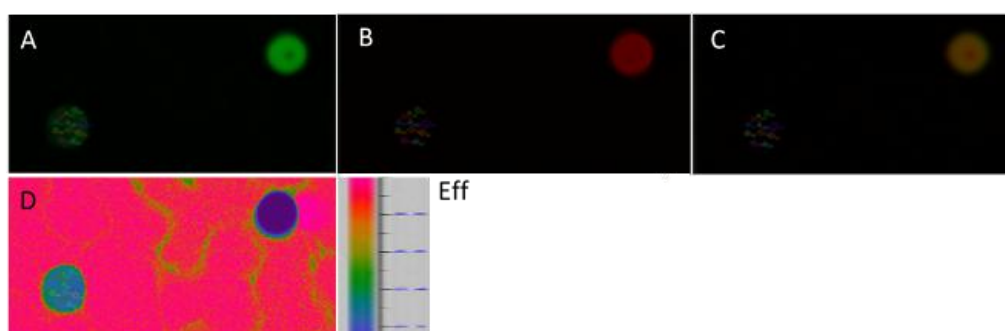


Figure 3.9 FRET between MYB26-GFP and RFP-Y2H970 fusion proteins. (A) Donor MYB26-GFP emission under donor (GFP) excitation. (B) Acceptor RFP-Y2H970 emission under donor (GFP) excitation. (C) MYB26-GFP and RFP-Y2H970 merge. (D) FRET calculated by the FRET application wizard according to manufacturer's instruction (Leica); Eff= scale bar indicating FRET efficiency.

In brief, GFP was taken as the donor and RFP as the acceptor, the FRET efficiency was determined based on fluorescence from the donor and acceptor molecule using the previous FRET efficiency formula. After excitation of the donor GFP, interaction (FRET) led to quenching of GFP emission, but the acceptor RFP was sensitized, resulting in strong fluorescence detected in the RFP-Y2H320 acceptor's emission channel (Figure 3.7). This represented the energy transfer (FRET), and was calculated by FRET sensitized emission (Leica). By co-expression of MYB26-GFP and RFP-Y2H320 in tobacco leaf cells and subsequent FRET analysis, the molecular distance between MYB26 and Y2H320 was determined as 5.81 nm (Table 3.5). In contrast, when the two proteins RFP-Y2H620 and RFP-Y2H970 were used in conjunction with MYB26-GFP, energy transfer (FRET) did not occur, with little fluorescence detected in the acceptor emission channel upon donor excitation (Figures 3.8 and 3.9). The molecular distance between MYB26 and Y2H620 was 10.97 nm and 9.05 nm between MYB26 and Y2H970 (Table 3.5). In general, FRET positive signals with the expectation that two proteins will be interacting if the distance between them is less than 10 nm; positive FRET was, therefore, demonstrated and further confirmed for the interaction between MYB26 and Y2H320 in plant cells.

3.3.3 IMMUNODETECTION OF GFP IN TRANSGENIC TOBACCO PLANTS

Plant tissues from infiltrated transiently transformed *N. benthamiana* leaves were harvested for total protein extraction (Section 2.7.1) for immunodetection of the gene constructs harboring the *GFP* fused gene (Section 2.7.4). This test was done to ensure that the expression levels of the three genes

resulted in approximately similar levels of the translated proteins. In addition, this also confirms that existence of fusion tags after translation. The proteins were transferred to Hybond-C membrane and hybridised with antibodies to the fluorescent protein tag on the constructs. Western blot of total protein hybridized with anti-GFP antibody showed a band corresponding to the MYB26-GFP fusion protein (Figure 3.10). This band was specific to those clones that had been infiltrated with the fusion construct (Figure 3.10), however, the expected size was a bit smaller than expected for the full-length MYB26-GFP fusion protein (72.1 kDa; e.g., 41.5 kDa for MYB26 and 30.6 kDa for GFP). This may be a reflection of partial breakdown of the MYB26-GFP protein since this has been shown to have rapid turnover *in planta* (Yang *et al.*, 2007).

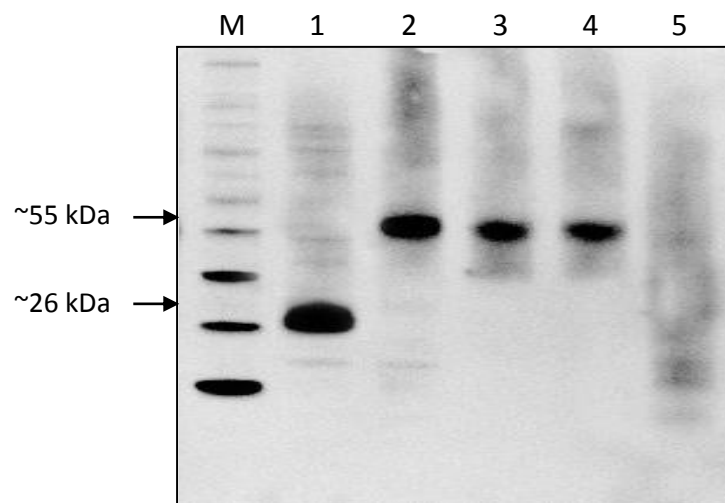


Figure 3.10 Western blot of total protein extracted from tobacco leaves using anti-GFP primary antibody. The exact concentration of the primary antibody used is described in Table 2.3. Lane 1= positive control (leaf of transiently transgenic plant with *GFP* gene, only). Lanes 2-4= leaves of the three transiently transgenics with *MYB26-GFP* gene fusion co-transformed with *RFP-Y2H320*, *RFP-Y2H620* or *RFP-Y2H970* gene fusion, respectively. Lane 5= negative control (leaf of wild type tobacco). A band corresponds to GFP protein (~26 kDa) is shown for the positive control. A band corresponds to the fusion MYB26-GFP protein (~55 kDa) is shown for the transgenics with *MYB26-GFP* gene fusion co-transformed with *RFP-Y2H320* (Lane 2), *RFP-Y2H620* (Lane 3) and *RFP-Y2H970* (Lane 4) gene fusions. Lane 5 showed absence of GFP in the non-transformed WT tobacco leaves as a negative control. M refers to protein marker (Nexus Western™ Wide Range, bionexus).

3.4 DISCUSSION AND CONCLUSION

The MYB26 protein was previously used to screen a stamen Y2H library and identified five putative interacting proteins (Table 3.2). These results suggest that MYB26 may function by interacting with these proteins; however Y2H screens are frequently associated with artifacts. It was, therefore, unknown whether the MYB26 protein interacted *in vivo* with any of the other identified Y2H proteins (Table 3.2). Data are presented in this chapter aimed at confirming putative protein-protein interactions that might occur *in vivo* in plant cells.

To understand the MYB26 transcription factor (TF) and its interaction with a bZIP family transcription factor Y2H320, bHLH-type transcription factor Y2H620 and zinc finger (C3HC4-type RING finger) transcription factor Y2H970 during pollen development, several approaches can be investigated (Table 3.1). In this work, the interaction between MYB26 and Y2H320 proteins was confirmed using the Y2H system and FRET. A clear nuclear localisation pattern was also observed for RFP-Y2H320, RFP-Y2H620 and RFP-Y2H970 fusion proteins. The latter candidates, therefore, co-localised with MYB26-GFP in the nucleus of tobacco leaves (Figures 3.7-3.9) in agreement with the previous localisation data for MYB26 and the expected localisation in the nucleus (Yang *et al.*, 2007).

FRET experiments demonstrated that Y2H320 and MYB26 proteins interact *in vivo* in which strong fluorescence was detected in the RFP-Y2H320 acceptor channel and MYB26-GFP donor after excitation of the GFP fluorescent protein indicating transference of energy (Figure 3.7). Furthermore, FRET analysis showed that the molecular distance between MYB26-GFP and RFP-Y2H320 is on average 5.81 nm (Table 3.5). In contrast, when the two other proteins RFP-Y2H620 and RFP-

Y2H970 co-expressed with GFP-MYB26, energy transfer (FRET) did not occur, with little fluorescence detected in the acceptor emission channel upon donor excitation (Figures 3.8 and 3.9). The FRET analysis indicated that the molecular distance between MYB26-GFP and RFP-Y2H620 fusion proteins is 10.97 nm, while 9.05 nm between MYB26-GFP and RFP-Y2H970 (Table 3.5). These results indicate strong energy transfer between MYB26-GFP and RFP-Y2H320 fusion proteins, while weak energy transfer between MYB26-GFP and Y2H620-RFP, and between MYB26-GFP and RFP-Y2H970. This indicates that the donor MYB26-GFP fluorescent molecule and the acceptor RFP-Y2H320 came into very close proximity (<10 nm) (Immink *et al.*, 2002) (Figure 3.3) and suggests that this interaction is genuine and occurring *in planta* and not only in the yeast 2-hybrid screens.

Agrobacterium tumefaciens-mediated transient transformation is a useful procedure for characterisation of proteins and their functions in plants, including analysis of protein-protein interactions (Tsuda *et al.*, 2012). *Agrobacterium*-mediated transient transformation of *Nicotiana benthamiana* by leaf infiltration is widely used due to its ease and high efficiency for transient expression of exogenous proteins (Tsuda *et al.*, 2012). It has also shown the advantages of being simple, fast, economical and effective (Zheng *et al.*, 2012).

The subcellular localisation of the Y2H proteins was investigated to confirm whether they were likely to interact with MYB26. The Y2H620 and Y2H970 proteins are all transcription factors and predicted to be co-localised with MYB26. A previous study by Song (2009) demonstrated that Y2H128 was localised in the endoplasmic reticulum (ER) and when co-expressed in onion epidermal cells with MYB26, FRET

analysis confirmed physical interaction between MYB26 and Y2H560 *in planta*.

Expression of *MYB26* occurs early during endothelial development, with high expression in the anther during pollen mitosis I (PM I), while very low levels were detected during bicellular stages in pollen mitosis II (PM II) (Yang *et al.*, 2007). It seems likely that MYB26 acts in a complex, however, the type of protein complexes formed during interaction could be monomer, homo- or hetero-dimer, trimer or tetramer (Immink *et al.*, 2002; Lalonde *et al.*, 2008). There are also larger protein complexes discovered in yeast and mammals, for example, the RNA polymerase II (pol II) system comprises six proteins, pol II and five general transcription factors (Kornberg, 2007). Other MYB factors have been shown to have diverse functions, which are achieved via various protein complexes, for example an MYB-bHLH-WD40 protein complex was found to control epidermal cell identity (Ramsay and Glover, 2005). Three MYB factors, MYB23 WEREWOLF (WER) and GLABROUS1 (GL1), are thought to be involved in this complex (Kirik *et al.*, 2005; Lee and Schiefelbein, 1999). There are four proteins that were identified as having a possible interaction with MYB26 in yeast, all of which are co-localised in the nucleus with MYB26 in plant cells. Further studies are needed on the two candidate genes *Y2H620* and *Y2H970* as they are members in this gene family (e.g., bHLH) that have been reported to positively associate with MYBs (Du *et al.*, 2009; Qu and Zhu, 2006). FRET analysis indicates that Y2H560 and Y2H320 interact with MYB26 *in vivo*, hence, these are also important proteins to analyse for their potential role in secondary thickening and anther dehiscence. Therefore, functional analysis of the effect of down- and up-regulation of these genes was investigated (Chapter 4).

CHAPTER 4: CHARACTERISATION OF THE PUTATIVE MYB26 INTERACTING PROTEINS

4.1 INTRODUCTION

A number of proteins have been identified which may interact with MYB26 to facilitate activity in regulating secondary thickening in the anther (Chapter 3). The function of these proteins was therefore investigated by altering their expression, by reducing levels of expression via insertional mutagenesis or RNAi gene silencing, by increasing their expression by transgene over-expression and via localization of their expression patterns. Four different genes (*At5g25560*, *At1g47128*, *At1g08320* and *At3g62970*) from the Y2H screen were selected for knockout analysis. Interaction of the proteins encoded by *At1g08320* and *At5g25560* genes with MYB26 had previously been confirmed by FRET analysis (Chapter 3; Song, 2009). *At3g47620* and *At3g62970* genes are members of the bHLH gene family whose encoded proteins have been reported to positively associate with MYBs (Du *et al.*, 2009; Qu and Zhu, 2006). The latter proteins were, therefore, also likely candidates to be associated with MYB26.

Several mutational approaches have been widely used to analyse the genetic and molecular traits in plant biology. This process involves the generation of mutants with altered phenotypes, enabling the biological function for a given gene to be assigned by identifying a mutant allele and comparing the performance of the plant harbouring it with that in the respective wild-type plant (Østergaard *et al.*, 2004). One of the principal approaches used to create mutations is via insertion of DNA (T-DNA) as a consequence of transformation

by *Agrobacterium tumefaciens*, or *A. rhizogenes*. T-DNA stands for 'transferred DNA' from the tumor-inducing (Ti) plasmid of *A. tumefaciens* and *A. rhizogenes*. T-DNA insertion is a highly effective mutagen for genome-wide site-directed mutagenesis (Krysan *et al.*, 1999). It has been widely used to produce insertion mutants in *Arabidopsis thaliana* for functional characterization of all genes in the genome (Krysan *et al.*, 1999; Sessions *et al.*, 2002; Alonso *et al.*, 2003). Over 360,000 insertions have been mapped in the *Arabidopsis* genome, covering >90% of the genes in the genome (Alonso and Ecker, 2006). T-DNA tends to insert as concatemers (Krysan *et al.*, 1999), therefore most T-DNA insertions result in loss-of-function alleles with entire disruption of gene function, although semi-dominant T-DNA mutations have been reported (Bolle *et al.*, 2000). Nevertheless, in most cases functional protein is absent in the homozygous mutant plants and even if mRNA is transcribed, the T-DNA sequence frequently contains intervening sequence(s), resulting in early translation termination and the recovery of truncated non-functioning proteins (Krysan *et al.*, 1999).

T-DNA insertion mutagenesis has been a powerful reverse genetics tool to link candidate genes to their consequent mutant phenotypes and to determine their biological function(s) in growth and development within the whole plant (Østergaard *et al.*, 2004). Additionally, the generation of diverse mutant alleles in a given gene of interest provides important tools to understand the structure of the gene (Kim *et al.*, 2005). To enable genome-wide analysis large populations of tagged mutants have been generated, such as the SALK insertional line population (Alonso *et al.*, 2003), which have been sequenced and compiled in databases that can be searched for a gene disruption event of interest; this

means that genomic sequences of many insertion sites are now available through the *Arabidopsis* Stock Centres.

RNA interference (RNAi) is an evolutionary conserved mechanism for silencing genes that is critical for many examples of growth or development and nowadays, it is frequently used in functional genomics studies by inducing silencing of a target gene. RNA-induced gene silencing (RNAi) was originally observed as an unusual expression pattern of a transgene designed to induce over-expression in plants (Napoli *et al.*, 1990). Similar results were reported in a range of organisms (Fire *et al.*, 1991; Pandit and Russo, 1992). Silencing requires the production of small interfering RNAs (siRNA), corresponding to the target gene. This is facilitated for functional analysis by the construction of stable transgenic plants in which the transgene construct generates double stranded (ds) RNA or hpRNA. dsRNAs are usually processed to siRNA (20-25 base pairs) *in vivo* by the endogenous enzyme Dicer (Fire *et al.*, 1998). These types of experiments have contributed to rapid advancement, in many model systems, in understanding the underlying mechanism, and RNA-mediated gene silencing processes came to be collectively known as RNA interference (RNAi).

The *MYB26* gene shows a very specific expression pattern (Yang *et al.*, 2007) during floral development. If the gene functions by interaction with the proteins that have been identified from the yeast-2-hybrid screen (Chapter 3), then these proteins should show an equivalent localisation of expression. Promoter-fusions have been frequently used as a means of determining temporal and spatial gene expression in a cell-specific manner. *Beta-glucuronidase* (*GUS*) is a frequently used reporter enzyme for plant genetic research. It

was originally isolated from *Escherichia coli* (*E. coli*) (Jefferson *et al.*, 1987). Since then, more than 5000 citations in the primary literature have been reported for its use, and over 1000 field releases of transgenic plants containing GUS are available worldwide. The enzyme has many characteristics of an ideal reporter. It is remarkably stable, has no cofactors, tolerates many commonly used chemicals, the assay is sensitive, rapid and its experimental conditions are simple (temperature and pH). In addition, the *uidA* (*beta-glucuronidase, GUS*) gene fusion system has extensive applications in plant gene expression studies because of the suitability of the assay for the detection by either fluorometric or histochemical approaches. Further advantages lie in the straightforward approach of the GUS assays that do not require expensive equipment, and in the variety of substrates commercially available (Fior and Gerola, 2009). *In planta*, no endogenous enzyme or substrate that interferes with GUS assay have been reported. In addition, GUS does not seem to interfere with plant physiology and metabolism after transgenesis. It is also regarded as safe for the environment (Gilissen *et al.*, 1998). Nevertheless, a major drawback of the GUS system is its destructive assay; the cell membrane must be disrupted so that the cytosol-localized enzyme can come into contact with its substrate.

4.2 MATERIALS AND METHODS

4.2.1 SALK-LINES ANALYSIS

Data relating to *At5g25560*, *At1g47128*, *At1g08320* and *At3g62970* genes were retrieved from the Ensembl and TAIR databases (Table 2.1, Section 2.3). Available mutants were identified and ordered from the Nottingham *Arabidopsis* stock Centre (NASC). Seeds were grown (Section 2.1) and leaf materials were collected in order to extract genomic DNA (gDNA) using Extract-N-Amp plant kit (Sigma) and the plants were genotyped for the insert (Section 2.9.1) using appropriate primers (Tables 4.2 and 4.3). RNA was extracted from inflorescences (Section 2.9.2) of homozygous T-DNA plants and cDNA generated (Section 2.9.3).

The TAIR database (<http://www.arabidopsis.org/servlets/sv>) was visited to retrieve sequence information, which was analysed using MacVector software (<http://www.macvector.com/>). The link was also used for creating maps consisting of the 3' and 5' UTR ends of the gene of interest, their upstream and downstream genes, the left and right primers to be used for genotyping and T-DNA insertion site (Figure 4.1).

4.2.2 PREPARATION OF RNAi SILENCING CONSTRUCTS FOR THE PUTATIVE MYB26-INTERACTING PROTEINS

Two *Y2H* genes, namely *Y2H128* and *Y2H970*, were selected for silencing analysis. *At1g47128*-pK7GW1GW2^{RNAi} (*Y2H128*^{RNAi}) and *At3g62970*-pK7GW1GW2^{RNAi} (*Y2H970*^{RNAi}) constructs were made to characterise the functions of the two genes by RNAi silencing. The coding sequence fragments of these two genes, *At1g47128* and *At3g62970*, were fused in to

entry vector pENTER™/D-TOPO (Invitrogen) using Gateway Technology (Section 2.9.7). The plasmids were then transformed into *E. coli* strain DH5a using heat-shock transformation (Sambrook *et al.*, 1989) (Section 2.9.7).

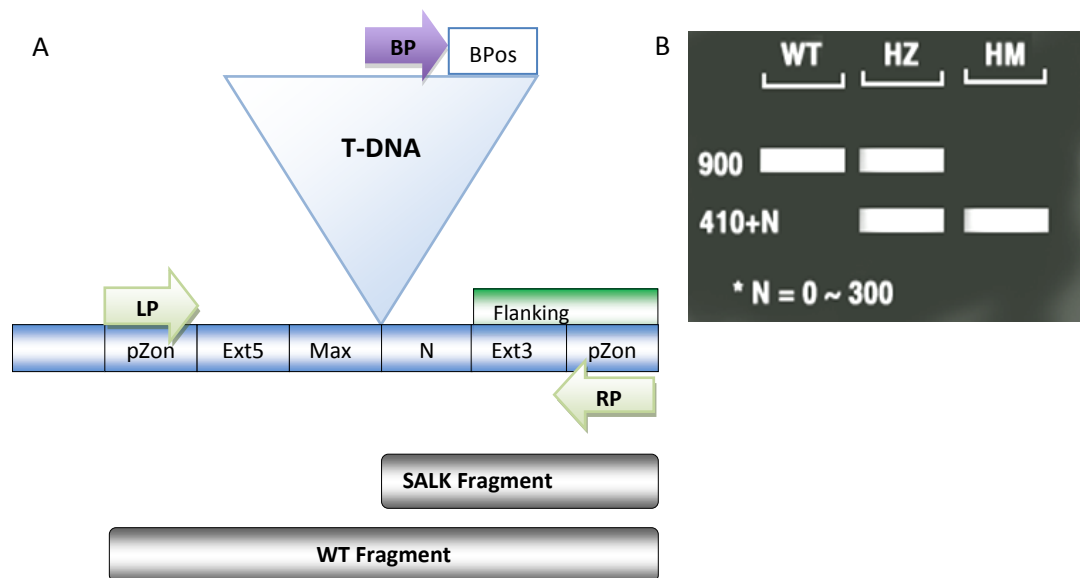


Figure 4.1 (A) Guide for the localization of T-DNA Insertion. N: difference of the actual insertion site and the flanking sequence position, usually 0-300 bases. MaxN: maximum difference of the actual insertion site and the sequence, default 300 bp. Ext5/Ext3: 5' and 3' regions between the MaxN and pZone LP/RP: Left and right genomic primers. BP: T-DNA border primer. BPos: the distance from BP to the insertion site. (B) Guide for the PCR genotyping and gel analysis of the insertion lines in the heterozygous (HZ) and homozygous (HM) lines as compared to their respective wild type (WT), provided by the SALK Institute, Genomic Analysis Laboratory (SIGnAL) (<http://signal.salk.edu/tdnaprimers.2.html>).

The transformed cells were selected by spreading the cells on LB medium plates containing 50 µg/ml kanamycin. The plasmids were isolated and purified after selection for the *kan* resistance gene (Section 2.9.10) and sent for sequencing (Section 2.9.11). The two RNAi constructs were then made by fusing the fragments into a destination vector pK7GWIWG2 (II) (RNAi GATEWAY ready) following Karimi *et al.* (2005). The Gateway LR reaction was applied following the procedure described in Section 2.9.7. The resultant pK7GW1GW2 vector

was transferred into chemically competent DH5α *E. coli* cells and the final constructs were named Y2H128^{RNAi} and Y2H970^{RNAi}. The two constructs were then transformed into *Agrobacterium tumefaciens* C58 before they were transformed into *Arabidopsis thaliana* flowers by the “floral dip method” (Clough and Bent, 1998) (Section 2.9.12). A total of 15 independent transformants for Y2H128^{RNAi} and Y2H970^{RNAi} were obtained and PCR checked (Section 2.9.1). In order to confirm the down-regulation of Y2H970 and Y2H128 gene expression, total RNA was isolated from inflorescences of plants from the T1 and T2 generations for each construct and compared to respective wild type (Ler) (Section 2.9.2). RT-PCR was carried out (Section 2.9.5) by using gene-specific primers (APPENDIX II). Inflorescences from individual transgenic plants and wild type were collected to detect the pollen viability and the dehiscence anthers. The pollen were analysed by Alexander staining (Section 2.6.1) and visualised by light microscopy.

4.2.3 PREPARATION OF OVER-EXPRESSION CONSTRUCTS FOR THE PUTATIVE MYB26-INTERACTING PROTEINS

Transgenic *Arabidopsis* plants over-expressing the coding sequences (CDS) of the four target genes were prepared using the PGWB402Ω vector (APPENDIX III). This construct possesses the P2x35sΩ promoter to drive over-expression. The entry clones of Y2H970, Y2H320, Y2H128 and Y2H620 pENTERTM/D-TOPO were inserted into a destination vector PGWB402Ω (APPENDIX III). The LR reactions were then carried out as described in Section 2.9.7 and PCR was checked using the 35S_forward primer and each of reverse gene

specific primers of *At3g62970*, *At3g47620*, *At1g08320* and *At1g47128* genes (APPENDIX II).

In order to confirm the ectopic expression of the four over-expression lines, total RNAs were isolated from inflorescences of plants at the T1 and T2 generations for each over-expressed gene and compared to their respective wild type (*Ler*) (Section 2.9.2). RT-PCR analysis was carried out to detect the expression levels of the four transgenes as compared to their respective WT genes (Section 2.9.5) using pairs of forward and reverse gene-specific primers. Transgenic plants of each over-expressed gene were checked for altered phenotypes.

4.2.4 PREPARATION OF PROMOTER: GUS CONSTRUCTS FOR THE PUTATIVE MYB26-INTERACTING PROTEINS

The *At1g08320* gene was selected for expression localization study; the entry clone of Y2H320 pENTER™/D-TOPO was inserted into a destination vector pGWB433 (APPENDIX III). The LR reaction was then carried out as described in Section 2.9.7. To confirm occurrence of genetic transformation, genomic PCR was carried out using the reverse primer of pGWB8GUS, namely pGWB8GUS_Reverse, and forward gene-specific primer (APPENDIX II). Seeds from transformed plants were sown onto 50 µg/ml kanamycin MS (APPENDIX I) selection plates (Section 2.4). Following transfer to soil, plants were grown until inflorescences and two fully extended siliques were developed. Inflorescences were then collected and placed in GUS staining solution (Section 2.6.4). Wild type *Ler* plants were also germinated on MS plates without selection and transferred to soil to act as negative controls for GUS activity. GUS analysis was carried out on the T1 population of 12

independent transformants for each transgene. Blue staining was visualized due to the action of β -glucuronidase in inflorescences assayed overnight (Section 2.6.4).

4.3 RESULTS

4.3.1 GENOTYPIC AND EXPRESSION ANALYSES OF THE SALK KNOCKOUT LINES

SALK insertional mutants with T-DNA insertion lines in the *Col* background were chosen based on the yeast-two-hybrid assay. These mutants correspond to genes encoding the five previously identified putative MYB26 interacting proteins (Y2H560, Y2H128, Y2H320, Y2H620 and Y2H970) from screening a stamen Y2H library using the full length MYB26 protein as bait (Table 3.2) (Yang and Wilson, unpublished data) (Chapter 3). The Knockout genes include *AT5G25560* or *chy* (encoding a ubiquitin-protein ligase), *At1g47128* or *rd21* encoding a cysteine protease, *At1g08320* or *bzip* encoding a member of the basic leucine zipper transcription factor family (Table 3.2) and *At3g62970* or *c3hc4* gene encoding a zinc ring finger transcription factor (Table 4.1). *At3g47620* and *At3g62970* candidate genes are members of the bHLH gene family, a group of proteins that have been reported to associate with MYB factors (Du *et al.*, 2009; Qu and Zhu, 2006). Therefore the SALK T-DNA line of *At3g62970* gene was investigated. Basic description of the genes and scientific literature associated with them were retrieved from the Ensembl and TAIR databases (<http://arabidopsis.info/BrowsePage>) (Table 4.1). SALK knockout mutants were identified and used for genotypic, phenotypic and expression analyses as compared to the wild type *Col*.

Table 4.1 Description of SALK gene mutants.

Gene ID and Y2H code	SALK line	GENE DESCRIPTION	REFERENCES
<i>At5g25560</i> , <i>Y2H560</i>	SALK_008223	CHY-type/CTCHYtype/RING-type Zinc finger gene. Functions in zinc ion binding and expressed in leaf, embryo, flower, cells, stamen and stem	https://www.arabidopsis.org/servlets/TairObject?id=135385&type=locus (Kosarev <i>et al.</i> , 2002)
<i>At1g08320</i> , <i>Y2H320</i>	SALK_091349	bZIP transcription factor family protein DNA binding, sequence-specific DNA binding transcription factor activity involved in regulation of transcription, DNA -dependent; and gene is expressed in leaf, flower, petal, embryo, pollen tube, seed and sepal	https://www.arabidopsis.org/servlets/TairObject?id=137011&type=locus (Jakoby <i>et al.</i> , 2002)
<i>At3g62970</i> , <i>Y2H970</i>	SALK_106671	Zinc finger (C3HC4-type RING finger) family gene. Functions in zinc ion binding; and involved in: N-terminal protein plant structures during growth stages and gene is expressed in carpel, flower, leaf apex, pollen, root, stamen and sepal	https://www.arabidopsis.org/servlets/TairObject?id=39947&type=locus (Kosarev <i>et al.</i> , 2002)
<i>At1g47128</i> , <i>Y2H128</i>	SALK_090551	cysteine proteinase precursor-like gene or dehydration stress-responsive gene (<i>RD21</i>). Enzyme has peptide ligase activity and protease activity <i>in vitro</i> . <i>RD21</i> is involved in immunity to the necrotrophic fungal pathogen <i>Botrytis cinerea</i> and is expressed in carpel, leaf, flower, petal, pollen, root, seed, sepal, stamen and stem	https://www.arabidopsis.org/servlets/TairObject?id=226917&type=locus (Lampl <i>et al.</i> , 2013).

4.3.1.1 ANALYSIS OF *AT5G25560* GENE

The *At5g25560* gene (3839 bp) encodes a CHY-type/CTCHY-type/RING type Zinc finger protein, which functions in zinc ion binding. The gene includes 12 exons in which the T-DNA was inserted in exon 12. According to TAIR (The *Arabidopsis* Information Resource), URL (<http://www.arabidopsis.org/>), the gene is expressed during growth stages in leaf, embryo, flower, pedicel, petal, pollen tubes, roots, seeds, sepals, shoot, sperm cells, stamen and stem. It contains InterPro domains of Zinc finger, CTCHY-type (InterPro: IPR017921), Zinc finger, CHY-type (InterPro: IPR008913), Zinc finger, RING-type

(InterPro: IPR001841). Figure 4.2 shows the T-DNA localization map of the gene along with the positions of the forward and reverse SALK primers for this gene.

Using gene-specific as well as forward SALK-LBb1 primers (Figures 4.2 and Table 4.2), PCR genotyping showed that the seven plants of SALK_008223 were homozygous for the T-DNA insertion (amplification of 307 bp, Figure 4.3). No amplification of the wild type (*At5g25560*) band was seen in the insertion lines, whilst amplification of the WT showed the expected gene size (884 bp). RT-PCR expression analysis was conducted using gene-specific primers (Figure 4.4 and Table 4.3) on lines homozygous for the T-DNA insertion; expression was normalized by comparison to *ACTIN7* gene (Figure 4.5A and B, respectively). The results of the target gene showed no amplification for the homozygous mutant lines, while the products size were generated for the WT (681 bp) indicating that the gene function is disrupted in the mutant lines (Figure 4.5A).

Table 4.2 Primers used for PCR genotyping of *Arabidopsis* T-DNA Insertion lines.

Gene ID	Primer name	Primer sequence (5' to 3')	Tm (°C)	Size of T-DNA band	Size of WT band
<i>At5g25560</i>	SALK_008223R SALK_008223F	TCCTTTGTAATTCTGCGGCTT AATCCTCCTCAAGAACGGTCA	55.9 57.9	307 bp	884 bp
<i>At1g47128</i>	SALK_090551R SALK_090551F	CGGTACAAATTTAACCATCTTCTCA GGTCACAAGGCAGAAAGAACA	58.1 57.9	700 bp	974 bp
<i>At1g08320</i>	SALK_091349R SALK_091349F	GACCACCAGGACCTAACATCA TCACATGAGTCGACTTCACTCAC	58.4 57.9	566 bp	966 bp
<i>At3g62970</i>	SALK_106671R SALK_106671F	GCCAAGTCAATGGTGGATATG TCGAATTGTGGCGTCAATATG	52 57.9	750 bp	1070 bp
SALK T-DNA insertion	SALK-LBb1	GCGTGGACCGCTTGCTGCAACT	57.9	-	-

Table 4.3 Gene-specific primers used for RT-PCR analysis of T-DNA Insertion lines.

Gene ID	Primer name	Primer sequence (5' to 3')	Tm (°C)	Band size
<i>At5g25560</i>	At5g25560_F At5g25560_R	CGTCAACTCTGGAAAGGGTAGCGCA GATTGCGGCTACACCAATGC	61.0 64.0	681 bp
<i>At1g47128</i>	At1g47128_F At1g47128_R	GCATGGTTGGTAAAACACGG TTGCTGCCCTCACGAGTACC	60.6 66.4	1114 bp
<i>At1g08320</i>	At1g08320_F At1g08320_R	GTCAGGAGGAGAGAGCAGCGA GCTGCACGGTGTTCCTAGTC	61.3 64.6	1000 bp
<i>At3g62970</i>	At3g62970_F At3g62970_R	TCTCTGCAATGACTGCAACAAGG CTCATCTTCTCATGCCGCCA	63.2 69.5	607 bp
<i>Actin</i>	ACT7F ACT7R	TGCTGACCGTATGAGCAAAG CAGCATCATCACAAGCATAA	58 58	400 bp

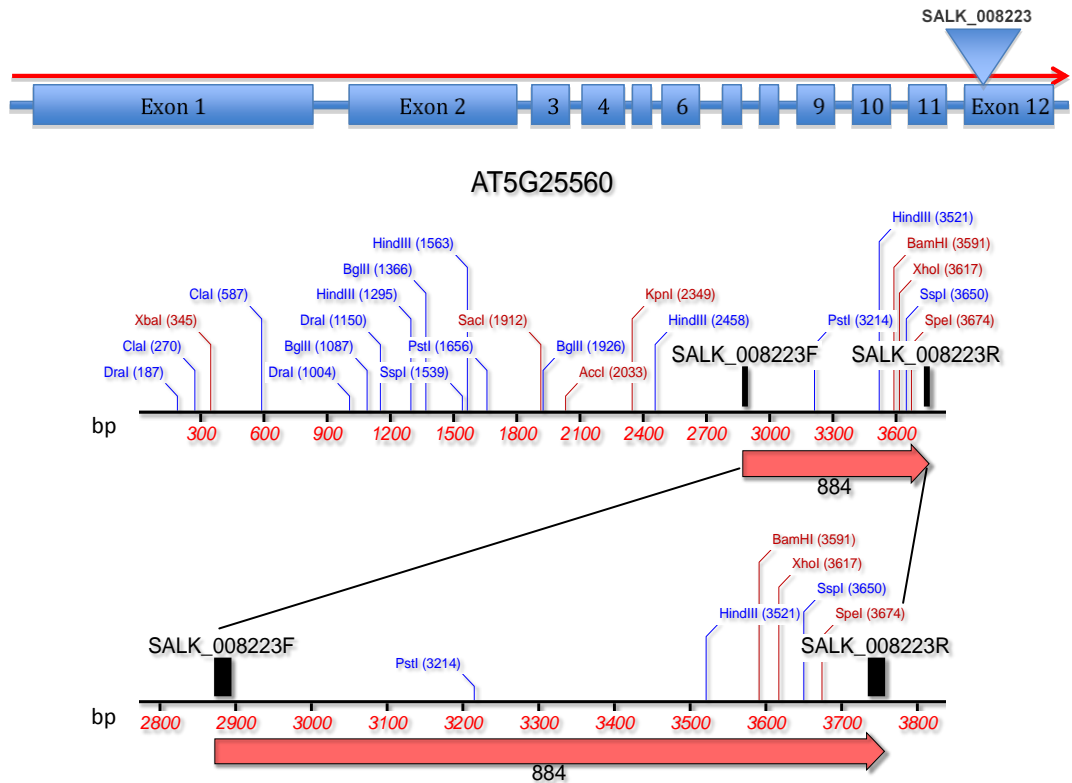


Figure 4.2 T-DNA localization map of SALK_008223 insertion line for *At5g25560* gene (3839 bp). The gene includes 12 exons in which T-DNA was inserted in exon 12. Arrows indicate the direction of the coding sequence of the gene. Black Squares show the positions of forward and reverse gene-specific primers used for genotyping analysis.

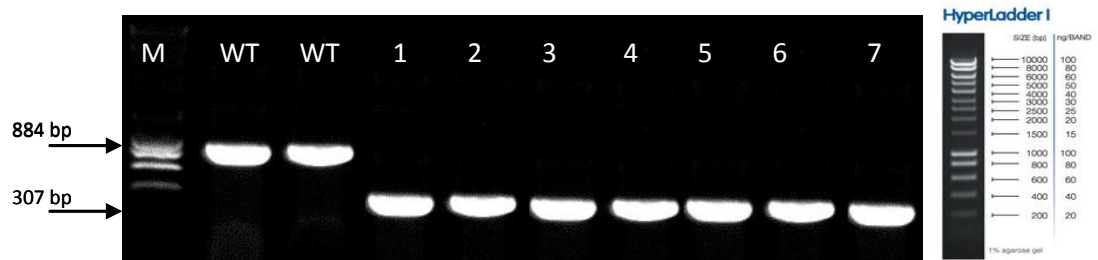


Figure 4.3 Genotyping analysis via PCR for SALK_008223 line with the *At5g25560* gene. Amplification was conducted using three primers, forward SALK-LBb1 generated from the SALK T-DNA insert and two forward and reverse gene-specific primers (Figure 4.2 and Table 4.2). Lanes 1-7 size (~307 bp) of individual homozygous lines as compared to those of the WT (*Col*) ~ (~884 bp). M = HyperLadder I with sizes shown in the figure.

inflorescence meristem, pedicel, petal, plant embryo, pollen, root, seed, sepal, shoot apex, shoot system, stamen, stem and vascular leaf (TAIR).

Gene-specific primers and T-DNA insertion forward primer, e.g., SALK-LBb1 (Figure 4.6 and Table 4.2) were used for genotypic analysis of the insertion line. Figure 4.7 shows that only two of the segregating SALK plants were homozygous (lines 7 and 10; generated an amplification product of 700 bp), while one plant was heterozygous (line 1) and the rest were wild type (generating an amplification product of 974 bp). RT-PCR of *At1g47128* gene was conducted using primers to generate a 1114 bp WT product. A corresponding product was also seen for the two homozygous lines using gene-specific primers (Figures 4.9 and Table 4.3); samples were compared using *ACTIN7* gene expression levels (Figures 4.9A and B, respectively). The results of the target gene showed amplification for the two homozygous lines at an equivalent level to those of the WT control, indicating that the gene is expressed as normal in the T-DNA line (Figure 4.9A).

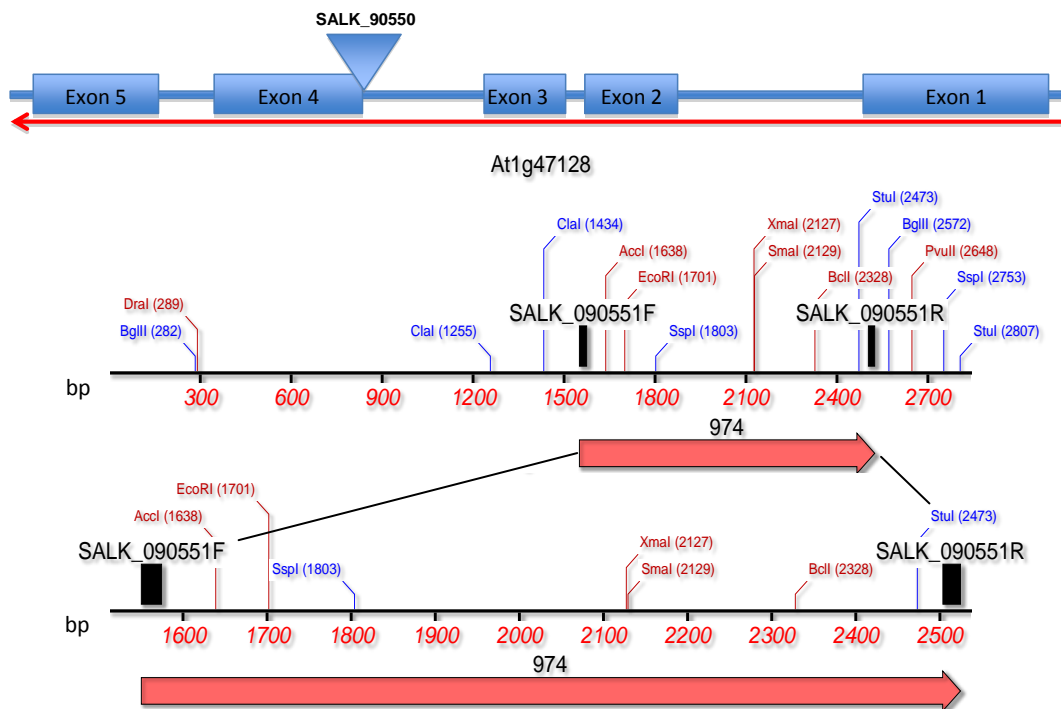


Figure 4.6 T-DNA localization map of SALK_90550 insertion line in the *At1g47128* gene (2846 bp). The gene includes 5 exons in which T-DNA was inserted in the intron between exons 3 and 4. Arrows indicate the direction of the coding sequence of the gene. Black Squares show the positions of forward and reverse gene-specific primers used for genotyping analysis.

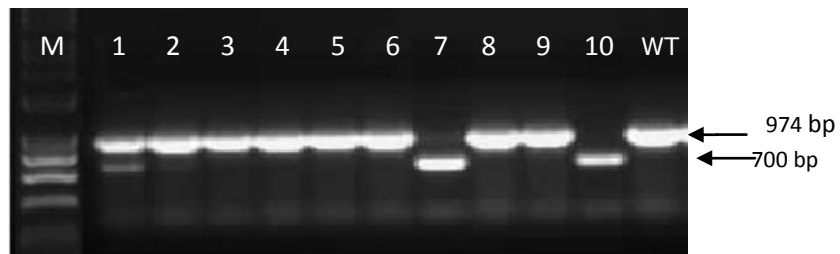


Figure 4.7 Genotyping analysis by PCR for Salk_090550 for the *At1g47128* gene. Amplification was conducted using three primers, forward SALK-LBb1 generated from the SALK T-DNA insert and two forward and reverse gene-specific primers (Figure 4.6 and Table 4.2). Lanes 7 and 10 size ~ (700 bp) of individual homozygous lines as compared to that of the WT (*Col*) ~ (974 bp). Lane 1 indicates a heterozygous (HT) T-DNA line. M=HyperLadder I.

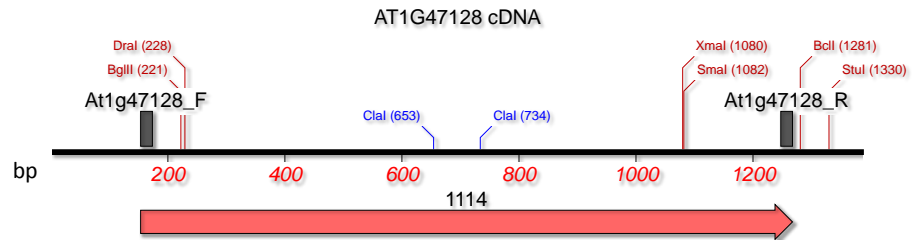


Figure 4.8 Localization map of Salk_090550 with *At1g47128* forward and reverse gene-specific primers used for RT-PCR. Arrow indicates the direction of the coding sequence of the gene. Black squares show the position of forward and reverse primers used for expression analysis.

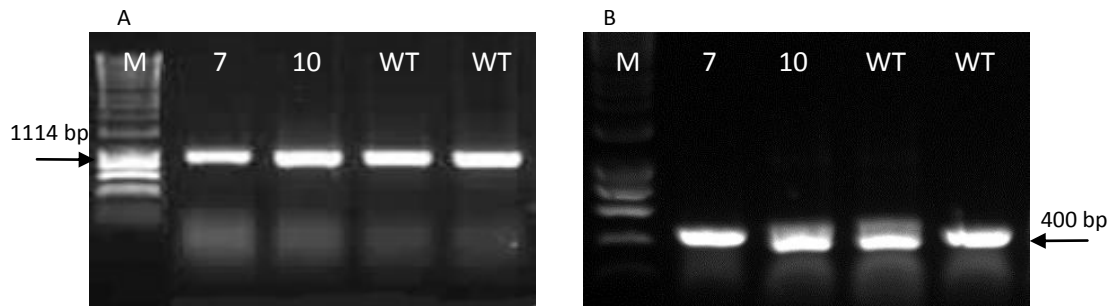


Figure 4.9 (A) RT-PCR expression analysis for individual plants of Salk_090550 insertion line with the *At1g47128* forward and reverse gene-specific primers (Figure 4.8 and Table 4.3). Expression was shown in samples 7 and 10 at the equivalent level as compared with the WT (*Col*). The latter showed gene expression of expected size ~1114 bp. (B) RT-PCR expression analysis of the *ACTIN7* house-keeping gene in the segregating SALK_090550 insertion line using the ACT7F and ACT7R primers. The latter gene showed expected size of 400 bp. All samples showed equivalent levels of expression. M=HyperLadder I.

4.3.1.3 ANALYSIS OF *AT1G08320* GENE

The *At1g08320* gene (5945 bp) encodes a bZIP transcription factor family protein that functions in DNA binding with sequence-specific DNA binding transcription factor activity. The gene includes 13 exons in which the T-DNA was inserted in exon 7. The predicted protein encodes for an InterPro domain basic-leucine zipper (bZIP) transcription factor (InterPro: IPR004827). This gene appears to be expressed in leaf, flower, petal, embryo, pollen tube, root, seed, sepal and in male gametophyte (TAIR).

Genotyping was conducted using gene-specific primers (Figure 4.10 and Table 4.2). Figure 4.11 shows that the ten SALK plants were homozygous (generated an amplification product of 566 bp), as compared to the wild type which generated products of 966 bp. RT-PCR of the *At1g08320* gene was conducted for the three homozygous lines using gene-specific primers (Figure 4.12 and Table 4.3) to generate an amplification product of 1000 bp, which was compared with *ACTIN7* gene expression levels (Figure 4.13A and B, respectively). The results of the target gene showed no amplification for the homozygous lines, while amplification were generated for the WT indicating no expression of the target gene in the T-DNA line (Figure 4.13A); equivalent expression of the *ACTIN7* gene was seen in all lines.

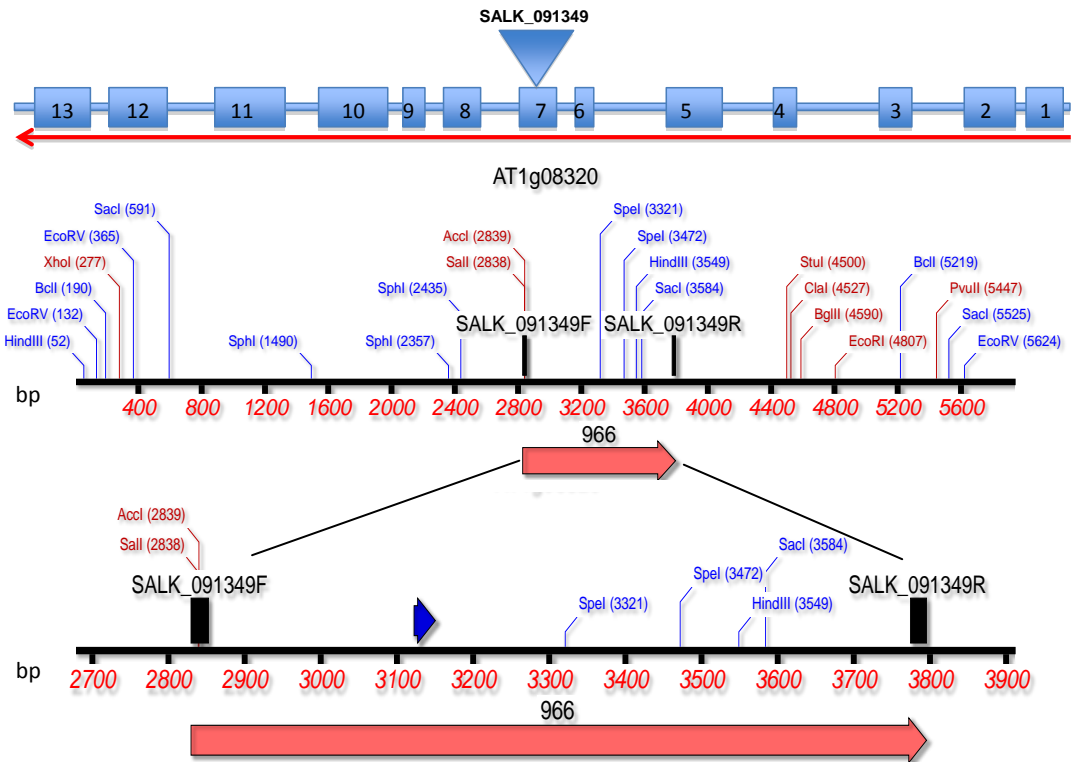


Figure 4.10 T-DNA localization map of SALK_091349 insertion line with *At1g08320* gene (5945 bp). The gene includes 13 exons in which T-DNA was inserted in exon 7. Arrows indicate the direction of the coding sequence of the gene. Black Squares show the positions of forward and reverse gene-specific primers used for genotyping analysis.

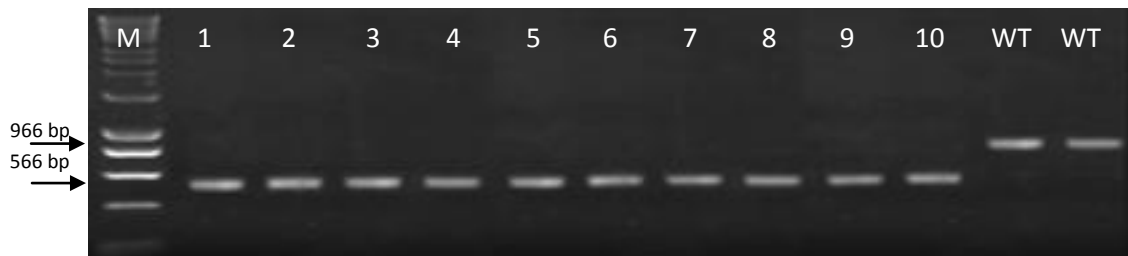


Figure 4.11 Genotyping analysis via PCR for Salk_091349 in the *At1g08320* gene. Amplification was conducted using three primers, forward SALK-LBb1 generated from the SALK T-DNA insert and two forward and reverse gene-specific primers (Figure 4.10 and Table 4.2). Lanes 1-10 size (~566 bp) of individual homozygous lines as compared to those of the WT (*Col*) (~966 bp). M=HyperLadder I.

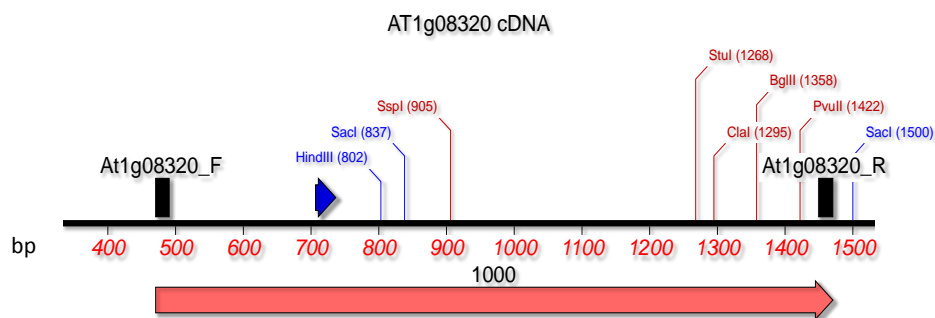


Figure 4.12 T-DNA localization map of Salk_ 091349 with *At1g08320* forward and reverse gene-specific primers used for RT-PCR. Arrow indicates the direction of the coding sequence of the gene. Black squares show the position of forward and reverse primers used for expression analysis.

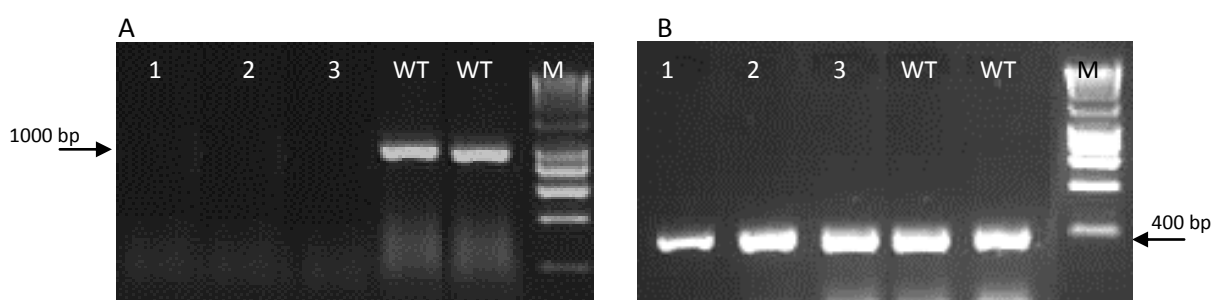


Figure 4.13 (A) RT-PCR expression analysis for individual plants of Salk_ 091349 insertion line with *At1g08320* forward and reverse gene-specific primers (Figure 4.12 and Table 4.3). No expression was shown in samples 1-3 as compared with the WT (*Col*). The latter showed gene expression of expected size ~1000 bp. (B) RT-PCR expression analysis of the *ACTIN7* house-keeping gene in the segregating SALK_ 091349 insertion line using the ACT7F and ACT7R primers. The latter gene showed expected size ~400 bp. All samples showed equivalent levels of expression. M=HyperLadder I.

4.3.1.4 ANALYSIS OF *AT3G62970* GENE

The *At3g62970* gene (2291 bp) encodes a Zinc finger (C3HC4-type RING finger) family protein that functions in zinc ion binding. The gene includes 12 exons in which the T-DNA was inserted between exons 7 and 8. Again, it was likely that the insertion would not affect the expression of the gene as it can be spliced along with the introns of the gene during post-transcriptional processing. It was predicted to be expressed in carpels, leaves, cotyledon, flower, hypocotyl, inflorescence meristem, leaf apex, leaf lamina base, pedicel, petal, petiole, plant embryo, plant sperm cell, pollen, root, seed, sepal, shoot

apex, shoot system, stamen, stem and vascular leaf (TAIR). The encoded protein is predicted to contain the InterPro Domains: Zinc finger, CTCHY-type (InterPro: IPR017921), Zinc finger, CHY-type (InterPro: IPR008913), Zinc finger, RING-type (InterPro: IPR001841), C3HC4 RING-type (InterPro: IPR018957).

A technical problem was encountered with using three primers (Figure 4.14 and Table 4.2) for genotyping as the two forward primers required different annealing temperatures. Therefore, two PCRs, rather than one, were conducted, one to characterise the T-DNA insertion and the other to characterise the WT gene. During the first PCR, forward SALK-LBb1 and reverse gene-specific primers (SALK_106671R) were used, while the forward and reverse gene-specific primers (SALK_106671F and SALK_106671R) were used during the second PCR. The results of the first PCR indicated that samples 1, 2, 6-16 could be either homozygous (HM) or heterozygous (HZ) for the T-DNA insertion as they generated the expected band size of 750 bp (Figure 4.15), while the results for samples 3-5 generated no products indicating that they are WT (data not shown). The second PCR was done for samples 3-5 as well as the original two WT samples and expected size of 1070 bp was generated using the two gene-specific primers (Figures 4.15). RT-PCR with gene-specific primers (Figure 4.16 and Table 4.3) for three randomly selected homozygous T-DNA lines showed expression of the gene at different levels as they generated products with the expected wt size of 607 bp (Figure 4.17A). The intensity of bands in the T-DNA lines was lower than that in the WT control, particularly for samples 1 and 7, with sample 9 slightly lower than that of wt. This indicate that the T-DNA insert is not preventing gene expression in the insertion mutant. The same T-DNA insertion

lines resulted in the amplification of expected size 400 bp for the *ACTIN7* gene used as a control (Figure 4.17B).

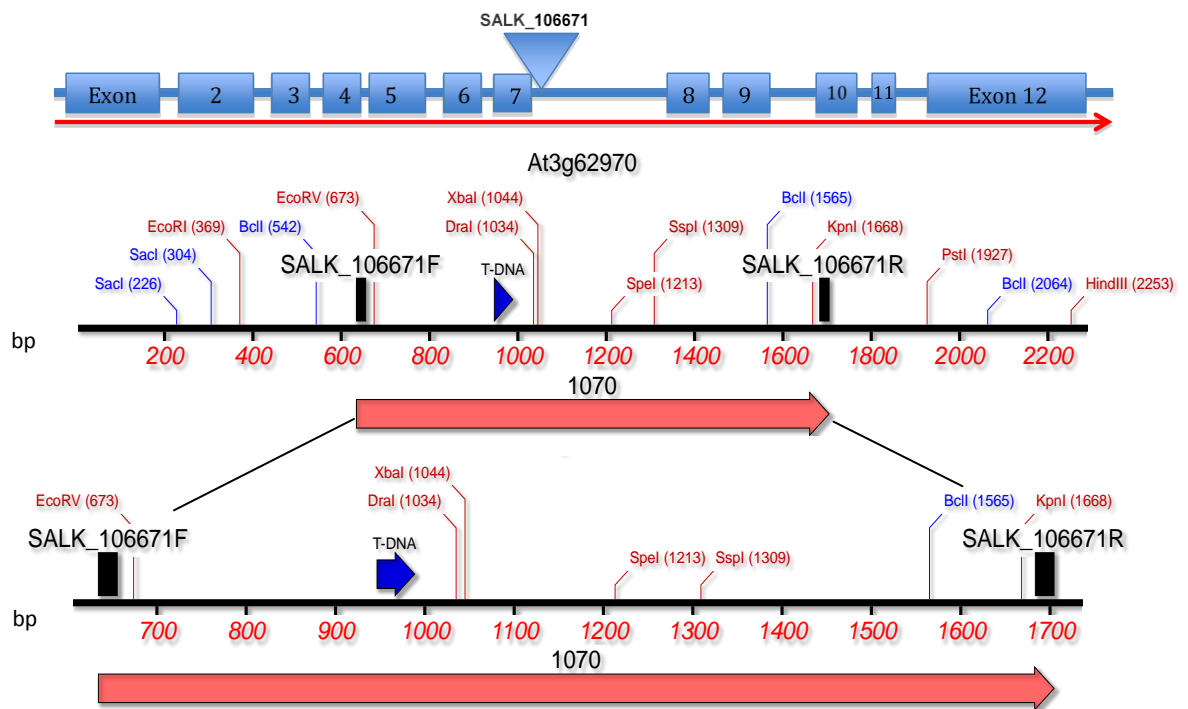


Figure 4.14 T-DNA localization map of SALK_106671 insertion line for the *At3g62970* gene (2291 bp). The gene includes 12 exons in which the T-DNA was inserted into the intron between exons 7 and 8. Arrows indicate the direction of the coding sequence of the gene. Black Squares show the positions of forward and reverse gene-specific primers used for genotyping analysis.

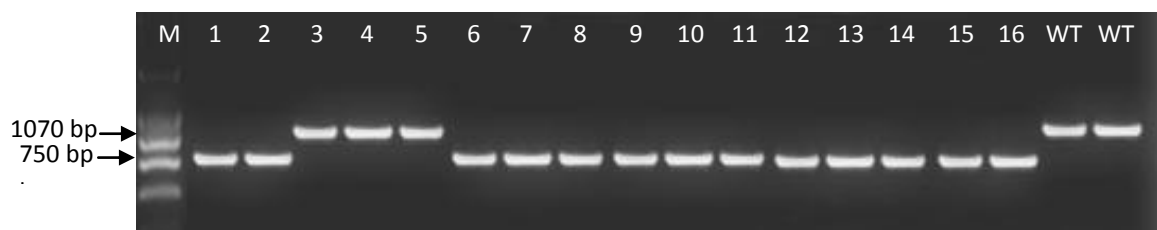


Figure 4.15 Genotyping analysis via PCR for Salk_106671 for the *At3g62970* gene. First PCR conducted for T-DNA insertion indicated homozygous (HM) lines in lanes 1, 2, 6-16, using forward SALK-LBb1 and reverse gene-specific primers generated ~750 bp. Second PCR for gene specific amplification conducted for lanes 3-5 and WT using forward and reverse gene-specific primers generated a ~1070 bp amplification product. M=HyperLadder I.

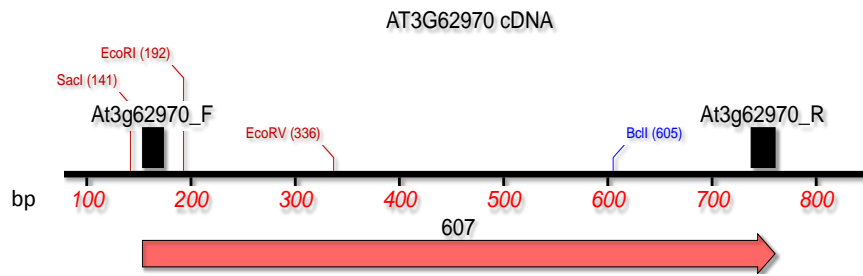


Figure 4.16 Localization map of SALK_106671 with *At3G62970* gene-specific primers. Arrow represents the direction of the coding sequence of the gene. Black squares show the position of forward and reverse primers used for expression analysis.

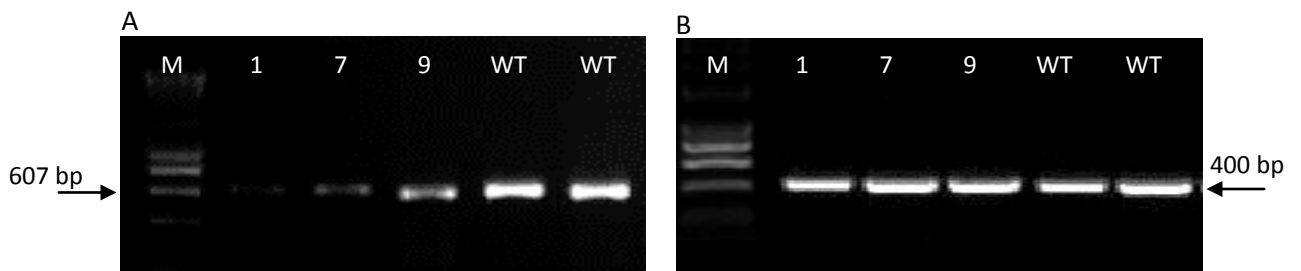


Figure 4.17 (A) RT-PCR expression analysis for three individual plants of Salk_106671 insertion line using forward and reverse *At3G62970* gene-specific primers (Figure 4.16 and Table 4.3). Low expression was shown in samples 1, 7 and 9 as compared with the WT (*Col*). Samples 1, 7 and 9 and WT showed gene expression, albeit at a reduced level, of an expected size of ~607 bp. (B) RT-PCR expression analysis of the *ACTIN7* house-keeping gene in the SALK_N591349 insertion line using the ACT7F and ACT7R primers. The latter gene showed expected size ~400 bp. All samples showed equivalent levels of expression. M=HyperLadder I.

4.3.2 GENERAL MORPHOLOGY OF THE SALK INSERTION LINES

The four SALK mutant insertion lines were analysed for changes in their phenotype. All mutants of *At5g25560* (*chy*⁻), *At1g47128* (*rd21*⁻), *At1g08320* (*bzip*⁻) and *At3g62970* (*c3hc4*⁻) exhibited normal vegetative growth and induction of flowering (Figure 4.18). They were also fertile, with long siliques containing seeds as in the wild type *Col* (Figure 4.19). Anthers from open flowers of the SALK lines were stained red with Alexander pollen viability stain (Section 2.6.1), indicating the presence of viable pollen. All the SALK knockout mutants analysed (Figure 4.20B, C, D and E) dehisced normally at the same time as the wild type *Col* (Figure 4.20A). Generally, morphology of the different lines appeared normal as in the wild type suggesting that each of the four genes might have no major effect on plant fertility, or that they might act redundantly with other genes involved in pollen development.

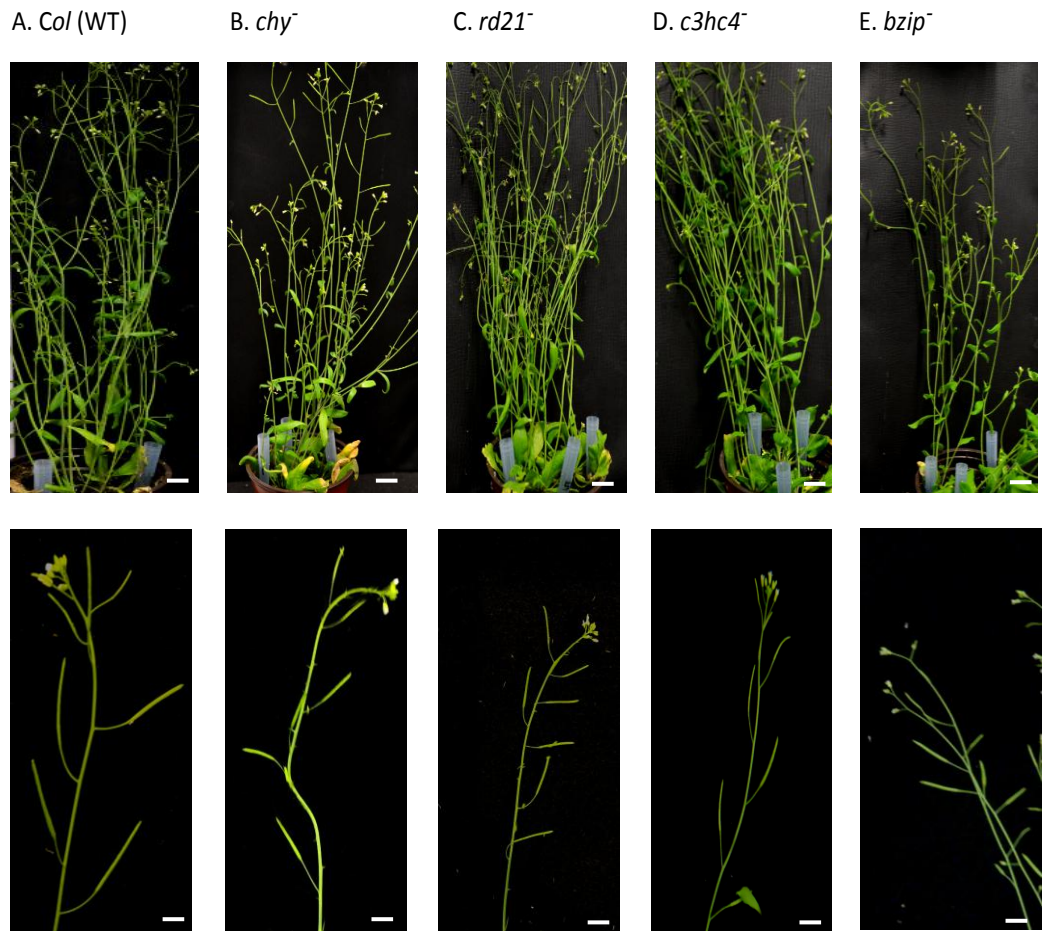


Figure 4.18 General plant morphology of the homozygous SALK insertional lines. Images were taken after 36 days of growth. The general morphology of all mutants (B-E) appeared similar to the wild type *Col* (A). Scale bar = 0.25 cm.

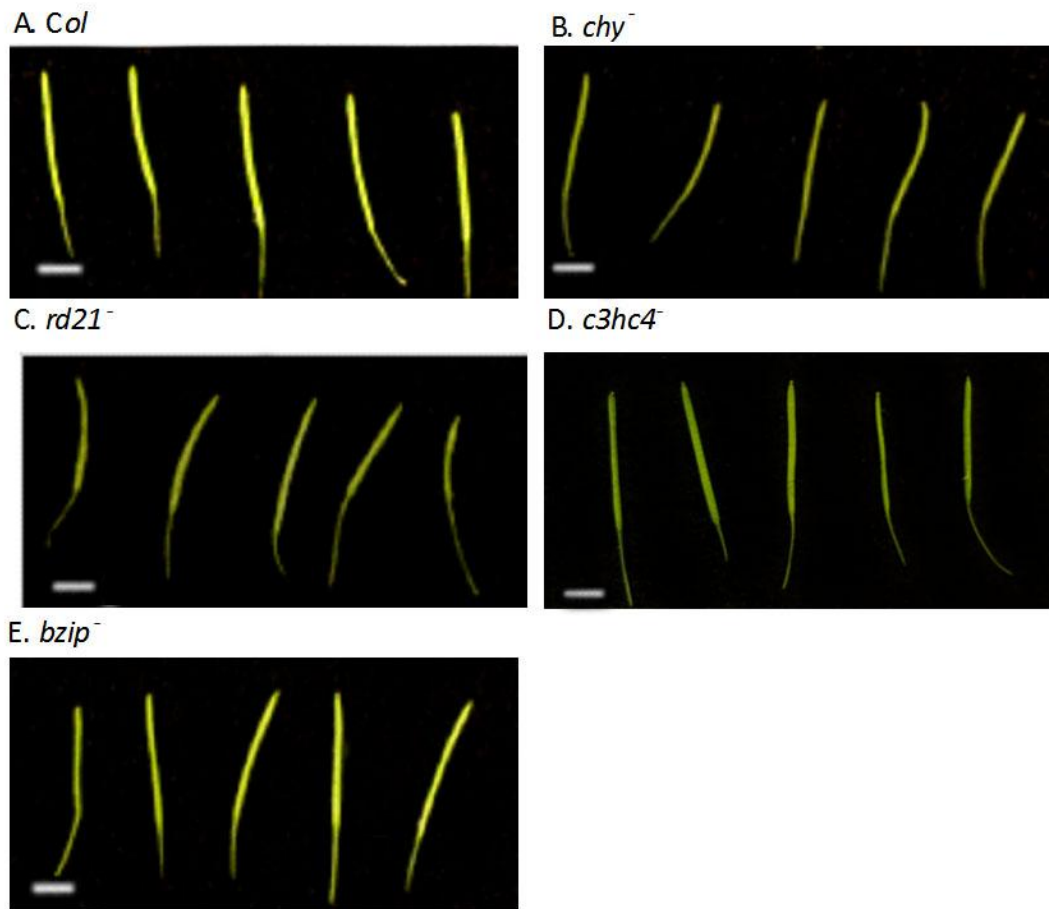


Figure 4.19 The siliques from primary inflorescences of different insertional mutants (B-E) taken after 36 days of growth as compared with the wild type *Col* (A). Scale bar = 0.5 cm.

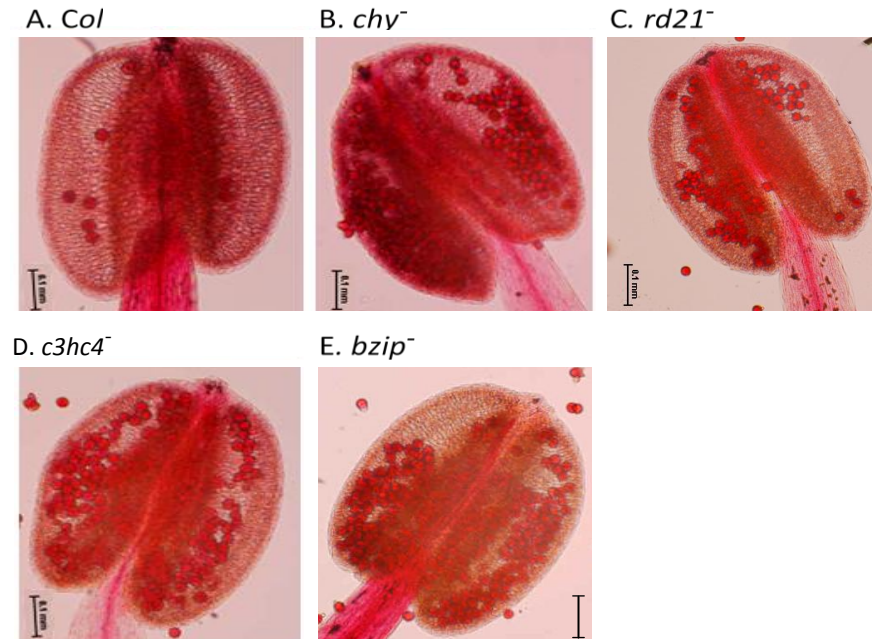


Figure 4.20 *Arabidopsis* anthers of the different mutants (B-E) which were capable of producing viable dehisced pollen as compared with the wild type (*Col*) (A) scale bar = 0.1 mm.

4.3.3 OVER-EXPRESSION LINES

Over-expression constructs were prepared using entry clones pENTR D TOPO vectors (APPENDIX III) *At1g47128*, *At3g62970*, *At1g08320* and *At3g47620*. These constructs were transferred into the vector pGWB402Ω, which possesses a promoter containing P2x35sΩ elements.

4.3.3.1 GENOTYPING ANALYSIS

Plant lines carrying the over expression constructs pGWB402Ω-*At3g62970*, pGWB402Ω-*At3g47620*, pGWB402Ω-*At1-g08320* and pGWB402Ω-*At1g47128* were identified by genomic PCR (Section 2.9.1) (Figures 4.21, 4.22, 4.23 and 4.24, respectively) using a gene specific primer for each gene as a reverse primer (APPENDIX II) and a Forward primer from the CaMV35S promoter (35S_For) to confirm the over-expression transgenic plants.

4.3.3.2 EXPRESSION ANALYSIS OF TRANSGENIC PLANTS

RT-PCR expression analysis from buds was used to determine levels of transgene expression. The expression in the buds showed an increase in transgenic plants pGWB402 Ω -At3g62970, pGWB402 Ω -At3g47620, pGWB402 Ω -At1g08320 and pGWB402 Ω -At1g47128 compared with the wild type *Ler* (Figures 4.25A, 4.26A, 4.27A and 4.28A, respectively). Expression level appeared higher compared with wild type *Ler* when normalized using *ACTIN7* expression (Figure 4.25B, 4.26B, 4.27B and 4.28B).

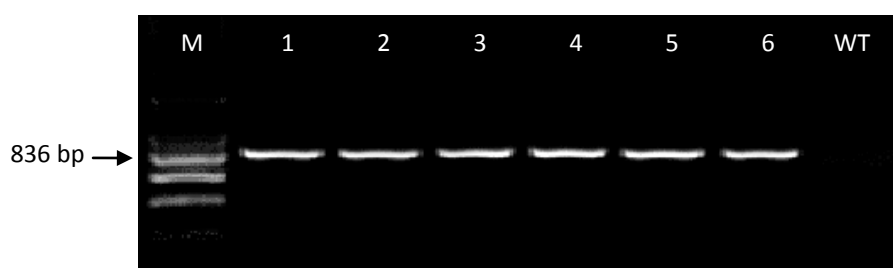


Figure 4.21 PCR confirmation of the presence of over-expressed transgene in plant leaf material using pGWB402 Ω At3g62970 (970R) as a reverse primer and 35SF as a forward primer (APPENDIX II). Plants 1-6 were identified as transgenic as compared with the WT (*Ler*) using genomic DNA as a template. Expected band size is ~836 bp. M=HyperLadder I.

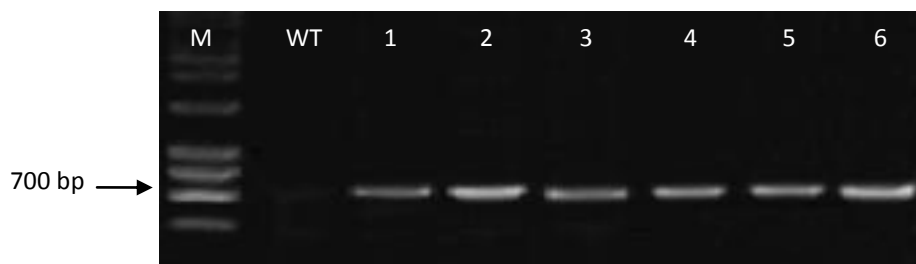


Figure 4.22 PCR confirmation of the presence of over-expression transgene in plant leaf material using pGWB402 Ω At1g47620 (620R) as a reverse primer and 35SF as a forward primer (APPENDIX II). Plants 1-6 were identified as transgenic as compared with the WT (Ler) using genomic DNA as a template. Expected band size is \sim 700 bp. M=HyperLadder I.

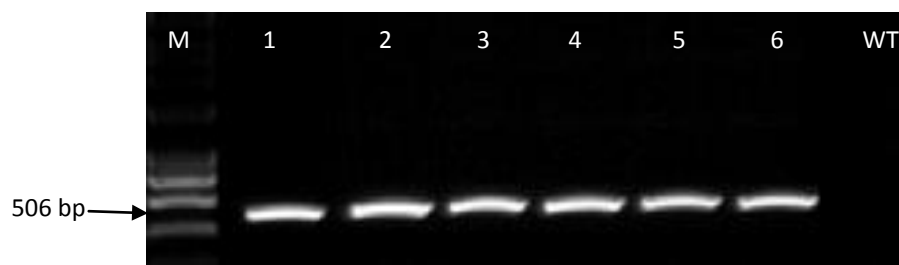


Figure 4.23 PCR confirmation of the presence of over-expression transgene in plant leaf material using pGWB402 Ω At1g08320 (320R) as a reverse primer and 35SF as a forward primer (APPENDIX II). Plants 1-6 were identified as transgenic as compared with the WT (Ler) using genomic DNA as a template. Expected band size is \sim 506 bp. M=HyperLadder I.

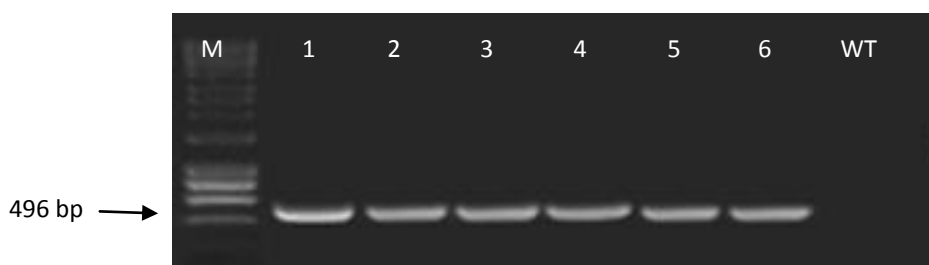


Figure 4.24 PCR confirmation of the presence of over-expression transgene in plant leaf material using PGWB402 Ω At1g47128 (128R) as a reverse primer and 35SF as a forward primer (APPENDIX II). Plants 1-6 were identified as transgenic as compared with the WT (Ler) using genomic DNA as a template. Expected size is \sim 496 bp. M=HyperLadder I.

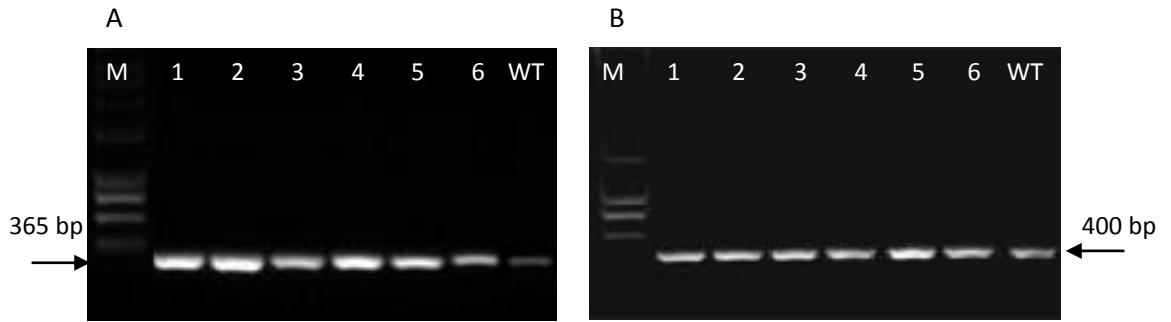


Figure 4.25 (A) RT-PCR expression analysis of *At3g62970* in the PGWB402 Ω *At3g62970* transgenic lines (samples 1-6). PCR products were amplified from cDNA buds as a template using forward and reverse gene-specific primers. Expected band size is \sim 365 bp. (B) RT-PCR using *ACTIN7* gene (ACT7F and ACT7R) primers to normalize expression in the transgenic lines as compared with the WT (*Ler*). Expected band size is \sim 400 bp (APPENDIX II). M=HyperLadder I.

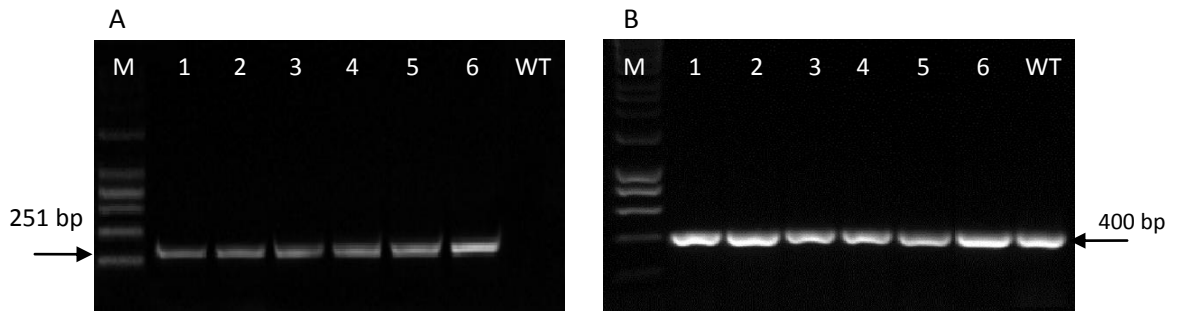


Figure 4.26 (A) RT-PCR expression analysis of *At1g47620* in the PGWB402 Ω *At1g47620* transgenic lines (samples 1-6). PCR products were amplified from cDNA buds as a template using forward and reverse gene-specific primers. Expected band size is \sim 251 bp. (B) RT-PCR using *ACTIN7* gene (ACT7F and ACT7R) primers to normalize expression in the transgenic lines as compared with the WT (*Ler*). Expected band size is \sim 400 bp (APPENDIX II). M=HyperLadder I.

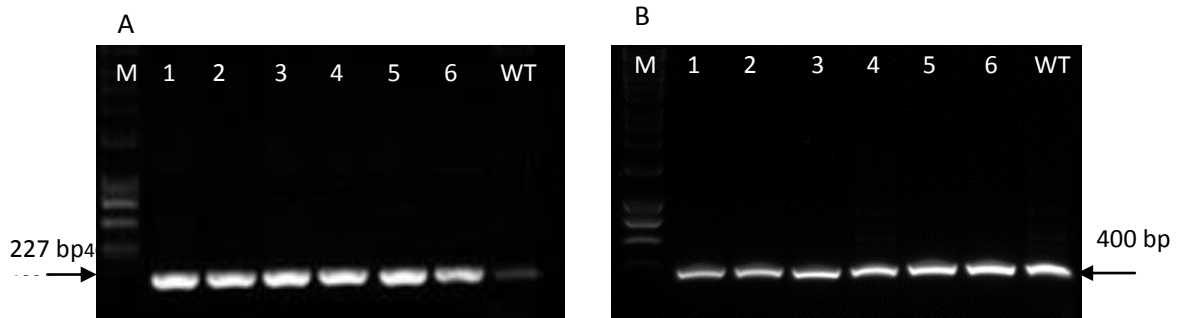


Figure 4.27 (A) RT-PCR expression analysis of *At1g08320* expression in the PGWB402 Ω -1g08320 transgenic lines (samples 1-6). PCR products were amplified from cDNA buds as a template using forward and reverse gene-specific primers. Expected band size is \sim 227 bp. (B) RT-PCR using *ACTIN7* gene (ACT7F and ACT7R) primers to normalize expression in the transgenic lines as compared with the WT (*Ler*). Expected band size is \sim 400 bp (APPENDIX II). M=HyperLadder I.

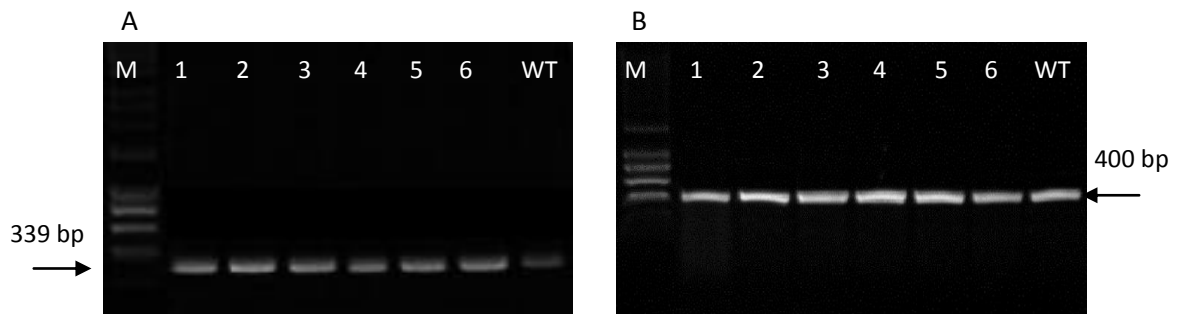


Figure 4.28 (A) RT-PCR expression analysis of *At1g47128* in the PGWB402 Ω -1g47128 transgenic lines (samples 1-6). PCR products were amplified from cDNA buds as a template using forward and reverse gene-specific primers. Expected band size is \sim 339 bp. (B) RT-PCR using *ACTIN7* gene (ACT7F and ACT7R) primers to normalize expression in the transgenic lines as compared with the WT (*Ler*). Expected band size is \sim 400 bp (APPENDIX II). M=HyperLadder I.

Quantitative RT-PCR (QRT-PCR) was also performed to confirm the over-expression of the transgenes in the transgenic plants (Figure 4.29) using gene-specific primers (APPENDIX II). The results showed that transgenic plants had a higher level of expression of the respective genes in the transgenic lines harbouring the expression constructs pGWB402Ω-At3g47620, pGWB402Ω-At1g08320 pGWB402Ω-At1g47128 and pGWB402Ω-At3g62970, ranging from 2 - 4.8 fold, as compared with the wild type (Ler) (Figure 4.29).

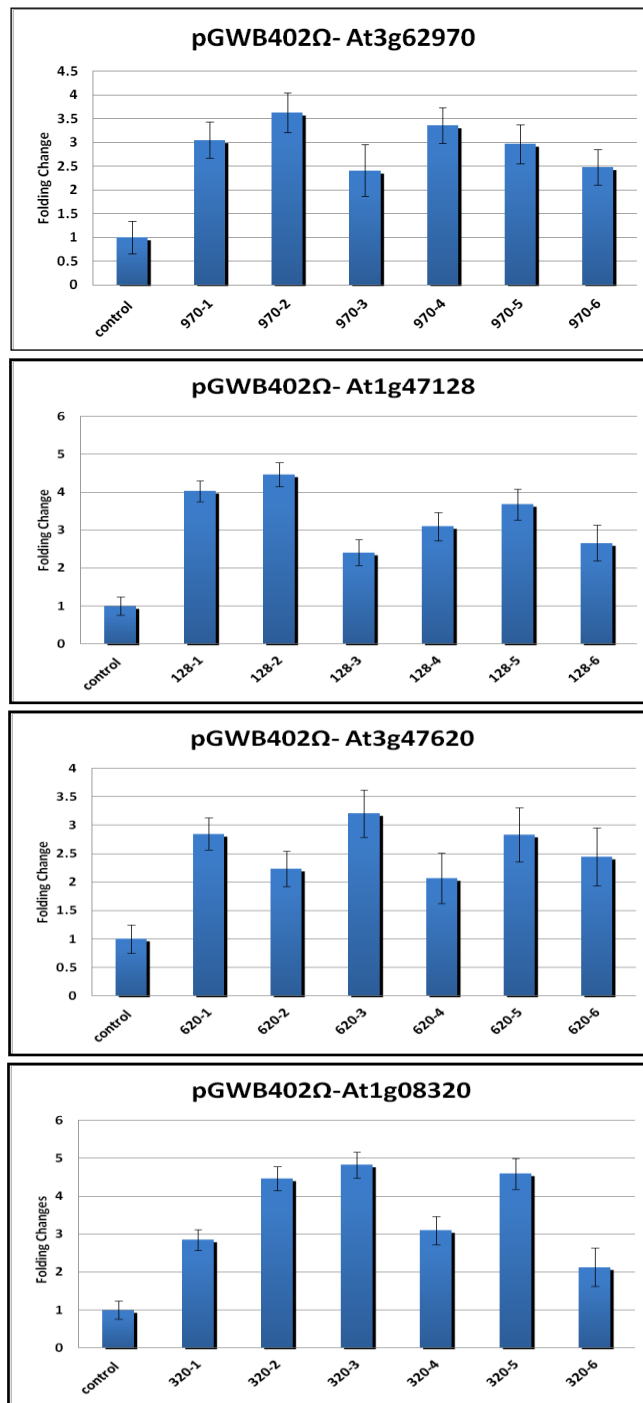


Figure 4.29 Quantitative RT-PCR (QRT-PCR) used to determine the levels of expression of the respective genes in transgenic lines harbouring the over-expression constructs pGWB402Ω-At3g62970, pGWB402Ω-At1g47128, pGWB402Ω-At3g47620 and pGWB402Ω-At1g08320 as compared with the *Ler* used as a wild type control.

4.3.3.3 PHENOTYPING ANALYSIS OF OVER-EXPRESSION (OEx) LINES

Phenotypic analysis of over-expression (OEx) lines was conducted by general growth observations of 15-day-old plants leaves. The results showed enhanced vegetative development in leaf size in the transgenic lines as compared with the WT (*Ler*) control (Figure 4.30). No clear explanation can be given for the OEx plants being larger in growth than the WT. Anthers from open flowers of the OEx lines stained with acridine orange (Section 2.6.3) indicated normal secondary thickening as compared with the wild type (*Ler*) (Figure 4.31). Staining of lignin stem sections of 30-day-old OEx plants was conducted using phloroglucinol HCl (Section 2.6.2). Tissues of OEx lines produced normal xylem development and lignin deposition as compared to the wild type (*Ler*) (Figure 4.32).

A. WT (*Ler*)



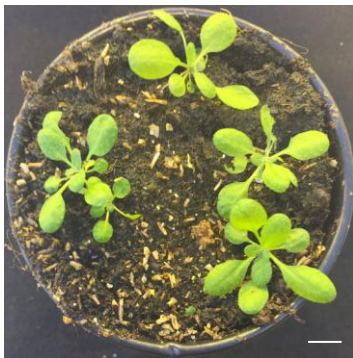
B. pGWB402 Ω At3g62970



C. pGWB402 Ω At1g47128



D. pGWB402 Ω At1g08320



E. pGWB402 Ω At3g47620



Figure 4.30 General growth of 15-day-old OEx plants containing the four transgenes (B-E) as compared to the wild type (*Ler*) (A). Scale bar = 1 cm.

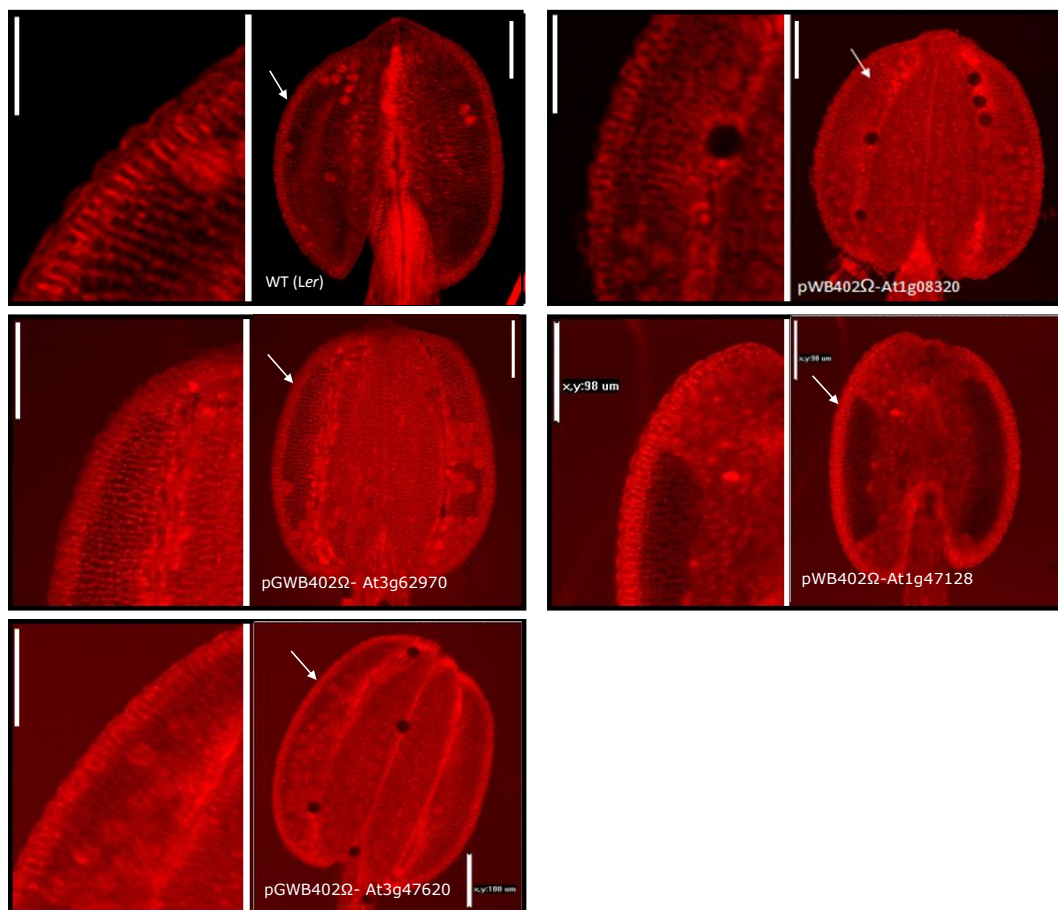


Figure 4.31 Anther secondary thickening (indicated by arrows) in endothecium of the OEx plants as compared to the wild type (Ler). Scale bar = 100 μm.

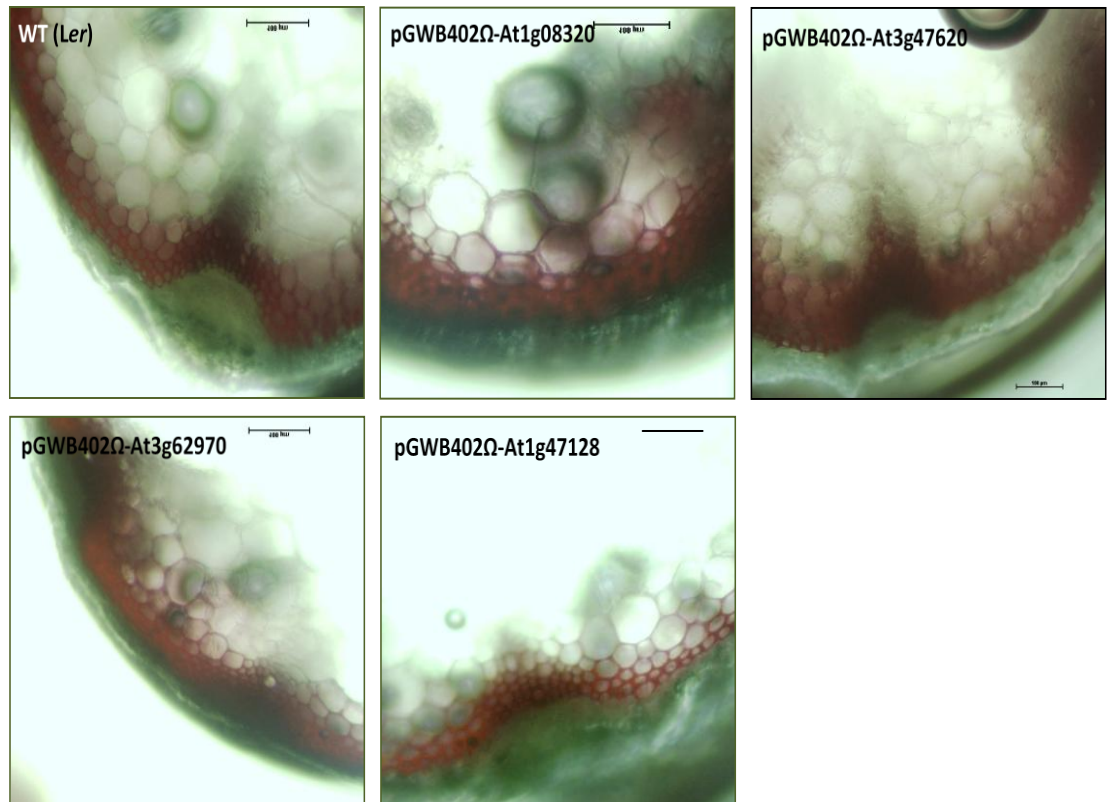


Figure 4.32 Lignin stain in stems of the OEx plants as compared to the wild type (Ler). Scale bar = 100 μ m.

4.3.4 AT3G62970 AND AT1G47128 GENE SILENCING CONSTRUCTS

4.3.4.1 GENOTYPIC AND EXPRESSION ANALYSIS OF 970^{RNAi} and 128^{RNAi} LINES

RNAi gene silencing constructs were prepared for the *Y2H970^{RNAi}* and *Y2H128^{RNAi}* genes using the destination vector pK7GW1WG2 (II) (Karimi *et al.*, 2005). Previously T-DNA insertions in these two genes had been shown to have maintained gene expression via RT-PCR albeit at different levels. This was possibly since they were inserted into the intron regions and may have been spliced out along with the introns during post-transcriptional processes. Furthermore, lignin staining indicated regular lignification when the genes

were over-expressed as compared to the WT control. Therefore, silencing of these two genes was conducted via RNAi in order to determine the effect of down-regulation of the expression of these two genes. Individual T1 plants were analysed by PCR to confirm the presence of *At3g62970^{RNAi}* and *At1g47128^{RNAi}* transgenes. For the first transgene, *At3g62970^{RNAi}R* (reverse) and 35SF (forward) primers were used for PCR of sense insertion and *At3g62970^{RNAi}F* (forward) and PK7F (forward) primers for PCR of the antisense insertions (APPENDIX II) (Figure 4.33A and B). For the second transgene, *At1g47128^{RNAi}R* (reverse) and 35SF (forward) primers were used for PCR of sense insertion and *At1g47128^{RNAi}F* (forward) and PK7F (forward) primers for PCR of antisense insertions (APPENDIX II) (Figure 4.34A and B).

QRT-PCR was performed on the same T1 individuals to confirm the expression levels of *At3g62970^{RNAi}* and *At1g47128^{RNAi}* genes in inflorescences of the transgenic plant lines. The results in Figure 4.35A showed that the expression was significantly decreased in three out of four T1 transgenic lines for each transgene as compared to the wild type (*Ler*). Two of them showed greater decrease of expression, hence, might be homozygous. Those homozygous lines were selfed and the results of QRT-PCR obtained at T2 generation were similar to those of their respective T1 individuals (Figure 4.35B and C).

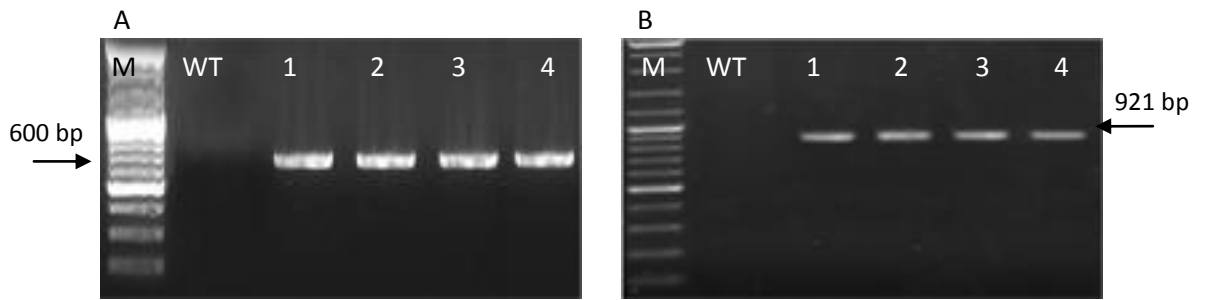


Figure 4.33 Genotyping of T1 transformed plants carrying the *At3g62970^{RNAi}* transgene. (A) PCR of sense insertion using the *At3g62970^{RNAi}R* with 35SF primers to recover size of 600 bp 1 and 2 representing line 7, samples 3 and 4 representing line 9. (B) PCR of antisense insertion using *At3g62970^{RNAi}F* with PK7F primers to generate a band size of 921 bp. The Wild type (*Ler*) resulted no amplification in the two PCRs. M=HyperLadder II.

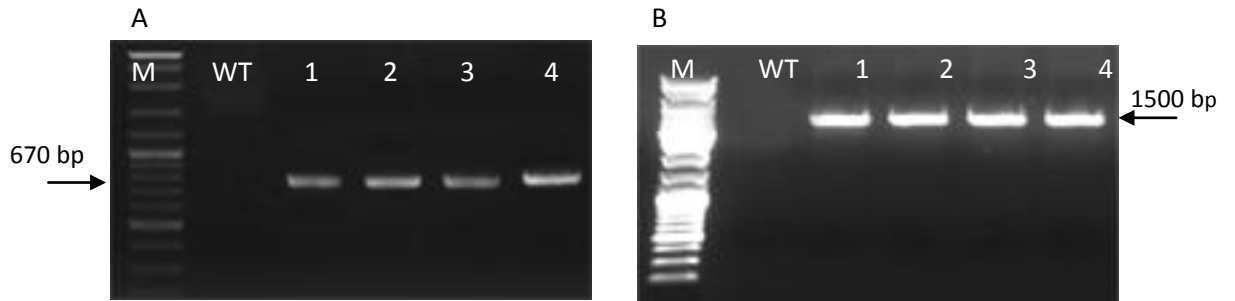
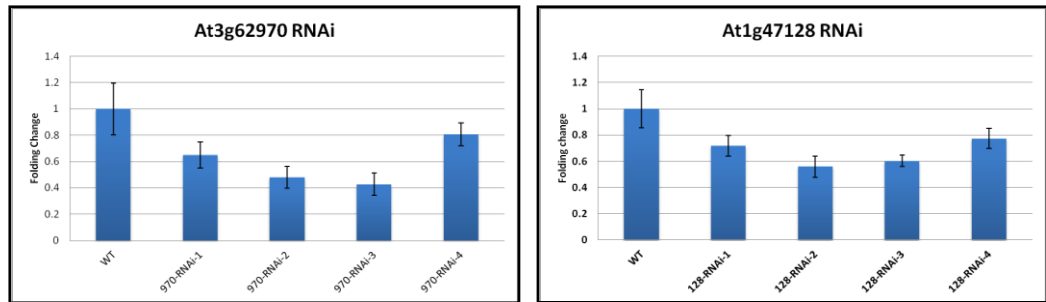


Figure 4.34 Genotyping of T1 transformed plants carrying the *At1g47128^{RNAi}* transgene. (A) PCR of sense insertion using the *At1g47128^{RNAi}R* with 35SF primers to recover size of 670 bp. 1 and 2 representing line 7 samples 3 and 4 representing line 10 (B) PCR of antisense insertion using *At1g47128^{RNAi}F* with PK7F primers to generate a band of 1500 bp. The Wild type (*Ler*) resulted in no amplification in the two PCRs. M1=HyperLadder II. M2=HyperLadder I.

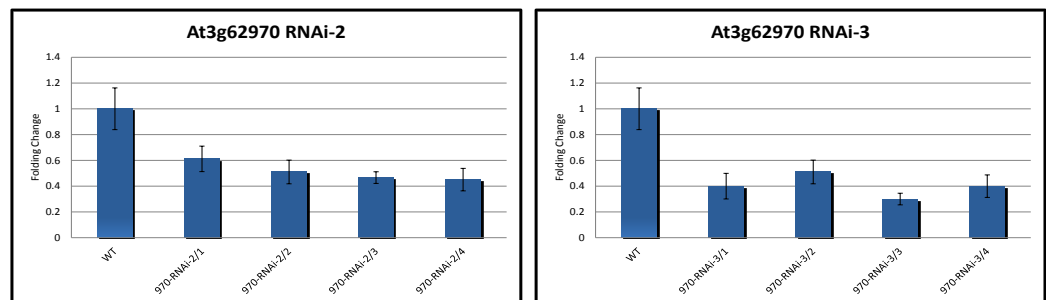
4.3.4.2 PHENOTYPING ANALYSIS OF 970^{RNAi} and 128^{RNAi} LINES

Plants of the RNAi line *At3g62970^{RNAi}* were fertile and normal seed set occurred as compared to that of the wild type (*Ler*) (Figures 4.36 and 4.37). The same data were generated for plants of the RNAi line *At1g47128^{RNAi}*. These data confirms the previous finding of T-DNA lines where gene mutants resulted in no change in plant fertility. Anthers from open flowers of the two RNAi lines stained with Alexander stain (Section 2.6.1) indicated the presence of viable pollen equivalent to those of the wild type (*Ler*) (Figure 4.38A, B and C) (Table 4.4) and showed normal dehiscence (Figure 4.37).

A. T1 generation



B. *At3g62970*^{RNAi} (T2 generation)



C. *At1g47128*^{RNAi} (T2 generation)

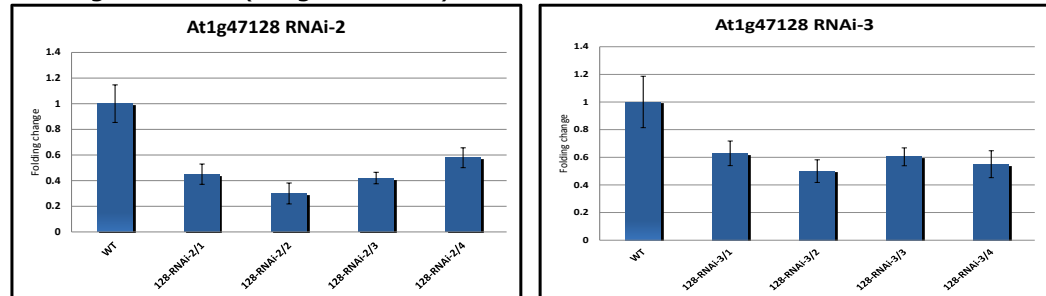


Figure 4.35 Quantitative RT-PCR of transgene expression in RNAi transgenic lines with *At3g62970*^{RNAi} and *At1g47128*^{RNAi} transgenes at T1 (A) and T2 (B and C) generations using *At3g62970*^{RNAi}F/R primers and *At1g47128*^{RNAi}F/R primers, respectively, as compared to the wild type(Ler) genes. Four transgenic events for each transgene were used in the T1 generation (A), of which two of them (events 2 and 3) with the lowest gene expression due to RNAi were proceeded to the T2 generation and four individuals from each gene family were tested (B and C).

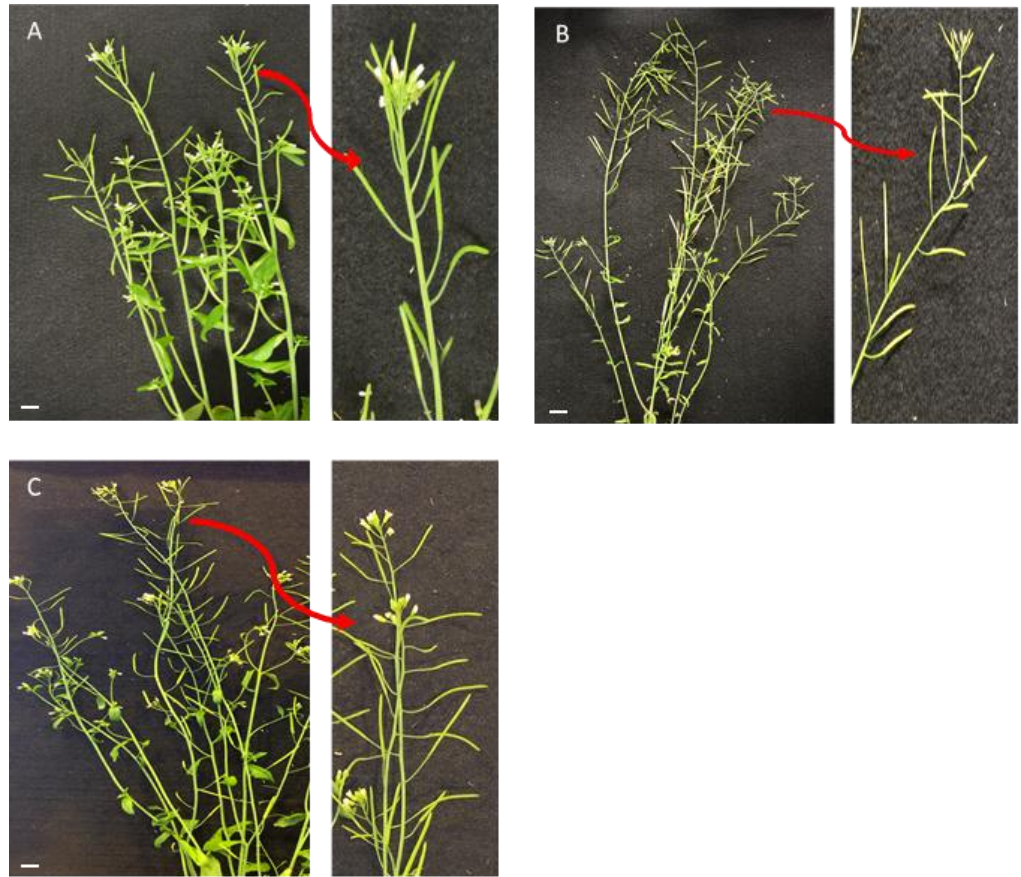


Figure 4.36 General plant morphology and silique formation of T1 RNAi lines *At3g62970^{RNAi}* and *At1g47128^{RNAi}* (lanes B and C, respectively). The two RNAi lines were fertile and set seeds equivalent to those of the wild type (A, *Ler*). Scale bar = 1 cm.



Figure 4.37 Anther dehiscence from T1 RNAi *At3g62970*^{RNAi} lines 7 and 9 (B and C, respectively), and *At1g47128*^{RNAi} lines 7 and 10 (D and E, respectively) as compared to that of the wild type (Ler) (A). Scale bar=50 μ m.

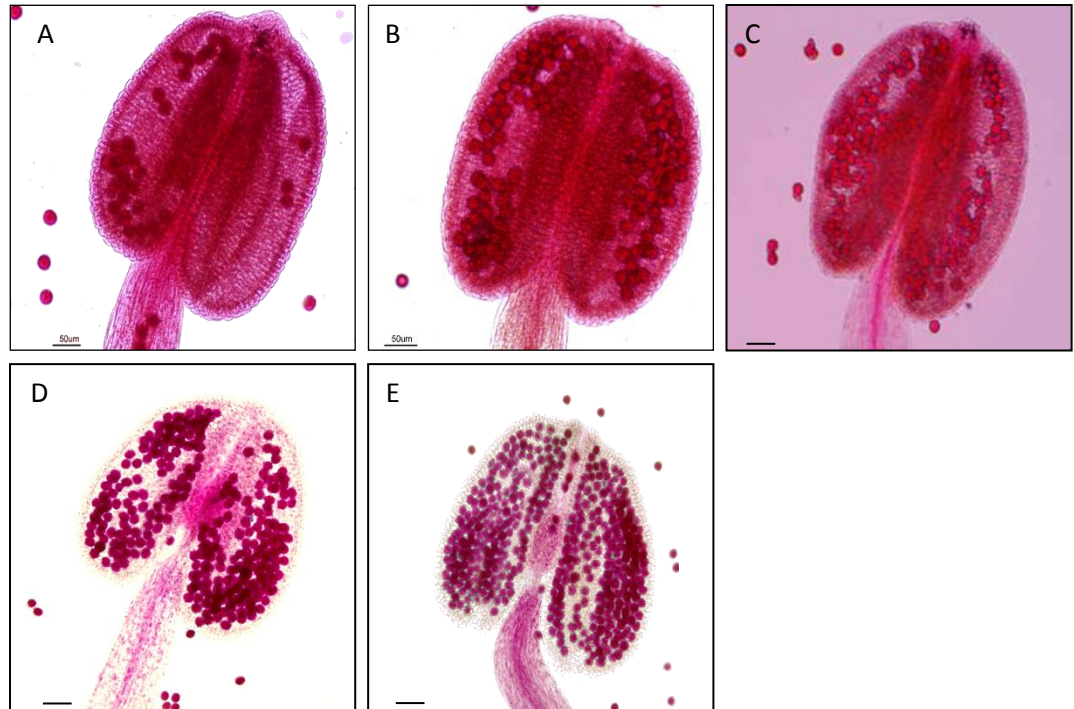


Figure 4.38 Anthers from T1 RNAi *At3g62970*^{RNAi} lines 7 and 9 (B and C, respectively), and *At1g47128*^{RNAi} lines 7 and 10 (D and E, respectively) stained with Alexander pollen viability stain. The anthers contained viable dehiscence pollen equivalent to that of the wild type (Ler) (A) as well as to their respective T-DNA lines. Scale bar=50 μ m.

4.3.5 SUMMARY OF SALK LINES INSERTIONAL

MUTANT AND RNAi LINES ANALYSIS

Data from the genotyping and phenotyping of T-DNA insertional mutants and RNAi Lines of *At1g47128*^{RNAi} and *At3g62970*^{RNAi} are summarized in Table 4.4. However, no expression was seen in the *At1g08320* and *At5g25560* insertion lines. However, the different SALK homozygous lines analysed had normal growth characteristics as compared with the wild type *Col*. In addition, the two RNAi lines silenced for *At1g47128* and *At3g62970* genes were also fertile and set normal seeds equivalent to those of the wild type *Ler* indicating that the different candidate genes under study may have no major or direct effect on anther dehiscence, or might act redundantly with other genes in this pathway.

Table 4.4 Summary of Analysis of insertional mutants and RNAi Lines.

Gene	Gene ID	SALK mutant lines	Insertion lines/Total plants analysed	Expression of gene in mutant or RNAi	Phenotype
Y2H970 C3HC4-type RING finger	At3g62970	SALK- N606671 <i>At3g62970^{RNAi}</i>	13/16	Yes	fertile, pollen released and silique contains seeds
Y2H320 is belong to the bZIP family	At1g08320	SALK- N591349	10/10	No	
Y2H128 is a cysteine proteinase	At1g47128	SALK- N590551 <i>At1g47128^{RNAi}</i>	2/12	Yes	
Y2H560-type Zinc finger protein	At5g25560	SALK_508223	7/7	No	

4.3.6 LOCALIZATION OF EXPRESSION OF *AT1G08320* PROMOTER IN DIFFERENT TISSUES

A promoter: β -glucuronidase gene (*GUS* or *uidA*) fusion was constructed to detect the tissue-specific expression pattern of *At1g08320* gene in different tissues as described by Jefferson *et al.* (1987). The reason for choosing *At1g08320* gene for Promoter::*GUS* fusion construction for localization of *GUS* expression is that it had been shown to be the closest distance (5.81 nm) to MYB26 via FRET analysis as compared to the other Y2H genes (Section 3.3.2). The upstream region (3 Kb) of the *At1g08320* gene was fused to the *GUS* reporter gene in pGWB433 and transformed into *Arabidopsis* WT plants (Ler) (Section 4.2.4).

Transgenic plants were identified by gDNA PCR (Figure 4.39) using the forward gene specific primer (320F) of the Y2H320 promoter and *GUS* reverse primer (*GUS*-R) of the *GUS* gene (APPENDIX II). Expression of *Prom320:GUS* was shown only in floral tissues, with signals observed in the inflorescence

(Figure 4.40A), and anthers (Figure 4.40B). It appears that strong expression signal was detected in the pollen (Figure 4.40 C), whereas, weak GUS expression was shown in nectaries, in the siliques, flowers and in the leaves (Figure 4.40D, E and F).

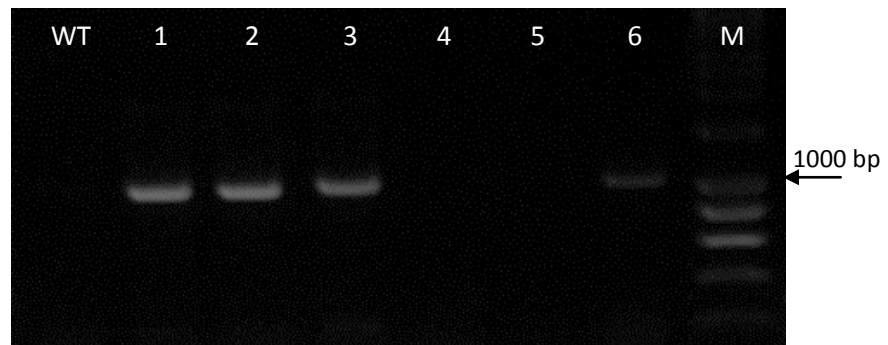


Figure 4.39 Genotypic analysis of pGWB433-At1g08320 transgenic plants using gene specific primer 320F as a forward primer and pGWB433 GUS as a reverse primer (APPENDIX II). Plants 1, 2, 3 and 6 contained the transgenes as indicated by the amplification of a band with the expected size of ~1000bp. WT (*Ler*) plant was used as a negative control. M=HyperLadder I.

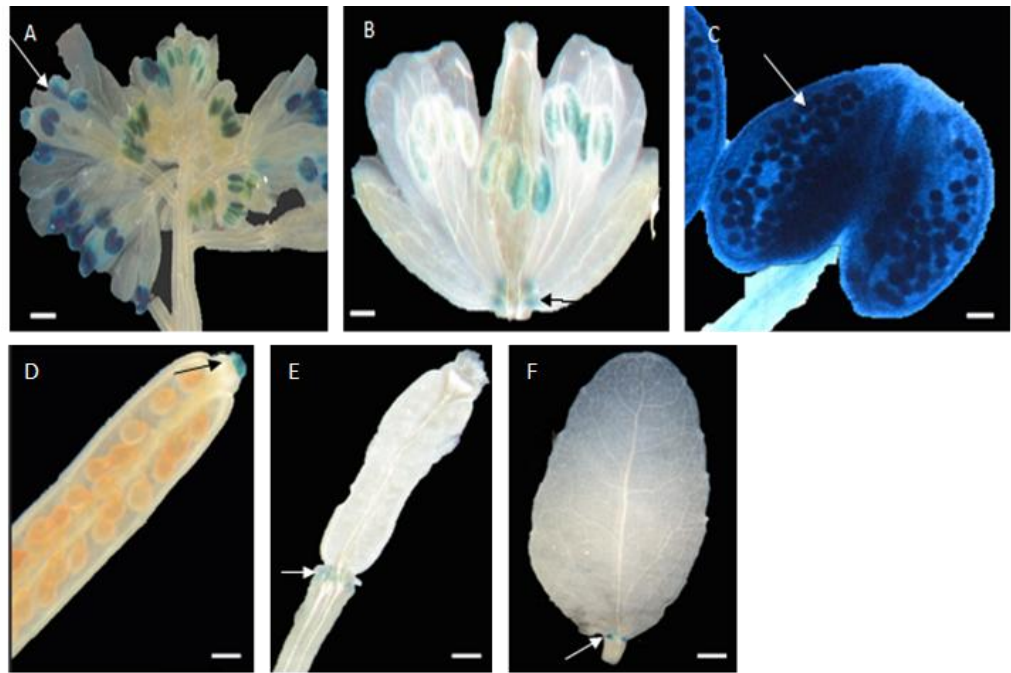


Figure 4.40 Expression of Prom320::GUS fusion in transgenic plants. Expression was observed in the inflorescence (A), anthers and nectaries (B), pollen (C), while weak signals of expression were shown in the silique (D), nectaries (E) and in the young leaves (F). Arrows indicated stained tissues as an indication of *GUS* gene expression. Scale bar = 1 μ m.

4.4 DISCUSSION AND CONCLUSION

Analysis of the *myb26* mutant revealed the same previously reported phenotypic analysis (Yang *et al.*, 2007) as the mutant showed that the vegetative phenotype was similar to that of the wild type (*Ler*), but *myb26* mutant differed in the failure of expansion of the siliques and lack of seeds. The *ms35* mutant had short siliques, which were devoid of seeds and the anther produces pollen but was indehiscent. The endothecium fails to expand and shrinkage of the anther walls does not occur in the mutant, which results in failure of pollen release (Dawson *et al.*, 1999). Previous studies showed that anther wall expansion and lignified secondary thickening occur in the endothecium during pollen mitosis (Sanders *et al.*, 1999). *MYB26* plays an important role during development of the endothecium, by determining cell fate in the endothecium prior to secondary wall biosynthesis (Yang *et al.*, 2007).

In the present study, morphological observations of fertility were conducted in SALK mutants, RNAi lines and over-expression lines corresponding to the genes encoding proteins that putatively interacted with *MYB26*. Analysis of the homozygous insertion lines for changes in their phenotype and expression levels showed that the T-DNA insertion changed gene expression levels. Two out of the four genes analysed, *At5g25560* (SALK_008223) and *At1g08320* (SALK_091349), showed complete loss of expression in the RT-PCR analysis due to the presence of T-DNA insert (Figures 4.5A and 4.13A). However, the other two genes, *At1g47128* (SALK_090551), and *At3g62970* (SALK_106671), were still expressed (Figures 4.9A and 4.17A). The map of the insertion sites in these two genes indicated that these two genes were unlikely to be knocked out as the inserts are located in the intervening

sequences or introns. The latter is therefore likely to be spliced out during the post-transcriptional processes and thus unlikely to interfere with the final transcripts being expressed. Nevertheless, none of the SALK mutant lines showed alterations in fertility or obvious defects in development. The same lack of phenotypic changes were also observed by reducing the expression of the *At1g47128* and *At3g62970* genes by silencing using an RNAi approach, however some residual expression was still maintained in these lines.

Despite the T-DNA insertion lines for *At5g25560* and *At1g08320* being homozygous with no evident expression of these genes, the lines did not show significantly altered phenotypes, and, in particular, no effect on male fertility was observed (Figures 4.18, 4.19 and 4.20). All SALK knockout lines appeared to be fully fertile and produced viable pollen as those of the WT (*Col*) (Figures 4.18, 4.19 and 4.20). This may be due to the possible occurrence of gene redundancy in which other gene family members might function in the absence of the mutated/knocked out gene. There is also a possibility that the genes under study might not be linked to the *myb26* pathway. An other explanation can be the minor additive influence of the genes under study. Therefore, there is a possibility that occurrence of double mutants with *myb26* might have a greater influence and results in a change in the phenotype and male fertility. An additional approach that could be utilized to determine if these transcription factors are involved in this pathway is to make alternative constructs to analyse gene function by inclusion of a motif into a transcription factor that can convert it into a repressor. Examples of these motifs include SRDX (plant-specific EAR-motif repression domain) (Mitsuda and Ohme-Takagi, 2009). Mutants can also be generated using novel techniques such as

targeted mutagenesis by TALENs (Transcription Activator-like Effectors) (Sun and Zhao, 2013) or CRISPRs-Cas9 (Clustered Regularly Interspaced Short Palindromic Repeats-Cas9) (Ran *et al.*, 2013), which guide RNA to activate specific endogenous genes.

RNAi has been used as a research tool to discover the functions of genes (Eamens *et al.*, 2008). It has been shown to be an effective mechanism for gene silencing in many organisms, including several agriculturally significant plants (Eamens *et al.*, 2008). However, in many cases transgenic lines may only carry one of the two inserts (Kerschen *et al.*, 2004), therefore, the RNAi constructs were carefully selected and checked in the present study for the presence of both the sense and antisense insertions. RNAi T1 transgenic lines analysed showed the presence of the *At3g62970^{RNAi}* and *At1g47128^{RNAi}* inserts (Figure 4.33A and B). Quantitative RT-PCR analysis of expression in the *At3g62970^{RNAi}* and *At1g47128^{RNAi}* transgenic lines indicated that the expression was significantly decreased as compared to that of the wild type *Col* (Figure 4.35A and 4.35B). Nevertheless, phenotype of plants harbouring either *At1g47128^{RNAi}* or *At3g62970^{RNAi}* insert was fertile and seed setting still occurred (Figures 4.36, 4.37A, B and C). Anthers from open flowers indicated the presence of dehiscence with released pollen as seen in the wild type (*Ler*) (Figure 4.38A, B and C).

RNAi lines are frequently knocked down, rather than knocked out, for the target gene expression (Yin *et al.*, 2005), then, the expression of the gene is likely to be reduced but some expression can still be maintained. Some expression was still observed in the RNAi lines. This incomplete silencing may

explain the presence of normal viable pollen and occurrence of fertility in the RNAi lines.

Over-expression analysis was conducted to determine if this would alter the process of dehiscence or secondary thickening. High expression (2 - 4.8 fold) of the pGWB402Ω-At3g62970, pGWB402Ω-At1g08320, pGWB402Ω-At1g47128 and pGWB402Ω-At3g47620 transcripts was observed as compared with the wild type *Ler* (Figures 4.25-4.28). Quantitative RT-PCR was performed to examine the expression level of OEx lines. The results indicated higher expression levels and a different performance of the plants in different OEx lines as compared with the wild type (*Ler*) (Figures 4.29 and 4.30). PGWB402Ω was reported to carry a modified CaMV35s promoter in which the enhancer regions are duplicated. Therefore, it is suitable for gene over-expression (Nakagawa *et al.*, 2007). Transgenic plants over-expressing the transgenes in the present study showed a different phenotype as compared with the wild type (*Ler*), although, no differences were observed in secondary thickening of their anthers in endothecium as compared with the wild type (*Ler*) (Figure 4.31). In addition, lignification of the stem in the four OEx lines was shown normal as compared to that of the wild type (*Ler*) (Figure 4.32). Over-expression of *MYB26* has been shown to induce ectopic thickening, with a net-like pattern of thickening observed in the leaf epidermis and xylem-like thickening in other tissues. Ectopic thickening was also shown in tobacco when *MYB26* was over-expressed (Yang *et al.*, 2007). This suggests that the putative interacting factors are insufficient to activate the secondary thickening pathway in the anther.

CHAPTER 5: CHARACTERIZATION AND ANALYSIS OF MALE STERILE INDUCED MUTATIONS

5.1 INTRODUCTION

Forward genetics is frequently used as an approach to identify genes of interest in a particular biological process whose genes are defined by phenotypic change in a mutant. This is in contrast to reverse genetics where gene sequences are selectively manipulated and the associated phenotypic changes are investigated. Forward genetics has typically entailed the generation of random mutations in an organism, and then via a series of breeding of subsequent generations, been used to isolate individuals with an aberrant phenotype associated with a mutation at a single locus. The mechanisms to generate such aberrations involve the use of different physical or chemical mutagens. In this study, the approach used was to induce mutations and identify male sterile phenotypes in which the anther fails to proceed through normal dehiscence. Backcrossing of the recovered male sterile mutants with the parental plants and checking for allelism to the *myb26* mutation was subsequently conducted. Crosses were also conducted to enable molecular genetic mapping of one of these mutants.

Jasmonic acid (JA) is thought to control anther dehiscence by regulating degradation of the septum and water transport (Scott *et al.*, 2004). Studies have also shown that mutations linked to the JA pathway can also cause delayed anther maturation and disruption of pollen development (Cecchetti *et al.*, 2008; Cheng *et al.*, 2006). For instance, the *myb108* mutation disrupts JA-mediated stamen maturation and results

in slightly shorter siliques (Mandaoker and Browse, 2008). The involvement of JA in anther dehiscence is supported by the JA signal transduction mutant *coronatine insensitive (coi1)*. Sterility was shown to occur due to non-dehiscence, which cannot be rescued by exogenous jasmonate (Devoto *et al.*, 2002; Xie *et al.*, 1998). The mutant fails to respond to JA treatment because of a failure in the SCF^{COI1}26S proteasome pathway (Katsir *et al.*, 2008) (Section 1.4.1.1).

Previous mutagenesis studies (Wilson's lab, University of Nottingham, UK) using X-rays and EMS identified a number of male sterile mutants (e.g., *c12*, *c20*, *mss*, and *msak*). Several of these mutants had been previously shown to produce viable pollen, but the anthers failed to dehisce. These lines were selected for further analysis of their phenotypes and the characterization of their mutations.

5.2 MATERIALS AND METHODS

5.2.1 PHENOTYPIC AND MICROSCOPIC ANALYSIS OF MUTANTS

Seeds of the M2 and M4 generations of WT plants that had been previously mutagenised by X-rays or EMS (Kalantidis *et al.*, 1994) were obtained from (Wilson's lab, University of Nottingham, UK). These lines were analysed for phenotypes associated with male sterility (lack of silique elongation, seed setting and pollen viability) (Section 2.6.1) (APPENDIX I) as compared to their wild type *Ler* ecotype. To establish whether viable pollen was present, Alexander staining (Alexander, 1969) (Section 2.6.1) was used for testing pollen viability as compared to the wild type *Ler* ecotype.

In order to rescue the M2 male sterile plants and also to test if the sterility was a result of dysfunctional pollen, the M2 male

sterile lines, used as a female parent, were backcrossed with the *Col* parental line, used as the male parent. To ensure that the lines were free from additional mutations and to select the desired mutant lines, the resulting F1 generation was allowed to self to form an F2 segregating population for each mutant. The male sterile lines were then screened for the phenotype in which the mutants should represent one-fourth the numbers of individuals in the F2 generation. For genetic mapping analysis, only male sterile individuals in the F2 generation were investigated.

5.2.2 ANALYSIS OF ANTHER DEVELOPMENT

Male sterile lines (*c12*, *c20*, *mss* and *msak*) were grown under glasshouse conditions (Section 2.1) and compared to WT (*Ler*) for phenotypic changes in pollen development by using Alexander's staining (Section 2.6.1) (APPENDIX I). To visualize anthers and pollen development, *Arabidopsis* inflorescences were fixed and embedded in resin for sectioning. Flowers were selected and immediately placed in 4% (v:v) freshly prepared paraformaldehyde solution (APPENDIX I) and kept on ice. To prevent air bubbles within the samples, vacuum infiltration was performed for 30 min. The fixative was then changed and vials incubated overnight (4°C under rotating). Then, the tissues were washed twice (30 min each) with 1x PBS (APPENDIX I). Fixed inflorescences were immediately dehydrated by treatment with increasing concentration of ethanol, e.g., 30, 50, 70, 90 and 100% (v:v) for 1 h each, except at 100% where samples were left for 2 h (or samples could be left at 70% (v:v) ethanol at 4°C for extended period before carrying on to the 90% ethanol (v:v), if needed). Pre-infiltration of the tissue was carried out using a mixture of ethanol/resin (100 ml of Technovit 7100 resin + 1 g of

Hardener I, solution A) at increasing proportions of resin, e.g., 2:1, 1:1, 1:2 for 1 h, finishing with 100% resin. After leaving the tissue overnight in 100% resin (4°C), material was placed into a capsule and the solution A was replaced by solution B (375 µl of solution A + 25 µl of hardener II). This was conducted as quickly as possible since solution B polymerises immediately in contact with air. Then, after 24 h, the capsule was removed using a blade and samples were placed into a mould orientated to the top. The samples were fixed using the Technovit resin (Technovit 3040, Heraeus Kulzer, Wehrheim, Germany). After 24 h, samples were ready for serial sectioning with a microtome (Model: 5040; Bright Instrument Company, Huntingdon, UK). The block was firmly attached to the balancing head and then the blade. The block was cut into 5.5 µm sections which were placed in clean water to expand the slices. Expanded sections were then recovered from the water using a cover-slip. After drying them using a warm plate (20-25°C), sections were stained using toluidine blue (0.05%, w/v). A drop of toluidine blue was placed on each tissue slice and then left for 30 sec and washed out and a cover-slip was placed on the sample. Slides were then left on a hotplate for drying. After 24 h on the hotplate, a drop of DePex (BHD, Pool, England) was placed on each slide and then covered with a cover-slip. After a further 24 h, the samples were ready for observation (Zeiss microscope).

5.2.3 POLLEN GERMINATION AND POLLEN TUBE GROWTH MEASUREMENTS

Flowers obtained from the different *Arabidopsis thaliana* mutants and WT (*Ler*) were used to examine pollen tube phenotypes. Pollen was harvested from newly opened flowers and placed onto pollen germination medium [1 mM CaCl₂, 1

mM Ca(NO₃)₂, 1 mM MgSO₄, 0.01% (w/v) H₃BO₃, and 18% (w/v) sucrose solidified with 1% (w/v) agar, pH 7.0] (Li *et al.*, 1999) as droplets on slides. The slides were placed into Petri dishes and cultured at 28°C under high humidity. Percentage of germinated pollen grains was determined after 8 h. Pollen growth rate was measured by microscopic analysis.

5.2.4 RESCUE TREATMENT OF MALE STERILE MUTANTS WITH JASMONIC ACID

Plants were grown as previously described (Section 2.1). Once flowering had commenced, the plants were treated with JA at 100 mM (using 250 µl of JA acid in 50 ml of Tween20, v/v) and using Tween20 (v/v) as a negative control. Plants were sprayed with JA/Tween20 solution (5 ml/plant) once every other day for two weeks. Then, plantlets were analysed for fertility and for elongation of the siliques.

5.2.5 TEST FOR ALLELISM AND COMPLEMENTATION

Four male sterile mutants (*c12*, *c20*, *mss* and *msak*) were identified and crossed to the *myb26* mutant to determine whether their mutations were a consequence of a mutation of the *MYB26* gene. Heterozygous plants of the mutant lines (male), which were fertile, were used to cross to the *myb26* homozygous mutant (female) and the resultant population screened for fertility. If the mutant gene is an allele of *myb26* then the resulting ratio of fertility versus sterility should be 1:1. The fertile individuals would be heterozygous for the mutant and its allele *myb26* and the sterile individuals would be the *myb26* homozygotes. If no sterile plants were recovered from the crossing then the mutated gene was expected to be located at a different locus from that of *MYB26*.

5.2.6 MUTATION MAPPING

To generate an approximate map position for the new male sterile mutant(s), a segregating population was generated from a cross between the male sterile homozygous mutant (in *Ler* background) and the *Columbia* (*Col*) ecotype. The F1 generation was allowed to self and the subsequent F2 segregating generation was screened for the presence of male sterile mutants for first-pass mapping. Leaves from the male sterile F2 plants were harvested and used for DNA analysis (Section 2.9.1). The DNA samples were analyzed using 11 markers corresponding to selected polymorphic loci on different chromosomes (Figure 5.1 and Table 5.1) to define genetic linkage between one or more of these markers and the gene(s) under study. The markers were initially confirmed by amplification using gDNAs of *Arabidopsis Ler* and *Col* ecotypes to confirm the sizes and the occurrence of the polymorphisms. Markers that showed a clear polymorphism using the parental lines were then used to amplify DNA from the segregating mapping population. The amplifications from the F2 mapping population of male sterile mutants were compared to those of *Col* and *Ler* to identify recombinants around the mutant locus. The data were then analyzed for linkage and distortion of segregation associated with the mutant locus. A high percentage (estimated to be >50%) of male sterile F2 individuals with *Ler* genotypes indicates the linkage between the given polymorphic locus and the gene under study. Initial mapping identifying that the male sterile mutant mapped to chromosome 1 and was linked to one polymorphic locus. The gDNAs from the male sterile F2 plants were subsequently analyzed using six additional co-dominant markers, e.g., simple sequence length polymorphism or SSLP (Table 5.2), on

chromosome 1 in the vicinity of the polymorphic locus (orange double-headed arrow region (Figure 5.1). This second linkage analysis was done in order to obtain a higher resolution map for the gene of interest.

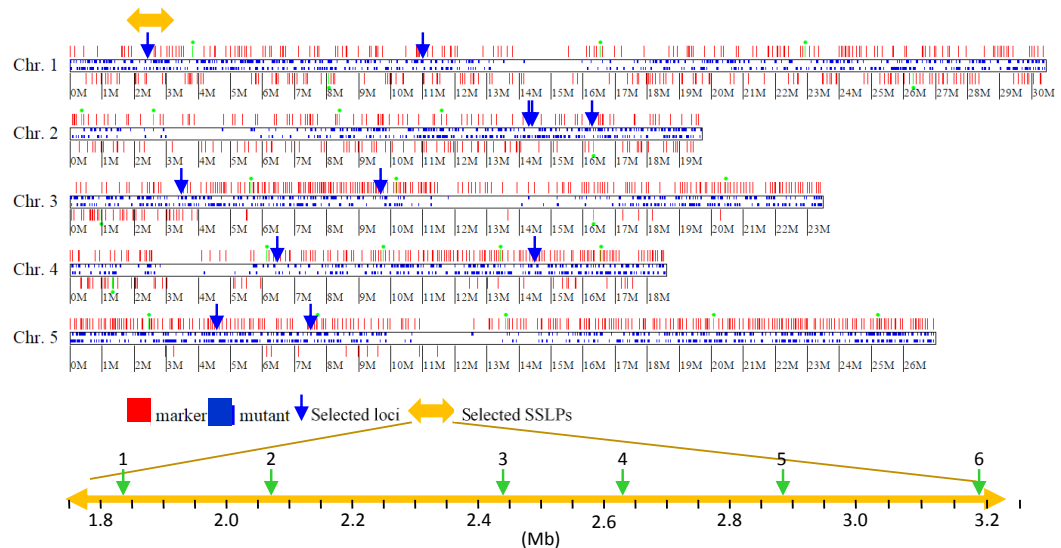


Figure 5.1 Map position of the selected 11 polymorphic loci (indicated by blue arrows, see Table 5.1) on the five *Arabidopsis* chromosomes (<http://amp.genomics.org.cn/>). Red lines indicate location of SSLP markers and orange double-headed arrow indicates the region (1,837,561-3,192,707 bp) where SSLPs were analysed. Green arrows indicate location of SSLP markers (1-6, see Table 5.2) used in the high-resolution linkage map analysis of chromosome 1.

Table 5.1 Polymorphic molecular markers and their locations on the different *Arabidopsis* chromosomes along with PCR conditions used to map the gene(s) of interest (www.arabidopsis.org/).

Chromosome	Gene ID	Location (bp)	Primers	Expected	Expected	Annealing
				size (bp) <i>Col</i>	size (bp) <i>Ler</i>	
1	<i>At1g07810</i>	2,416,265- 2,420,757	(F)= GTTCACGGACAAAGAGCCTGAAAT (R)= AAGCAGTCAATATTCAGGAAGGG	>300	<300	55
	<i>At1g30930</i>	11,014,783- 11,015,913	(F)= TCAATGGGATCGAACTGGT (R)= ACTGAAAAGCGAGCCAAAAG	239	142	55
2	<i>CER459006</i>	14,297,784- 14,297,986	(F)= TCGCAAACCAAATATCAACT (R)= AGCTGATGAACAAAAGACTGA	203	158	50
	<i>CER459010</i>	14,320,519- 14,320,606	(F)= ACATTGAAAGTTCCCGATTCT (R)= CAACAGATTTTCTTTGACCCA	90	72	50
	<i>CER461057</i>	16,291,858- 16,291,970	(F)= GAGGACATGTATAGGAGCCTCG (R)= TCGTCTACTGCACTGCCG	151	135	50
3	<i>At3g11220</i>	3,513,531- 3,516,408	(F)= GGATTAGATGGGGATTTCTGG (R)= TTGCTCGTATCAACACACAG	193	174	55
	<i>At3g26605</i>	9,773,018- 9,773,500	(F)= CCCCAGTTGAGGTATT (R)= GAAGAAATTCCTAAAGCATTTC	<200	>200	53
4	<i>At4g10360</i>	6,420,455- 6,422,380	(F)= GCCAAACCCAAAATTGTAAAAC (R)= TAGAGGGAACAATCGGATGC	268	188	55
	<i>At4g29860</i>	14,601,698- 14,605,796	(F)=GCCCAGAGGAAAGAAGAGCAAAC (R)=TGGGAATTCATGAGAGAATATGTGGG	492	404	55
5	<i>At5g14320</i>	4,617,650- 4,618,912	(F)= GGCCTAAGAACCAAATCAAACAA (R)= CGTGATGAAGTCTCCAAGTACATG	225	271	55
	<i>At5g22545</i>	7,483,253- 7,483,811	(F)= TAGTGAAACCTTTCTCAGAT (R)= TTATGTTTTCTTCAATCAGTT	100	>130	50

Table 5.2 Molecular markers (SSLP) used to recover a higher resolution map containing the gene(s) of interest in the vicinity of *At1g07810* locus on chromosome 1 (<http://amp.genomics.org.cn/>).

No.	Marker ID	Forward primer position (bp)	Primers	Expected size (bp) <i>Col</i>	Expected size (bp) <i>Ler</i>	Annealing temp. (°C)
1	AC024174-0604	1,837,561	(F)= CAGAGAGATCCGACGAGAGA (R)= GTACCACTTACCCGAACCAA	161	146	49.3
2	AC011001-0681	2,073,469	(F)=GAACAATGTCAATGGAGATA (R)= CTTCTCTCTCCTCACAGAGT	137	125	55
3	AC026875-0804	2,445,556	(F)= TTACTTTTCTGCAACTAAAT (R)= TCGTCTAGGGTGAGAAGATG	108	118	55
4	AC011438-0865	2,630,625	(F)= TTTGGGCTGTTAGATTGT (R)= TTTGAGGCTTTCAGTTTG	113	103	56.3
5	AC000106-0948	2,884,921	(F)= ATTACGCATATTATTATTCC (R)= CGCTTATTCAACAAGAGACT	204	181	52.5
6	AC000132-1049	3,192,707	(F)= TGCTTCCTAAGTTCATCAT (R)= TGTAACCAAGAATCCAAA	155	134	45.5

5.3 RESULTS

5.3.1 PHENOTYPING AND MICROSCOPIC ANALYSIS OF MALE STERILE MUTANTS

The four mutants generally showed normal growth characteristics as compared to wild type *Ler* plants. The wild type *Ler* had elongated siliques that contained seeds (Figure 5.2 A). However, the mutants produced short siliques lacking seeds, indicating that the plants were sterile (Figure 5.2B-E). Observations of open flowers from these plants indicated a range of phenotypes. Flowers from the sterile plants had a normal external morphology, except that in some lines the stamen filament development appeared to be generally shorter as compared to that of the wild type (*Ler*) (Figure 5.3). Flowers of the *msak* mutant (Figure 5.3B) had filaments, which were approximately half the length of those in wild type (*Ler*). Microscopic observation showed that the pollen was viable (red) in all phenotypes as indicated by Alexander stain (Alexander, 1969) (Section 2.6.1) (Figure 5.5). The secondary thickening of the anthers was analysed by confocal microscopy using acridine orange/ethidium bromide stains, which differentially stain cellulose and lignin (Yang *et al.*, 2007) (Section 2.6.3)(Figure 5.4). The endothecium cells of *msak*, *c12*, *c20* and *mss* mutants showed abnormal secondary thickening, which was reduced and disorganized as compared to the wild type (*Ler*) (Figure 5.5). Analysis of open flowers from plants of the four male sterile mutants indicated that dehiscence and pollen release failed to occur as compared to the wild type, which dehisced and pollen was released (Figure 5.5).

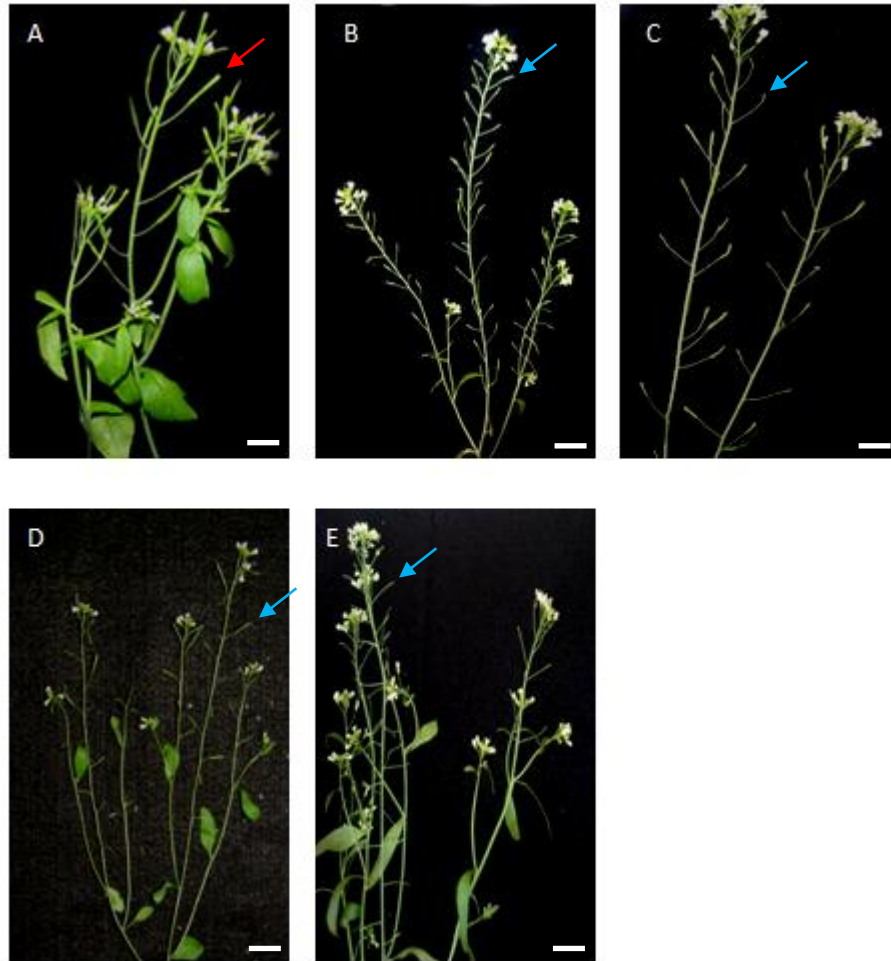


Figure 5.2 Whole plant phenotypes showing silique formation of (A) *Ler* wild type and the four mutants, (B) *mask*, (C) *mss*, (D) *c12* and (E) *c20*. The wild type was fertile with long siliques (red arrow) and full seed set, the mutants were sterile with short siliques (blue arrow) and no seeds. Scale bars = 0.25 cm. Red arrow indicates the long silique while the blue arrows indicate the short siliques.

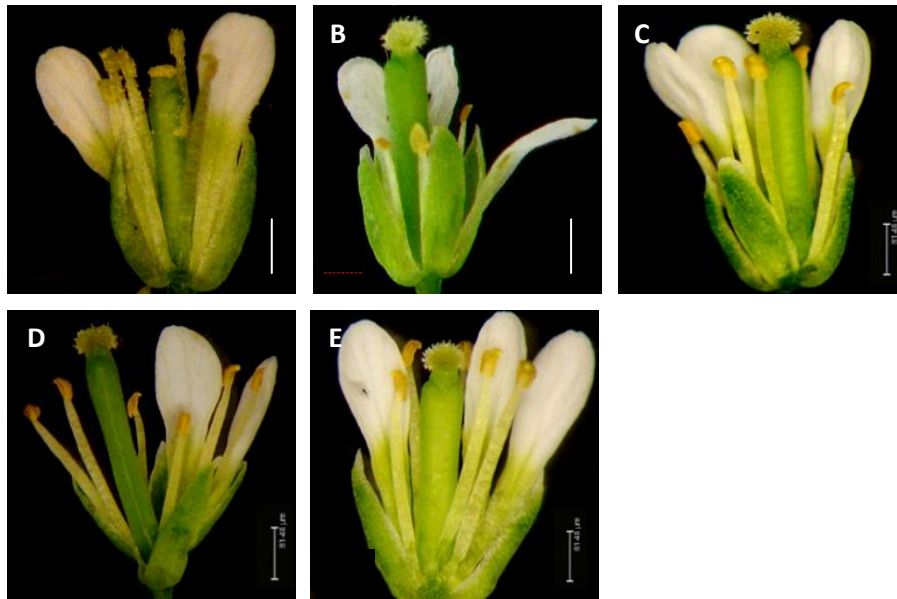


Figure 5.3 Flowers Phenotypic analysis of flowers from (A) *Ler* and the mutants (B) *msak*, (C) *mss*, (D) *c12*, and (E) *c20* as compared to the wild type (A). Wild type flower showed pollen grains on the stigmatic surface and on the dehiscing anthers. Mutants showed open flowers but no pollen was visible on the stigmas. Scale bars = 40 μ m.

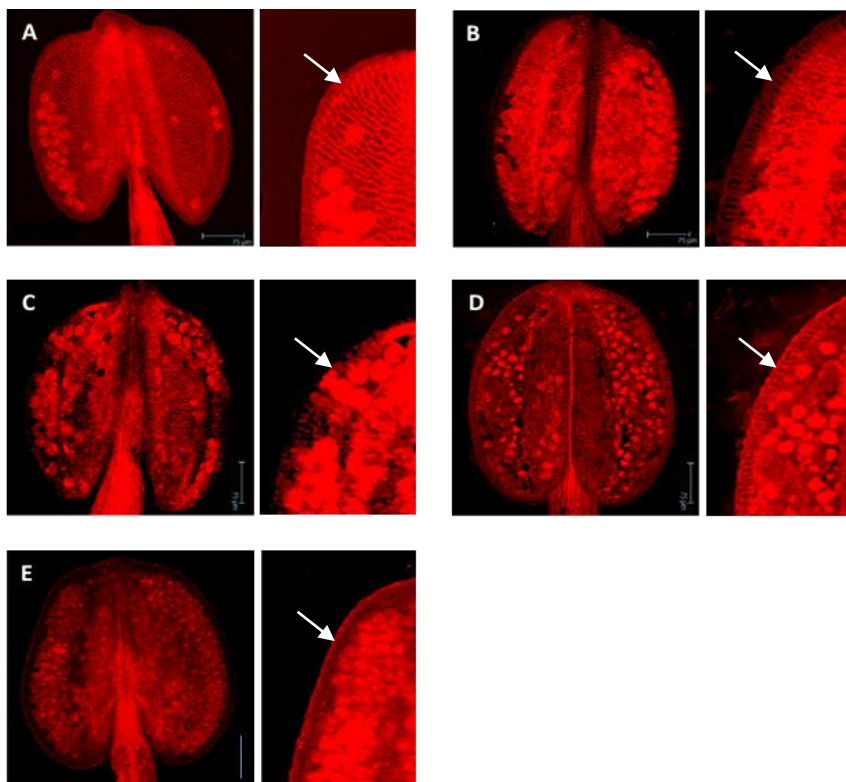


Figure 5.4 Anthers from wild type *Ler* (A) and the mutants B-E, showing endothecium cells and secondary thickening in the four mutants (B) *msak*, (C) *mss*, (D) *c12*, and (E) *c20*. The mutants exhibited decreased and disorganized secondary thickening in the endothecium as compared to the wild type (*Ler*). Scale bars = 70 μ m.

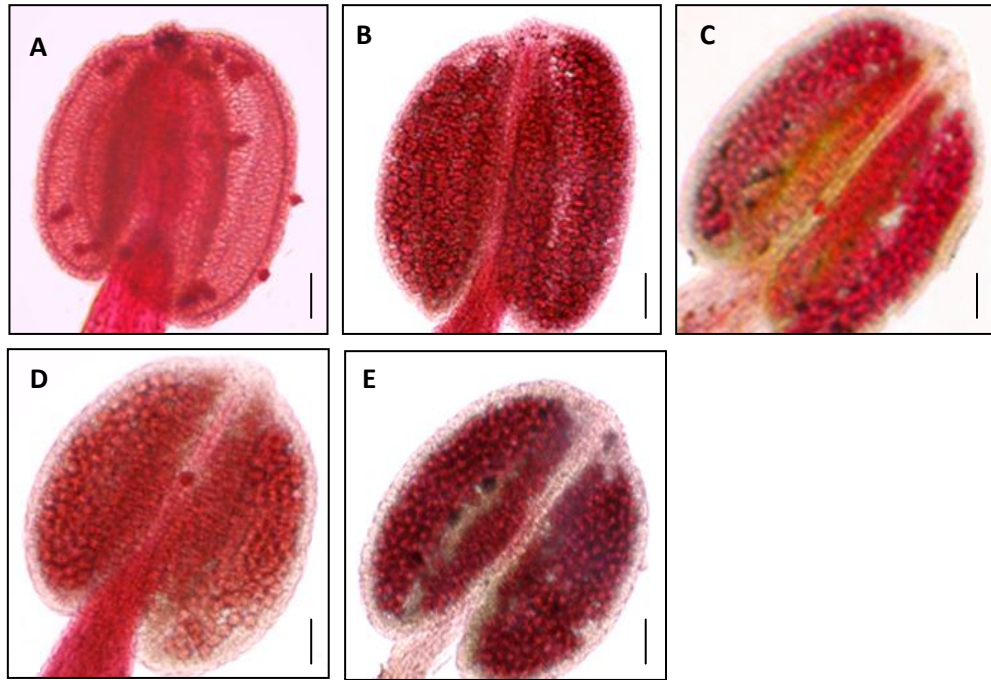


Figure 5.5 Viable pollen was observed using Alexander staining in the anthers of (A) *Ler* and the four mutants (B) *msak*, (C) *mss*, (D) *c12*, and (E) *c20*. No release of pollen was observed in the mutants as compared to the wild (*Ler*), which dehisced and visible pollen was released. Scale bars = 50 μ m.

5.3.2 TESTING FOR RESCUE OF MALE STERILE MUTANTS WITH JASMONIC ACID TREATMENTS

JA is essential for stamen development in *Arabidopsis thaliana*. JA-deficient mutants are male sterile with short stamen filaments, failure of anther dehiscence, and non-viable pollen. Application of exogenous jasmonic acid can restore the male fertility of the JA-deficient mutants and regulates dehiscence by controlling water transport in the filament and anther.

In the recent study, the wild type (*Ler*) and mutant plants of *msak*, *mss*, *c12* and *c20* were sprayed with JA (100 mM) or Tween20 (as a control) once the plants were flowering. This was repeated every other day for a period of two weeks. Male sterile mutants were smaller with short siliques due to the failure of silique expansion as a result of a lack of seed setting. A quantitative analysis of fertility was subsequently made by (i) measuring the length of five siliques in the upper region of

the mutant and wild type lines, (ii) checking that seed formation was reduced and corresponded to the length of silique elongation, and by (iii) assessing the total number of fully developed seed-containing siliques per plant. Average siliques length and thus fertility did not appear to be significantly affected by JA treatment (Figure 5.6).

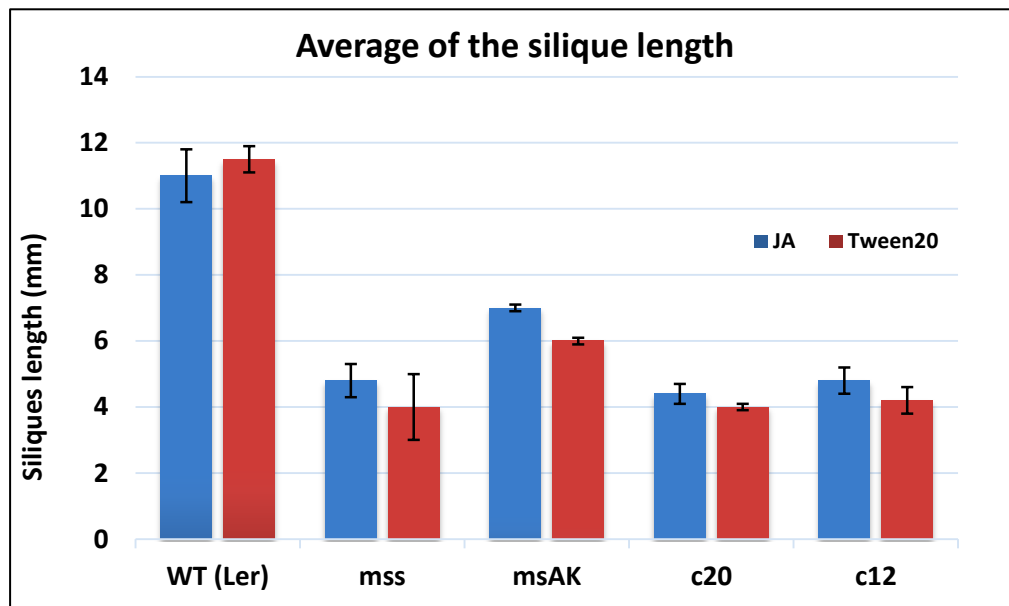


Figure 5.6 Siliques length of the four mutants *mss*, *msak*, *c20* and *c12* after jasmonic acid (100 mM) and Tween20 (control) treatment as compared to the wild type (*Ler*).

5.3.3 ALLELISM TESTS

The four male sterile mutants were first crossed as females to the wild type (*Ler*) in order to get heterozygous fertile lines. The latter heterozygous lines were further crossed as males to the *myb26* mutant to determine whether they are alleles of the *myb26* mutation or whether they result from mutations in novel genes at other loci. As a consequence, a series of crosses were done between the sterile homozygous *myb26myb26* mutant (female parent) with each fertile heterozygous (male parent) mutant line. It was expected that if the mutation was in a novel gene and

not *myb26*, gene complementation would occur, therefore, all the individuals in the F1 progeny should be fertile. Whereas, if the mutation occurred in the same gene (e.g. *myb26*), then 50% of the progeny should be sterile (1 fertile:1 sterile). Based upon this complementation analysis (Table 5.3), lines *c20* and *mss* showed segregation of sterility, although sterile individuals occurred at a lower frequency than expected. On the other hand, crossing of the heterozygous fertile plants of the other two mutant lines *msak* and *c12* with the homozygous mutant (*myb26myb26*) showed no segregation of sterility. These results suggest that *mss* and *c20* are alleles of the *myb26* mutation, whilst *c12* and *msak* are novel mutations at other loci.

Therefore, line *msak* was used for molecular mapping analysis to identify the location of the mutation. There was insufficient time for mapping of the other mutant, *c12*, which was decided to be beyond the scope of the present study. In addition to mapping analysis, further phenotypic observations of *msak* and *c12* mutants were made to confirm the male sterility phenotype (Section 5.3.4).

Table 5.3 Allelism test for the four mutants. Crosses were conducted between heterozygous fertile lines of the mutants and homozygous (X *myb26myb26*) sterile plants.

Cross of mutant lines	Total number of plants after crossing	Number and genotype of fertile plants after crossing	Number of sterile plants after crossing
<i>C12 c12</i> // <i>MYB26MYB26</i> X <i>C12C12</i> // <i>myb26myb26</i>	20	20 <i>C12</i> <i>C12</i> // <i>MYB26myb26</i> and/or <i>C12</i> <i>c12</i> // <i>MYB26myb26</i>	0
<i>MSS mss</i> ** X <i>myb26myb26</i>	20	17 <i>MSS myb26</i>	3 <i>mss myb26</i>
<i>C20 c20</i> ** x <i>myb26myb26</i>	20	15 <i>C20 myb26</i>	5 <i>c20 myb26</i>
<i>MSAK msak</i> *// <i>MYB26MYB26</i> X <i>MSAK MSAK</i> // <i>myb26myb26</i>	20	20 <i>MSAK MSAK</i> // <i>MYB26myb26</i> and <i>MSAK msak</i> // <i>MYB26myb26</i>	0

* *c12* and *msak* are not alleles of *myb26* (*c12* ≠ *msak* ≠ *myb26*)

** *mss* and *c20* are alleles of *myb26* (*mss* = *c20* = *myb26*)

5.3.4 ANTHHER DEVELOPMENT IN MUTANTS

The early stages of anther and pollen development in *msak* and *c12* lines appeared generally normal, with normal tetrad formation and microspore release (Figure 5.7D and G) as compared to the wild type (*Ler*) (Figure 5.7A). However, at the later stages of pollen formation, although septum lysis occurred a failure of dehiscence was observed, abnormal tapetal development and pollen were also seen in the two mutants (Figure 5.7E, F, H and I) as compared to the wild type (*Ler*) (Figure 5.7B and C). Complete tapetum breakdown was observed in the wild type (Figure 5.7B) whereas at the corresponding stage in *msak* and *c12* accumulation of tapetum breakdown materials was observed (Figure 5.7E, F, H and I).

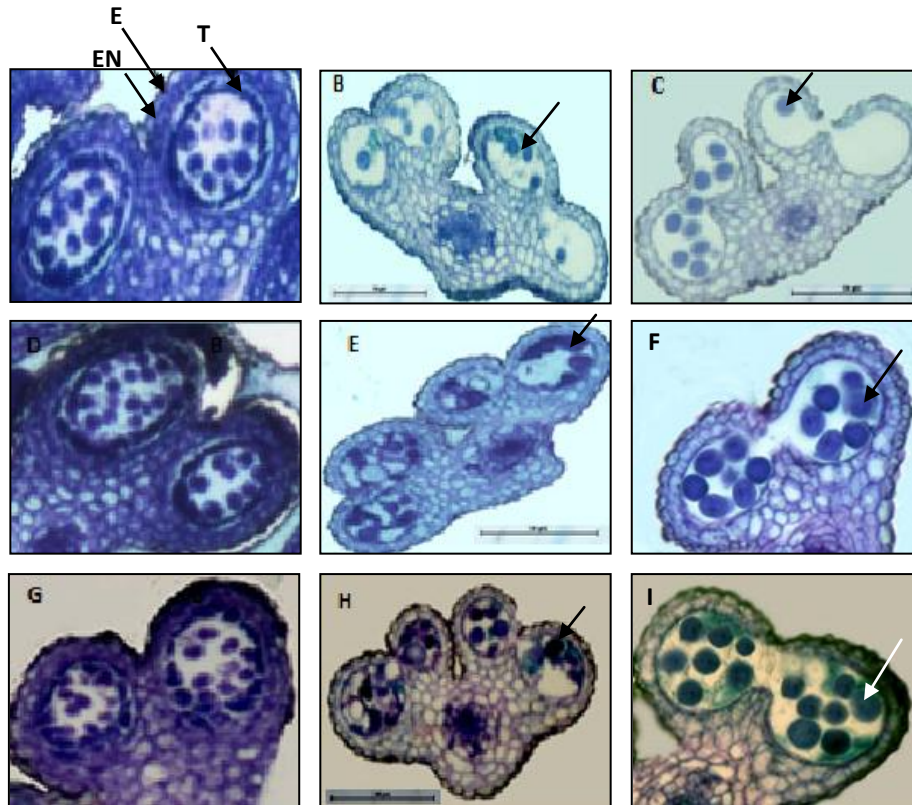


Figure 5.7 Anthers and pollen development in (A-C) wild type (*Ler*), (D-F) *msak* and (G-I) *c12* mutants. Flower sections were stained with toluidine blue. Epidermis (E), Endothecium (EN) and Tapetum (T). Scale bars = 50 μ m. Arrows indicate the pollen development.

5.3.5 POLLEN GERMINATION IN MALE STERILE MUTANTS

Pollen germination was examined by *in vitro* culture of pollen to determine whether the pollen was fully functional in the two mutants. Approximately 25% of the wild type (*Ler*) pollen grains germinated *in vitro* (Figure 5.8A). However, this ratio was significantly reduced in the mutants as less than 5% of pollen grains of *c12* and 10% of pollen grains from *msak* mutant produced normal pollen tubes (Figure 5.8B and C, respectively). The frequency of pollen tube growth varied, nevertheless, a limited number of normal pollen tubes were observed in the two mutants (Figure 5.8A, B and C).

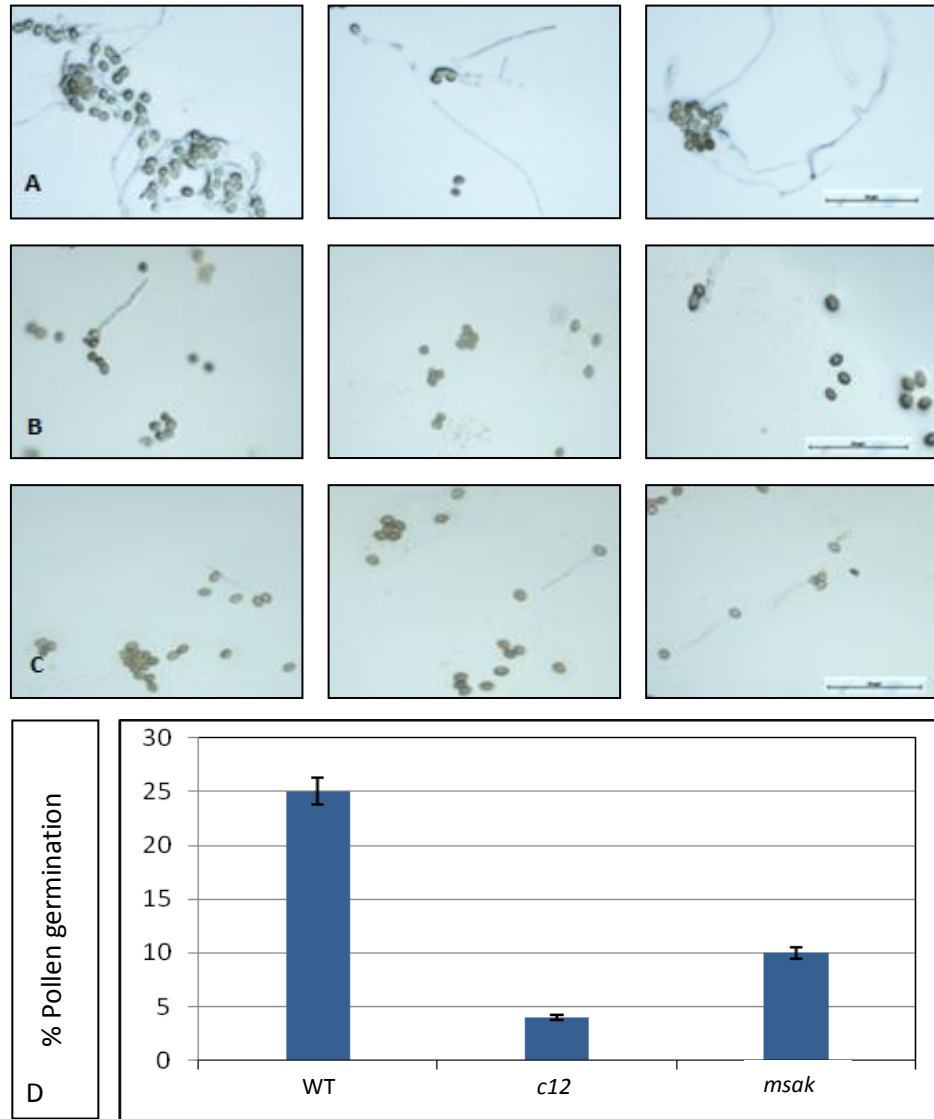


Figure 5.8 *In vitro* pollen tube growth in the wild type (A) and in the mutants (B) *c12* and *msak* (C). (D) Rates of the pollen germination of the mutants *c12* and *mask* as compared to the wild type (*Ler*) after 8 hours of culturing on pollen medium germination.

5.3.6 MAPPING ANALYSIS FOR THE *msak* MUTANT

In order to help identify the identity of the *MSAK* gene, the *msak* mutant in the *Ler* background was crossed to wild type *Columbia* (*Col*) to generate a segregating mapping population. A series of polymorphic molecular markers (11), distributed across the five *Arabidopsis* chromosomes (Table 5.1), were analysed for co-segregation with the mutation in the F2 generation. The primers used were initially tested on gDNA from *Arabidopsis* wild type *Ler* and *Col* ecotypes to confirm the products sizes and the presence of polymorphisms (Figure 5.9 and Table 5.1). PCR analysis was subsequently performed on the segregating F2 male sterile lines. Lines were expected to randomly segregate for the genetic background (*Ler/Col*), but to be consistently *Ler* background in the critical region associated with the gene of interest.

Amplifications sizes from the male sterile lines at the F2 segregation were compared to *Col* and *Ler* and scored for their genotypes (homozygous *Ler*: heterozygous *Ler/Col*: homozygous *Col*) for each marker to identify recombinants around the mutant locus. Linkage was detected to locate the *MSAK* gene on a chromosome after calculating the genetic linkage as recombinant frequency (RF) [$RF = (\text{recombinant} / \text{parental} + \text{recombinant}) \times 100$] (Table 5.4) converted to map units measured in centiMorgans (cM).

The recombination frequency, thus the distance between each two loci, was measured between *MSAK* gene and the different molecular markers on different chromosomes. The results of the RF indicated different linkages to the markers on all chromosomes, however, the lowest distance (21.73 cM) was scored between the *MSAK* gene and a marker on chromosome

1 namely *At1g07810* (located in 2,416,265-2,420,757 bp) (Tables 5.1 and 5.4). PCR of the segregating F2 population of the locus with ID *At4g10360* is shown in Figure 5.10 as a model. PCR of other markers are shown in Appendix III. Therefore, further genetic linkage mapping was conducted at higher resolution using simple sequence length polymorphism (SSLP) molecular markers in the vicinity around the *At1g07810* locus (Figure 5.1; Tables 5.2 and 5.5). Six SSLP markers in the region between 1.8-3.2 Mb that flanks the locus *At1g07810* (~2.42 Mb) (Figure 5.1 and Table 5.5) were used. These SSLP markers were initially tested on gDNA from *Arabidopsis* wild type *Ler* and *Col* ecotypes to confirm the products sizes and the presence of polymorphisms (Figure 5.11). Then, PCR products from the male sterile lines at the F2 generation were compared to *Col* and *Ler* and scored for their genotypes for each marker on this region of chromosome 1. The results of the RF indicated different linkages to the SSLP markers on chromosome 1 in the defined region. The shortest distance (12.57 cM) was scored between the *MSAK* gene and the SSLP marker AC000132-1049 (*At1g09560*) located at ~3.2 Mb of chromosome 1 (Figure 5.12 and Table 5.5). The further downstream from downstream this location (>3.2 Mb), the further the distance between the marker and the gene of interest is scored. However, this criterion was not straightforward as the estimated distances between the different markers and the gene of interest did not exactly reflect the real distances between the different SSLP markers (Figure 5.12). The reason for these inconsistent results might be due to the small number of individuals in the F2 population used in the present study. This result indicates that the location of the dehiscence-related gene is likely to be in the region beyond 3.0 Mb from the start of chromosome 1.

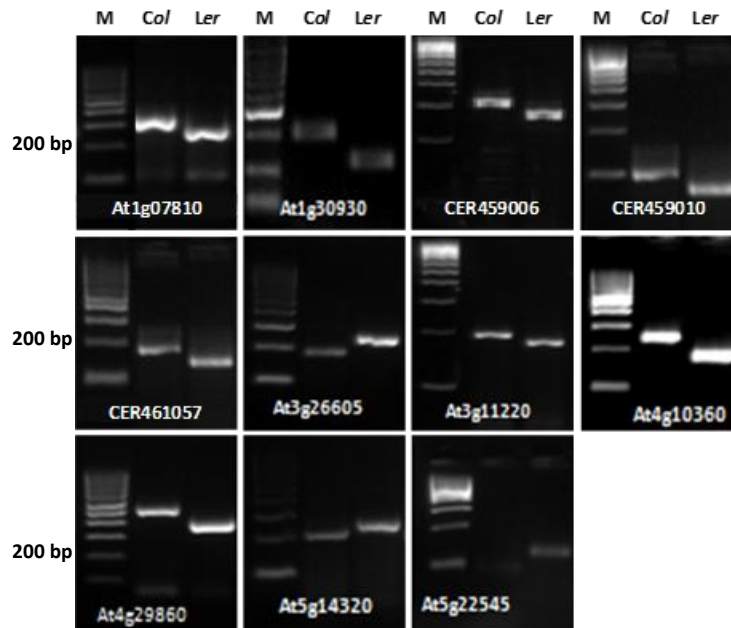


Figure 5.9 Discrimination between *Ler* and *Col* genotypes using 11 polymorphic markers on the five *Arabidopsis* chromosomes (<http://amp.genomics.org.cn/>). M: HyperLadder II.

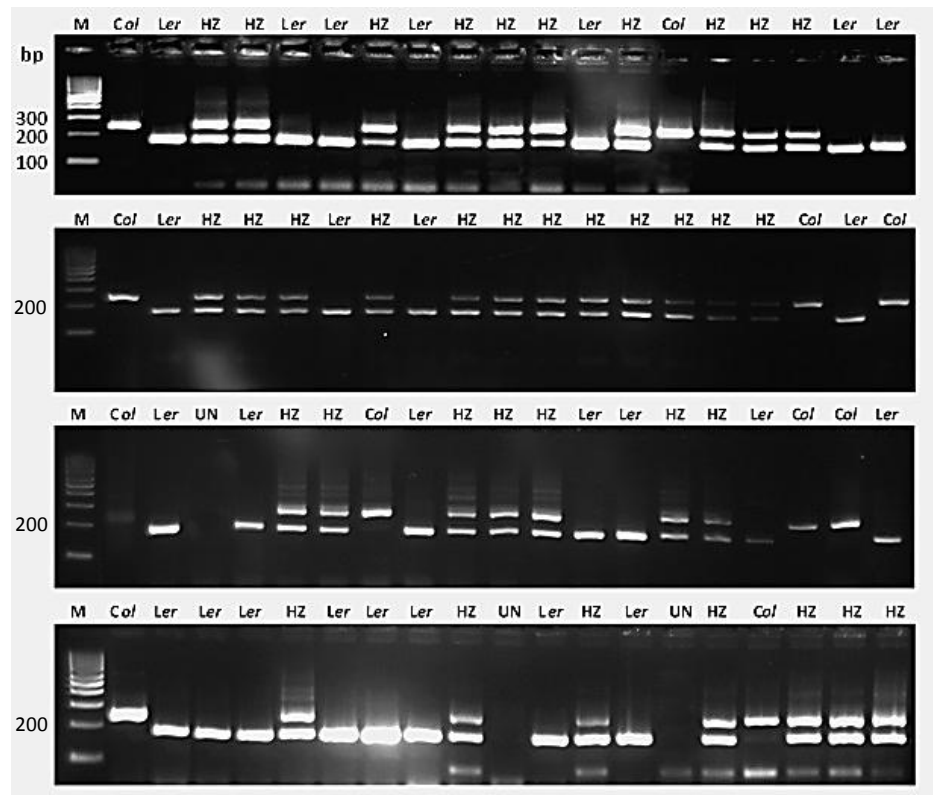


Figure 5.10 PCR amplification of the F2 male sterile population for the *msak* mutant using the *At4g10360* polymorphic genetic marker on chromosome 4 (<http://amp.genomics.org.cn/>). PCR indicates products size of the homozygous *Col* (268 bp) or *Ler* (188 bp) genotypes as well as the heterozygous (HZ) with *Col/Ler* background. The segregating F2 population indicated 22 individuals with *Ler* homozygous genotype, while 7 with *Col* homozygous genotype and 37 were heterozygous with the two genetic background of *Ler/Col* (See Table 5.4). M: HyperLadder II.

Table 5.4 Linkage map analysis of *msak* mutation with loci on different *Arabidopsis* chromosomes. RF= recombinant frequency, D (cM)= distance in centiMorgan.

Chromosome	Locus ID	Observed (Ler)	Observed HZ (Ler/Col)	Observed (Col)	SUM of Unknown	Exp <i>Ler</i>	Exp HZ	Exp <i>col</i>	Chi-Square	RF	D (cM)
1	At1g07810	48	9	9	2	16.5	33	16.5	2.577 ^{E-18}	0.205	21.73
	At1g30930	2	51	8	7	15.25	30.5	15.25	5.75 ^{E-07}	0.549	>100
2	CER459006	4	55	6	3	16.25	32.5	16.25	1.615 ^{E-07}	0.515	>100
	CER459010	12	45	8	3	16.25	32.5	16.25	0.006	0.469	86.25
	CER461057	14	41	8	5	15.75	31.5	15.75	0.032	0.452	74.89
3	At3g11220	30	10	15	13	13.75	27.5	13.75	2.437 ^{E-07}	0.364	46.15
	At3g26605	13	15	12	28	10	20	10	0.279	0.488	>100
4	At4g10360	22	36	7	3	16.25	32.5	16.25	0.022	0.385	50.92
	At4g29860	35	14	13	6	15.5	31	15.5	3.639 ^{E-08}	0.323	38.35
5	At5g14320	24	20	13	11	14.25	28.5	14.25	0.100	0.404	55.92
	At5g22545	20	18	10	20	12	24	12	0.028	0.396	53.79

Table 5.5 Linkage map analysis of *msak* mutation with SLP markers on chromosome 1 of *Arabidopsis* in the region between 1,837,561-3,192,707. RF= recombinant frequency, D (cM)= distance in centiMorgan.

Locus or marker location (bp)	Marker ID	Observed (Ler)	Observed HZ (Ler/Col)	Observed (Col)	SUM of Unknown	Exp <i>Ler</i>	Exp HZ	EXP <i>col</i>	Chi-Square	RF	D (cM)
1,837,561	AC024174-0604	22	33	9	4	16	32	16	0.069	0.398	54.50
2,073,469	AC011001-0681	32	21	6	9	14.75	29.5	14.75	9.128 ^{E-07}	0.280	31.59
2,416,265	At1g07810	48	9	9	2	16.5	33	16.5	2.577 ^{E-18}	0.205	21.73
2,445,556	AC026875-0804	33	32	2	1	16.75	33.5	16.75	5.516 ^{E-07}	0.269	30.02
2,630,625	AC011438-0865	35	17	8	8	15	30	15	1.892 ^{E-08}	0.275	30.92
2,884,921	AC000106-0948	38	25	4	1	16.75	33.5	16.75	3.717 ^{E-09}	0.246	26.97
3,192,707	AC000132-1049	55	4	6	3	16.25	32.5	16.25	1.270 ^{E-27}	0.123	12.57

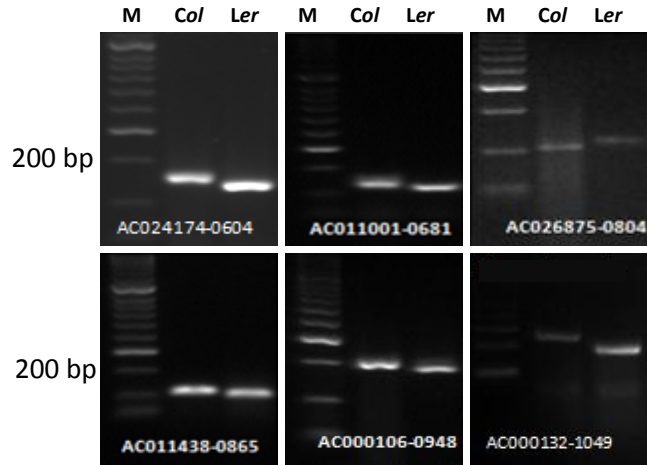


Figure 5.11 Discrimination between *Ler* and *Col* genotypes using six SSLP markers on *Arabidopsis* chromosome 1 of *Arabidopsis* (<http://amp.genomics.org.cn/>) in the region between 1,837,561-3,192,707 bp. M: HyperLadder II.

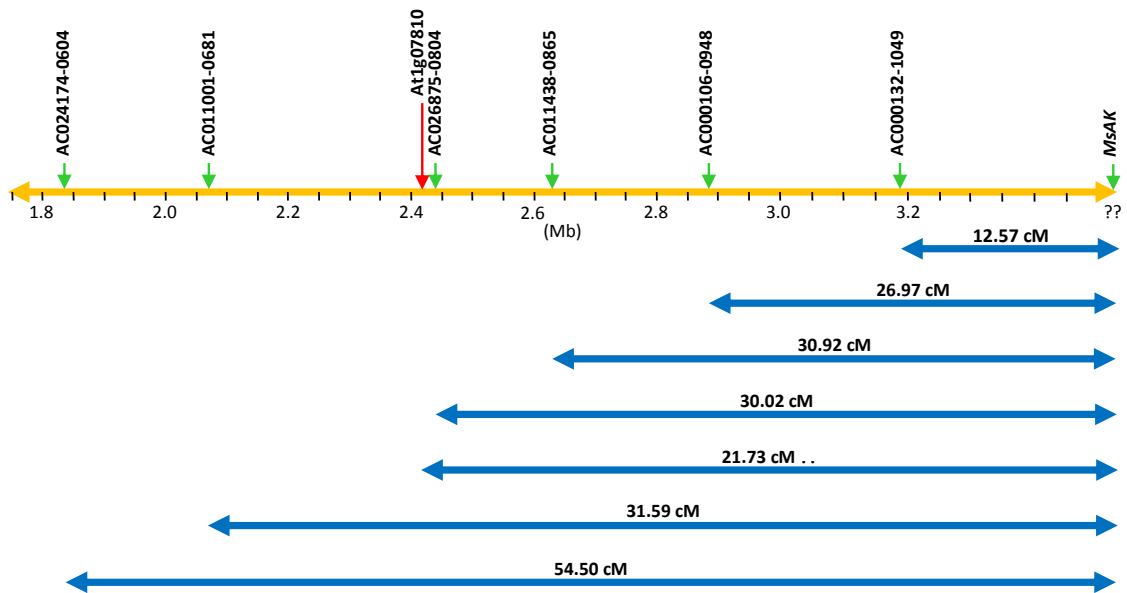


Figure 5.12 The genetic map indicating the possible location of the *MSAK* gene on chromosome 1 of *Arabidopsis*. The region (1,837,561-3,192,707 bp), where SSLP analysis was conducted, is indicated by the orange double-headed arrow. Locations of SSLP markers on chromosome 1 are indicated by the green arrows. Distances in cM between the gene and the SSLP markers as well as the locus *At1g07810* are shown by the blue double-headed arrows. Red arrow indicates the original marker (*At1g07810*) from the initial linkage mapping analysis.

Further mathematical analysis using the recombination data (cM) and physical distances (bps) between the markers (Table 5.5) was conducted to determine the average distance per cM in this region of chromosome 1 and to estimate the possible location of the *MSAK* gene. The results suggested that 1 cM was equivalent to between 10-237 kb (Table 5.6). Based on these estimates of distance/recombination, calculations were made to determine the approximate distance between the AC000132-1049 SSLP marker and *MSAK* gene; three estimates of distance were used assuming that 1 cM might be equivalent to 21, 250 or 500 kb. The results indicated that the corresponding distances between the AC000132-1049 SSLP marker and the *MSAK* gene could be 268.7, 3142.5 or 6285.0 kb, respectively. This indicates that the possible location of *MSAK* gene could be be ~3.46, 6.34 or 9.48 Mb from the start of chromosome 1, respectively. This region was then analysed for possible candidates corresponding to the *MSAK* gene. Transcription factors (TFs) previously located in the vicinities in these regions (3.4-3.5, 6.3-6.4 and 9.4-9.5 Mb) of chromosome 1 were investigated (TAIR, <https://www.arabidopsis.org/servlets/TairObject?id=28652&type=locus>). The results are shown in Figure 5.13 and detailed information on description and exact locations of the TFs in these regions are shown in Table 5.7. The results indicated the existence of four, three and nine TFs, respectively, in these three regions of the chromosome. However, from our initial linkage analysis, no linkage was detected between *MSAK* and *At1g30930* genes (>100 cM). The latter gene is located on chromosome 1 at ~11.02 Mb, which is about 1.5 or 4.6 Mb downstream *MSAK* gene in case that 1 cM is equivalent to 500 or 250 kb, respectively. Therefore, it is more likely that 1 cM is closer to the

lower distance/cM of 21 kb, than the high estimate of 500Kb/cM, in the region of chromosome 1 where *MSAK* gene is located. Consequently, it is likely that *MSAK* gene is approximately located at ~3.46 Mb of the chromosome. The four TFs in the vicinity of 3.4-3.5 Mb include SIN3-LIKE 6 (or SNL6), ZINC FINGER PROTEIN 5 (or ZFP5), Transducin/WD40 repeat-like protein and a basic helix-loop-helix (bHLH). Genes encoding these transcription factors are *At1g10450*, *At1g10480*, *At1g10580* and *At1g10585*, respectively (Table 5.7). Analysis of the four genes in the Flowernet gene correlation database (<https://www.cpib.ac.uk/anther/>) recently generated by Prof. Zoe A. Wilson's group (Pearce *et al.*, 2015) indicated no relation to pollen development except for *At1g10580* (<https://www.cpib.ac.uk/anther/?species=Arabidopsis&gene=AT1G10580#gene>) (Figure 5.14). This gene is located at ~3.49 Mb of chromosome 1 and encodes a transducin/WD40 repeat-like protein. These results suggest the possibility that *MSAK* gene is a Transducin/WD40 repeat-like TF. Further analysis of the T-DNA knockout SALK line of this gene (e.g., SALK_068763) might help in confirming the entity of the *MSAK* gene.

Furthermore, analysis of other genes located in the region between 3.0-4.0 Mb of chromosome 1 related to male gametophyte, pollen development or belong to MYB superfamily was also conducted in order to determine the possible identity of the *MSAK* gene. The analysis indicated the presence of 16 previously characterised genes, which are also possible candidates for the gene of interest (Table 5.8). These genes were categorised into three groupings.

The first category involves only one gene, a putative pectin methylesterase/invertase inhibitor (*At1g10770*; located at ~3.59 Mb), which results in pollen tube growth retardation, partial male sterility and reduced seed set. Detection of other activities in the Flowernet indicated high relation of this gene to pollen development (<https://www.cpib.ac.uk/anther/?species=Arabidopsis&gene=AT1G10770#gene>) (Figure 5.15). This gene is also a strong candidate allele for the *MSAK* gene. Again, study of the T-DNA knockout SALK line of this gene (e.g., SALK_040257) will help to detect its role in pollen development and dehiscence.

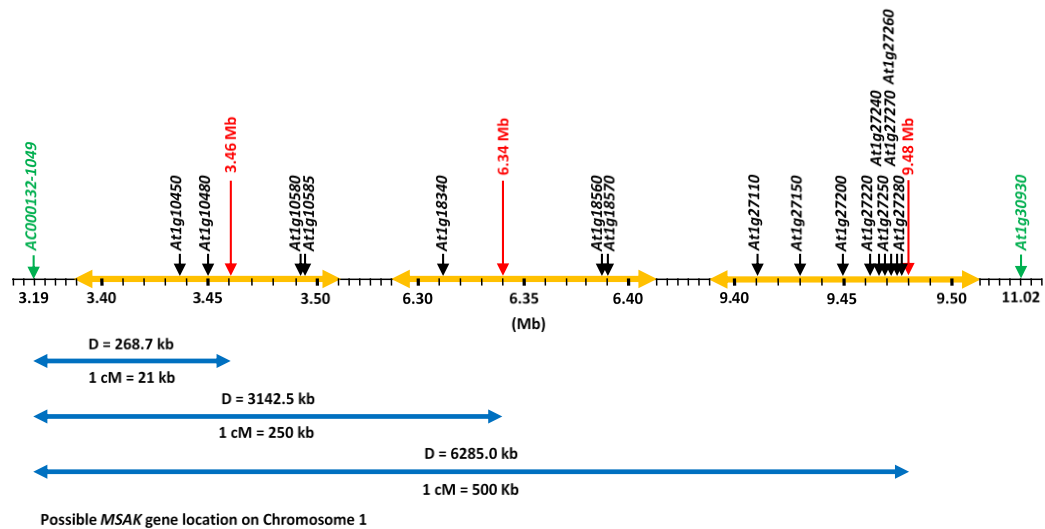


Figure 5.13 The genetic/physical distances (cM/kb) between *MSAK* gene and the AC000132-1049 SSLP marker, the possible location of *MSAK* gene as well as the location of genes encoding transcription factors in the vicinities of 3.4-3.5, 6.3-6.4 and 9.49.5 Mb on chromosome 1 of *Arabidopsis*.

The second category includes 13 genes with involvement in pollen development. Three of these genes (*At1g09640* (*EF1B*), *At1g11040* (*HSP40/DnaJ*) and *At1g11520*; located at ~3.12, 3.68 and 3.87 Mb, respectively) were shown to

be involved in male gametophyte and in pollen development during mature and pollen germination stages. The gene *At1g09690* (*SH3*-like) (located at ~3.14 Mb) is involved in juvenile leaf and pollen tube development. The genes *At1g10680* (*ABCB10*) and *At1g11770* (located at ~3.54 and 4.0, respectively) are involved in mature pollen stage and pollen germination, while *At1g11540* gene (located at ~3.88) is involved only during germinated pollen stage. The third category involves two *MYB* gene family members, *MYB61* and *MYB3R*-type (*At1g09540* and *At1g09770*; located at ~3.09 and 3.17 Mb, respectively). Neither of them has been shown to be involved in pollen development or male sterility (Table 5.8). However, as members of the *MYB* gene family, it is possible that one or both of these transcription factor-encoding genes have influence during anther and pollen tube development stage and possibly the generation of sterile flowers in *Arabidopsis*. Thus, *MSAK* gene could potentially be an allele of *MYB61* or *MYB3R*-type gene (Table 5.8).

AT1G10580

Transducin/WD40 repeat-like superfamily protein; CONTAINS InterPro DOMAIN/s: WD40 repeat 2 (InterPro:IPR019782), WD40 repeat, conserved site (InterPro:IPR019775), WD40 repeat (InterPro:IPR001680), G-protein beta WD-40 repeat, region (InterPro:IPR020472), WD40 repeat-like-containing domain (InterPro:IPR011046), WD40-repeat-containing domain

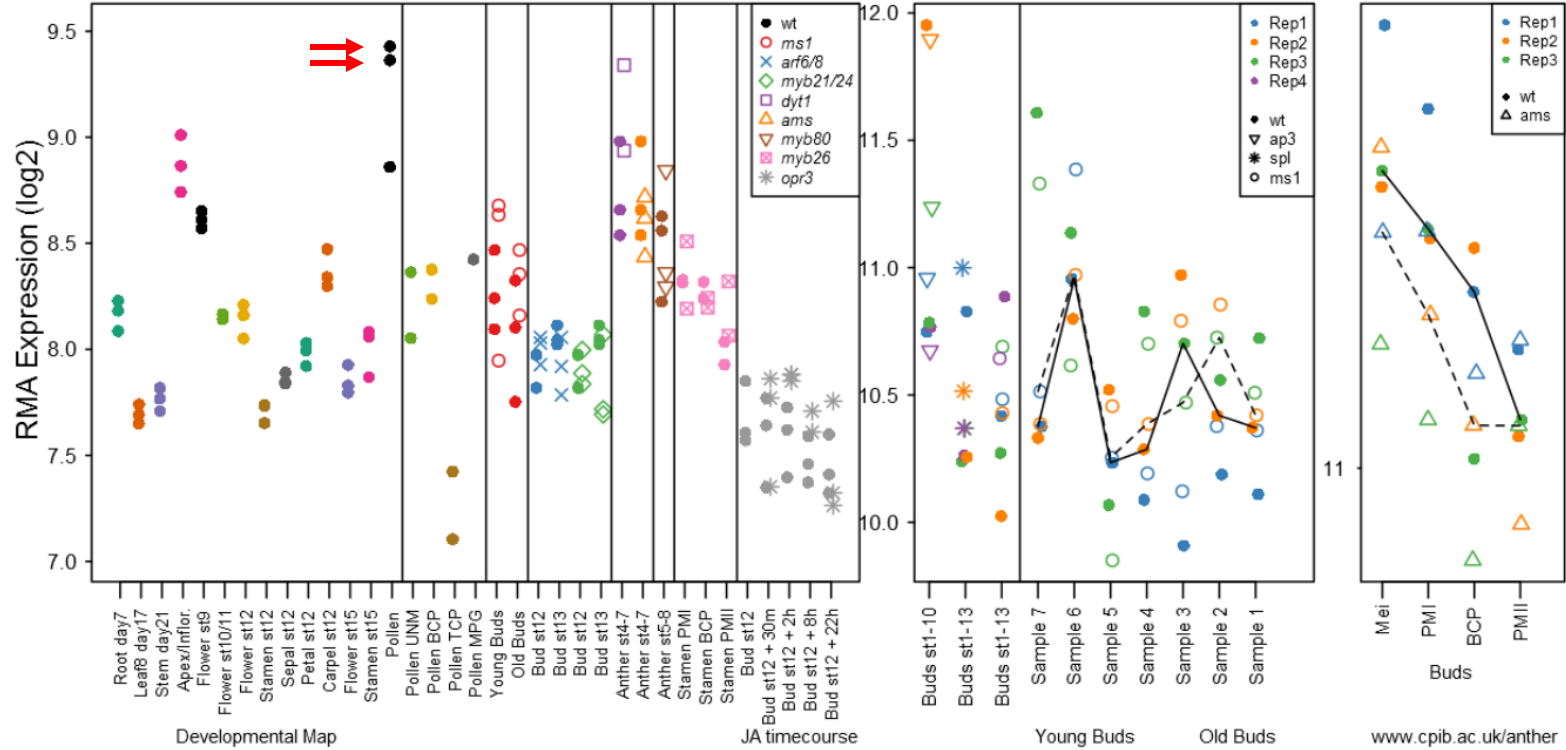


Figure 5.14 Plot from the Web site tool showing the expression of Transducin/WD40 in various anther and floral microarrays (<http://www.cpib.ac.uk/anther>). Horizontal red arrows indicate the expression level of the *At1g10580* gene in the pollen.

AT1G10770

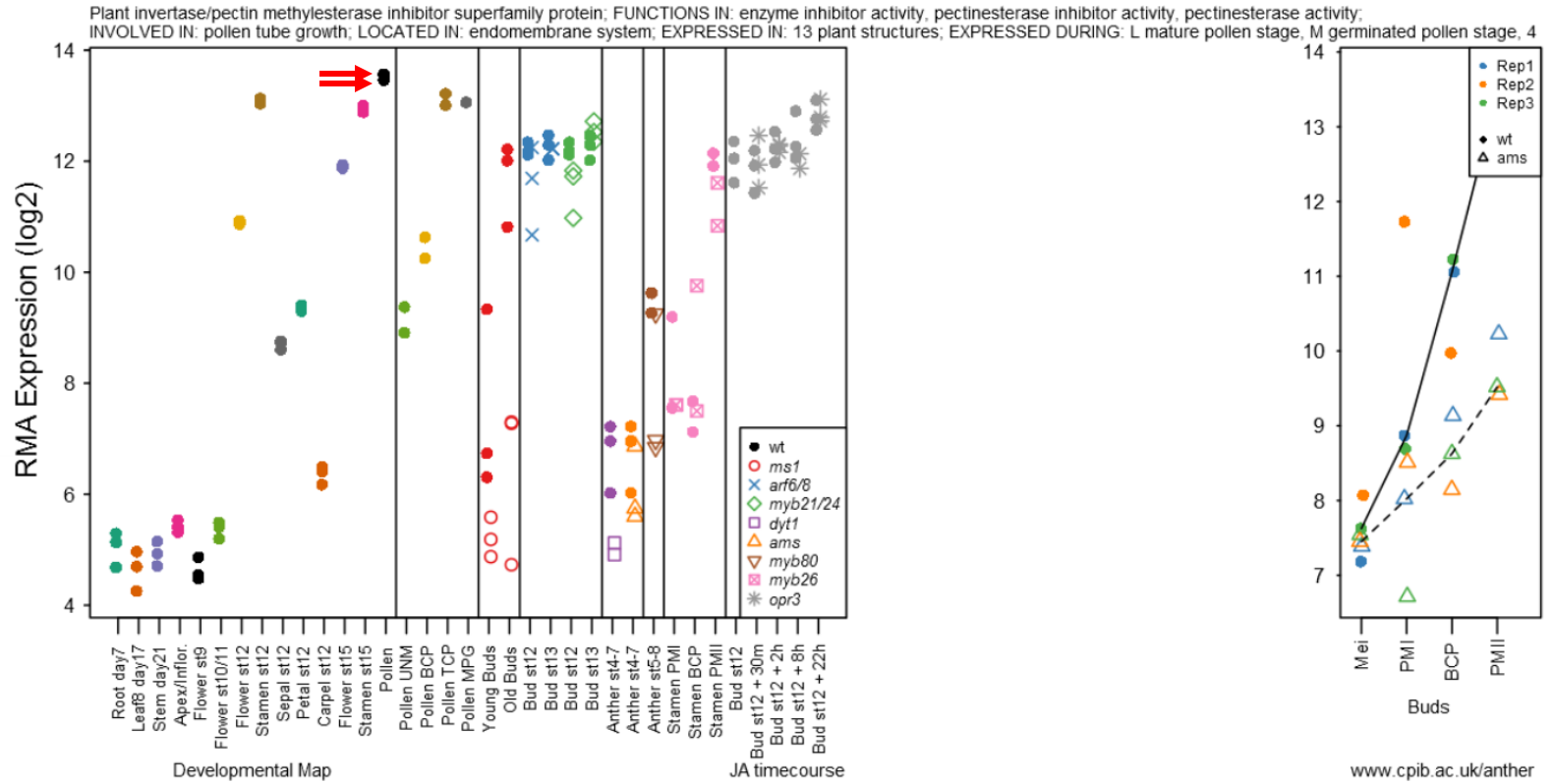


Figure 5.15 Plot from the Web site tool showing the expression of putative pectin methylesterase/invertase inhibitor in various anther and floral microarrays (<http://www.cpib.ac.uk/anther>). Horizontal red arrows indicate the expression level of the *At1g10770* gene in the pollen.

Table 5.6 Estimation of the physical distance per cM in the region around the *MSAK* gene on chromosome 1.

No.	SSLP marker	Location on Chromosome 1 (bp)	Distance between markers in bp	Distance in cM	Average physical distance (kb) per cM
1	AC024174-0604	1,837,561	-	-	-
2	AC011001-0681	2,073,469	235,908	22.91	10
3	AC026875-0804	2,445,556	372,087	1.57	237
4	AC011438-0865	2,630,625	185,069	0.89	208
5	AC000106-0948	2,884,921	254,296	3.95	64
6	AC000132-1049	3,192,707	307,786	14.4	21
			based on 1 cM = 21 kb	based on 1 cM = 250 kb	based on 1 cM = 500 kb
Approximate distance to <i>MSAK</i> in kb			268.7*	3142.5**	6285.0***
Approximate distance to <i>MSAK</i> in bp			268,672	3,142,500	6,285,000
possible location of <i>MSAK</i> if 1 cM = 21 kb*			3,461,379 bp		
possible location of <i>MSAK</i> if 1 cM = 250 kb**			6,335,207 bp		
possible location of <i>MSAK</i> if 1 cM = 500 kb***			9,477,707 bp		

* low kb/cM ratio seen in this region

** highest kb/cM ratio

*** very high kb/cM ratio

Table 5.7 Previously characterised transcription factors (<http://amp.genomics.org.cn/>) in the regions of 3.4-3.5, 6.3-6.4 (in green boxes) and 9.4-9.5 Mb of chromosome 1 of *Arabidopsis* that might be alleles of *MSAK* gene.

Gene ID	Position (bp)	Gene name and description	Reference
<i>At1g10450</i>	3,431,780-3,438,370	SIN3-LIKE 6, SNL6, Encodes SIN3-like 6, a homolog of the transcriptional repressor SIN3 (AT1G24190).	https://www.arabidopsis.org/servlets/TairObject?id=136238&type=locus
<i>At1g10480</i>	3,449,691-3,451,226	ZFP5, ZINC FINGER PROTEIN 5, Encodes a zinc finger protein containing only a single zinc finger that acts downstream of ZFP6 in regulating trichome development by integrating GA and cytokinin signaling	https://www.arabidopsis.org/servlets/TairObject?id=136246&type=locus
<i>At1g10580</i>	3,491,281-3,493,737	Transducin/WD40 repeat-like superfamily protein; CONTAINS InterPro DOMAIN/s: WD40 repeat 2 (InterPro:IPR019782), WD40 repeat, conserved site (InterPro:IPR019775), WD40 repeat (InterPro:IPR001680), G-protein beta WD-40 repeat, region (InterPro:IPR020472), WD40 repeat-like-containing domain (InterPro:IPR011046), WD40-repeat-containing domain (InterPro:IPR017986), WD40/YVTN repeat-like-containing domain (InterPro:IPR015943), WD40 repeat, subgroup (InterPro:IPR019781); BEST Arabidopsis thaliana protein match is: Transducin/WD40 repeat-like superfamily protein (TAIR:AT5G54520.1); Has 62674 Blast hits to 30927 proteins in 942 species: Archae - 75; Bacteria - 8018; Metazoa - 23835; Fungi - 13551; Plants - 7464; Viruses - 27; Other Eukaryotes - 9704 (source: NCBI BLink).	https://www.arabidopsis.org/servlets/TairObject?id=136244&type=locus
<i>At1g10585</i>	3,493,940-3,495,144	basic helix-loop-helix (bHLH) DNA-binding superfamily protein; FUNCTIONS IN: sequence-specific DNA binding transcription factor activity; INVOLVED IN: regulation of transcription; LOCATED IN: nucleus; EXPRESSED IN: 7 plant structures; EXPRESSED DURING: LP.06 six leaves visible, 4 anthesis, LP.10 ten leaves visible, petal differentiation and expansion stage, LP.08 eight leaves visible; CONTAINS InterPro DOMAIN/s: Helix-loop-helix DNA-binding domain (InterPro:IPR001092), Helix-loop-helix DNA-binding (InterPro:IPR011598); BEST Arabidopsis thaliana protein match is: basic helix-loop-helix (bHLH) DNA-binding superfamily protein (TAIR:AT1G10586.1); Has 97 Blast hits to 96 proteins in 11 species: Archae - 0; Bacteria - 0; Metazoa - 0; Fungi - 0; Plants - 97; Viruses - 0; Other Eukaryotes - 0 (source: NCBI BLink).	https://www.arabidopsis.org/servlets/TairObject?id=500231430&type=locus
<i>At1g18340</i>	6,311,483-6,313,931	basal transcription factor complex subunit-related; FUNCTIONS IN: general RNA polymerase II transcription factor activity; INVOLVED IN: DNA repair, regulation of transcription, DNA-dependent; LOCATED IN: core TFIIH complex; EXPRESSED IN: 17 plant structures; EXPRESSED DURING: 9 growth stages; CONTAINS InterPro DOMAIN/s: Transcription factor Tfb4 (InterPro:IPR004600); Has 359 Blast hits to 354 proteins in 179 species: Archae - 0; Bacteria - 0; Metazoa - 118; Fungi - 143; Plants - 47; Viruses - 0; Other Eukaryotes - 51 (source: NCBI BLink).	https://www.arabidopsis.org/servlets/TairObject?id=27816&type=locus
<i>At1g18560</i>	6,385,449-6,388,080	BED zinc finger ;hAT family dimerisation domain; FUNCTIONS IN: protein dimerization activity, DNA binding; INVOLVED IN: biological_process unknown; LOCATED IN: cellular_component unknown; EXPRESSED IN: 16 plant structures; EXPRESSED DURING: 6 growth stages; CONTAINS InterPro DOMAIN/s: HAT dimerisation (InterPro:IPR008906), Zinc finger, BED-type predicted (InterPro:IPR003656); BEST Arabidopsis thaliana protein match is: BED zinc finger ;hAT family dimerisation domain (TAIR:AT3G42170.1); Has 1077 Blast hits to 1005	https://www.arabidopsis.org/servlets/TairObject?id=29506&type=locus

		proteins in 94 species: Archae - 0; Bacteria - 2; Metazoa - 242; Fungi - 210; Plants - 602; Viruses - 0; Other Eukaryotes - 21 (source: NCBI BLink).	
<i>At1g18570</i>	6,389,411-6,391,267	ATMYB51, BW51A, BW51B, HIG1, HIGH INDOLIC GLUCOSINOLATE 1, MYB DOMAIN PROTEIN 51, MYB51, Encodes a member of the R2R3-MYB transcription family. Involved in indole glucosinolate biosynthesis.	https://www.arabidopsis.org/servlets/TairObject?id=29505&type=locus
<i>At1g27110</i>	9,412,820-9,417,504	Tetratricopeptide repeat (TPR)-like superfamily protein; FUNCTIONS IN: binding; INVOLVED IN: biological_process unknown; LOCATED IN: cellular_component unknown; CONTAINS InterPro DOMAIN/s: Tetratricopeptide-like helical (InterPro:IPR011990); BEST Arabidopsis thaliana protein match is: Tetratricopeptide repeat (TPR)-like superfamily protein (TAIR:AT1G27150.1); Has 512 Blast hits to 499 proteins in 150 species: Archae - 27; Bacteria - 221; Metazoa - 81; Fungi - 0; Plants - 62; Viruses - 0; Other Eukaryotes - 121 (source: NCBI BLink).	https://www.arabidopsis.org/servlets/TairObject?id=137784&type=locus
<i>At1g27150</i>	9,429,047-9,432,274	Tetratricopeptide repeat (TPR)-like superfamily protein; FUNCTIONS IN: binding; INVOLVED IN: biological_process unknown; LOCATED IN: cellular_component unknown; EXPRESSED IN: 23 plant structures; EXPRESSED DURING: 13 growth stages; CONTAINS InterPro DOMAIN/s: Tetratricopeptide-like helical (InterPro:IPR011990); BEST Arabidopsis thaliana protein match is: Tetratricopeptide repeat (TPR)-like superfamily protein (TAIR:AT1G27110.1); Has 429 Blast hits to 423 proteins in 137 species: Archae - 5; Bacteria - 191; Metazoa - 78; Fungi - 0; Plants - 66; Viruses - 0; Other Eukaryotes - 89 (source: NCBI BLink).	https://www.arabidopsis.org/servlets/TairObject?id=137793&type=locus
<i>At1g27200</i>	9,449,549-9,451,750	CONTAINS InterPro DOMAIN/s: Protein of unknown function DUF23 (InterPro:IPR008166); BEST Arabidopsis thaliana protein match is: zinc finger (C3HC4-type RING finger) family protein (TAIR:AT3G27330.1); Has 321 Blast hits to 319 proteins in 87 species: Archae - 0; Bacteria - 165; Metazoa - 2; Fungi - 4; Plants - 113; Viruses - 0; Other Eukaryotes - 37 (source: NCBI BLink).	https://www.arabidopsis.org/servlets/TairObject?id=137797&type=locus
<i>At1g27220</i>	9,463,806-9,465,444	Paired amphipathic helix repeat-containing protein; FUNCTIONS IN: nucleic acid binding; INVOLVED IN: regulation of transcription, DNA-dependent; LOCATED IN: nucleus; EXPRESSED IN: sperm cell; CONTAINS InterPro DOMAIN/s: Polynucleotidyl transferase, ribonuclease H fold (InterPro:IPR012337), Paired amphipathic helix (InterPro:IPR003822); BEST Arabidopsis thaliana protein match is: Paired amphipathic helix (PAH2) superfamily protein (TAIR:AT1G27250.1); Has 833 Blast hits to 732 proteins in 188 species: Archae - 0; Bacteria - 52; Metazoa - 196; Fungi - 169; Plants - 372; Viruses - 0; Other Eukaryotes - 44 (source: NCBI BLink).	https://www.arabidopsis.org/servlets/TairObject?id=137782&type=locus
<i>At1g27240</i>	9,466,237-9,467,076	Paired amphipathic helix (PAH2) superfamily protein; FUNCTIONS IN: molecular_function unknown; INVOLVED IN: regulation of transcription, DNA-dependent; LOCATED IN: nucleus; EXPRESSED IN: 18 plant structures; EXPRESSED DURING: 12 growth stages; CONTAINS InterPro DOMAIN/s: Paired amphipathic helix (InterPro:IPR003822); BEST Arabidopsis thaliana protein match is: Paired amphipathic helix (PAH2) superfamily protein (TAIR:AT1G24210.1); Has 568 Blast hits to 542 proteins in 154 species: Archae - 0; Bacteria - 4; Metazoa - 189; Fungi - 136; Plants - 215; Viruses - 0; Other Eukaryotes - 24 (source: NCBI BLink).	https://www.arabidopsis.org/servlets/TairObject?id=28118&type=locus
<i>At1g27250</i>	9,468,568-9,469,634	Paired amphipathic helix (PAH2) superfamily protein; FUNCTIONS IN: molecular_function unknown; INVOLVED IN: regulation of transcription, DNA-dependent; LOCATED IN: nucleus; CONTAINS InterPro DOMAIN/s: Paired amphipathic helix (InterPro:IPR003822); BEST Arabidopsis thaliana protein match is: paired amphipathic helix repeat-containing protein (TAIR:AT1G27220.1); Has 603 Blast hits to 572 proteins in 159 species: Archae - 0; Bacteria - 0; Metazoa - 198;	https://www.arabidopsis.org/servlets/TairObject?id=28133&type=locus

		Fungi - 151; Plants - 225; Viruses - 0; Other Eukaryotes - 29 (source: NCBI BLink).	
<i>At1g27260</i>	9,469,948-9,470,967	Paired amphipathic helix (PAH2) superfamily protein; FUNCTIONS IN: molecular_function unknown; INVOLVED IN: regulation of transcription, DNA-dependent; LOCATED IN: nucleus; CONTAINS InterPro DOMAIN/s: Paired amphipathic helix (InterPro:IPR003822); BEST Arabidopsis thaliana protein match is: Paired amphipathic helix (PAH2) superfamily protein (TAIR:AT1G23810.1); Has 1078 Blast hits to 561 proteins in 156 species: Archae - 0; Bacteria - 0; Metazoa - 392; Fungi - 252; Plants - 385; Viruses - 0; Other Eukaryotes - 49 (source: NCBI BLink).	https://www.arabidopsis.org/servlets/TairObject?id=28127&type=locus
<i>At1g27270</i>	9,472,077-9,473,149	Paired amphipathic helix (PAH2) superfamily protein; FUNCTIONS IN: molecular_function unknown; INVOLVED IN: regulation of transcription, DNA-dependent; LOCATED IN: nucleus; CONTAINS InterPro DOMAIN/s: Paired amphipathic helix (InterPro:IPR003822); BEST Arabidopsis thaliana protein match is: Paired amphipathic helix (PAH2) superfamily protein (TAIR:AT1G23810.1); Has 680 Blast hits to 519 proteins in 139 species: Archae - 0; Bacteria - 0; Metazoa - 210; Fungi - 129; Plants - 307; Viruses - 0; Other Eukaryotes - 34 (source: NCBI BLink).	https://www.arabidopsis.org/servlets/TairObject?id=28108&type=locus
<i>At1g27280</i>	9,474,027-9,474,990	Paired amphipathic helix (PAH2) superfamily protein; FUNCTIONS IN: molecular_function unknown; INVOLVED IN: regulation of transcription, DNA-dependent; LOCATED IN: nucleus; CONTAINS InterPro DOMAIN/s: Paired amphipathic helix (InterPro:IPR003822); BEST Arabidopsis thaliana protein match is: Paired amphipathic helix (PAH2) superfamily protein (TAIR:AT1G24230.1); Has 730 Blast hits to 554 proteins in 156 species: Archae - 0; Bacteria - 0; Metazoa - 199; Fungi - 160; Plants - 334; Viruses - 0; Other Eukaryotes - 37 (source: NCBI BLink).	https://www.arabidopsis.org/servlets/TairObject?id=28112&type=locus

Table 5.8 Previously characterised genes in the region of 3.0-4.0 Mb of *Arabidopsis* chromosome 1 (<http://amp.genomics.org.cn/>) and downstream of AC000132-1049 *At1g09560* SSLP marker (3.2 Mb) with possible linkage to *MSAK* gene. These genes are involved in male sterility (one gene in yellow boxes), pollen development (13 genes in uncoloured boxes) or belong to *MYB* gene family (two genes in green boxes).

Locus	Position (bp)	Gene name and description	Reference
<i>At1g10770</i>	3,591,633-3,592,411	Encodes a putative pectin methylesterase/invertase inhibitor. Anti-sense reduction of this gene's transcript results in pollen tube growth retardation and then partial male sterility and reduced seed set.	http://www.arabidopsis.org/servlets/TairObject?id=28652&dtype=locus
<i>At1g09640</i>	3,119,878-3,122,526	Translation elongation factor <i>EF1B</i> , gamma chain; EXPRESSED IN: male gametophyte, cultured cell, pollen tube, leaf, seed; DURING: L mature pollen stage, M germinated pollen and seed development stages	https://www.arabidopsis.org/servlets/TairObject?name=AT1G09640&dtype=locus
<i>At1g09690</i>	3,136,188-3,137,475	Translation protein <i>SH3</i> -like family protein; EXPRESSED IN: juvenile leaf, pollen tube	https://www.arabidopsis.org/servlets/TairObject?type=gene&id=30270
<i>At1g09780</i>	3,165,370-3,167,869	2,3-BIPHOSPHOGLYCERATE-INDEPENDENT PHOSPHOGLYCERATE MUTASE 1, <i>IPGAM1</i> ; INVOLVED IN pollen development and stomatal movement	http://www.arabidopsis.org/servlets/TairObject?id=28936&dtype=locus
<i>At1g10200</i>	3,346,390-3,347,885	<i>ATWLIM1</i> ; Encodes a member of the <i>Arabidopsis</i> LIM proteins. <i>WLIM1</i> , <i>WLIM2a</i> , and <i>WLIM2b</i> are widely expressed, whereas <i>PLIM2a</i> , <i>PLIM2b</i> , and <i>PLIM2c</i> are predominantly expressed in pollen	http://www.arabidopsis.org/servlets/TairObject?id=27638&dtype=locus
<i>At1g10680</i>	3,538,470-3,543,782	<i>ABCB10</i> , ATP-BINDING CASSETTE B10, P-GLYCOPROTEIN 10, EXPRESSED DURING: I mature pollen stage, M germinated pollen stage	http://www.arabidopsis.org/servlets/TairObject?id=28650&dtype=locus
<i>At1g11040</i>	3,679,225-3,680,924	HSP40/DnaJ peptide-binding protein; EXPRESSED IN: petal, leaf whorl, male gametophyte, flower, pollen tube; EXPRESSED DURING: L mature pollen stage, M germinated pollen stage, 4 anthesis, petal differentiation and expansion stage	http://www.arabidopsis.org/servlets/TairObject?id=136626&dtype=locus
<i>At1g11280</i>	3,787,334-3,790,876	S-locus lectin protein kinase family protein; EXPRESSED IN: 23 plant structures; EXPRESSED DURING: 15 growth stages	http://www.arabidopsis.org/servlets/TairObject?id=137306&dtype=locus
<i>At1g11330</i>	3,810,093-3,813,607	S-locus lectin protein kinase family protein; EXPRESSED IN: 21 plant structures; EXPRESSED DURING: 13 growth stages	http://www.arabidopsis.org/servlets/TairObject?id=137299&dtype=locus
<i>At1g11340</i>	3,814,116-3,817,420	S-locus lectin protein kinase family protein; EXPRESSED IN: 8 plant structures; EXPRESSED DURING: 6 growth stages	http://www.arabidopsis.org/servlets/TairObject?id=137039&dtype=locus
<i>At1g11410</i>	3,841,286-3,844,432	S-locus lectin protein kinase family protein; INVOLVED IN: protein amino acid phosphorylation, recognition of pollen; EXPRESSED IN: 21 plant structures; EXPRESSED DURING: 13 growth stages	http://www.arabidopsis.org/servlets/TairObject?id=137044&dtype=locus

<i>At1g11520</i>	3,873,029-3,873,819	Spliceosome associated protein-related; EXPRESSED IN: male gametophyte, pollen tube; EXPRESSED DURING: L mature pollen stage, M germinated pollen stage	http://www.arabidopsis.org/servlets/TairObject?id=137042&dtype=locus
<i>At1g11540</i>	3,875,442-3,877,155	Sulfite exporter <i>TauE/SafE</i> family protein; EXPRESSED IN: 13 plant structures; EXPRESSED DURING: M germinated pollen stage, 4 anthesis, C globular stage, 4 leaf senescence stage, petal differentiation and expansion stage	http://www.arabidopsis.org/servlets/TairObject?id=137029&dtype=locus
<i>At1g11770</i>	3,975,679-3,977,379	FAD-binding Berberine family protein; EXPRESSED DURING: L mature pollen stage, M germinated pollen stage, 4 anthesis, C globular stage, petal differentiation and expansion stage	http://www.arabidopsis.org/servlets/TairObject?id=29486&dtype=locus
<i>At1g09540</i>	3,086,159-3,087,912	<i>ARABIDOPSIS THALIANA</i> MYB DOMAIN PROTEIN 61, <i>ATMYB61</i> , MYB DOMAIN PROTEIN 61, <i>MYB61</i> ; Encodes putative transcription factor. Mutants lack of mucilage extrusion from the seeds during imbibition. Reduced quantities of mucilage are deposited during the development of the seed coat epidermis in <i>myb61</i> mutants	http://www.arabidopsis.org/servlets/TairObject?id=27560&dtype=locus
<i>At1g09770</i>	3,161,841-3,165,360	<i>ARABIDOPSIS THALIANA</i> CELL DIVISION CYCLE 5, <i>ARABIDOPSIS THALIANA</i> MYB DOMAIN CELL DIVISION CYCLE 5, <i>ATCDC5</i> , <i>ATMYBCDC5</i> , <i>CDC5</i> , CELL DIVISION CYCLE 5, Member of <i>MYB3R</i> - and <i>R2R3</i> -type MYB-encoding genes. Essential for plant innate immunity. Interacts with <i>MOS4</i> and <i>PRL1</i>	http://www.arabidopsis.org/servlets/TairObject?id=28932&dtype=locus

5.4 DISCUSSION AND CONCLUSION

Understanding pollen development is important in genetic and genomic technologies at the molecular level. Male sterility can arise as cytoplasmic, nuclear (genetic) or genetic-cytoplasmic male sterility (Jain, 1959). Interactions between transcription factors such as MYB26 and their target genes during pollen development have been studied. The activities of transcription factors are needed in order to understand and predict the regulatory relationships between transcription factors and their target genes (Wang *et al.*, 2011; Lamesch *et al.*, 2012). The recent Plant Male Reproduction Database (PMRD; <http://www.pmr.org>) has made significant progress in collating and presenting pollen development at each development stage.

In this work, X-ray and EMS radiation were used as mutagens to create random mutations in genes linked to male fertility and in particular those causing failure of pollen development resulting in male sterility. X-rays and EMS have been previously reported as highly effective mutagens resulting in mutations at individual loci in *Arabidopsis thaliana* (Koornneef *et al.*, 1982). In this study, four mutants were characterised, which stably showed male sterility in the M2 and M4 generations. Plants of the four mutants showed normal vegetative growth characteristics (Figure 5.2B-E) as compared to wild type *Ler* plants (Figure 5.2A). However, they failed to produce elongated siliques, indicating that the plants were sterile (Figure 5.3B-E) as compared to the wild type *Ler*, which had long siliques with full seed set (Figure 5.3A). The filament length in the mutants was also reduced (Figure 5.4B-E) as compared to the wild type (*Ler*) (Figure 5.4A).

Viable (red) pollen (Alexander, 1969) was evident in the mutants as compared to the wild type *Ler*, but this was not associated with pollen release in the mutants (Figure 5.4B-E), while the wild type dehisced and released viable pollen (Figure 5.4A). Microscopic observation of open flowers from these male sterile mutants indicated that dehiscence and pollen release failed to occur. A lack of secondary thickening in the anther endothecium when analysed by confocal microscopy resulted in no development of secondary thickening in the anther endothecium (Figure 5.4B-E) as compared to the wild type *Ler* (Figure 5.4A). Analysis of open flowers of the four male sterile mutants indicated that dehiscence and pollen release failed to occur (Figure 5.5B-E) in contrast to the evidence of the wild type (*Ler*) (Figure 5.5A).

Male sterility can occur due to lack of production of viable pollen, but it can also occur due to the failure of release of the pollen. The phenotype of the *myb26* male sterile mutant showed that the anther produced pollen grains, but fertilization was still unable to occur due to the failure of dehiscence (Yang *et al.*, 2007). Analysis of male sterile mutants is necessary to help understand the mechanism by which pollen develops. The target of the present study particularly focused upon genes that had an effect on anther dehiscence. The phenotypes of these mutants were very similar to that of the *myb26* mutant (Dawson *et al.*, 1999; Steiner-Lange *et al.*, 2003).

Many of the previously described male sterile mutants showed aberrations in anther dehiscence due to defects in jasmonic acid biosynthesis (Park *et al.*, 2002). The mutants that had been previously identified showed defects in anther dehiscence in this

work. However, these defects could not be rescued by JA treatment.

The length of the siliques did not change significantly after JA treatment in any of the mutants as compared to the wild type (Figure 5.6). As a negative control, Tween20 treatment did not rescue fertility suggesting that the defect is not linked to the JA biosynthesis pathway. Nevertheless, the male sterility observed in the JA signaling mutant, *coronatine insensitive1 (coi1)*, is due to non-dehiscence but cannot be rescued by exogenous jasmonate, since the defect is associated with JA perception rather than biosynthesis (Devoto *et al.*, 2002; Xie *et al.*, 1998). The *Arabidopsis thaliana* *CORONATINE INSENSITIVE1 (COI1)* *At2g39940* gene encodes an F-box protein essential for response to jasmonates (JAs). Recessive *coi1* mutant failed to respond to JA or phytotoxin (structurally similar to jasmonic acid) because protein was not degraded in the presence of the signals displaying defects in JA-regulated gene expression. The latter criterion exhibits male sterility and shows a propensity to insect attack and pathogen infection (Feys *et al.*, 1994; Katsir *et al.*, 2008; Xiao *et al.*, 2004).

The phenotype of the *msak* mutant has short filaments (Figure 5.3B), suggesting that JA and gibberellin pathways may be affected in this mutant (Plackett *et al.*, 2011). The study of anther and pollen development in *msak* and *c12* lines at early stages of pollen formation indicated normal development (Figure 5.7D and G) as seen in the wild type (*Ler*) (Figure 5.7A). At the later stages, abnormal tapetal development and pollen release failed to occur were seen in the two *mutants* (Figure 5.7E, F, H and I) as compared with the wild type (*Ler*) (Figure 5.7B and C).

In vitro pollen germination can be useful to detect alterations in germination or tube growth performance (Cole *et al.*, 2005). In this work, pollen germination was examined *in vitro* to determine whether the pollen was fully functional. Approximately, 25% of the wild type Landsberg (Ler) pollen germinated *in vitro* (Figure 5.8A). However, the rate of germination was significantly reduced in the mutants with less than 5.0% of pollen grains from *c12* and 10.0% of pollen grains from *mask* plants producing normal pollen tubes (Figure 5.8B and C, respectively). Both the mutants and wild type produced apparently normal pollen tubes (Figure 5.8B and C).

Allelism tests indicated that two of the four mutants (e.g. *c20* and *mss*) were alleles of *myb26*, whilst *msak* and *c12* represented novel mutations in other loci. Based upon the complementation analysis (Table 5.3), lines *c20* and *mss* showed segregation for sterility, although at a lower frequency than expected. On the other hand, crosses between heterozygous lines of *msak* or *c12* with the homozygous *myb26myb26* mutant did not show any male sterile progeny (Table 5.3). Sterile individuals were only shown in the crosses between heterozygous lines of *c20* or *mss* and the homozygous *myb26myb26* mutant. This suggests that the latter two genes are alleles of the *myb26* gene, therefore, we did not proceed to the further analyses. The line *msak* was used for genetic mapping analysis, while *c12* line was not as this type of study requires a large F2 population in order to detect the exact position of the gene on the chromosome.

Mapping of *MSAK* gene indicated that it may be located on chromosome 1, after calculating the recombinant frequency (RF)

and the distance between the gene and a number of polymorphic loci of different chromosomes (Figure 1 and Table 5.4). The closest marker to the gene of interest was *At1g07810* that is located in the region of ~2.42 Mb of chromosome 1 (Figures 5.1 and 5.12 and Table 5.4). Further genetic linkage analysis was conducted to get a map with higher resolution for the gene of interest. This study was done consulting the simple sequence length polymorphism (SSLP) molecular markers flanking the *At1g07810* locus (1.8-3.2 Mb) (Figure 5.1 and Table 5.5). The results of the RF indicated estimated distances between each of the SSLP markers and the gene of interest; the closest (12.57 cM) involved the SSLP marker AC000132-1049 (*At1g09560*) located at ~3.2 Mb of chromosome 1 (Figure 5.12 and Table 5.5).

Mathematical analysis utilizing the linkage data of the SSLP markers indicated that 1 cM may be equivalent to 10-237 kb in the region of chromosome 1 where *MSAK* gene is located (Table 5.6). Calculations indicated that the approximate distance between AC000132-1049 SSLP marker and *MSAK* gene, speculating that 1 cM might be equivalent to 21 kb, is 268.7 kb. This indicates that the *MSAK* gene can possibly be located at ~3.46 Mb region of chromosome 1. Investigation on the transcription factors (TFs) located in the vicinity of 3.4-3.5 Mb of chromosome 1 consulting TAIR and Flowernet databases indicated the possibility that *MSAK* gene is a Transducin/WD40 repeat-like TF as it is highly expressed during pollen development (Table 5.7 , Figures 5.13 and 5.14).

Further analysis of the other genes previously investigated from the *Arabidopsis* databases (<http://amp.genomics.org.cn/> and

[http://www. Arabidopsis .org/](http://www.Arabidopsis.org/)) in region between 3.0-4.0 Mb indicated the existence of 16 other genes that might be alleles of the *MSAK* gene (Table 5.8). One of them, namely methylesterase/invertase inhibitor (*At1g10770*; located at ~3.59 Mb), is reported to be involved in pollen tube growth retardation, partial male sterility and reduced seed set. Information in the Flowernet data (Pearce *et al.*, 2015) also supported its involvement in pollen development (Figure 5.15). There are 13 other genes in the region that are also involved in pollen development. Some of them (e.g., *EF1B*, *HSP40/DnaJ*, *SH3*-like, *ABCB10*, etc.) are involved in male gametophyte and in pollen development mostly during mature and germinated pollen stages. The last category involves two *MYB* genes (*MYB61* and *MYB3R*-type); *MYB26* and *MYB128* are also members of this gene family. Thus, it might be that the genes *MYB61* and *MYB3R*-type are also involved in pollen development and/or male sterility. This option raises the possibility that the encoded protein might act as a transcription factor with an influence on pollen tube growth and the generation of sterile flowers in *Arabidopsis*. This conclusion can be confirmed in the future by complementation analysis to detect the gene identity.

Nevertheless, although the gene of interest is likely to lie in the 3.0-4.0 Mb region, no close marker flanking the upstream region of *MSAK* has been identified. Therefore, no upstream point has been defined beyond which the gene is not associated. Gene confirmation can also be assisted using SALK insertion mutant lines of the different candidate genes.

CHAPTER 6: FINAL DISCUSSION AND CONCLUSIONS

6.1 HYBRID PLANT BREEDING AND MALE STERILITY

Hybridization forms the basis of evolution and biodiversity of living organisms, which is used for the development of new varieties in economically important crop plants. Hybrid plant breeding is important in producing plants with superior growth rates and high yield due to the occurrence of hybrid vigour or heterosis due to combining complementary characteristics originating from the two parents (Lippman and Zamir, 2007). Hybrid plants can be produced by effective control of male fertility, but a major requirement in hybrid breeding is the control of viable pollen release so as to prevent self-fertilization., but also the ability to rescue fertility. In some self-fertilizing species like maize, manual emasculation is practiced as an intensive, laborious method to remove the male portion of a plant (Leland, 1985) However, this approach is not practical for crops such as rice and wheat. This method is used to either prevent the pollen production (e.g., maize, tomato, pepper, etc.) or pollen competition (e.g., brassicas, chicory, etc.). In some cases, failure to avoid self-pollination of the female line may cause subsequent seed quality problems with regard to high purity standards complying with the regulations of the market place. Therefore, breeders are interested in novel, reliable systems for plant breeding and hybrid seed production.

Various systems are used for hybrid development, these include the utilization of genic (GMS) and/or cytoplasmic (CMS) male

sterility characteristics as well as the use of chemical gametocides in hybrid development. Although chemical gametocides is a promising protocol that is used for barley hybrid production, it is not practical for large-scale application (Rao *et al.*, 1990). Male sterile lines often favoured for hybrid seed production in breeding programmes as they avoid expensive labour and intensive emasculation process (Wilson and Zhang, 2009). Plant male sterility is a biological characteristic commonly present in nature. It has been identified in over 150 plant species including maize, wheat, sorghum, barley, rice, cotton, flax, sunflower, sugar beet, tomato, pepper, eggplant, cucurbits, onion, asparagus, celery, cauliflower, broccoli, cabbage, etc. The development and use of CMS varieties complies with EU or Member States legislation (http://www.sementi.it/informazione/download/materiali/ESA_13_0834_3.pdf).

In the present study, emphasis has been given to the understanding of anther and pollen development and the mechanism by which pollen is released, as key elements to the successful application of male sterility for plant breeding and efficient hybrid production.

6.2 ROLE OF *MYB26* GENE IN MALE STERILITY AND CO-EXPRESSED GENES

It is interesting to study the biological pathway of male sterility, which is a system of pollination control that growers use to produce hybrids with greater ease (Gardner *et al.*, 2009). The male sterility in the *myb26* mutant plant occurs as a consequence of failed pollen release, rather than due to pollen

inviability and pollen degeneration or abortion. This failure of dehiscence occurs due to the lack of secondary thickening in the endothecium layer of the anther wall resulting in the endothecium failing to expand, hence, shrinkage of the anther walls does not occur and pollen fails to release (Dawson *et al.*, 1999; Steiner-Lange *et al.*, 2003; Yang *et al.*, 2007). These characteristics make it potentially a valuable tool for generating hybrids in species of agricultural significance. An example of potential applications in other plant species, the *Arabidopsis MYB26* gene was introduced into tobacco (*Nicotiana tabacum*) under the control of the CaMV35S promoter. The gene induced ectopic secondary thickening in various aboveground tissues resulting in sterility and prolonged vegetative growth (Yang *et al.*, 2007).

In its expression network, *MYB26* gene (*At3g13890*) has been indicated as potentially co-expressed with a number of genes (Figure 6.1). These co-expressed genes include genes *At3g23130*, *At5g66370* and *At4g32375*. Expectedly, proteins encoded by the three genes are predicted to be localised in the nucleus (TAIR website). *At3g23130* is expressed in flowers and controls the boundary of the stamen and carpel whorls with similar functions to zinc finger transcription factors. The encoded protein of this gene is the closest in location (flower) to that encoded by *MYB26* gene. *At4g32375* encodes a pectin lyase-like superfamily protein involved in polygalacturonase activity carbohydrate metabolic process. These processes take place in many organs in the plant including the flower. *At5g66370* is of unknown function. The gene is co-expressed with the three other genes *At1g28160*, *At4g01490* and *At4g07460*. The first gene

encodes a member of the ERF (ethylene response factor) subfamily B-1 of ERF/AP-2 transcription factor family. The encoded protein contains an AP-2 domain. Transcription factors harbouring this domain play a critical role in regulating gene expression during plant early development (Hilger-Eversheim *et al.*, 2000). The encoded protein was reported to be localized predominantly in the nucleus and was shown to interfere with other signal transduction pathways (Li and Dashwood, 2004; Eckert *et al.*, 2005). The other two genes *At4g01490* and *At4g07460* are transposable element genes in which co-expression with the above-mentioned genes may be coincidental.

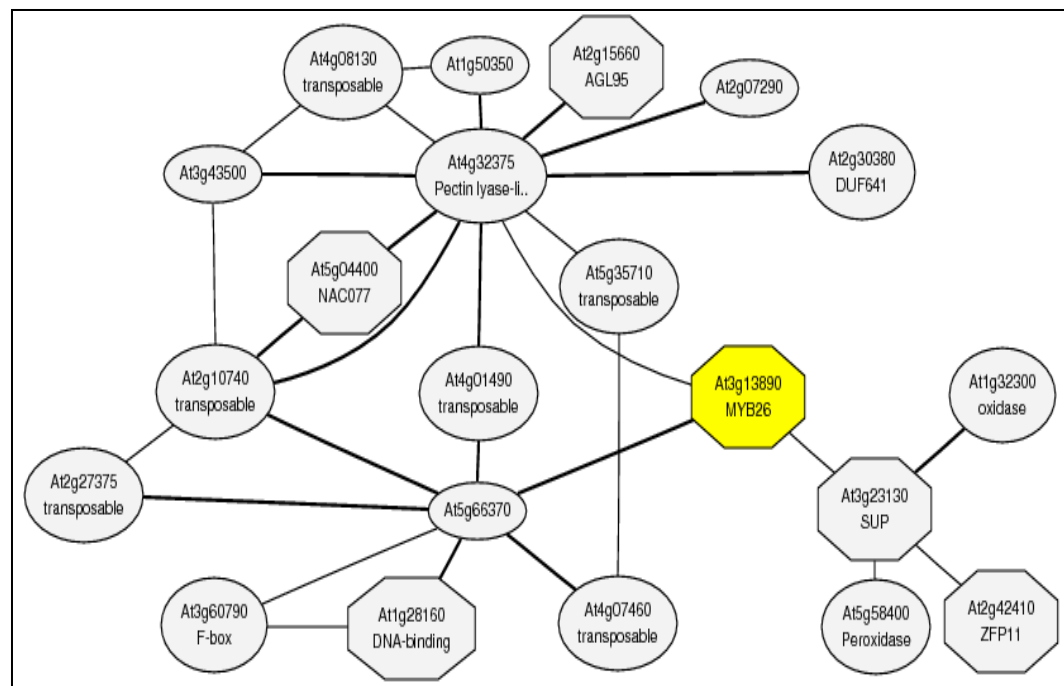


Figure 6.1 Co-expressed gene network of gene *At3g13890*. Taken from the *Arabidopsis* Information Resource (TAIR) website.

In general, co-expression analysis indicated that all the genes co-expressed with *MYB26* gene have no obvious role in pollen development, hence, alternative techniques based upon protein-protein interaction approaches, e.g., yeast-two-hybrid and FRET,

were used in order to experimentally detect other candidate genes that might directly be involved in the MYB26-associated pathway of pollen development or male sterility.

6.3 MYB26 PROTEIN-PROTEIN INTERACTIONS

Studying protein-protein interactions is essential to uncover unknown functions of proteins at the molecular level. However, false-positive interactions present problems in such analyses. Therefore, despite the previous identification of possible candidate interacting proteins with MYB26 protein by yeast-two-hybrid analysis, it was important to confirm whether these interactions were genuine using other reliable approaches, e.g., Förster resonance energy transfer (FRET) analysis (Kuroda *et al.*, 2012; Piotrkowski *et al.*, 2012; Sparkes and Brandizzi, 2012; Steiner *et al.*, 2012).

Most proteins function in complexes of homo- or hetero-oligomers and thus fulfill their roles via protein interactions (Immink *et al.*, 2002). For example, MYB-bHLH-WD40 protein complexes have been found in the control of epidermal cellular diversity (Ramsay and Glover, 2005). The transcription complex of MYB-bHLH-WD40 is involved in the control of anthocyanin biosynthesis in a range of plant species, via the regulation of expression of multiple different target genes (Spelt *et al.*, 2002). Three other MYB factors, WEREWOLF (WER), GLABROUS1 (GL1) and MYB23, are thought to be involved in these complexes (Lee and Schiefelbein, 1999; Kirik *et al.*, 2005).

In the present study, the Y2H screen using the MYB26 full-length protein as the bait identified five proteins showing a possible interaction with MYB26 (Yang and Wilson, unpublished data).

However, given the probability of false positive results from Y2H assays (Lalonde *et al.*, 2008), these interactions were tested by an alternative approach, e.g., FRET.

For interactions to occur, the proteins have to be present at the same location and at the same time. The expression profiles of the identified Y2H proteins were investigated to help confirm their interaction with MYB26. MYB26 is localised in the nucleus (Yang *et al.*, 2007), which is commonly seen for transcription factors. A similar expression pattern was seen for the Y2H proteins identified by screening with the MYB26 protein. Further tests were done to confirm their interaction in *planta*. Transcription factors Y2H320, Y2H560, Y2H620 and Y2H970, when co-expressed with MYB26, were co-localised with MYB26 in the nucleus of *Nicotiana benthamiana* epidermal cells. Y2H128 had previously been localised to the endoplasmic reticulum. The Y2H320, Y2H970 and Y2H620 transcription factors are all expressed in floral tissues suggesting that spatial interaction is possible. Förster resonance energy transfer (FRET) assay was successfully used to demonstrate that physical interaction between MYB26 and Y2H320 occurred in *Nicotiana benthamiana* leaves cells. It is unknown whether MYB26 interacts only with Y2H320, or with one or more of the other of Y2H proteins. However, protein interactions can involve varying numbers proteins in a given complex, e.g., the mammalian RNA polymerase II (pol II) system, which comprises the pol II and five transcription factors (Immink *et al.*, 2002; Kornberg, 2007; Lalonde *et al.*, 2008).

The bZIP protein Y2H320 is of particular interest, since many of its family members have been found to interact with MYB factors

in the phenylpropanoid and flavonoid pathways in secondary metabolism (Du *et al.*, 2009). Genetic and physical interaction studies have also suggested common functions for MYBs and bHLH (basic helix-loop-helix) proteins (Du *et al.*, 2009). Protein complexes, composed of members of the MADS family, have been demonstrated to control floral transition (Immink *et al.*, 2002). Protein complexes composed of the bHLH transcription factors GLABRA3 (GL3) and ENHANCER OF GLABRA3 (EGL3) and different MYBs that associate with a WD-repeat protein (TRANSPARENT TESTA GLABRA1, TTG1), are involved in controlling epidermal cell identity (Qu and Zhu, 2006).

The three CesA proteins, IRX1, IRX3 and IRX5, are involved in forming the cellulose synthesising rosette, which is a stable protein complex that forms in a highly ordered manner (Taylor *et al.*, 2003). Protein interactions can occur briefly via contact with each other, as commonly seen in the signalling pathway (Yoo *et al.*, 2009), or they can be recruited separately to the promoter(s) to initiate translation (Kornberg, 2007). Protein-protein interactions are highly tissue- or cell-specific and in some pathways, the physical interaction between MYBs and bHLHs has not been experimentally confirmed (Nakatsuka *et al.*, 2008; Zhang *et al.*, 2003). In further work, it would be worth testing protein interactions via pull downs of complete protein complexes.

6.4 CHARACTERISATION OF PUTATIVE MYB26-INTERACTING PROTEINS

Yeast-two-hybrid screens using the MYB26 protein previously identified a number of proteins that may interact with MYB26. T-

DNA SALK insertion mutants of the genes encoding these proteins were subsequently analysed to help provide an understanding of the gene function at the molecular level. In addition, morphological observations of these lines were used to detect the gene's physiological and developmental roles in anther and pollen development. However, T-DNA insertion in these genes did not present phenotypes different from the wild type (*Col*) and in particular did not show significant effects on male fertility despite some of them being homozygous. Gene knockout was confirmed by RT-PCR for two, e.g, *At1g08320* (SALK-N591349), and *At5g25560* (SALK-N508223), out of four genes used in the study. However, expression was seen during RT-PCR in knockouts of the other two genes *At3g62970* (SALK-N606671) and *At1g47128* (SALK-N590551) probably due to the occurrence of T-DNA insertions within the intron regions. This indicated that insertion lines within the exon region have the chance to increase the possibility of getting loss-of-function alleles. A number of recent reports have shown that the gene with T-DNA inserted in the intron region can still function (Chehab *et al.*, 2011). However, insertions into an intron can be spliced out during post-transcriptional regulation, which reduces the chance of getting these insertions present in the final transcript (Hurtado *et al.*, 2006). This conclusion was previously reached for the insertion mutant of *AGL104* (Verelst *et al.*, 2007). Such expression of mutated genes due to intron splicing also proved useful in rescuing an otherwise lethal mutation (Sato *et al.*, 2005).

Analysis of the homozygous insertion lines for changes in their phenotype and expression levels showed that the T-DNA

insertion could change gene expression levels. Two of the genes being analysed, e.g., *At1g08320* (SALK-N591349), and *At5g25560* (SALK-N508223), showed complete loss of expression as indicated by RT-PCR due to the T-DNA insert. Nevertheless, despite some of them being homozygous, the SALK insertion mutant lines did not show significantly altered phenotypes, and in particular, no effect on male fertility was observed. The T-DNA insertion in genes *At3g62970* (SALK-N606671) and *At1g47128* (SALK-N590551) showed expression as compared with the wild type (*Col*). However, none of the homozygous KO lines showed male sterility, with all plants appearing similar to wild type. This may be due to possible gene redundancy, where other gene family members may function in the absence of function of the original gene. There is also the possibility that the candidate genes may not be linked to MYB26 pathway. However, these genes might also have minor effects, in which case the use of double mutants might produce a phenotype change and male sterility. This is going to require our further experimentation to reach a final conclusion whether these candidate genes are involved in flower fertility or not.

Analysis of RNAi T1 transgenic lines showed the presence of the *At3g62970^{RNAi}* and *At1g47128^{RNAi}* inserts. Quantitative RT-PCR analysis of expression in the *At3g62970^{RNAi}* and *At1g47128^{RNAi}* transgenic lines indicated that the expression was significantly decreased as compared with the wild type (*Ler*). Gene-silenced plants of *At1g47128^{RNAi}* and *At3g62970^{RNAi}* have presented a similar phenotype to that observed in the respective T-DNA insertion lines, where the gene-silenced lines showed normal

pollen viability confirming the results of their respective SALK T-DNA lines.

RNAi gene silencing is normally associated with knocking down gene expression rather than knocking it out (Yin *et al.*, 2005). Therefore, although the expression of the target mRNA is likely to be reduced, a small amount of transcript may remain, which may be sufficient to maintain wild type function. In addition, it has been reported that the biggest obstacles in genetic engineering of crops is that of the likely transgene silencing (Anand *et al.*, 2003). In addition, unstable gene expression is often related to the integration of multiple copies of the transgene in the plant genome (Muller *et al.*, 1996). All these problems might complicate the results of silencing taking place due to the induction of the RNAi machinery as the phenomenon of multiple copies of the two RNAi transgenes might co-exist.

Quantitative RT-PCR expression analysis of over-expression (OEx) of transgenic plants with genes *At3g47620*, *At1g47128*, *At1g08320* and *At3g62970* under the *CaMV35S* promoter indicated that the level of the expression has been increased. PGWB402 Ω vector, used in inducing gene over-expression, carries a modified *CaMV35S* promoter in which the enhancer region is duplicated; therefore, it is suitable for highly increased expression of genes (Nakagawa *et al.*, 2010). The results showed enhanced vegetative development in terms of leaf size in the transgenics as compared to the WT control. Tissues of OEx lines produced normal xylem development, with no change in lignin deposition as compared to the wild type (*Ler*). Ectopic thickening was previously seen in tobacco when *MYB26* is over-expressed (Yang *et al.*, 2007). This suggests that the putative

interacting factors in the present study might not be sufficient to activate the secondary thickening pathway in the anther.

Results of the expression of Y2H320 gene as tested in the fusion *Prom320:GUS* indicated that GUS signals have been shown in floral tissues, with signal observed in the inflorescence, anthers and nectaries of siliques. A strong signal was also detected in the pollen, although the expression was weak in the nectaries of the flower, silique, vegetative tissues and in the base of the young leaves. Similar observations were previously made using a *MYB26prom::GUS* fusion with Yang *et al.* (2007) demonstrating GUS expression in a number of floral organs but with no expression in the vegetative tissues. Future work is needed to characterise the tissue-specific expression patterns of the other Y2H genes by GUS or GFP fusions.

Y2H320 is an uncharacterised bZIP family transcription factor. Y2H560 and Y2H970 belong to the zinc finger (C3HC4-type RING finger) family. Y2H620 (AtTCP14) is a member of the bHLH family. There is very limited information available for these four proteins, except for Y2H620 that has been demonstrated to regulate seed germination (Tatematsu *et al.*, 2008). Since individual knockout mutants led to no reduction in secondary thickening, double mutants can be used to test gene function and relationships between the individual genes (Koornneef *et al.*, 1982; Putterill *et al.*, 1995).

Furthermore, to test the function of importance of transcriptional activators, specific motifs can be fused to transcription factors in order to convert the transcriptional complex into a repressor. This approach can be used to test the function of components in a protein complex. These motifs include SRDX (plant-specific

EAR-motif) repression domain (Mitsuda and Ohme-Takagi, 2009). In addition, targeted mutations can be generated by TALENs (Transcription Activator-Like Effectors) (Sun and Zhao, 2013) or CRISPRs-Cas9 (Clustered Regularly Interspaced Short Palindromic Repeats-Cas9) (Ran *et al.*, 2013), which guide RNA to interact with specific endogenous genes. Mitsuda *et al.* (2007) showed that plant-specific transcription factors, designated *NAC SECONDARY WALL THICKENING PROMOTING FACTOR1 (NST1)* and *NST2*, are key gene regulators of the secondary wall thickening in *Arabidopsis thaliana*. They showed that the expression of chimeric repressors derived from *NST1* and *NST2* suppressed secondary wall thickenings in the presumptive inter-fascicular fibers. These two transcription factors were shown to regulate expression of genes related to secondary wall synthesis. As a future prospect, it may be interesting to detect expression of the four *Y2H* genes in SALK KO lines of *NST1* (SALK_120377 and SALK_149993) and *NST2* (SALK_022022) to detect the relationship between the two transcription factors and the four *Y2H* genes. In addition, we can knock down the *NST1* and *NST2* genes and detect the consequent change in expression of the four *Y2H* genes. These experiments will help elucidate the possible role of the MYB26-*Y2H* genes, especially *Y2H320*, in the formation of secondary wall thickening.

6.5 CHARACTERIZATION OF NOVEL MALE STERILE MUTANT PLANTS

X-ray and EMS were used in the present study as mutagens to induce mutations in genes related to male sterility and in particular those causing failure of pollen release (Chaudhury, 1993). Male sterility was previously induced using various

transgenesis methods (Acquaah, 2012). A forward genetics approach was utilised in the present work in order to identify the genes that might be critical to anther development and male sterility. The resulted mutant lines showed arrested elongation of the stamen filament. However, the variety of phenotypes observed, such as failure of dehiscence and pollen release, lack of secondary thickening in the anther endothecium, and viable pollen, are similar to those of the *myb26* male sterile mutant. Pollen tube growth and rate of pollen germination were significantly reduced in the *msak* and *c12* mutants. Treatment with JA failed to rescue the fertility and dehiscence of the mutant lines. JA is thought to regulate septum degradation and water transport in anther and, therefore, control anther dehiscence as reported previously, e.g., *dde1* (Sanders *et al.*, 2000), *dad1* (Ishiguro *et al.*, 2001) and GA mutants (Plackett *et al.*, 2011). These results suggest that these new mutants are not associated with JA pathway.

The recovered mutants were then crossed to the *myb26* mutant to test for gene complementation or allelism. Two lines *c12* and *msak* were identified as novel mutants since they were able to complement the *myb26* mutant, and were, therefore, selected for further analysis. The analysis of *c12* was postponed, as we were required to generate a large F2 population for mapping analysis of the mutant. The *msak* mutant plant was crossed as female with wild type Columbia (*Col*) ecotype to generate F2 generation of recombinants and localisation of the gene locus on the chromosome map. Initial analysis showed linkage of the *msak* mutation to a locus *At1g07810* on chromosome 1, which is located at ~2,416,265 bp. Further Simple Sequence Length

Polymorphisms (SSLPs) marker analysis indicated that the *MSAK* gene is located downstream the identified locus. The closest marker to the gene is located 12.57 cM upstream the gene.

The genetic linkage data of the SSLP markers in the vicinity of the *MSAK* gene and the physical distances between these markers was used to predict the location of *MSAK* gene on chromosome 1. This analysis converting the available genetic distance (cM) to a physical distance (kb), indicated that *MSAK* gene could possibly be located at ~3.46 Mb locus of chromosome 1. Interestingly, a transcription factor (TF) namely Transducin/WD40 repeat-like protein is located in this region of chromosome 1. The encoding gene (*At1g10580* located at ~3.49 Mb) was found the highly expressed during pollen development in the recently published Flowernet database (Pearce *et al.*, 2015).

Many other candidate genes are located within the region 3-4 Mb of chromosome 1 with involvement in male gametophyte and in pollen development during mature and germinated pollen stages, three particular candidates are located at ~3.12, 3.68 and 3.87 Mb (*At1g09640*, *At1g11040* and *At1g11520*, respectively). However, the strongest candidate gene, *At1g10770* (located at ~3.59 Mb), has been shown to have a role in pollen development. Anti-sense reduction of *AT1g10770* results in pollen tube growth retardation, partial male sterility and reduced seed set. In addition, the gene is also highly expressed during pollen development as screened by the Flowernet database (Pearce *et al.*, 2015). Several *MYB* genes are also located within this region; however, none of them has been shown to be involved in pollen development or male sterility.

Further work is needed to complete the *msak* mutant for gene identification. This could also be conducted by further mapping and, then, high-throughput sequencing of the whole genome (James *et al.*, 2013) with emphasis on chromosome 1 within the allocated region. Also, *msak* locus could be analysed using KO insertion mutants in the possible candidate genes within the region of 3-4 Mb, that were indicated earlier, to see if a phenotype similar to that of the *msak* mutant line is observed. Complementation analysis using the different candidate genes against the *msak* mutant gene could also be conducted to confirm the gene identity.

6.6 FUTURE PROSPECTS

There are many genes involved in anther and pollen development that have been observed in different species. For example, the rice orthologs of *dyl1*, *ms1* or *ams* genes maintain similar function to their analogs in *Arabidopsis* (Wilson and Zhang, 2009). This conservation in regulation is allowing researchers to go further in finding similar orthologous genes in different less or non-characterised species, e.g., the anther-specific expression of the *Cm-ERS1/H70A* gene from melon in tobacco (Takada *et al.*, 2006). Studying the characterization of the developmental events in the anther is crucial to understand the regulation of this process, which can lead to future crop improvement.

More work could involve finding out the changes in different biological processes in these putative mutants during anther and pollen development. This could be achieved by analysing the chemical composition of the pollen wall and the anther tissue.

Additional work could involve comparing the sequences of putative mutant and identifying any conserved regions with specialised functions and then linking this to possible events that occur during anther and pollen wall formation.

REFERENCES

Aarts, M.G.M., Hodge, R., Kalantidis, K., Florack, D. and Wilson, Z.A. (1997). The *Arabidopsis* MALE STERILITY2 protein shares similarity with reductases in elongation/condensation complexes. *Plant Journal* **12**: 615–23.

Achard, P., Baghour, M., Chapple, A., Hedden, P., Van Der Straeten, D., Genschik, P., Moritz, T. and Harberd, N.P. (2007). The plant stress hormone ethylene controls floral transition via DELLA-dependent regulation of floral meristem-identity genes. *Proceedings of the National Academy of Sciences* **104**(15): 6484-6489.

Acquaah, G. (2012). Mutagenesis in Plant Breeding. *In*: Principles of Plant Genetics and Breeding, 2nd Edition, John Wiley and Sons Ltd, Chichester, UK.

Aharoni, A., Ric De Vos, C.H., Wein, M., Sun, Z., Greco, R., Kroon, A., Mol, J.N.M. and O'Connell, A.P. (2001). The strawberry FaMYB1 transcription factor suppresses anthocyanin and flavonol accumulation in transgenic tobacco. *The Plant Journal* **28**: 319-332.

Alexander, M.P. (1969). Differential staining of aborted and nonaborted pollen. *Stain Technology* **44**: 117-122.

Alexander, M. P. (1980). Aversatile stain for pollen, fungi, yeast and bacteria. *Stain Technology* **55**:13-18.

Aloni, R., Aloni, E., Langhans, M. and Ullrich, C. (2006). Role of auxin in regulating *Arabidopsis* flower development. *Planta* **223**(2): 315-328.

Alonso, J.M. and ECKER, J.R. (2006). Moving forward in reverse: genetic technologies to enable genome-wide phenomic screens in *Arabidopsis*. *Nature reviews. Nature Reviews Genetics* **7**: 524-536.

Alonso, J.M., Stepanova, A.N., Leisse, T.J., Kim, C.J., Chen, H., Shinn, P., Stevenson, D.K., Zimmerman, J., Barajas, P., Cheuk, R., Gadrinab, C., Heller, C., Jeske, A., Koesema, E., Meyers, C.C., Parker, H., Prednis, L., Ansari, Y., Choy, N., Deen, H., Geralt, M., Hazari, N., Hom, E., Karnes, M., Mulholland, C., Ndubaku, R., Schmidt, I., Guzman, P., Aguilar-henonin, L., Schmid, M., Weigel, D., Carter, D.E., Marchand, T., Risseeuw, E., Brogden, D., Zeko, A., Crosby, W.L., Berry, C.C. and Ecker, J.R. (2003). Genome-wide insertional mutagenesis of *Arabidopsis thaliana*. *Science* **301**: 653-657.

Anand, A., Harold, N., Bikram, T., Gill, S. and Muthukrishnan, S. (2003). Stable transgene expression and random gene silencing in wheat. *Plant Biotechnology Journal* **1**: 241-251.

Ariizumi, T. and Toriyama, K. (2011). Genetic regulation of sporopollenin synthesis and pollen exine development. *Annual Review of Plant Biology* **62**: 437-460.

Baudry, A., Heim, M.A., Dubreucq, B., Caboche, M., Weisshaar, B. and Lepiniec, L. (2004). TT2, TT8, and TTG1 synergistically specify the expression of BANYULS and proanthocyanidin biosynthesis in *Arabidopsis thaliana*. *The Plant Journal*, **39**(3): 366-380.

Bennett, M.D., Leitch, I.J., Price, H.J. and Johnston, J.S. (2003). Comparisons with *Caenorhabditis* (approximately 100 Mb) and *Drosophila* (approximately 175 Mb) using flow cytometry show genome size in *Arabidopsis* to be approximately 157 Mb and thus approximately 25% larger than the *Arabidopsis* genome initiative estimate of approximately 125 Mb. *Annals of Botany* **91**(5): 547-557.

Bennett, M.J., Marchant, A., Green, H.G., May, S.T., Ward, S.P., Milliner, P.A., Walker, A. R., Schuiz, B. and Feldmann, K.A. (1996). *Arabidopsis* AUX1 Gene: A pemeas-like regulator of root gravitropism. *Science* **273**(5277): 948-950.

Bennett, S.R.M., Alvarez, J., Bossinger, G. and Smyth, D.R. (1995). Morphogenesis in pinoid mutants of *Arabidopsis thaliana*. *The plant Journal* **8**(4): 505-520.

Bhat, R.A., Lahaye, T. and Panstruga, R. (2006). The visible touch: *in planta* visualization of protein-protein interactions by fluorophore-based methods. *Plant Methods* **26**: 2-12.

Blazquez, M.A., Green, R., Nilsson, O., Sussman, M.R. and Weigel, D. (1998). Gibberellins promote flowering of *Arabidopsis* by activating the LEAFY promoter. *Plant Cell* **10**(5): 791-800.

Bleecker, A.B. and Kende, H. (2000). Ethylene: a gaseous signal molecule in plants. *Annual review of cell and developmental biology* **16**(1): 1-18.

Bolle, C., Koncz, C. and Chua, N.H. (2000). PAT1, a new member of the GRAS family, is involved in phytochrome A signal transduction. *Genes Dev* **14**: 1269-1278.

Bonner, L.J. and Dickinson, H.G. (1989). Anther dehiscence in *Lycopersicon esculentum* Mill. I. Structural aspects. *New Phytologist* **113**(1): 97-115.

Borg, M., Brownfield, L. and Twell, D. (2009). Male gametophyte development: a molecular perspective. *J Exp Bot* **60**(5): 1465-1478.

Bowman, J.L., Smyth, D.R. and Meyerowitz, E.M. (1991). Genetic interactions among floral homeotic genes of *Arabidopsis*. *Development* **112**(1): 1-20.

Bradley, D.J., Kjellbom, P. and Lamb, C.J. (1992). Elicitor- and wound induced oxidative cross-linking of a proline-rich plant cell wall protein: a novel, rapid defense response. *Cell* **70**: 21-30.

Brown, D.M., Zeef, L.A.H., Ellis, J., Goodacre, R. and Turner, S.R. (2005). Identification of novel genes in *Arabidopsis* involved in secondary cell wall formation using expression profiling and reverse genetics. *Plant Cell* **17**(8): 2281-2295.

Brown, D.M., Zhang, Z., Stephens, E., Dupree, P. and Turner, S.R. (2009). Characterization of *IRX10* and *IRX10*-like reveals an essential role in glucuronoxylan biosynthesis in *Arabidopsis*. *The Plant Journal* **57**: 732-746.

Brown, R.L., Kazan, K., McGrath, K.C., Maclean, D.J. and Manners, J.M. (2003). A role for the GCC-box in jasmonate-mediated activation of the PDF1.2 gene of *Arabidopsis*. *Plant Physiol* **132**(2): 1020-1032.

Canales, C., Bhatt, A.M., Scott, R. and Dickinson, H. (2002). EXS, a putative LRR receptor kinase, regulates male

germline cell number and tapetal identity and promotes seed development in *Arabidopsis*. *Current Biology* **12**: 1718-1727.

Carroll, A. and Somerville, C. (2009). Cellulosic biofuels. *Annual Review of Plant Biology*, 60.

Cecchetti, V., Altamura, M.M., Brunetti, P., Petrocelli, V., Falasca, G., Ljung, K., Costantino, P. and Cardarelli, M. (2013). Auxin controls *Arabidopsis* anther dehiscence by regulating endothecium lignification and jasmonic acid biosynthesis. *Plant J* **74**: 411-422.

Cecchetti, V., Altamura, M.M., Falasca, G., Costantino, P. and Cardarelli, M. (2008). Auxin regulates *Arabidopsis* anther dehiscence, pollen maturation, and filament elongation. *Plant Cell* **20**(7): 1760-1774.

Chaudhury, A.M. (1993). Nuclear genes controlling male Fertility. *The Plant Cell* **5**(10): 1277-1283.

Chase, C. and Babay-Laughnan, S. (2004). Cytoplasmic male sterility and fertility restoration by nuclear genes. In *Molecular Biology and Biotechnology of Plant Organelles*, H. Daniell and C. Chase, eds .Dordrecht, The Netherlands: Kluwer Academic Publishers, p593-622.

Chehab, E., W., Kim, S., Savchenko, T., Kliebenstein, D., Dehesh, K. and Braam, J. (2011). Intronic T-DNA insertion renders *Arabidopsis opr3* a conditional jasmonic acid-producing mutant. *Plant Physiol* **156**: 770-778.

Chen, W., Yu, X.H., Zhang, K., Shi, J., Schreiber, L., Shanklin, J. and Zhang, D. (2011). Male sterile 2 encodes a plastid-localized fatty acyl ACP reductase required for pollen

exine development in *Arabidopsis thaliana*. *Plant Physiology* **157**: 842-853.

Cheng, H., Qin, L., Lee, S., Fu, X., Richards, D.E., Cao, D., Luo, D., Harberd, N.P. and Peng, J. (2004). Gibberellin regulates *Arabidopsis* floral development via suppression of DELLA protein function. *Development* **131**(5): 1055-1064.

Cheng, Y. and Zhao, Y. (2007). A Role for auxin in flower development. *Journal of Integrative Plant Biology* **49**(1): 99-104.

Cheng, Y., Dai, X. and Zhao, Y. (2006). Auxin biosynthesis by the YUCCA flavin monooxygenases controls the formation of floral organs and vascular tissues in *Arabidopsis*. *Genes Dev* **20**: 1790-1799.

Cheng, S.H., Zhuang, J.Y., Fan, Y.Y., Du, J.H. and Cao, L.Y (2007). Progress in research and development on hybrid rice: a super-domesticated in China. *Ann Bot (Lond)* **100**: 959-966.

Chhun, T., Aya, K., Asano, K., Yamamoto, E., Morinaka, Y., Watanabe, M., Kitano, H., Ashikari, M., Matsuoka, M. and Ueguchi-Tanaka, M. (2007). Gibberellin regulates pollen viability and pollen tube growth in rice. *Plant Cell* **19**(12): 3876-3888.

Clough, S.J. and Bent, A.F. (1998). Floral dip: a simplified method for *Agrobacterium*-mediated transformation of *Arabidopsis thaliana*. *Plant J* **16**(6): 735-743.

Cole, R.A., Synek, L., Zarsky, V. and Fowler, J.E. (2005). SEC8, a subunit of the putative *Arabidopsis* exocyst complex, facilitates pollen germination and competitive pollen tube growth. *Plant Physiol* **138**: 2005–2018.

Cosgrove, D.J. (2000). Expansive growth of plant cell walls. *Plant physical biochem* **38**(1-2): 109-124.

Dawson, J., Sozan, E., Vizir, I., van Waeyenberge, S., Wilson, Z. A. and Mulligan, B.J. (1999). Characterization and genetic mapping of a mutation (ms35) which prevents anther dehiscence in *Arabidopsis thaliana* by affecting secondary wall thickening in the endothecium. *New Phytol* **144**: 213-222.

Dawson, J., Wilson, Z.A., Aarts, M.G.M., Braithwaite, A.F., Briarty, L.G. and Mulligan, B.J. (1993). Microspore and pollen development in six male-sterile mutants of *Arabidopsis thaliana*. *Canadian Journal of Botany-Revue Canadienne de Botanique* **71**(4): 629-638.

De Cnodder, T., Vissenberg, K., Van Deer Straeten, D. and Verbelen, J.P. (2005). Regulation of cell length in the *Arabidopsis thaliana* root by the ethylene precursor 1-aminocyclopropane-1-carboxylic acid: a matter of apoplastic reactions. *New Phytologist* **168**(3): 541-550.

Delmer, D.P. and Amor, Y. (1995). Cellulose biosynthesis. *Plant Cell* (**7**): 987-1000.

Devarshi, S., Robin, G.P. and Kachroo, A. (2013). GmRIN4 protein family members function nonredundantly in soybean race-specific resistance against *Pseudomonas syringae*. *New Phytologist* **197**(4): 1225-1235.

Devoto, A., Nieto-Rostro, M., Xie, D., Ellis, C., Harmston, R., Patrick, E., Davis, J., Sherratt, L., Coleman, M. and Turner, J.G. (2002). COI1 links Jasmonate signalling and

fertility to the SCF ubiquitin-ligase complex in *Arabidopsis*. *Plant J* **32**: 457-466.

Dharmasiri, N., Dharmasiri, S. and Estelle, M. (2005). The F-box protein TIR1 is an auxin receptor. *Nature* **435**(7041): 441-445.

Du, H., Zhang, L., Liu, L., Tang, X.F., Yang, W.J., Wu, Y.M., Huang, Y.B. and Tang, Y.X. (2009). Biochemical and molecular characterization of plant MYB transcription factor family. *Biochemistry (Mosc)* **74**: 1-11.

Dubos, C., Stracke, R., Grotewold, E., Weisshaar, B., Martin, C. and Lepiniec, L. (2010). MYB transcription factors in *Arabidopsis*. *Trends Plant Sci* **15**(10): 573-581.

Eamens, A., Wang, M.B., Smith, A.N. and Waterhouse, M. (2008). RNA silencing in plants: yesterday, today, and tomorrow. *Plant Physiology* **147**: 456-468.

Eckert, D., Buhl, S., Weber, S., Jäger, R. and Schorle, H. (2005). The AP-2 family of transcription factors. *Genome Biology* **6**: 246.

Farmer, E.E. and Ryan, C.A. (1990). Interplant communication: airborne methyl jasmonate induces synthesis of proteinase inhibitors in plant Leaves. *Proceedings of National Academy of Sciences* **87**(19): 7713-7716.

Feller, A., Machemer, K., Braun, E.L. and Grotewold, E. (2011). Evolutionary and comparative analysis of MYB and bHLH plant transcription factors. *Plant J* **66**(1): 94-116.

Feng, X. and Dickinson, H.G. (2007). Packaging the male germline in plants. *Trends Genet* **23**: 121-138.

Feng, X.L., Ni, W.M., Elge, S., Mueller-Roeber, B. B., Xu, Z. H. and Xue, H.W. (2006). Auxin flow in anther filaments is critical for pollen grain development through regulating pollen mitosis. *Plant Mol Biology* **61**: 215-226.

Feys, B.J.F., Benedetti, C.E., Penfold, C.N. and Turner, J.G. (1994). Arabidopsis mutants selected for resistance to the phytotoxin coronatine are male-sterile, insensitive to methyl jasmonate, and resistant to a bacterial pathogen. *Plant Cell* **6**: 751–759.

Fior, S. and Gerola, D.P. (2009). Impact of ubiquitous inhibitors on the GUS gene reporter system: evidence from the model plants *Arabidopsis*, tobacco and rice and correction methods for quantitative assays of transgenic and endogenous GUS. *Plant Methods* **5**: 19.

Fire, A., Albertson, D., Harrison, S. and Moerman, D. (1991). Production of antisense RNA leads to effective and specific inhibition of gene expression in *C. elegans* muscle. *Development* **113**: 503–514.

Fire A., Xu, S., Montgomery, M.K., Kostas, S.A., Driver, S.E. and Mello, C.C. (1998). Potent and specific genetic interference by double-stranded RNA in *Caenorhabditis elegans*. *Nature* **391**: 806–811.

Fleet, C.M. and Sun, T.P. (2005). A DELLA cate balance: the role of gibberellin in plant morphogenesis. *Plant Biology* **8**(1): 77-85.

Fobert, P.R. and Després, C. (2005). Redox control of systemic acquired resistance. *Current Opinion in Plant Biology* **8**: 378-382.

Fernández Gómez, J. and Wilson, Z. (2014). A barley PHD-finger transcription factor that confers male sterility by affecting tapetal development. *Plant Biotechnology Journal* **12**(6): 765-777.

Frimi, J., Yang, X., Michniewicz, M., Weijers, D., uint, A., Tietz, O., Benjamins, R., Ouwerkerk, P.B.F., Ljung, K., Sandberg, G., Hooykaas, P.J.J., Palme, K. and Offringa, R. (2004). A PINOID-Dependent Binary Switch in Apical-Basal PIN Polar Targeting Directs Auxin Efflux. *Science* **306**(5697): 862-865.

Galweiler, L., Guan, C., Muller, A., Wisman, E., Mendgen, K., Yephremov, A. and Palme, K. (1998). Regulation of polar auxin transport by AtPIN1 in *Arabidopsis* vascular tissue. *Science* **282**(5397): 2226-2230.

Gardner, N., Felsheim, R. and Smith, A.G. (2009). Production of male- and female-sterile plants through reproductive tissue ablation. *Journal of Plant Physiology* **166**: 871-881.

Gehring, W.J., Qian, Y.Q., Billeter, M., Furukubo-Tokunaga, K., Schier, A.F., Resendez-Perez, D., Affolter, M., Otting, G. and Wuthrich, K. (1994). Homeodomain-DNA recognition. *Cell* **78**(2): 211-223.

Gilissen, L.J., Metz, P.L., Stiekema, W.J. and Nap (1998). Biosafety of *E. coli* beta-glucuronidase (GUS) in plants. *Transgenic Res* **7**(3): 157-163.

Goff, S.A., Cone, K.C. and Chandler, V.L. (1992). Functional analysis of the transcriptional activator encoded by the maize B gene: evidence for a direct functional interaction between two classes of regulatory proteins. *Genes Dev* **6**: 864-875.

Goldberg, R.B., Beals, T.P. and Sanders, P.M. (1993). Anther development: basic principles and practical applications. *Plant Cell* **5**: 1217-1229.

Grefen, C., Donald, S., Hashimoto, K., Kudla, J., Schumacher, K. and Blatt, M.R. (2010). A ubiquitin-10 promoter-based vector set for fluorescent protein tagging facilitates temporal stability and native protein distribution in transient and stable expression studies. *The plant Journal* **64**: 355-365.

Griffiths, J., Murase, K., Rieu, I., Zentelia, R., Zhang, Z.L., Powers, S.J., Gong, F., Phillips, A.L., Hedden, P., Sun, T.P. and Thomas, S.G. (2006). Genetic characterization and functional analysis of the GID1 gibberellin receptors in *Arabidopsis*. *Plant Cell* **18**(12): 3399-3414.

Gundlach, H., Muller, M.J., Kutchan, T.M. and Zenk, M.H. (1992). Jasmonic acid is a signal transducer in elicitor-induced plant cell cultures. *Proc Natl Acad Sci USA* **89**(6): 2389-2393.

Guo, H. and Ecker, J.R. (2004). The ethylene signalling pathway: new insights. *Current Opinion in Plant Biology* **7**(1): 40-49.

Hagen, G. and Guilfoyle, T. (2002). Auxin-responsive gene expression: genes, promoters and regulatory factors. *Plant Molecular Biology* **49**(3): 373-385.

Henderson, J., Baulry, J.M., Ashford, D.A., Oliver, S.C., Hawes, C.R., Lazarus, C.M., Venis, M.A. and Napier, R.M. (1997). Retention of maize auxin-binding protein in the endoplasmic reticulum: quantifying escape and the role of auxin. *Planta* **202**(3): 313-323.

Harding, S.A., Leshkevich, J., Chiang, V.L. and Tsai, C.J. (2002). Differential substrate inhibition couples kinetically distinct 4-coumarate:coenzyme A ligases with spatially distinct metabolic roles in quaking aspen. *Plant Physiol* **128**: 428-438.

Harris, D. and De Bolt, S. (2010). Synthesis, regulation and utilization of lignocellulosic biomass. *Plant Biotechnol J* **8**(3): 244-262.

Hilger-Eversheim, K., Moser, M., Schorle, H. and Buettner, R. (2000). Regulatory roles of AP-2 transcription factors in vertebrate development, apoptosis and cell-cycle control. *Gene* **260**: 1-12.

Hill, J.P. and Lord, E.M. (1989). Floral development in *Arabidopsis thaliana*: A comparison of the wild type and the homeotic pistillata mutant. *Canadian Journal of Botany-Revue Canadienne de Botanique* **67**(10): 2922-2936.

Himanen, K., Vuylsteke, M., Vanneste, S., Vercruyssen, S., Boucheron, E., Alard, P., Chriqui, D., Van Montagu, M.,

Inze, D. and Beeckman, T. (2004). Transcript profiling of early lateral root initiation. *Proceedings of the National Academy of Sciences*, **101**(14): 5146-5151.

Hu, J., Mitchum, M.G., Barnaby, N., Ayele, B.T., Ogawa, M., Nam, E., Lai, W.C., Hanada, A., Alonso, J.M., Ecker, J.R., Swain, S.M., Yamaguchi, S., Kamiya, Y. and Sun, T.P. (2008). Potential sites of bioactive gibberellin production during reproductive growth in *Arabidopsis*. *Plant Cell* **20**(2): 320-336.

Huang, L., Ye, Y., Zhang, Y., Zhang, A., Liu, T. and Cao, J. (2009). *BcMF9*, a novel polygalacturonase gene, is required for both *Brassica campestris* intine and exine formation. *Annals of Botany* **104**: 1339–1351.

Hurtado, L., Farrona, S. and Reyes, J.C. (2006). The putative SWI/SNF complex subunit BRAHMA activates flower homeotic genes in *Arabidopsis thaliana*. *Plant Mol Biol* **62**: 291-304

Immink, R.G.H., Gadella, T.W.J., Ferrario, S., Busscher, M. and Angenent, G.C. (2002). Transcription factors do it together: the hows and whys of studying protein-protein interactions. *Trends Plant Science* **7**: 531-534.

Ishiguro, S., Kawai-Oda, A., Ueda, J., Nishida, I. and Okada, K. (2001). The DEFECTIVE IN ANTHOR DEHISCENCE gene encodes a novel phospholipase A1 catalyzing the initial step of jasmonic acid biosynthesis, which synchronizes pollen maturation, anther dehiscence, and flower opening in *Arabidopsis*. *Plant Cell* **13**(10): 2191-2209.

Jain, M., Kaur, N., Tyagi, A. and Khurana, J. (2006). The auxin-responsive GH3 gene family in rice (*Oryza sativa*). *Functional and integrative Genomics* **6**(1): 36-46.

Jain, S.K. (1959). Male sterility in flowering plants. *Biblioger Genet* **18**: 103-166.

Jakoby, M., Weisshear, B., Droge-Laser, W., Vicente-Carbajosa, J., Tiedemann, J., Kroj, T. and Parcy, F. (2002). bZIP transcription factors in Arabidopsis. *Trends in Plant Science* **7**(3): 106-111.

James, G.V., Patel, V., Nordström, K.J., Klasen, J.R., Salomé, A.P., Weigel, D. and Schneeberger, K.(2013). User guide for mapping-by-sequencing in *Arabidopsis*. *Genome Biology* **14**: R61.

Jefferson, R.A., Kavanagh, T.A. and Bevan, M.W. (1987). GUS fusions: β -glucuronidase as a sensitive and versatile gene fusion marker in higher plants. *The EMBO Journal* **13**: 3901-3907.

Jones, L., Ennos, A.R. and Turner, S.R. (2001). Cloning and characterization of irregular xylem4 (*irx4*): a severely lignindeficient mutant of Arabidopsis. *The Plant J* **26**: 205-216.

Jung, K.W., Seung-Ick, O., Kim, Y.Y., Yoo, K.S., Cui, M.H. and Shin, J.S.H. (2008). Arabidopsis histidine-containing phosphotransfer Factor 4 (AHP4). negatively regulates secondary wall thickening of the anther endothecium during flowering. *Mol Cells* **25**(2): 294-300.

Kalantidis, K., Dawson, J., Wilson, Z.A., Briartym, L.G. and Mulligan, B.J. (1994). Isolation and characterisation of twelve

male sterile mutants of *Arabidopsis thaliana*. *ISPMB*, Amsterdam, 750.

Kapila, J., Rycke, R.D., Montagu, M.V. and Angenon, G. (1997). An *Agrobacterium*-mediated transient gene expression system for intact leaves. *Plant Science* **122**: 101–108.

Karimi, M., De Meyer, B. and Hilson, P. (2005). Modular cloning in plant cells. *Trends Plant Sci* **10**: 103–105.

Katsir, L., Chung, H.S., Koo, A.J.K. and Howe, G.A. (2008). Jasmonate signaling: a conserved mechanism of hormone sensing. *Curr Opin Plant Biol* **11**: 428-435.

Kawaoka, A., Kaothien, P., Yoshida, K., Endo, S., Yamada, K. and Ebinuma, H. (2000). Functional analysis of tobacco LIM protein NtLIM1 involved in lignin biosynthesis. *The Plant J* **22**: 289-301.

Keijzer, C.J. (1987). The processes of anther dehiscence and pollen dispersal. *New Phytologist* **105**(3): 487-498.

Kepinski, S. and Leyser, O. (2005). The *Arabidopsis* F-box protein TIR1 is an auxin receptor. *Nature* **435**(7041): 446-451.

Kerschen, A., Napoli, C.A., Jorgensen, R.A. and Müller, A.E. (2004). Effectiveness of RNA interference in transgenic plants. *FEBS Letters* **566**(1-3): 223-228.

Kim, O.K., Jung, J.H. and Park, C.M. (2010). An *Arabidopsis* F-box protein regulates tapedum degeneration and pollen maturation during anther development. *Planta* **232**(2): 353–366.

Kim, S.J., Jeong, D.H., An, G.H. and Kim, S.R. (2005). Characterization of a drought-responsive gene *OsTPS1*

identified by the T-DNA gene-trap system in rice. *Journal of Plant Biology* **48**: 371-379.

Kim, S.Y., Hong, C.B. and Lee, I. (2001). Heat shock stress causes stage-specific male sterility in *Arabidopsis thaliana*. *Journal of Plant Research* **114**: 301-307.

Kim, W.C., Kim, J.Y., Ko, J.H., Kim, J. and Han, K.H. (2013). Transcription factor MYB46 is an obligate component of the transcriptional regulatory complex for functional expression of secondary wall-associated cellulose synthases in *Arabidopsis thaliana*. *Journal of Plant Physiology* **170**(15): 1374-1378.

Kirik, V., Lee, M.M., Wester, K., Herrmann, U., Zheng, Z., Oppenheimer, D., Schiefelbein, J. and Hulskamp, M. (2005). Functional diversification of *MYB23* and *GL1* genes in trichome morphogenesis and initiation. *Development* **132**: 1477-1485.

Knox, J.P. (2008). Revealing the structural and functional diversity of plant cell walls. *Plant Biology* **11**: 308-313.

Koornneef, M., Dellaert, L.W.M. and van der Veen, J.H. (1982). EMS- and relation-induced mutation frequencies at individual loci in *Arabidopsis thaliana* (L.) Heynh. *Mutation Research/Fundamental and Molecular Mechanisms of Mutagenesis* **93**(1): 109-123.

Kornberg, R.D. (2007). The molecular basis of eukaryotic transcription. *Proc Natl Acad Sci USA* **104**: 12955-12961.

Kosarev, P., Mayer, K.F. and Hardtke, C.S. (2002). Evaluation and classification of RING-finger domains encoded by the *Arabidopsis* genome. *Genome Biol* **3**(4): RESEARCH0016.

Kranz, H.D., Denekamp, M., Greco, R., Jin, H., Leyva, A., Meissner, R.C., Petroni, K., Urzainqui, A., Bevan, M. and Martin, C. (1998). Towards functional characterisation of the members of the R2R3-MYB gene family from *Arabidopsis thaliana*. *Plant J* **16**: 263-276.

Krysan, J.P., Young, C.J., Michael and Sussman, R.M. (1999). T-DNA as an insertional mutagen in *Arabidopsis*. *The Plant Cell* **11**: 2283–2290.

Kuroda, H., Yanagawa, Y., Takahashi, N., Horii, Y. and Matsui, M. (2012). Analysis of interaction and localization of *Arabidopsis* SKP1-LIKE (ASK) and F-Box (FBX) proteins. *PLoS ONE* **7**: e50009.

Lai, L.B., Nadeau, J.A., Lucas, J., Lee, E.K., Nakagawa, T., Zhao, L., Geisler, M. and Sack, F.D. (2005). The Arabidopsis R2R3 MYB proteins FOUR LIPS and MYB88 Restrict Divisions Late in the Stomatal Cell Lineage. *Plant Cell* **17**(10): 2754-2767.

Lalonde, S.W.E.D., Loque, D., Chen, J., Rhee, S.Y. and Frommer, W.B. (2008). Molecular and cellular approaches for the detection of protein-protein interactions: latest techniques and current limitations. *Plant J* **53**: 610-635.

Lamesch, P., Berardini, T.Z., Li, D., Swarbreck, D., Wilks, C., Sasidharan, R., Muller, R., Dreher, K., Alexander, D.L., Garcia-Hernandez, M., Karthikeyan, S.A., Lee, C.H., Nelson, W.D., Ploetz, L. Singh, S. Wensel, A. and Huala, E. (2012). The *Arabidopsis* Information Resource (TAIR): improved gene annotation and new tools. *Nucleic Acid Research* **40**: D1202–D1210.

- Lampl, N., Alkan, N., Davydov, O. and Fluhr, R. (2013).** Set-point control of RD21 protease activity by AtSerp1 controls cell death in *Arabidopsis*. *Plant Journal* **74**(3): 498-510.
- Lee, M.M. and Schiefelbein, J. (1999).** WEREWOLF, a MYB related protein in *Arabidopsis*, is a position-dependent regulator of epidermal cell patterning. *Cell* **99**: 473-483.
- Leland, R.H. (1985).** A Guide to Sorghum Breeding. International Crops Research Institute for the Semi-Arid Tropics ICRISAT Patancheru P.O. *Andhra Pradesh* 502, 324, India.
- Li, Q. and Dashwood, R.H. (2004).** Activator protein 2alpha associates with adenomatous polyposis coli/beta-catenin and inhibits beta-catenin/T-cell factor transcriptional activity in colorectal cancer cells. *J Biol Chem* **279**: 45669-45675.
- Li, H., Lin, Y., Heath, R.M., Zhu, M.X. and Yang, Z. (1999).** Control of pollen tube tip growth by a Rop GTPase-dependent pathway that leads to tip-localized calcium influx. *The Plant Cell* **11**: 1731-1742.
- Li, J., Li, X., Guo, L., Lu, F., Feng, X., He, K., Wei, L., Chen, Z., Qu, L.J. and Gu, H. (2006)** A subgroup of MYB transcription factor genes undergoes highly conserved alternative splicing in *Arabidopsis* and rice. *J Exp Bot* **57**(6): 1263-1273.
- Li, S.F., Iacuone, S. and Parish, R.W. (2007).** Suppression and restoration of male fertility using a transcription factor. *Plant Biotechnol J* **5**(2): 297-312.
- Lippman, Z.B. and Zamir, D. (2007).** Heterosis: revisiting the magic. *Trends Genet* **23**(2): 60-66.

Ljung, K., Hull, A., Celenza, J., Yamada, M., Estelle, M., Normanly, J. and Sandberga, G. (2005). Sites and Regulation of Auxin Biosynthesis in *Arabidopsis* Roots. *The plant cell* **17**: 1090–1104.

Ma, H. (2005). Molecular genetic analysis of microsporogenesis and microgametogenesis in flowering plants. *Annu Rev Plant Biol* **56**: 393-434.

Ma, J., Skibbe, D., Fernandes, J. and Walbot, V.(2008). Male reproductive development gene expression profiling of maize anther and pollen ontogeny. *Genome Biol* **9**: R181.

Ma, X., Feng, B. and Ma, H. (2012) AMS-dependent and independent regulation of anther transcriptome and comparison with those affected by other *Arabidopsis* anther genes. *BMC Plant Biology* **12**: 23.

Mandaokar, A., Thines, B., Shin, B., Markus Lange, B., Chol, G., Koo, Y.J., Yoo, Y.J., Choi, T.D., Choi, G. and Browse, J. (2006). Transcriptional regulators of stamen development in *Arabidopsis* identified by transcriptional profiling. *Plant J* **49**: 984-1008.

Mandaokar, A. and Browse, J. (2009). MYB108 acts together with MYB24 to regulate jasmonate-mediated stamen maturation in *Arabidopsis*. *Plant Physiology* **149**: 851-862.

Mashiguchia, K., Tanakaa, K., Sakaic, T., Sugawaraa, S., Kawaideb, H., Natsumeb, M., Hanadaa, A., Yaenaa, T., Shirasua, K., Yaod, H., McSteend, P., Zhaoe, Y., Hayashif, K., Kamiyaa, Y. and Kasaharaa, H. (2011). The main auxin biosynthesis pathway in *Arabidopsis*. *Proc Natl Acad Sci USA* **108**(45): 18512–18517.

McCarthy, R.L., Zhong, R. and Ye, Z.H. (2009). MYB83 is a direct target of SND1 and acts redundantly with MYB46 in the regulation of secondary cell wall biosynthesis in *Arabidopsis*. *Plant Cell Physiol* **50**: 1950–1964.

McCormick, S. (1993). Male gametophyte development. *Plant Cell* **5**(10): 1265-1275.

Meyerowitz, E.M. (2001). Prehistory and history of *Arabidopsis* research. *Plant Physiol* **125**(1): 15-19.

Millar, A.A. and Gubler, F. (2005). The *Arabidopsis* GAMYB-like genes, *MyB33* and *MYB56*, are microRNA-regulated genes that redundantly facilitate anther development. *Plant Cell* **17**: 705-721.

Mitsuda, N., Seki, M., Shinozaki, K. and Ohme-Takagi, M. (2005). The NAC transcription factors NST1 and NST2 of *Arabidopsis* regulate secondary wall thickenings and are required for anther dehiscence. *Plant Cell* **17**: 2993–3006.

Mitsuda, N., Iwase, A., Yamaoto, H., Yoshida, M., Seki, M., Shinozaki, K. and Ohme-Takagi, M. (2007). NAC transcription factors, NST1 and NST3, are key regulators of the formation of secondary walls in woody tissues of *Arabidopsis*. *Plant Cell* **19**: 270-280.

Mitsuda, N. and Ohme-Takagi, M. (2008). NAC transcription factors NST1 and NST3 regulate pod shattering in a partially redundant manner by promoting secondary wall formation after the establishment of tissue identity. *The Plant Journal* **56**: 768-778.

Mitsuda, N. and Ohme-Takagi, M (2009). Functional Analysis of Transcription Factors in Arabidopsis. *Plant Cell Physiol* **50**: 1232-1248.

Mueller, S., Hilbert, B., Dueckershoff, K., Roitsch, T., Krischke, M., Mueller, M.J. and Berger, S. (2008). General detoxification and stress responses are mediated by oxidized lipids through TGA transcription factors in Arabidopsis. *Plant Cell* **20**: 768-785.

Muller, E., Lorz, H., Lutticke, S. (1996). Variability of transgene expression in clonal cell lines of wheat. *Plant Science* **114**: 71-82.

Murashige, T. and Skoog, F. (1962). A Revised Medium for Rapid Growth and Bio Assays with Tobacco Tissue Cultures. *Physiologia Plantarum* **15**(3): 473-497.

Murmu, J., Bush, M.J., DeLong, C., Li, S.T., Xu, M.L., Khan, M., Malcolmson, C., Fobert, P.R., Zachgo, S. and Hepworth, S.R. (2010). Arabidopsis basic leucine-zipper transcription factors TGA9 and TGA10 interact with floral glutaredoxins ROXY1 and ROXY2 and are redundantly required for anther development. *Plant Physiol* **154**: 1492-1504.

Murray, F., Kalla, R., Jacobsen, J. and Gubler, F.(2003). A role for HvGAMYB in anther development. *Plant J* **33**: 481-491.

Nakagawa, T., Suzuki, T., Murata, S., Nakamura, S., Hino, T., Maeo, K., Tabata, R., Kawai, T., Tanaka, K., Niwa, Y., Watanabe, Y., Nakamura, K., Kimura, T. and Ishiguro, S. (2010). Improved Gateway binary vectors: high performance vectors for creation of fusion constructs in transgenic analysis of plants. *Biosci Biotechnol Biochem* **71**(8): 2095-2100.

Nakatsuka, T., Haruta, K.S., Pitaksutheepong, C., Abe, Y., Kakizaki, Y., Yamamoto, K., Shimada, N., Yamamura, S. and Nishihara, M. (2008). Identification and characterization of R2R3-MYB and bHLH transcription factors regulating anthocyanin biosynthesis in gentian flowers. *Plant Cell Physiol* **49**: 1818-1829.

Napoli, C., Lemieux, C. and Jorgensen, R. (1990). Introduction of chimeric chalcone synthase gene into *petunia* results in reversible cosuppression of homologous gene in trans. *Plant Cell* **2**: 279–289.

Neelam, A. and Sexton, R. (1995). Cellulase (endo-1,4 glucanase) and cell wall breakdown during anther development in the sweet pea (*Lathyrus odoratus* L.): isolation and characterization of partial cDNA clones. *Journal of Plant Physiology* **146**: 622–628.

Nelson, M.R., Band, L.R., Dyson, R.J., Lessinnes, T., Wells, D.M., Yang, C. and Wilson, Z.A. (2012). A biomechanical model of anther opening reveals the roles of dehydration and secondary thickening. *New Phytologist* **196**(4): 1030-1037.

Ogawa, M., Kay, P., Wilson, S. and Swain, S.M. (2009). ARABIDOPSIS DEHISCENCE ZONE POLYGALACTURONASE1 (ADPG1), ADPG2, and QUARTET2 are polygalacturonases required for cell separation during reproductive development in Arabidopsis. *The Plant Cell Online* **21**(1): 216-233.

Olsen, K.M., Lea, U.S., Slimestad, R., Verheul, M. and Lillo, C. (2008). Differential expression of four *Arabidopsis* PAL genes; PAL1 and PAL2 have functional specialization in abiotic

environmental-triggered flavonoid synthesis. *J Plant Physiol* **165**: 1491-1499.

Østergaard, L. and Yanofsky, M.F. (2004) Establishing gene function by mutagenesis in *Arabidopsis thaliana*. *The Plant Journal* **39**: 682–696.

Paciorek, T. and Friml, J. (2006). Auxin signaling. *J Cell Sci* **119**(7): 1199-1202.

Paciorek, T., Zazimalova, E., Ruthardt, N., Petrasek, J., Stierhof, Y.D., Kleine-Vehn, J., Morris, D.A., Emans, N., Jurgenes, G., Geldner, N. and Friml, J. (2005). Auxin inhibits endocytosis and promotes its own efflux from cells. *Nature* **435**(7046): 1251-1256.

Pandit, N.N. and Russo, V.E. (1992). Reversible inactivation of a foreign gene, *hph*, during the asexual cycle in *Neurospora crassa* transformants. *Molecular General Genetics* **234**(3): 412–22.

Park, J.H., Halitschke, R., Kim, H.B., Baldwin, I.T., Feldmann, K.A. and Feyereisen, R. (2002). A knock-out mutation in allene oxide synthase results in male sterility and defective wound signal transduction in *Arabidopsis* due to a block in jasmonic acid biosynthesis. *Plant J* **31**(1): 1-12.

Patten, A.M., Cardenas, C.L., Cochrane, F.C., Laskar, D.D., Bedgar, D.L., Davin, L.B. and Lewis, N.G. (2005). Reassessment of effects on lignification and vascular development in the *irx4* *Arabidopsis* mutant. *Phytochemistry* **66**: 2092-2107.

Pearce, S., Ferguson, A., King, J. and Wilson, Z.A. (2015). FlowerNet: A gene expression correlation network for anther and pollen development. *Plant Physiology* **167**: 1717–1730.

Penfield, S., Meissner, R.C., Shoue, D.A., Carpita, N.C. and Bevan, M.W. (2001). MYB61 is required for mucilage deposition and extrusion in the Arabidopsis seed coat. *Plant Cell* **13**: 2777-2791.

Phan, H.A., Iacuone, S., Li, S.F. and Parish, R.W. (2011). The MYB80 transcription factor is required for pollen development and the regulation of tapetal programmed cell death in *Arabidopsis thaliana*. *The Plant Cell Online* **23**(6): 2209-2224.

Piotrkowski, N., Schillberg, S. and Rasche, S. (2012). Tackling heterogeneity: A leaf disc-based assay for the high-throughput screening of transient gene expression in tobacco. *PLoS ONE* **9**: e45803.

Pireyre, M. and Burow, M. (2015). Regulation of MYB and bHLH transcription factors—a glance at the protein level. *Molecular Plant* **8**(3): 378–388.

Plackett, A.R., Thomas, S.G., Wilson, Z.A. and Hedden, P (2011). Gibberellin control of stamen development: a fertile field. *Trends Plant Sci* **16**: 568-578.

Plackett, A.R., Powers, S.J., Fernandez-Garcia, N., Urbanova, T., Takebayashi, Y., Seo, M., Jikumaru, Y., Benlloch, R., Nilsson, O., Ruiz-Rivero, O. (2012). Analysis of the developmental roles of the *Arabidopsis* gibberellin 20-oxidases demonstrates that GA20ox1, -2, and -3 are the dominant paralogs. *Plant Cell* **24**: 941–960.

Plackett, R. G.A., Ferguson, C.A., Powers, J.S., Aakriti Wanchoo-Kohli, A., Phillips, L.A., Wilson, A.Z., Hedden, P. and Thomas, G.S. (2014). DELLA activity is required for successful pollen development in the Columbia ecotype of *Arabidopsis*. *New Phytologist* **201**: 825–836.

Preston, J., Wheeler, J., Heazlewood, J., Li, S.F. and Parish, R.W. (2004). AtMYB32 is required for normal pollen development in *Arabidopsis thaliana*. *Plant J* **40**(6): 979-995.

Putterill, J., Robson, F., Lee, K., Simon, R. and Coupland, G. (1995). The CONSTANS gene of *Arabidopsis* promotes flowering and encodes a protein showing similarities to zinc finger transcription factors. *Cell* **80**: 847–857.

Qu, L.-J. and Zhu, Y.X. (2006). Transcription factor families in *Arabidopsis*: major progress and outstanding issues for future research. *Current Opinion in Plant Biology* **9**: 544-549.

Quilichini, T.D., Friedmann, M.C., Samuels, A.L. and Douglas, C.J. (2010). ATP-binding cassette transporter G26 is required for male fertility and pollen exine formation in *Arabidopsis*. *Plant Physiol* **154**(2): 678-690.

Ramsay, N.A. and Glover, B.J. (2005). MYB-bHLH-WD40 protein complex and the evolution of cellular diversity. *Trends in Plant Science* **10**: 63-70.

Ran, F.A., Hsu, P.D., Jason Wright, J., Agarwala, V., Scott, D.A. and Zhang, F. (2013). Genome engineering using the CRISPR-Cas9 system. *Nature Protocols* **8**: 2281-2308.

Rao, M.K., Devi, K.U. and Arundhati, A. (1990). Applications of genic male sterility in plant breeding. *Plant Breeding* **105**: 1-25.

Regan, S.M. and Moffatt, B.A. (1990). Cytochemical Analysis of Pollen Development in Wild-Type *Arabidopsis* and a Male-Sterile Mutant. *Plant Cell* **2**(9): 877-889.

Rhee, S.Y., Osborne, E., Poindexter, P.D. and Somerville, C.R. (2003). Microspore separation in the quartet 3 mutants of *Arabidopsis* is impaired by a defect in a developmentally regulated polygalacturonase required for pollen mother cell wall degradation. *Plant Physiology* **133**(3): 1170-1180.

Rhee, S.Y. and Somerville, C.R. (1998). Tetrads pollen formation in quartet mutants of *Arabidopsis thaliana* is associated with persistence of pectic polysaccharides of the pollen mother cell wall. *The Plant Journal* **15**(1): 79-88.

Rieu, I., Ruiz-Rivero, O., Fernandez-Garcia, N., Griffiths, J., Powers, S.J., Gong, F., Linhartova, T., Eriksson, S., Nilsson, O., Thomas, S.G., Phillips, A.L. and Hedden, P. (2008). The gibberellin biosynthetic genes *AtGA20ox1* and *AtGA20ox2* act, partially redundantly, to promote growth and development throughout the *Arabidopsis* life cycle. *Plant J* **53**(3): 488-504.

Rieu, I., Wolters-Arts, M., Derksen, J., Mariani, C. and Weterings, K. (2003). Ethylene regulates the timing of anther dehiscence in tobacco. *Planta* **217**(1): 131-137.

Ritter, H. and Schulz, G.E. (2004) Structural basis for the entrance into the phenylpropanoid metabolism catalyzed by phenylalanine ammonia-lyase. *Plant Cell* **16**: 3426-3436.

Rogers, L.A. and Campbell, M.M. (2004). The genetic control of lignin deposition during plant growth and development. *New Phytologist* **164**: 17-30.

Sakata, T. and Higashitani, A. (2008). Male sterility accompanies with abnormal anther development in plants – genes and environmental stresses with special reference to high temperature injury. *International Journal of plant Development and Biology* **2**(1): 42–51.

Sambrook, J., Fritsch, E.D. and Maniatis, T. (1989). Molecular Cloning: A Laboratory Manual, Cold Spring Harbor: Cold Spring Harbor Laboratory Press, Plainview, 2nd Ed., p49-55.

Sanders, P.M., Bui, A.Q., Weterings, K., McIntire, K.N., Hsu, Y. C., Lee, P.Y., Truong, M.T., Beals, T.P. and Goldberg, R.B. (1999). Anther developmental defects in *Arabidopsis thaliana* male-sterile mutants. *Sexual Plant Reprod* **11**(6): 297–322.

Sanders, P.M., Lee, P.Y., Biesgen, C., Boone, J.D., Beals, T.P., Weiler, E.W. and Goldberg, R.B. (2000). The arabidopsis DELAYED DEHISCENCE1 gene encodes an enzyme in the jasmonic acid synthesis pathway. *Plant Cell* **12**(7): 1041-1061.

Sato, H., Shibata, F. and Murata, M. (2005). Characterization of a Mis12 homologue in *Arabidopsis thaliana*. *Chromosome Res* **13**: 827–834

Schaller, F., Schaller, A. and Stintzi, A. (2004). Biosynthesis and metabolism of jasmonates. *Journal of Plant Growth Regulation* **23**(3): 179-199.

Scott, R.J., Spielman, M. and Dickinson, H.G. (2004). Stamen structure and function. *Plant Cell* **16**: 46-60.

Sessions, A., Burke, E., Presting, G., Aux, G., Mcelver, J., Patton, D., Dietrich, B., Ho, P., Bacwaden, J., Ko, C., Clarke, J. D., Cotton, D., Bullis, D., Snell, J., Miguel, T., Hutchison, D., Kimmerly, B., Mitzel, T., Katagiri, F., Glazebrook, J., Law, M. and Goff, S.A. (2002). A high-throughput Arabidopsis reverse genetics system. *The Plant cell* **14**: 2985-94.

Shan, X.Y., Wang, Z.L. and Xie, D. (2007). Jasmonate signal pathway in Arabidopsis. *Journal of Integrative Plant Biology* **49**(1): 81-86.

Singh, D.P., Jermakow, A.M. and Swain, S.M. (2002). Gibberellins are required for seed development and pollen tube growth in Arabidopsis. *Plant Cell* **14**(12): 3133-3147.

Smyth, D.R., Bowman, J.L. and Meyerowitz, E.M. (1990). Early flower development in *Arabidopsis*. *Plant Cell* **2**(8): 755-767.

Solano, R., Nieto, C., Avila, J., Canas, L., Diaz, I. and Paz-Ares, J. (1995). Dual DNA binding specificity of a petal epidermis-specific MYB transcription factor (MYB.ph3) from *Petunia* hybrid. *EMBO J* **14**(8): 1773-1784.

Sommer-Knudsen, J, Bacic., A. and Clarke. A.E. (1998). Hydroxyproline-rich plant glycoproteins. *Phytochemistry* **47**: 483-497.

Song, J. (2009). MYB26 controls arabidopsis anther dehiscence by regulating secondary thickening in the endothecium. The plants and crops sciences. PhD Thesis, Nottingham, The University of Nottingham.

Song, S., Qi, T., Huang Huang, A., Qingcuo Ren, A., Dewei Wu, A., Chang, C., Wen Peng, A., Yule Liu, A., Jinrong Peng, B. and Xiea, D. (2011). The Jasmonate-ZIM Domain Proteins Interact with the R2R3-MYB Transcription Factors MYB21 and MYB24 to Affect Jasmonate-Regulated Stamen Development in Arabidopsis. *The Plant Cell* **23**: 1000–1013.

Sparkes, I. and Brandizzi, F. (2012). Fluorescent protein-based technologies: shedding new light on the plant endomembrane system. *Plant J* **70**: 96-107.

Spelt, C., Quattrocchio, F., Mol, J. and Koes, R. (2002). ANTHOCYANIN1 of petunia controls pigment synthesis, vacuolar pH, and seed coat development by genetically distinct mechanisms. *Plant Cell* **14**: 2121–2135.

Steiner, F.A., Talbert, P.B., Kasinathan, S., Deal, R.B. and Henikoff, S. (2012). Cell-type-specific nuclei purification from whole animals for genome-wide expression and chromatin profiling. *Genome Research* **22**: 766-777.

Steiner-Lange, S., Unte, U.S., Eckstein, L., Yang, C., Wilson, Z.A., Schmelzer, E., Dekker, K. and Saedler, H. (2003). Disruption of *Arabidopsis thaliana* MYB26 results in male sterility due to non-dehiscent anthers. *Plant J* **34**(4): 519-528.

Stokes, D., Morgan, C., O'Neill, C. and Bancroft, I. (2007). Evaluating the utility of *Arabidopsis thaliana* as a model for understanding heterosis in hybrid crops. *Euphytica* **156**(1): 157-171.

Stracke, R., Werber, M. and Weisshaar, B. (2001). The R2R3-MYB gene family in *Arabidopsis thaliana*. *Curr Opin Plant Biol* **4**(5): 447-456.

Sun, N. and Zhao, H. (2013). Transcription activator-like effector nucleases (TALENs): A highly efficient and versatile tool for genome editing. *Biotechnology and Bioengineering* **110**: 1811-1821.

Suter, B., Kittanakom, S. and Stagljar, I. (2008). Twohybrid technologies in proteomics research. *Current Opinion in Biotechnology* **19**: 316-323.

Takada, K., Ishimaru, K. and Kamada, H. (2006) Anther-specific expression of mutated melon ethylene receptor gene *Cm-ERS1/H70A* affected tapetum degeneration and pollen grain production in transgenic tobacco plants. *Plant Cell Reports* **25**: 936-941.

Tatematsu, K., Kamiya, Y. and Nambara., E. (2008). Co-regulation of ribosomal protein genes as an indicator of growth status: Comparative transcriptome analysis on axillary shoots and seeds in *Arabidopsis*. *Plant signal behav* **3**(7): 450-452.

Taylor, N.G., Howells, R.M., Huttly, A.K., Vickers, K. and Turner, S.R. (2003). Interactions among three distinct Cesa proteins essential for cellulose synthesis. *Proc Natl Acad Sci USA* **100**: 1450-1455.

Tehseen, M., Imran, M., Hussain, M., Irum, S., Ali, S., MAnsoor, S. and Zafar, Y. (2010). Development of male sterility by silencing *Bcp1* gene of *Arabidopsis* through RNA interference. *African J Biotechnology* **9**(19): 2736-2741.

Thines, B., Katsir, L., Melotto, M., Niu, Y., Mandaokar, A., Liu, G., Nomura, K., He, S.Y., Howe, G.A. and Browse, J. (2007). JAZ repressor proteins are targets of the SCFCO11 comple during jasmonate signalling. *Nature* **448**: 661-666.

Thompson, E.P., Wilkins, C., Demidchik, V., Davies, J.M. and Glover, B.J. (2010). An Arabidopsis flavonoid transporter is required for anther dehiscence and pollen development. *J Exp Bot* **61**(2): 439-451.

Tiwari, S.B., Hagen, G. and Guilfoyle, T. (2003). The roles of auxin response factor domains in auxin-responsive transcription. *Plant Cell* **15**(2): 533-543.

Tominaga, R., Iwata, M., Okada, K. and Wada, T. (2007). Functional Analysis of the Epidermal-Specific MYB Genes CAPRICE and WEREWOLF in Arabidopsis. *Plant Cell* **19**(7): 2264-2277.

Tsuda, K., Qi, Y., Nguyen, I.V., Bethke, G., Tsuda, Y., Glazebrook, J. and Katagiri, F. (2012). An efficient Agrobacterium-mediated transient transformation of Arabidopsis. *Plant Journal* **69**: 713-719.

Ueguchi-Tanaka, M., Ashikari, M., NaKajima, M., Itoh, H., Katoh, E., Kobayashi, M., Chow, T. Y., Hsing, Y.i.C., Kitano, H., Yamaguchi, I. and Matsuoka, M. (2005). GIBBERELLIN INSENSITIVE DWARF1 encodes a soluble receptor for gibberellin. *Nature* **437**(7059): 693-698.

Vacca, R.A., Valenti, D., Bobba, A., de Pinto, M.C., Merafina, R.S., DeGara, L., Passarella, S. and Marra, E. (2007). Proteasome function is required for activation of

programmed cell death in heat shocked tobacco Bright-Yellow 2 cells. *FEBS Letters* **581**: 917-922.

Verelst, W., Saedler, H. and Munster, T. (2007). MIKC MADS-protein complexes bind motifs enriched in the proximal region of late pollen-specific Arabidopsis promoters. *Plant Physiol* **143**: 447-460.

von Malek, B., van der Graaff, E., Schneitz, K. and Keller, B. (2002). The Arabidopsis male-sterile mutant *dde2-2* is defective in the ALLENE OXIDE SYNTHASE gene encoding one of the key enzymes of the jasmonic acid biosynthesis pathway. *Planta* **216**(1): 187-192.

Wang, W., Wang, L., Chen, C., Xiong, G., Tan, X.-Y., Yang, K.-Z., Wang, Z.C., Zhou, Y., Ye, D. and Chen, L.-Q. (2011). *Arabidopsis CSLD1* and *CSLD4* are required for cellulose deposition and normal growth of pollen tubes. *J Exp Bot* **62**(14): 5161-5177.

Wen-Jun, S. and Forde, B.G. (1989). Efficient transformation of *Agrobacterium* spp. by high voltage electroporation. *Nucleic Acids Research* **17**: 8385.

Wilson, Z.A. and Zhang, D.B. (2009). From Arabidopsis torice: pathways in pollen development. *J Exp Bot* **60**: 1479-1492.

Wisniewska, J., Xu, J., Seifertova, D., Brewer, P.B., Ruzicka, K., Billou, I., Rouquie, D., Benkova, E., Scheres, B. And Frimi, J. (2006). Polar PIN localization directs auxin flow in plants. *Science* **312**(5775): 883.

Woodward, A.W. and Bartel, B. (2005). Auxin: regulation, action, and interaction. *Ann Bot* **95**: 707-735.

Xie, D.X., Feys, B.F., James, S., Nieto-Rostro, M. and Turner, J.G. (1998). *COI1*: an Arabidopsis gene required for jasmonate-regulated defense fertility. *Science* **280**: 1091-1094.

Xiao, S., Dai, L., Liu, F., Wang, Z., Peng, W. and Xie, D. (2004). *COS1*: An Arabidopsis coronatine insensitive1 suppressor essential for regulation of jasmonate-mediated plant defense and senescence. *The Plant Cell* **16**: 1132-1142.

Xu, J., Yang, C., Yuan, Z., Zhang, D., Gondwe, M.Y., Ding, Z., Liang, W., Zhang, D. and Wilson, Z.A. (2010). The ABORTED MICROSPORES regulatory network is required for postmeiotic male reproductive development in *Arabidopsis thaliana*. *Plant Cell* **22**: 91-107.

Xu, L., Liu, F., Wang, W., Huang, R., Huang, D. and Xie, D. (2001). An Arabidopsis mutant *cex1* exhibits constant accumulation of jasmonate-regulated *AtVSP*, *Thi2.1* and *PDF1.2*. *FEBS Letters* **494**(3): 161-164.

Yang, C., Xu, Z., Song, J., Conner, K., Vizcay Barrena, G. and Wilson, Z.A. (2007). Arabidopsis MYB26/MALE STERILE35 regulates secondary thickening in the endothecium and is essential for anther dehiscence. *Plant Cell* **19**(2): 534-548.

Yang, X., Makaroff, C.A. and Ma, H. (2003a). The Arabidopsis *MALE MEIOCYTE DEATH1* gene encodes a PHD-finger protein that is required for male meiosis. *Plant Cell* **15**: 1281-1295.

Yang, S.-L., Xie, L.-F., Mao, H.-Z., Pua, C.S., Yang, W.-C., Jiang, L., Sundaresan, V. and Ye, D. (2003b) *TAPETUM DETERMINANT1* is required for cell specialization in the Arabidopsis anther. *Plant Cell* **15**: 2792-2804.

Yang, W.C., Ye, D., Xu, J. and Sundaresan, V. (1999). The *SPOROXYTELESS* gene of Arabidopsis is required for initiation of sporogenesis and encodes a novel nuclear protein. *Genes Dev* **13**: 2108-2117.

Yin, Y., Chory, J. and Baulcombe, D. (2005). RNAi in Transgenic Plants. *Current Protocols in Molecular Biology*.

Yoo, S.D., Cho, Y. and Sheen, J. (2009). Emerging connections in the ethylene signaling network. *Trends in Plant Science* **14**: 270-279.

Zhao, K. and Bartley, L.E. (2014). Comparative genomic analysis of the R2R3 MYB secondary cell wall regulators of Arabidopsis, poplar, rice, maize, and switchgrass. *BMC plant biology* **14**(1): 135.

Zhao, D.Z., Wang, G.F., Speal, B. and Ma, H. (2002). The *EXCESS MICROSPOROXYTES1* gene encodes a putative leucine-rich repeat receptor protein kinase that controls somatic and reproductive cell fates in the *Arabidopsis* anther. *Genes Dev* **16**: 2021-2031.

Zhang, F., Gonzalez, A., Zhao, M., Payne, C.T. and Lloyd, A. (2003). A network of redundant bHLH proteins functions in all TTG1-dependent pathways of Arabidopsis. *Development* **130**: 4859-4869.

Zhang, W., Sun, Y., Timofejeva, L., Chen, C., Grossniklaus, U. and Ma, H. (2006). Regulation of Arabidopsis tapetum development and function by DYSFUNCTIONAL TAPETUM1 (DYT1) encoding a putative bHLH transcription factor. *Development* **133**: 3085-3095.

Zheng, L., Liu, G., Meng, X., Li, Y. and Wang, Y. (2012). A versatile Agrobacterium-mediated transient gene expression system for herbaceous plants and trees. *Biochemical Genetics* **50**: 761-9.

Zhong, R., Demura, T. and Ye, Z.H. (2006). SND1, a NAC domain transcription factor, is a key regulator of secondary wall synthesis in fibers of Arabidopsis. *The Plant Cell Online* **18**, 3158.

Zhong, R., Lee, C., Zhou, J., McCarthy, R.L. and Ye, Z.H. (2008). A battery of transcription factors involved in the regulation of secondary cell wall biosynthesis in Arabidopsis. *The Plant Cell Online* **20**: 2763.

Zhong, R. and Ye, Z.H. (2007). Regulation of cell wall biosynthesis. *Curr Opin Plant Biol* **10**: 564-572.

Zhong, R., Richardson, E.A. and Ye, Z.H. (2007a). Two NAC domain transcription factors, SND1 and NST1, function redundantly in regulation of secondary wall synthesis in fibers of Arabidopsis. *Planta* **225**: 1603-1611.

Zhong, R., Richardson, E.A. and Ye, Z.H. (2007b). The MYB46 transcription factor is a direct target of SND1 and regulates secondary wall biosynthesis in Arabidopsis. *Plant Cell* **19**(9): 2776-2792.

Zhong, R. and Ye, Z.H. (2012). MYB46 and MYB83 bind to the SMRE sites and directly activate a suite of transcription factors and secondary wall biosynthetic genes. *Plant Cell Physiol* **53**: 368-380.

Zhou, J., Lee, C., Zhong, R. and Ye, Z.H. (2009). MYB58 and MYB6 are transcriptional activators of the lignin biosynthetic

pathway during secondary cell wall formation in *Arabidopsis*.
Plant Cell **21**: 248–266.

APPENDIX

WEBSITES

[http://atensemble.arabidopsis.info/Arabidopsis thaliana TAIR.](http://atensemble.arabidopsis.info/Arabidopsis_thaliana_TAIR)

Website visited:2010.

(<http://atensembl.arabidopsis.info/index.html>)

[http://www.arabidopsis.org/.](http://www.arabidopsis.org/)

Website visited: 2010.

[http://signal.salk.edu/tdnaprimers.2.html.](http://signal.salk.edu/tdnaprimers.2.html)

Website visited: 2011.

[http://www. Invitrogen .com.](http://www. Invitrogen .com)

Website visited: 2011.

<http://frodo.wi.mit.edu/primer3>

Website visited: 2011.

<http://amp.genomics.org.cn/>

Website visited :2014.

<http://Eurofinedna.com>

Website visited :2014.

<http://atted.jp/cgi-bin/locus.cgi?loc=AT3G13890>

Website visited :2014.

[http://www.cbm.g.umd.edu/ files/cbm.g/corelab/ FRET AB.pdf](http://www.cbm.g.umd.edu/files/cbm.g/corelab/FRET_AB.pdf)

Website visited :2014.

<http://www.molecularbeacons.org/toto/>

<Marras energy transfer.html>

Website visited :2015.

[http://www.ebi.ac.uk /Tools/msa/kalign/\).](http://www.ebi.ac.uk /Tools/msa/kalign/)

APPENDIX I

CHEMICALS AND STAINING

10 X TBE BUFFER	
NaCl	0.89 M
Tris-HCl (PH 7.5)	10mM
Na ₂ -EDTA	1mM
Dilute to 0.5 x to use in electrophoresis	

Tris-HCl 1M (1000ml)	
121g of Tris	1000ml dH ₂ O
The pH was adjusted at 8.0 and the solution was autoclaved 121°C for 15 min. Solution was autoclaved 121°C for 15 min.	

1 X Running BUFFER	
10xTris/Glycine/SDS-PAGE buffer	100µl
Dilute to 1000ml with distilled water	

10x TBS	
NaCl	90g
1M Tris pH7.5	200ml
Dilute to 1000ml with distilled water	

1 X TBST BUFFER	
10x TBS	100ml
Tween [®] 20	1ml
Dilute to 1000ml with distilled water	

Murashige and Skoog Basal (MS) medium	
MS powder	2.15 g
Agar	9 g
ddH ₂ O	Add up to 1L
Total volume	1L
Adjust pH to 5.2-5.7 and autoclave to sterilize; antibiotics added when sterilized medium cools to 50°C.	

Luria-Bertani (LB) medium	
Bacto-Tryptone	20g
Bacto-yeast extract	10g
NaCl	10g
Agar (if solid medium)	15g
dH ₂ O	Add up to 1L
Total volume	1L
Adjust PH to 7.0 and autoclave to sterilize: antibiotic added when sterilized medium cools to ≈50°C	

Alexander Staining	
Ethanol 1%	20ml
Malachite green in ethanol	95%
dH ₂ O	50ml
Glycerol	40ml
Acid fuchsin 1% in dH ₂ O	10ml
Phenol	5g
Lactic acid	1-6ml
Pollen stained can be used immediately or stored for later use. Staining is hastened by lightly flaming the slides or by storing at 55±2 C for 24 hr.	

Paraformaldehyde4%	
Paraformaldehyde (Sigma)	2g
1xPBS	50ml
Tween20	50µl
Triton	50µl

APPENDIX II

PRIMERS

FOR RT PCR ANALYSIS			
Genes	Primer name	Primer sequence(5' to 3')	Tm°C
At3g62970	At3g62970_R At3g62970_F	GGATCTTGTGGCGTTGAGAT TGCCAAGTCAATGGTGGATA	56 55
At1g47128	At1g47128_R At1g47128_F	TCTTGCTCAATAAACAGGTTCC GAGAGAGTGGATACCTAA	54 52
At5g25560	At5g25560_R At5g25560_F	CGTCAACTCTGGAAAGGGTAGCA GATTGCGGCTACACCAATGC	61 64
At1g08320	AT1G08320_R At1g08320_F	CATTTGTTGCATTCCGTCAA CCGAACGTTGTTTTATTTGGA	53 53
At3g47620	At3g47620_R At3g47620_F	AATGGAAGGAAACGTCCAAA CGGATTTGCATCAACAACAA	53 53

For RT-PCR expression analysis			
Gene	Primer name	Primer sequence(5' to 3')	Tm°C
ACTIN	ACT2F	TGCTGACCGTATGAGCAAAG	58
ACTIN	ACT2R	CAGCATCATCACAAGCATCC	58
PP2A3_1355F	PP2F	TCCGTGAAGCTGCTGCAAAC	59.4
PP2A3_1677R	PP2R	CACCAAGCATGGCCGTATCA	59.4

FOR GENOTYPING			
Genes	Primer name	Primer sequence(5' to 3')	Tm°C
At3g62970	At3g62970-JIE-702 F At3g62970-JIE137 R	TCTCTGCAATGACTGCAACAAGG TGGCGGCATGAGAAGATGAG	69.5 63.2
At3g13890	At3g13890-JIE-RTL1 At3g13890-JIE- RTR1060	ATGGGTCATCACTCATGCT GTCCACAAGAGATTGGCGACGA	58 58
At3g47620	At3g47620_JIE_250F At3g47620_JIE_511R	TCGCTGCTCTCTCCTCCTGAC TCTTTCGTCGACGCTCGTTTC	61.6 60.6
At1g08320	At1g08320_JIE-1276 F At1g08320_JIE-491 R	GCTGCACGGTGTTTCCTAGTCA TCGCTGCTCTCTCCTCCTGAC	64.6 61.3
At1g47128	At1g47128_154R At1g47128_1248F	CCGTGTTTCACCAACCATGC TTGCTGCCCTCAGGATACC	60.6 66.4
At5g25560	At5g25560_774F At5g25560_Jie_430R	GATTGCGGCTACACCAATGC TGGTGGCGAGGAATATCATGC	64 64
Promoter	35S_For	CACAATCCCACTATCCTTCGCAAGAC	60

FOR OVEREXPRESSION GENOTYPING			
Genes	Primers name	Primer sequence(5' to 3')	Tm°C
At3g62970	At3g62970R	CGCCACAATTCGAGCAGACTT	59
At3g47620	At3g47620R	TCTTTCGTCGACGCTCGTTTC	60.6
At1g08320	At1g08320R	TCGCTGCTCTCTCCTCCTGAC	61.3
At1g47128	At1g47128 R	GATCCGCAAACGAGTCAAACC	58
Promoter	35S_For	CACAATCCCACTATCCTTCGCAAGAC	60

FOR qPCR			
Genes	Primer name	Primer sequence(5' to 3')	Tm°C
At1g08320	At1g08320F At1g08320R	CCGAACGTTGTTTTATTTGGA CATTGTTGCATTCCGTCAA	59.85 60.50
At3g62970	At3g62970- F At3g62970- R	TGCCAAGTCAATGGTGGATA GGATCTTGTGGCGTTGAGAT	59.92 60.08
At1g47128	At1g47128_154F At1g47128_307R	CCGTGTTTCACCAACCATGC GATCCGCAAAACGAGTCAAACC	60.6 58
At3g47620	At3g47620_F At3g47620_R	CGGATTTGCATCAACAACAA AATGGAAGGAAACGTCCAAA	60.50 59.41

FOR GUS PROMOTER			
Genes	Primer name	Primer sequence(5' to 3')	Tm°C
At1g08320	At1g08320F	GCTGCACGGTGTTCCTAGTCA	60
GUS	GUSR	TTTGATTTACGGGTTGGGGTTT	59

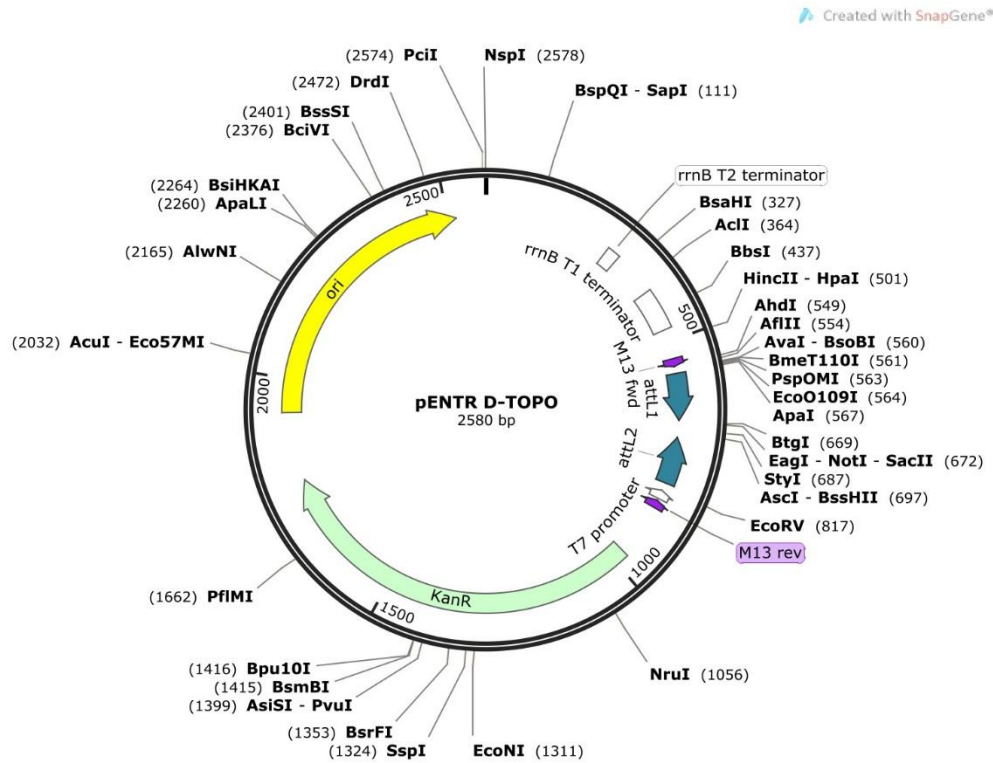
FOR RNAi			
Genes	Primer name	Primer sequence(5' to 3')	Tm oC
At3g62970	At3g62970- RNAiF At3g62970- RNAiR	CATTGAGAACTCTACAAA TGCAGAGAATTGAAACCTCAAA	58 58
At1g47128	At1g47128-RNAiF At1g47128-RNAiR	GAGAGAGTGGATACCTAA TCTTGCTCAATAAACAGGTTCC	58 58
PK7	PK7-F1 PK7-R2	TTACCCACTAAGCGTGACCA TTGATGGCCATAGGGGTTTA	57.3 55.3
35sF	35sF	CACAATCCCACTATCCTTCGCAAGAC	64.8

	FOR CLONING AND PROTEINS EXPRESSION		
Contrasts name	Primers name	Primer sequence (5' to 3')	Tm°C
pUBC-MYB26-GFP	GFP_PGWB5_R MYB26-RTL1	AAGTCGTGCTGCTTCATGTG ATGGGTCATCACTCATGCTG	57 57
pUBN-RFE-Y2H320	RFP-F At1g08320-R	ATGAGGCTGAAGCTGAAGGA CATTGTTGCATTCCGTCAA	60 60
pUBN-RFP-Y2H620	RFP-F At3g47620_R	ATGAGGCTGAAGCTGAAGGA AATGGAAGGAAACGTCCAAA	60 59
pUBN-RFP-Y2H970	RFP-F At3g62970-R	ATGAGGCTGAAGCTGAAGGA GGATCTTGTGGCGTTGAGAT	60 60

APPENDIX III

MAPS

(pENTR / D-TOPO)



NAME: pENTR/D-TOPO.

RESISTANT MARKER: Kanamycin resistant; 25µg/ml.

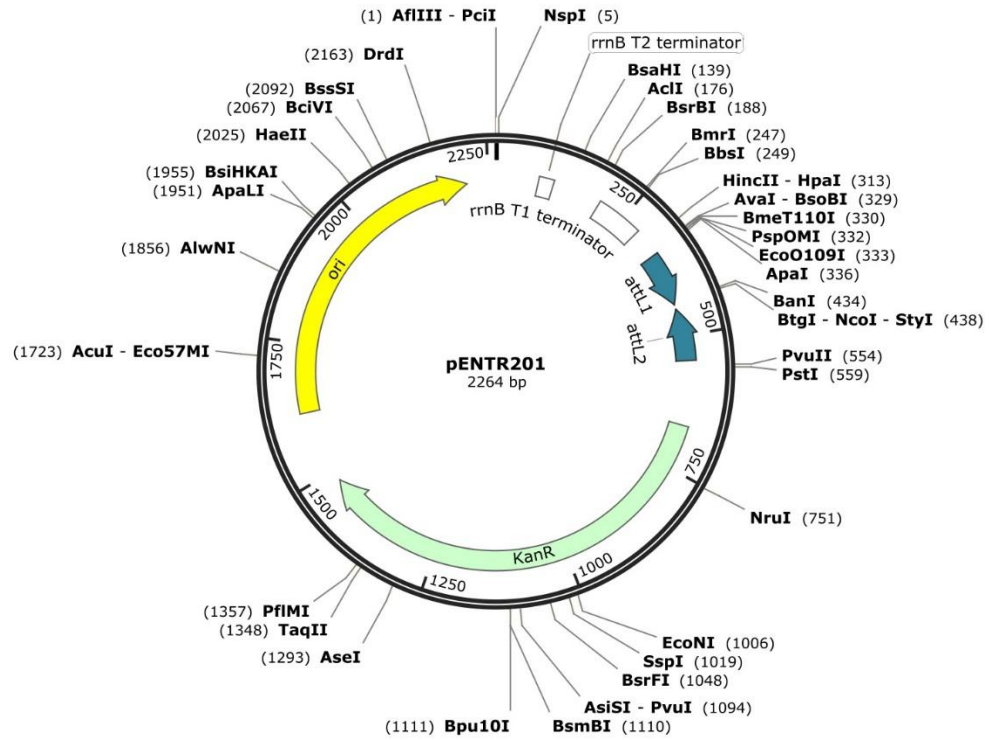
SOURCE: Invitrogen Life Technologies.

V_TYPE: Gateway entry vector.

SEQUENCING PRIMERS M13 reverse T17.

(pENTR201)

Created with SnapGene®



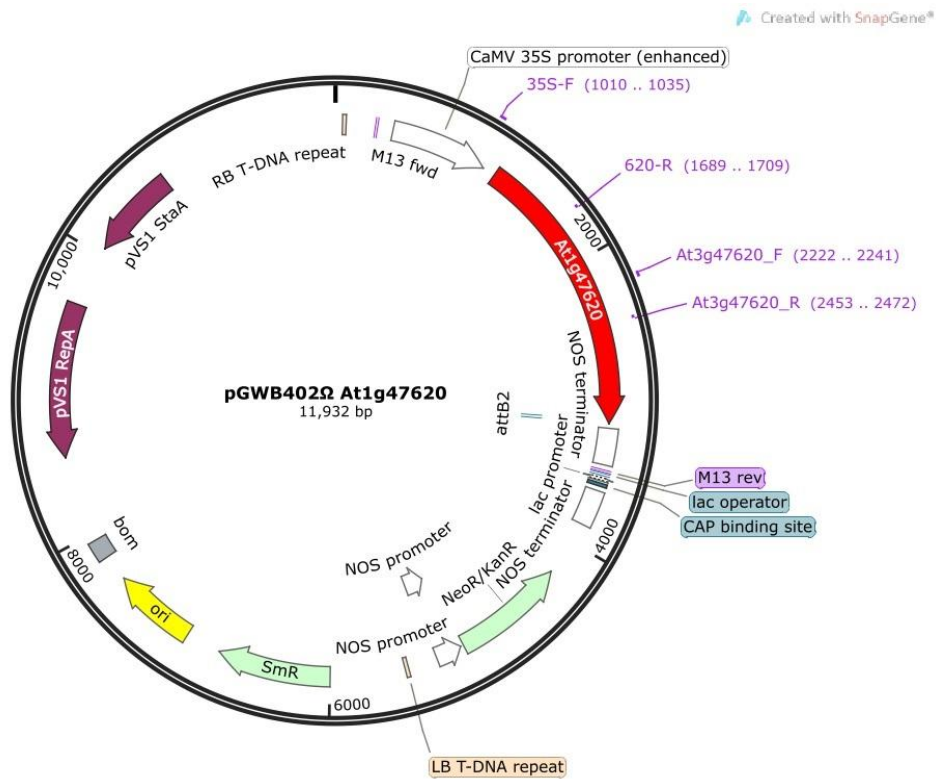
NAME: pENTR201.

RESISTANT MARKER: Kanamycin resistant; 25µg/ml.

SOURCE: Invitrogen Life Technologies.

V_TYPE: Gateway entry vector.

pGWB402Ω- At3g47620



NAME: pGWB402Ω- 620

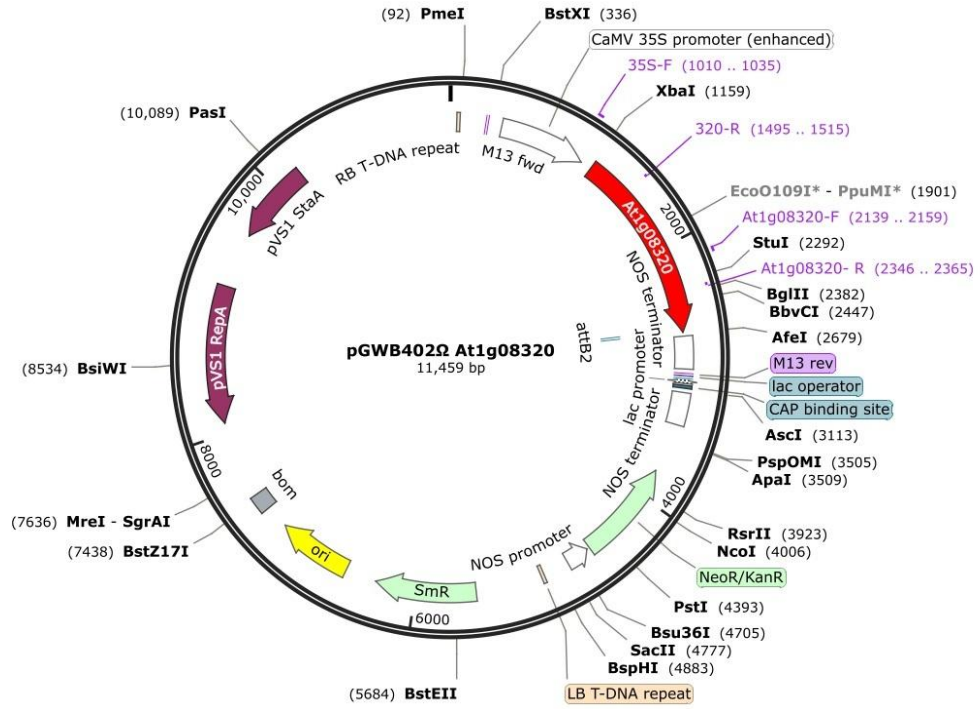
RESISTANT MARKER: Spectomaycin resistant.

SOURCE: Snap Gene viewer 2.3.2

TYPE: destination vector.

pGWB402Ω-At1g08320

Created with SnapGene®



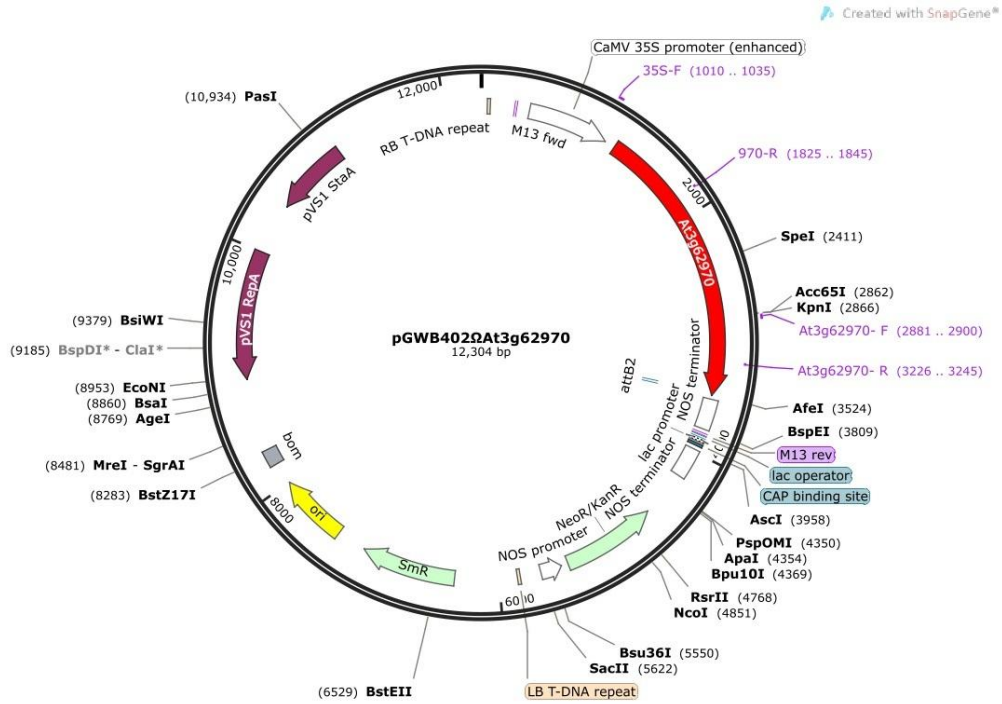
NAME: pGWB402Ω- 320

RESISTANT MARKER: Spectomaycin resistant.

SOURCE: Snap Gene viewer 2.3.2

TYPE: destination vector.

pGWB402Ω- At3g62970



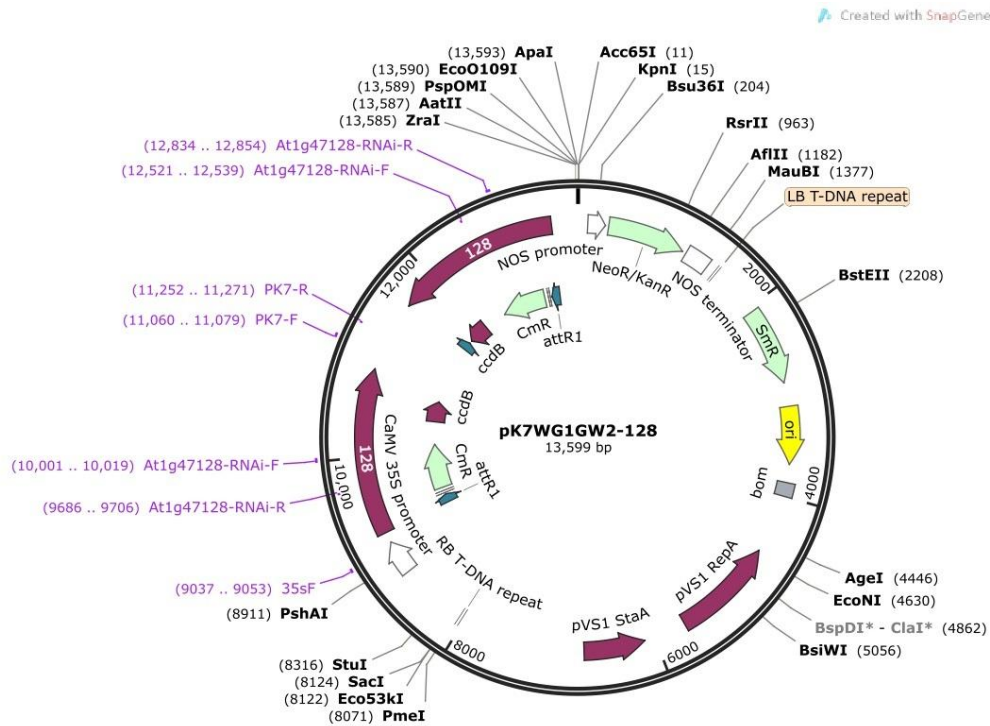
NAME: pGWB402Ω- 970

RESISTANT MARKER: Spectomycin resistant.

SOURCE: Snap Gene viewer 2.3.2

TYPE: destination vector.

At1g47128^{RNAi}



NAME: pK7WG1GW2- 128

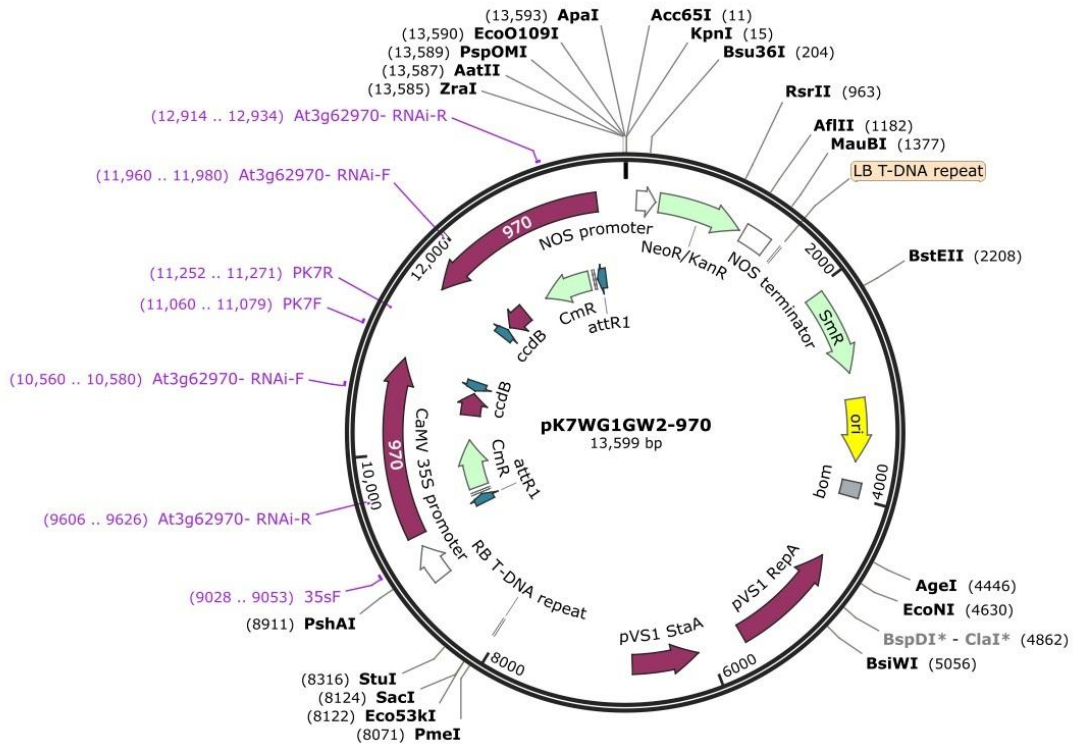
RESISTANT MARKER: Spectomaycin resistant.

SOURCE: Snap Gene viewer 2.3.2

TYPE: destination vector.

At3g62970^{RNAi}

Created with SnapGene®



NAME: pK7WG1GW2- 970

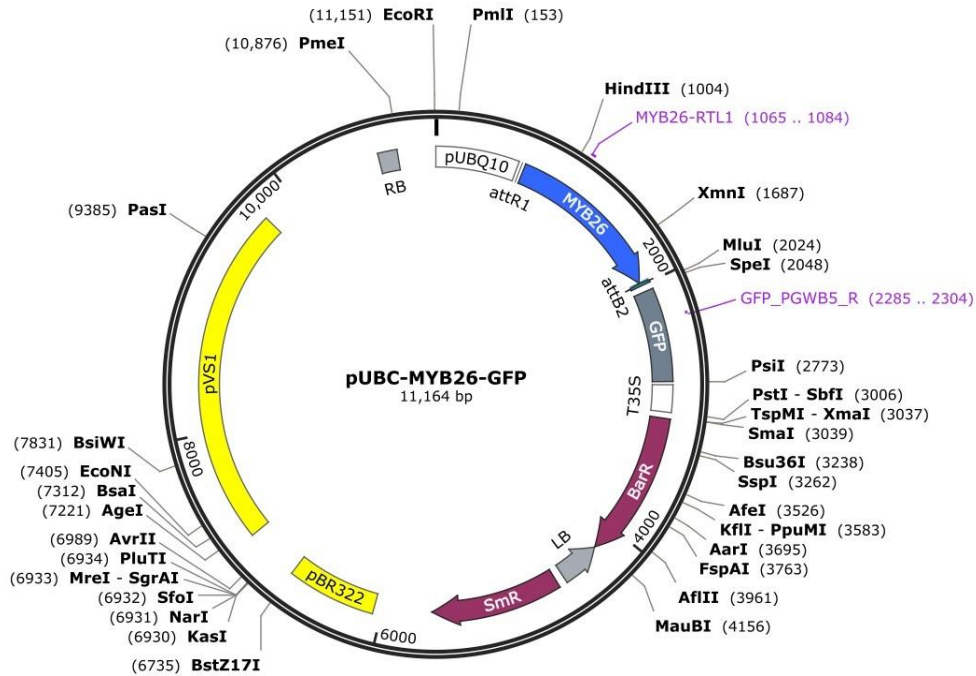
RESISTANT MARKER: Spectomycin resistant.

SOURCE: Snap Gene viewer 2.3.2

TYPE: destination vector.

pUBC-MYB26-GFP

Created with SnapGene®



NAME:pUB- MYB26-GFP

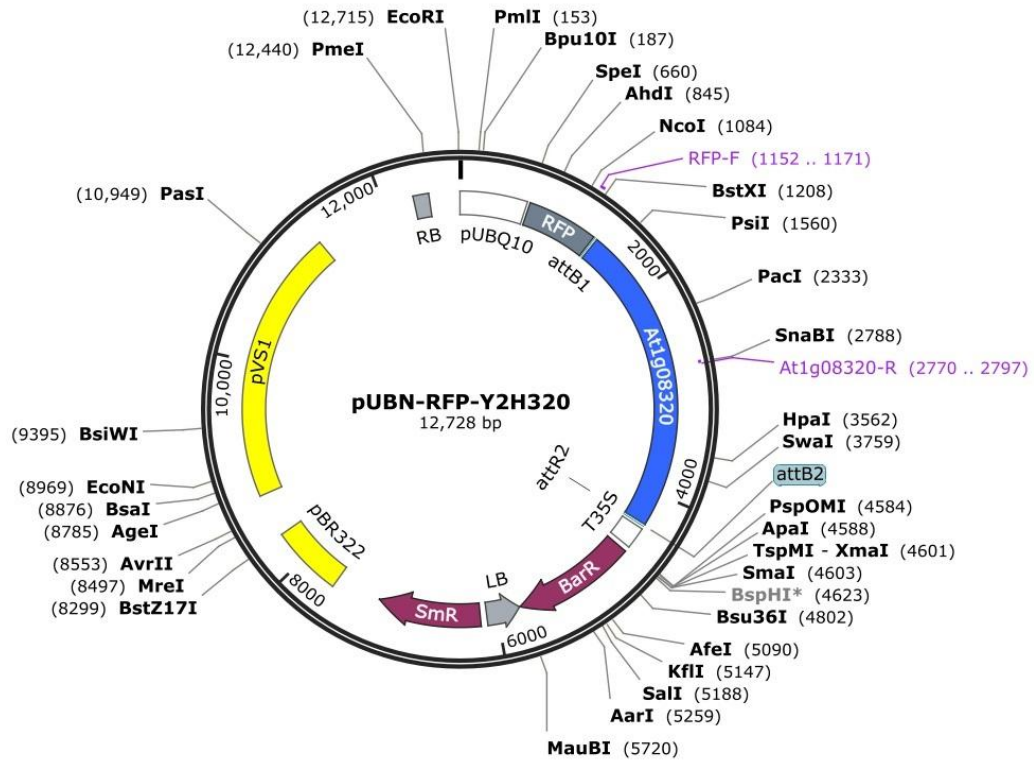
RESISTANT MARKER: Spectomaycin resistant.

SOURCE: Snap Gene viewer 2.3.2

TYPE: destination vector.

pUB-RFP-Y2H320

Created with SnapGene®



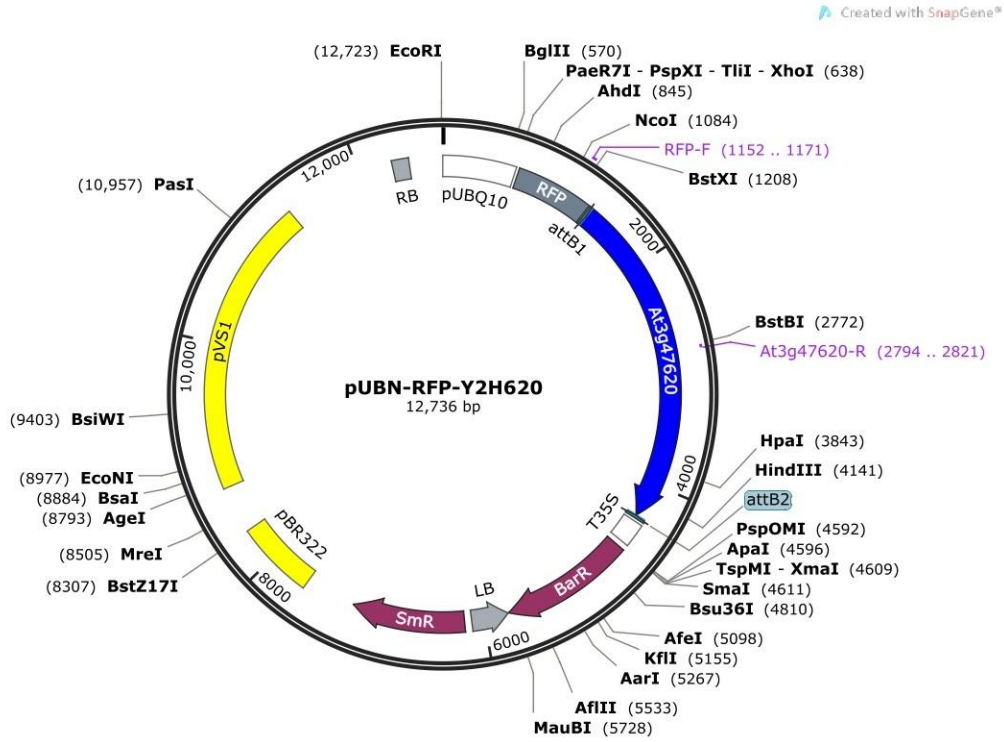
NAME:pUB-RFP – Y2H320

RESISTANT MARKER: Spectomycin resistant.

SOURCE: Snap Gene viewer 2.3.2

TYPE: destination vector.

pUB-RFP-Y2H620



NAME:pUB-RFP – Y2H620

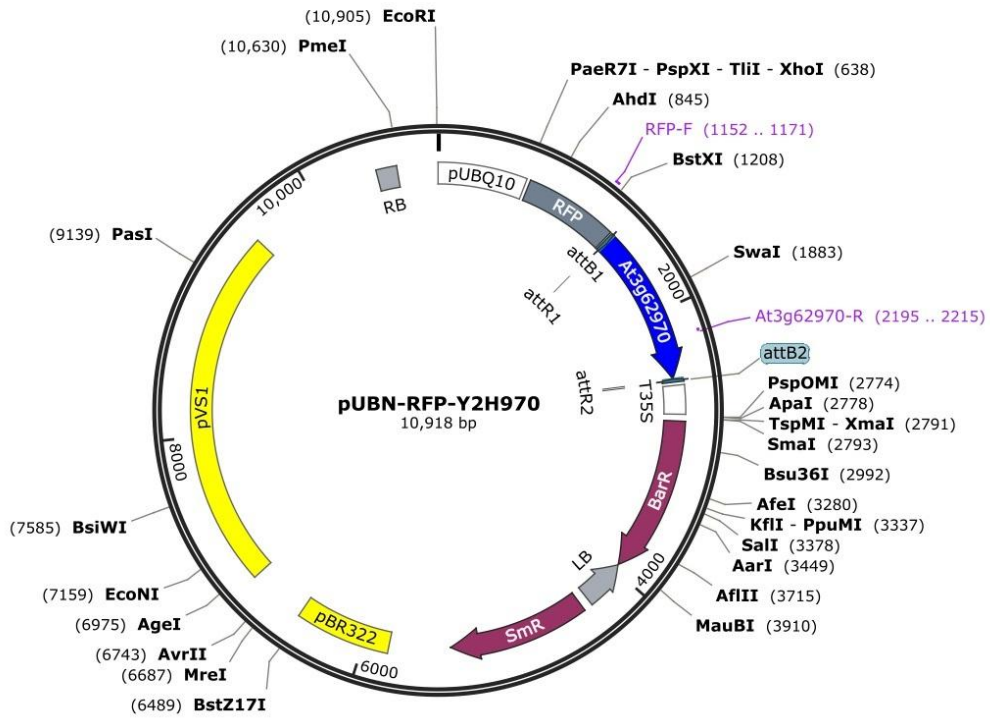
RESISTANT MARKER: Spectomycin resistant.

SOURCE: Snap Gene viewer 2.3.2

TYPE: destination vector.

pUB-RFP-Y2H970

Created with SnapGene®



NAME:pUB-RFP- Y2H970

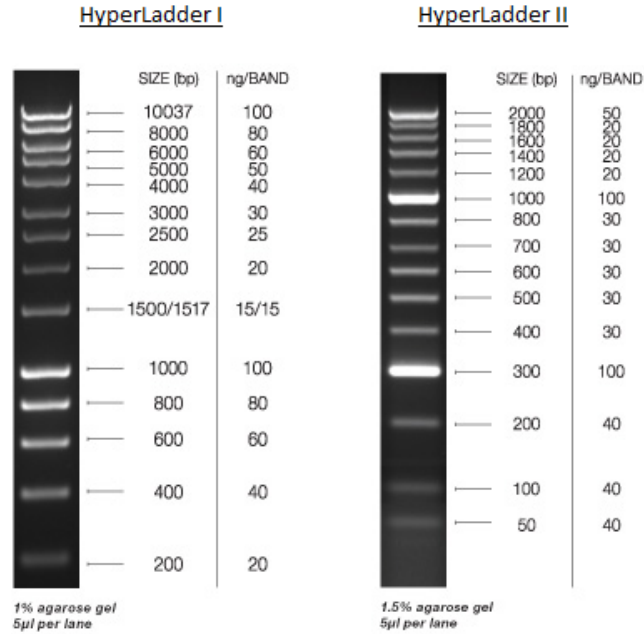
RESISTANT MARKER: Spectomycin resistant.

SOURCE: Snap Gene viewer 2.3.2

TYPE: destination vector.

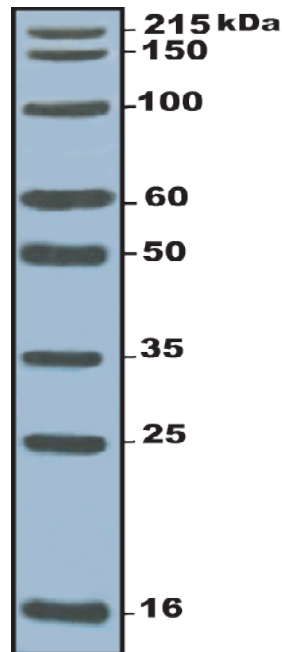
APPENDIX IV

-IMAGES OF DNA MOLECULAR MARKERS UTILISED (Bioline.com)



-PROTEIN LADDER

NexusWestern Percise Western Blot (Wide Range)



-TABLE OF χ^2 VALUE VERSUS P-VALUE

The table below gives a number of p-values matching to χ^2 for the first 10 degrees of freedom. A p-value of 0.05 or less is usually regarded as statistically significant, i.e. the observed deviation from the null hypothesis is significant.

Degrees of freedom (df)	χ^2 value											
1	0.004	0.02	0.06	0.15	0.46	1.07	1.64	2.71	3.84	6.64	10.83	
2	0.10	0.21	0.45	0.71	1.39	2.41	3.22	4.60	5.99	9.21	13.82	
3	0.35	0.58	1.01	1.42	2.37	3.66	4.64	6.25	7.82	11.34	16.27	
4	0.71	1.06	1.65	2.20	3.36	4.88	5.99	7.78	9.49	13.28	18.47	
5	1.14	1.61	2.34	3.00	4.35	6.06	7.29	9.24	11.07	15.09	20.52	
6	1.63	2.20	3.07	3.83	5.35	7.23	8.56	10.64	12.59	16.81	22.46	
7	2.17	2.83	3.82	4.67	6.35	8.38	9.80	12.02	14.07	18.48	24.32	
8	2.73	3.49	4.59	5.53	7.34	9.52	11.03	13.36	15.51	20.09	26.12	
9	3.32	4.17	5.38	6.39	8.34	10.66	12.24	14.68	16.92	21.67	27.88	
10	3.94	4.86	6.18	7.27	9.34	11.78	13.44	15.99	18.31	23.21	29.59	
P value (Probability)	0.95	0.90	0.80	0.70	0.50	0.30	0.20	0.10	0.05	0.01	0.001	
	Nonsignificant								Significant			

Polymorphic molecular markers and their locations on the different *Arabidopsis* chromosomes along with PCR conditions used to map the gene(s) of interest (www.arabidopsis.org/).

Chromosome	Gene ID	Location (bp)	Primers	Expected	Expected	Annealing
				size (bp) Col	size (bp) Ler	
1	At1g07810	2,416,265- 2,420,757	(F)= GTTCACGGACAAAGAGCCTGAAAT (R)= AAGCAGTCAATATTCAGGAAGGG	>300	<300	55
	At1g30930	11,014,783- 11,015,913	(F)= TCAATGGGATCGAACTGGT (R)= ACTGAAAAGCGAGCCAAAAG	239	142	55
2	CER459006	14,297,784- 14,297,986	(F)= TCGCAAACCAAATATCAACT (R)=AGCTGATGAACAAAAGACTGA	203	158	50
	CER459010	14,320,519- 14,320,606	(F)= ACATTGAAAGTTCCCGATTCT (R)= CAACAGATTTTCTTTGACCCA	90	72	50
	CER461057	16,291,858- 16,291,970	(F)= GAGGACATGTATAGGAGCCTCG (R)= TCGTCTACTGCACTGCCG	151	135	50
3	At3g11220	3,513,531- 3,516,408	(F)= GGATTAGATGGGGATTTCTGG (R)= TTGCTCGTATCAACACACAG	193	174	55
	At3g26605	9,773,018- 9,773,500	(F)= CCCCAGTTGAGGTATT (R)= GAAGAAATTCCTAAAGCATTTC	<200	>200	53
4	At4g10360	6,420,455- 6,422,380	(F)= GCCAAACCCAAAATTGTAAAAC (R)= TAGAGGGAACAATCGGATGC	268	188	55
	At4g29860	14,601,698- 14,605,796	(F)=GCCCAGAGGAAAGAAGAGCAAAC (R)=TGGGAATTCATGAGAGAATATGTGGG	492	404	55
5	At5g14320	4,617,650- 4,618,912	(F)= GGCCTAAGAACCAAATCAAAACAA (R)= CGTGATGAAGTCTCCAAGTACATG	225	271	55
	At5g22545	7,483,253- 7,483,811	(F)= TAGTGAAACCTTTCTCAGAT (R)= TTATGTTTTCTTCAATCAGTT	100	>130	50

Molecular markers (SSLP) used to recover a higher resolution map containing the gene(s) of interest in the vicinity of At1g07810 locus on chromosome 1 (<http://amp.genomics.org.cn/>).

No.	Marker ID	Forward primer position (bp)	Primers	Expected size (bp) Col	Expected size (bp) Ler	Annealing temp. (°C)
1	AC024174-0604	1,837,561	(F)= CAGAGAGATCCGACGAGAGA (R)= GTACCACTTACCCGAACCAA	161	146	49.3
2	AC011001-0681	2,073,469	(F)=GAACAATGTCAATGGAGATA (R)= CTTCTCTCTCCTCACAGAGT	137	125	55
3	AC026875-0804	2,445,556	(F)= TTACTTTTCTGCAACTAAAT (R)= TCGTCTAGGGTGAGAAGATG	108	118	55
4	AC011438-0865	2,630,625	(F)= TTTGGGCTGTTAGATTGT (R)= TTTGAGGCTTTCAGTTTG	113	103	56.3
5	AC000106-0948	2,884,921	(F)= ATTACGCATATTATTATTCC (R)= CGCTTATTCAACAAGAGACT	204	181	52.5
6	AC000132-1049	3,192,707	(F)= TGCTTCCTAAGTTCATCAT (R)= TGTAACAACAAGAATCCAAA	155	134	45.5

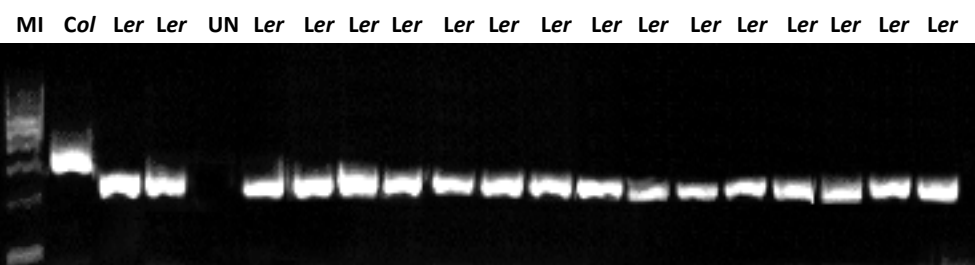
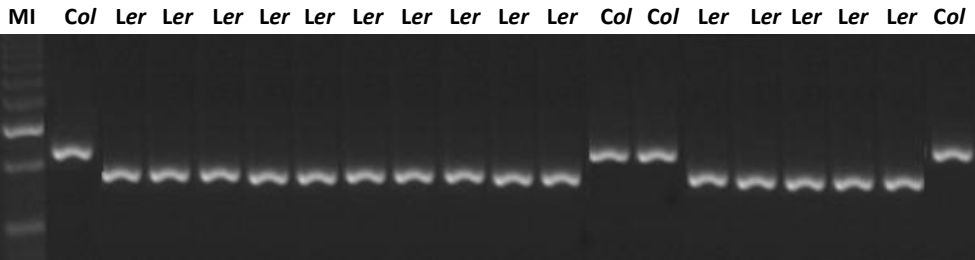
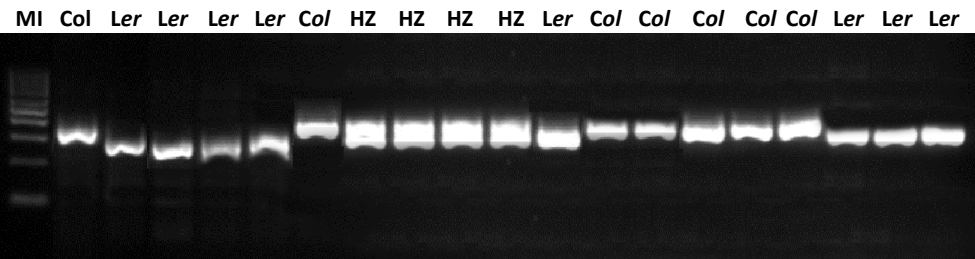
Linkage map analysis of *msAK* mutation with loci on different *Arabidopsis* chromosomes. RF= recombinant frequency, D (cM)= distance in centiMorgan.

Chromosome	Locus ID	Observed (Ler)	Observed HZ (Ler/Col)	Observed (Col)	SUM of Unknown	ExpLer	Exp HZ	Expcol	Chi-Square	RF	D (cM)
1	At1g07810	48	9	9	2	16.5	33	16.5	2.577 ^{E-18}	0.205	21.73
	At1g30930	2	51	8	7	15.25	30.5	15.25	5.75 ^{E-07}	0.549	>100
2	CER459006	4	55	6	3	16.25	32.5	16.25	1.615 ^{E-07}	0.515	>100
	CER459010	12	45	8	3	16.25	32.5	16.25	0.006	0.469	86.25
	CER461057	14	41	8	5	15.75	31.5	15.75	0.032	0.452	74.89
3	At3g11220	30	10	15	13	13.75	27.5	13.75	2.437 ^{E-07}	0.364	46.15
	At3g26605	13	15	12	28	10	20	10	0.279	0.488	>100
4	At4g10360	22	36	7	3	16.25	32.5	16.25	0.022	0.385	50.92
	At4g29860	35	14	13	6	15.5	31	15.5	3.639 ^{E-08}	0.323	38.35
5	At5g14320	24	20	13	11	14.25	28.5	14.25	0.100	0.404	55.92
	At5g22545	20	18	10	20	12	24	12	0.028	0.396	53.79

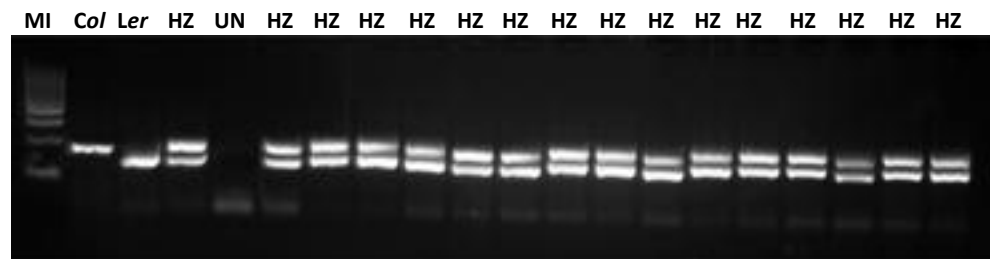
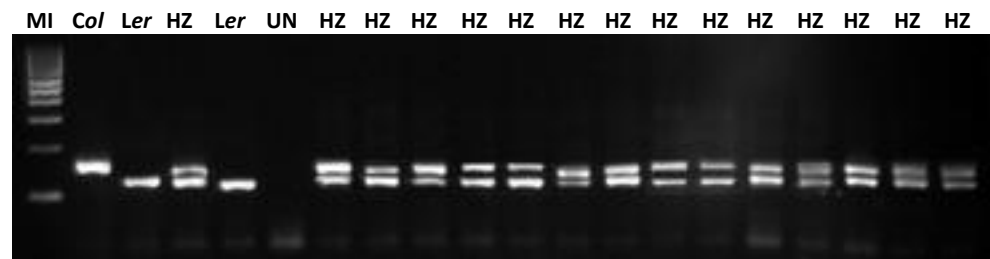
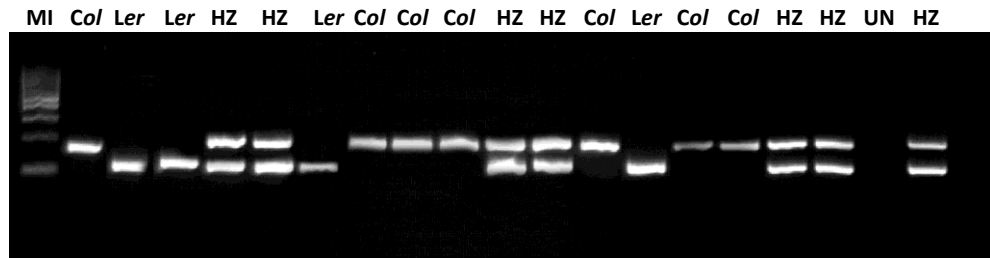
Linkage map analysis of *msAk* mutation with SSLP markers on chromosome 1 of *Arabidopsis* in the region between 1,837,561-3,192,707. RF= recombinant frequency, D (cM)= distance in centiMorgan.

Locus or marker location (bp)	Marker ID	Observed (Ler)	Observed HZ (Ler/Col)	Observed (Col)	SUM of Unknown	ExpLer	Exp HZ	EXP col	Chi-Square	RF	D (cM)
1,837,561	AC024174-0604	22	33	9	4	16	32	16	0.069	0.398	54.50
2,073,469	AC011001-0681	32	21	6	9	14.75	29.5	14.75	9.128 ^{E-07}	0.280	31.59
2,416,265	At1g07810	48	9	9	2	16.5	33	16.5	2.577 ^{E-18}	0.205	21.73
2,445,556	AC026875-0804	33	32	2	1	16.75	33.5	16.75	5.516 ^{E-07}	0.269	30.02
2,630,625	AC011438-0865	35	17	8	8	15	30	15	1.892 ^{E-08}	0.275	30.92
2,884,921	AC000106-0948	38	25	4	1	16.75	33.5	16.75	3.717 ^{E-09}	0.246	26.97
3,192,707	AC000132-1049	55	4	6	3	16.25	32.5	16.25	1.270 ^{E-27}	0.123	12.57

Mapping of the *msak* mutant based on polymorphic marker at *At1g07810* gene (expected size = *Col* <300 bp, *Ler* >300 bp). UN = unknown.

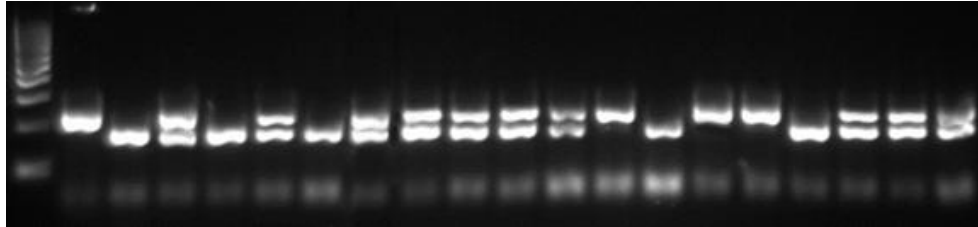


Mapping of the *msak* mutant based on polymorphic marker at *CER459006* gene (expected size = *Col* 203 bp, *Ler* 158 bp). UN = unknown.

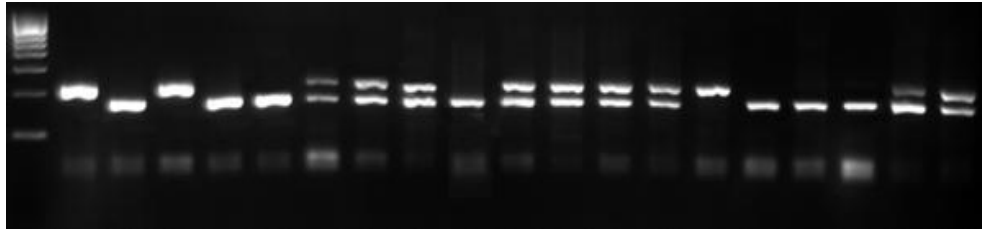


Mapping of the *msak* mutant based on polymorphic marker at *CER459010* gene (expected size = *Col* 90 bp, *Ler* 72 bp). UN = unknown.

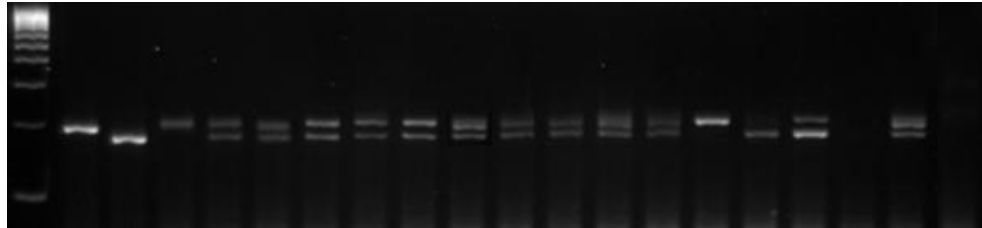
MI *Col* *Ler* HZ *Ler* HZ *Ler* HZ HZ HZ HZ HZ *Col* *Ler* *Col* *Col* *Ler* HZ HZ HZ



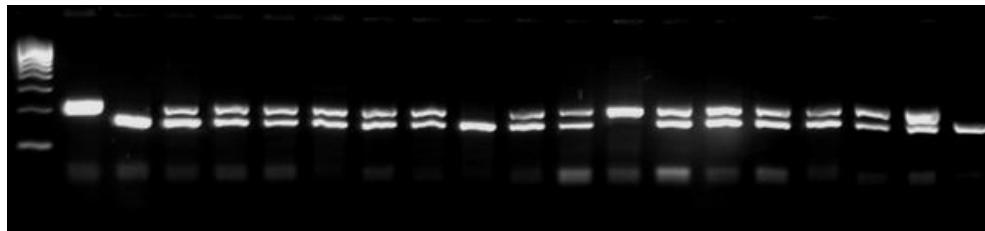
MI *Col* *Ler* *Col* *Ler* *Ler* HZ HZ HZ *Ler* HZ HZ HZ HZ *Col* *Ler* *Ler* *Ler* HZ HZ



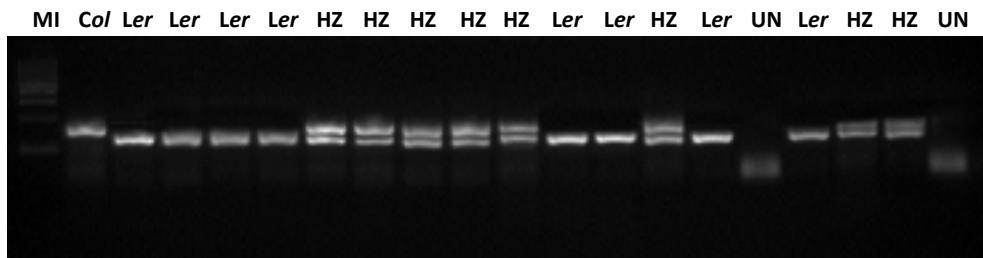
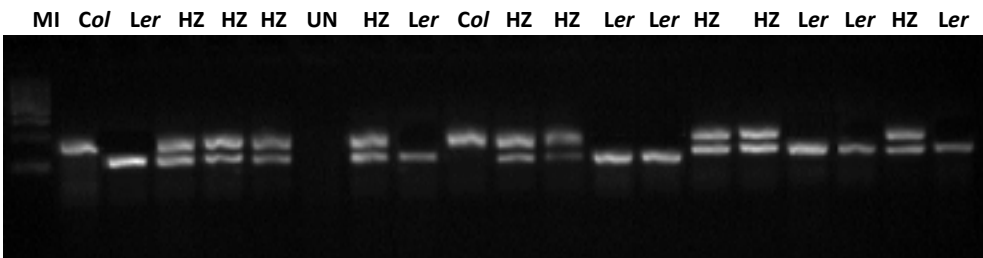
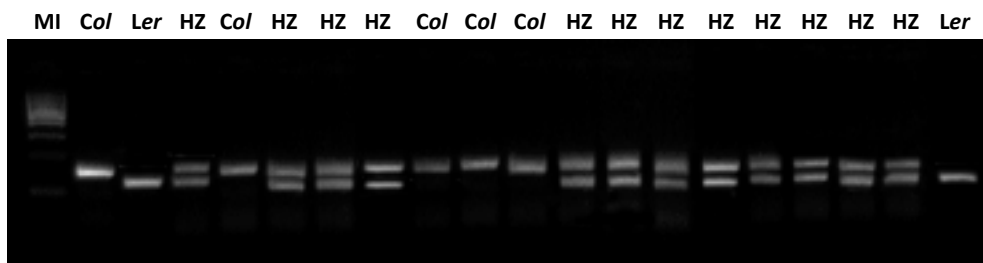
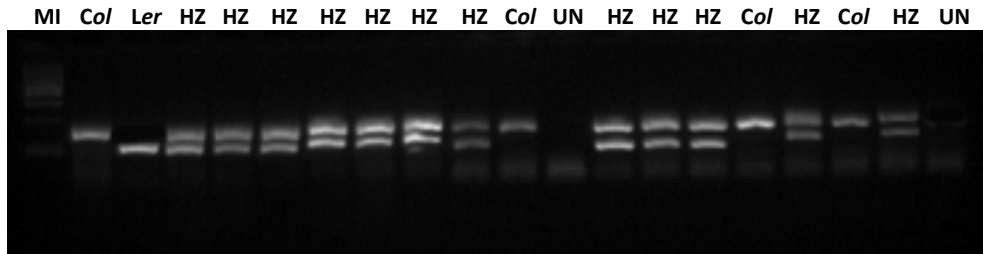
MI *Col* *Ler* *Col* HZ *Col* UN HZ UN HZ UN



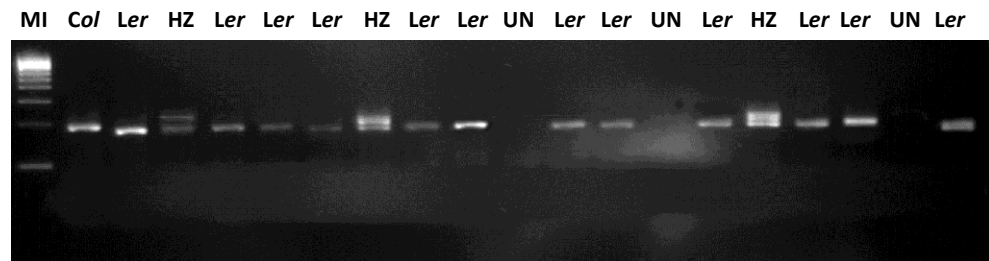
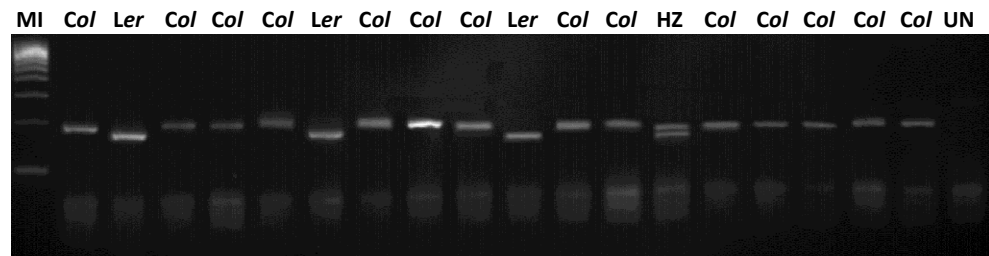
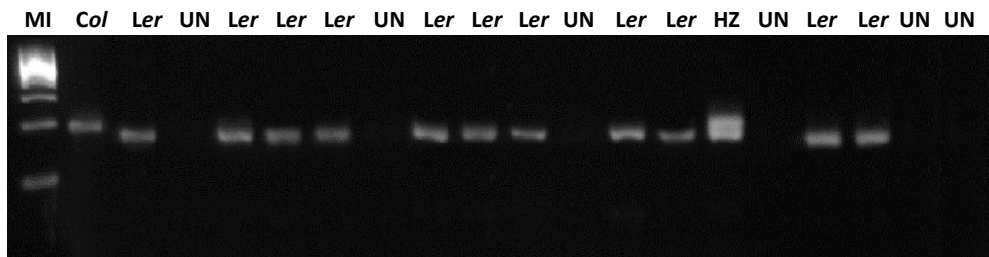
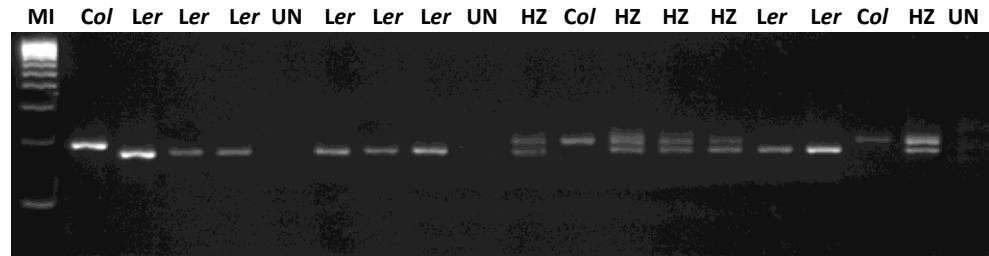
MI *Col* *Ler* HZ HZ HZ HZ HZ HZ *Ler* HZ HZ *Col* HZ HZ HZ HZ HZ HZ *Ler*



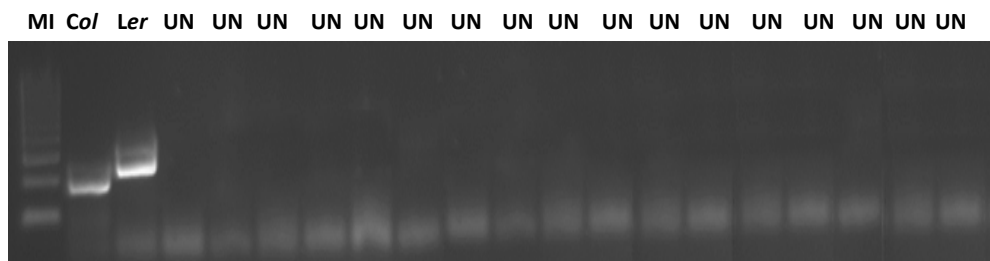
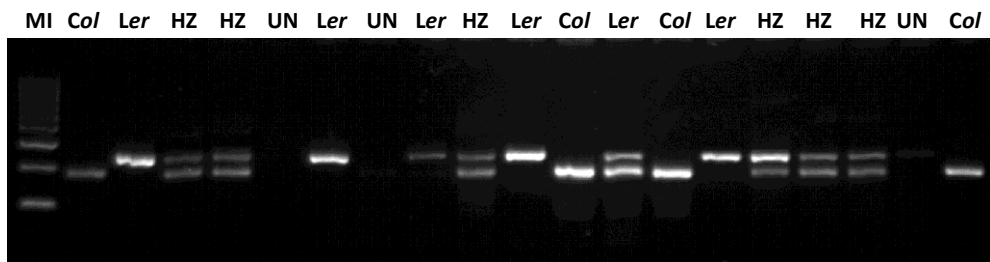
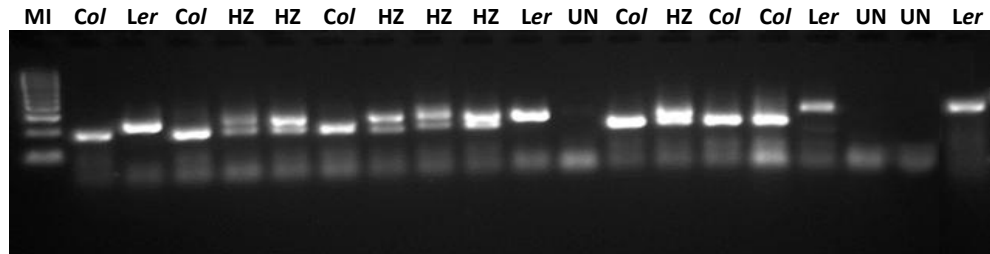
Mapping of the *msak* mutant based on polymorphic marker at *CER461057* gene (expected size = Col 151 bp, Ler 135 bp). UN = unknown.



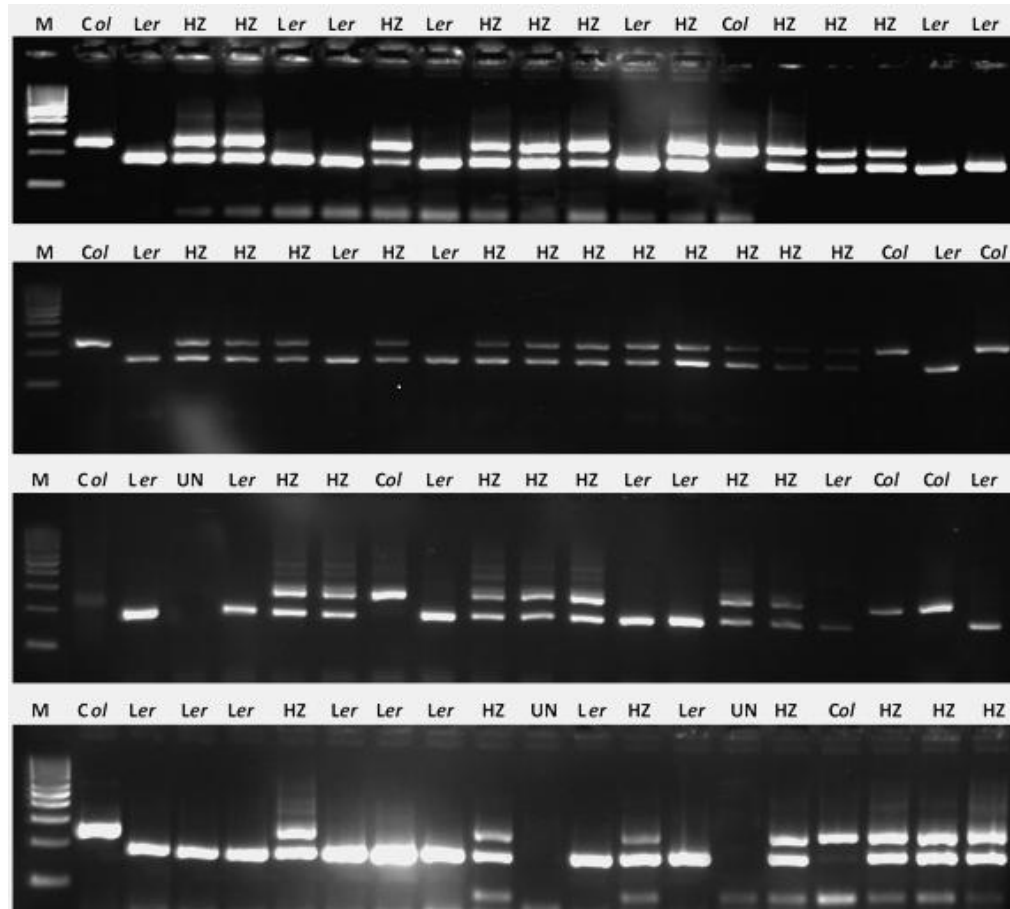
Mapping of the *msak* mutant based on polymorphic marker at *At3g11220* gene (expected size = Col 193 bp, Ler 174 bp). UN = unknown.



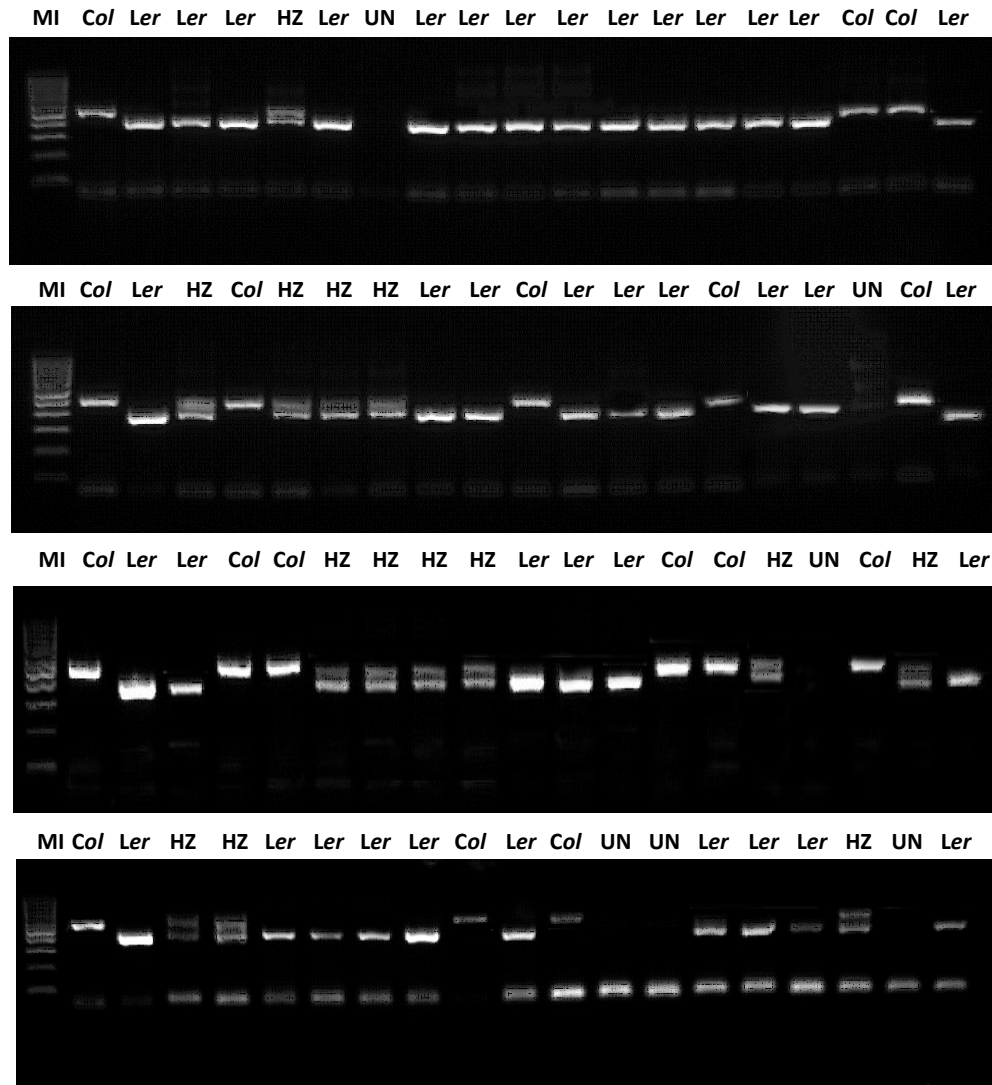
Mapping of the *msak* mutant based on polymorphic marker at *At3g26605* gene (expected size = *Col* <200 bp, *Ler* >200 bp). UN = unknown.



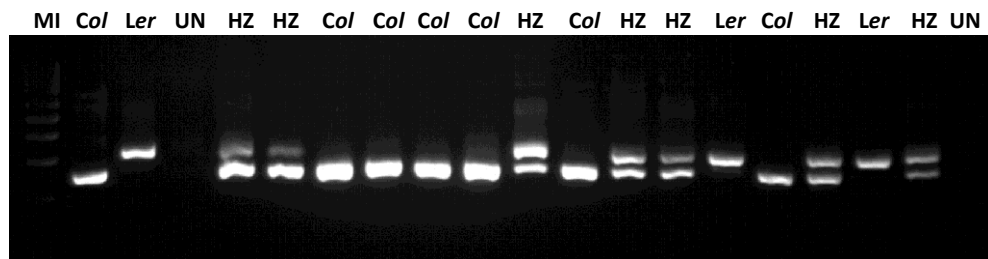
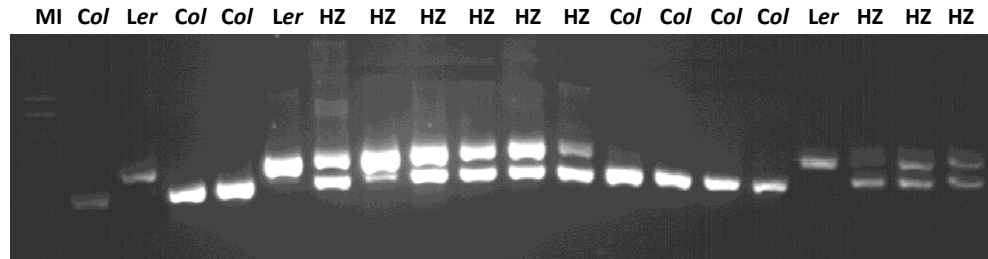
Mapping of the *msak* mutant based on polymorphic marker at *At4g10360* gene (expected size = *Col* 268 bp, *Ler* 188 bp). UN = unknown.



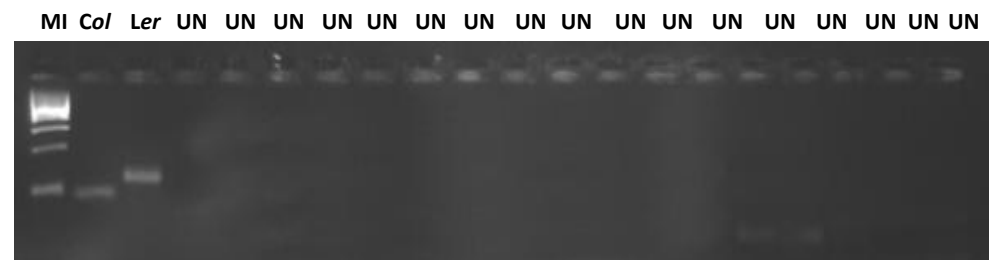
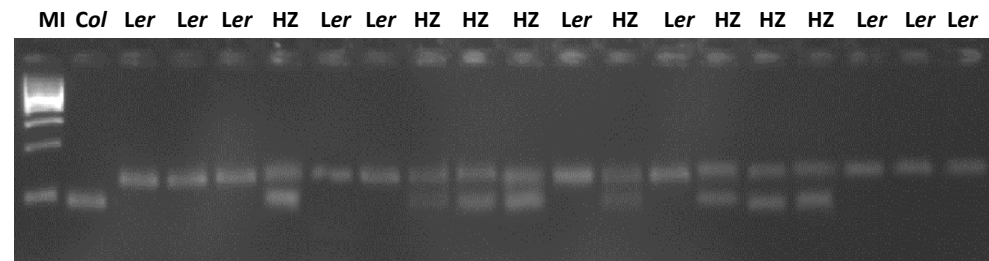
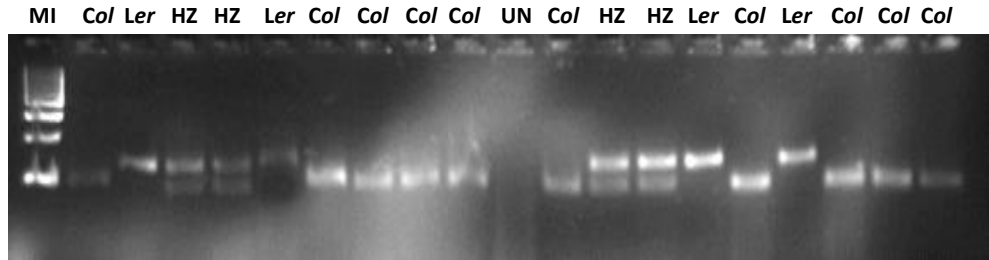
Mapping of the *msak* mutant based on polymorphic marker at *At4g29860* gene (expected size = Col 492 bp, Ler 404 bp). UN = unknown.



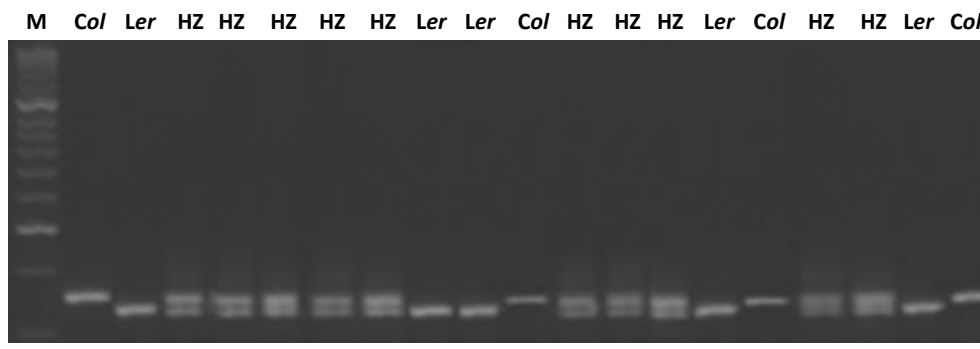
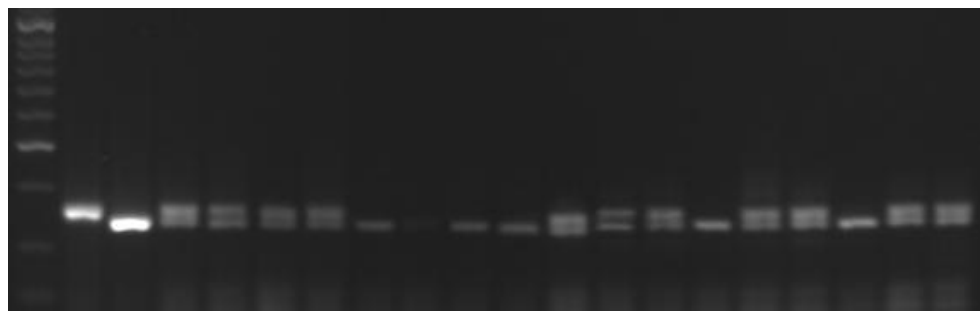
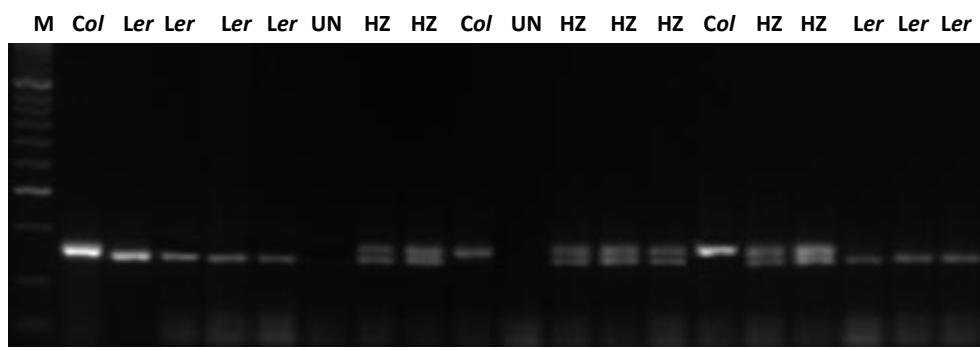
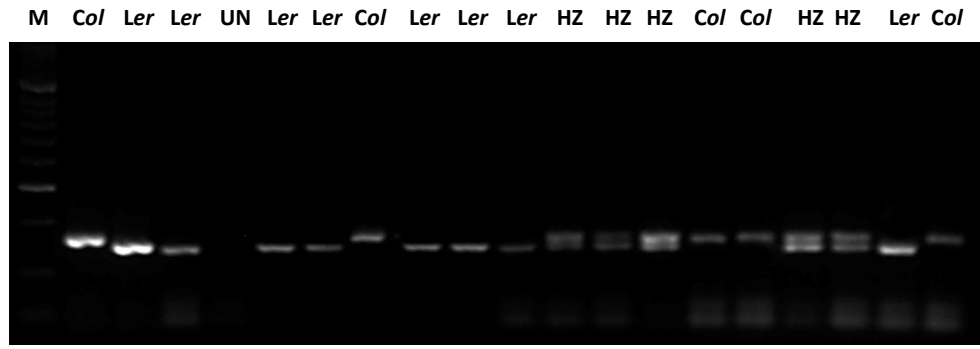
Mapping of the *msak* mutant based on polymorphic marker at *At5g14320* gene (expected size = *Col* 225 bp, *Ler* 271 bp). UN = unknown.



Mapping of the *msak* mutant based on polymorphic marker at *At5g22545* gene (expected size = *Col* 100 bp, *Ler* >130 bp). UN = unknown.

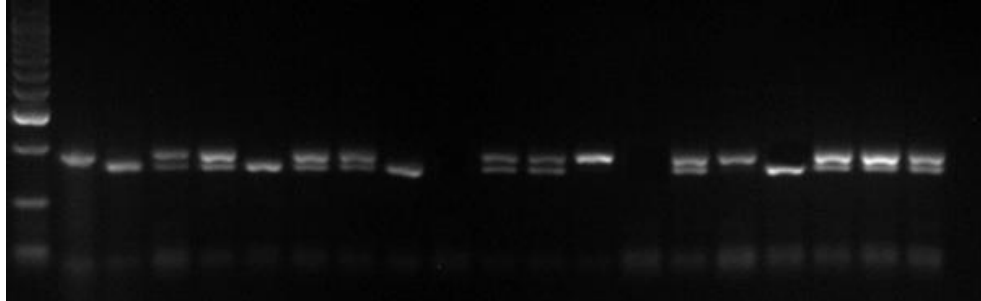


Mapping of the *msak* mutant based on SSLP marker AC024174-0604 (expected size = *Col* 161 bp, *Ler* 146 bp). UN = unknown.

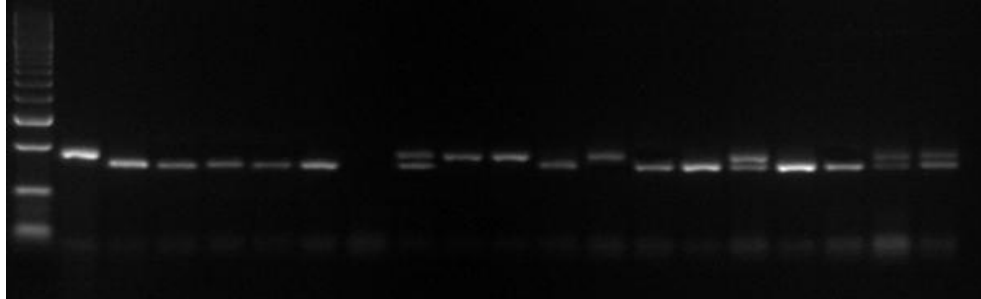


Mapping of the *msak* mutant based on SSLP marker AC011001-0681 (expected size = *Col* 137 bp, *Ler* 125 bp). UN = unknown.

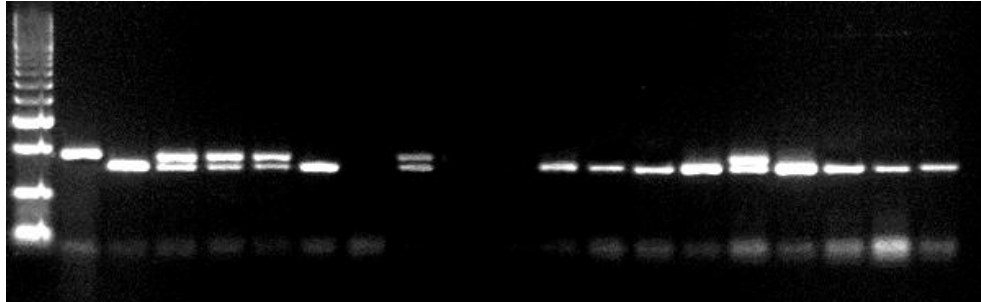
M *Col* *Ler* HZ HZ *Ler* HZ HZ *Ler* UN HZ HZ *Col* UN HZ *Col* *Ler* HZ HZ HZ



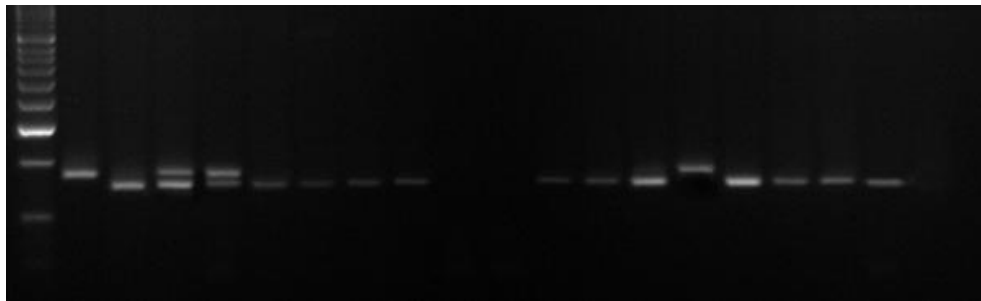
M *Col* *Ler* *Ler* *Ler* *Ler* *Ler* UN HZ *Col* *Col* *Ler* *Col* *Ler* *Ler* HZ *Ler* *Ler* HZ HZ



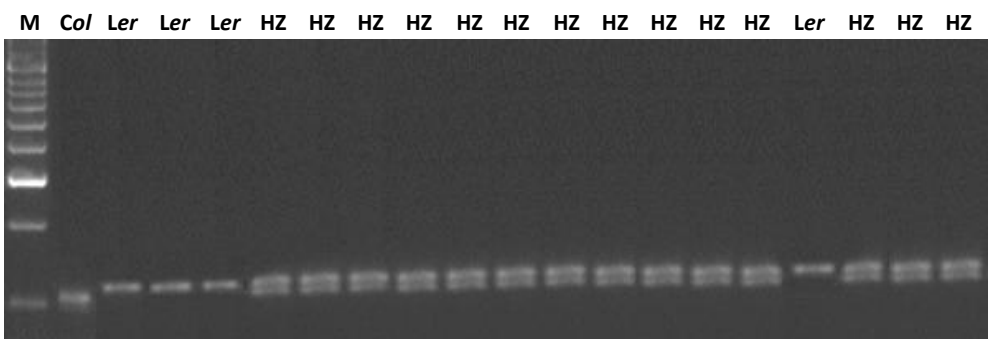
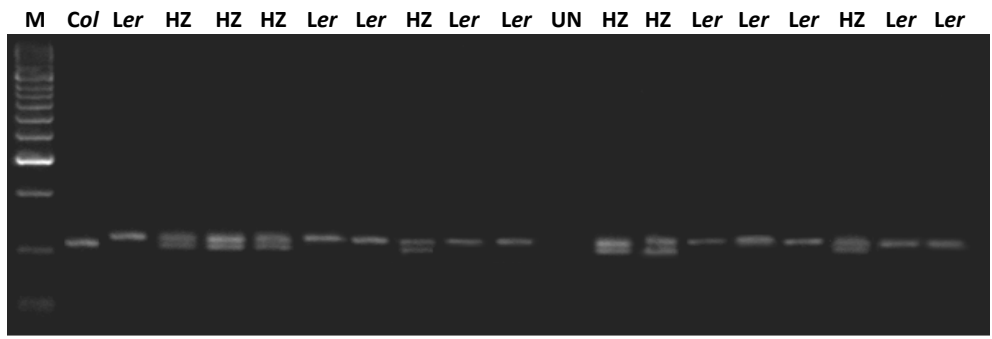
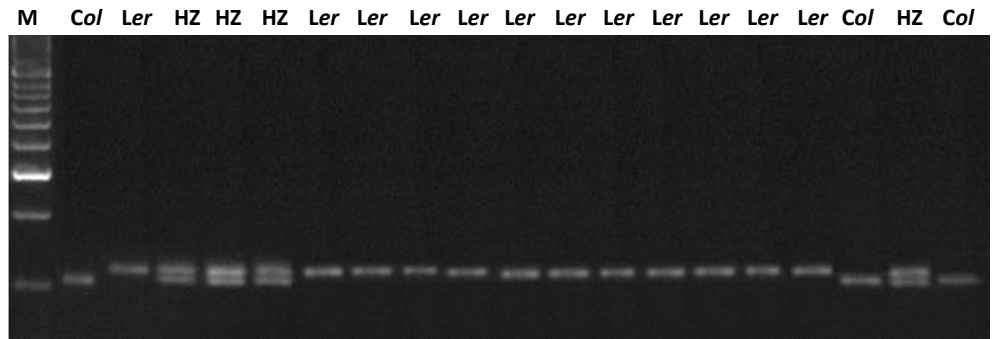
M *Col* *Ler* HZ HZ HZ *Ler* UN HZ UN UN *Ler* *Ler* *Ler* *Ler* HZ *Ler* *Ler* *Ler* *Ler*



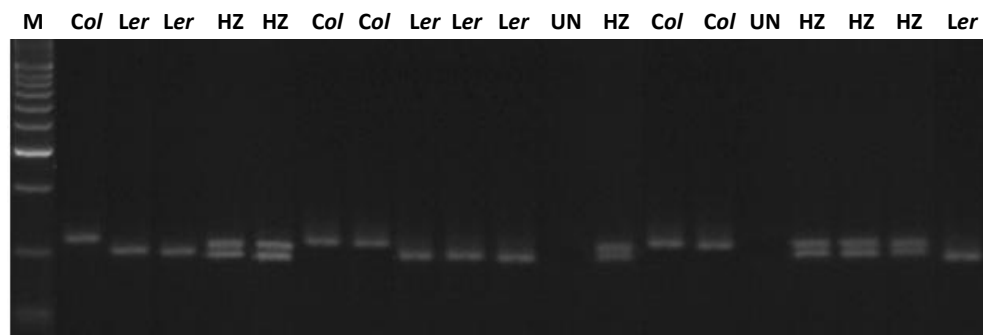
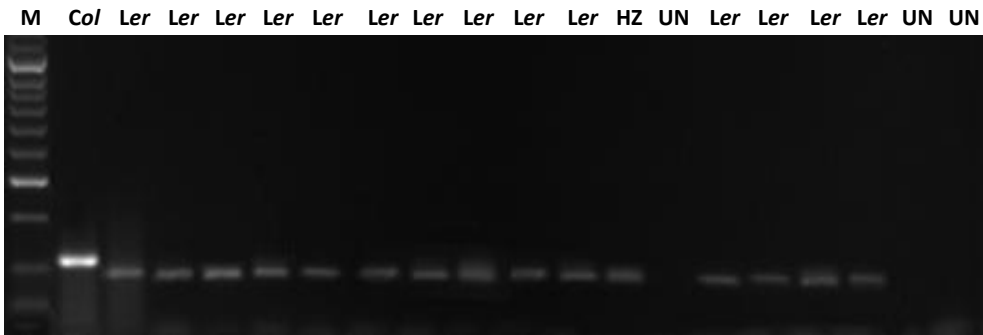
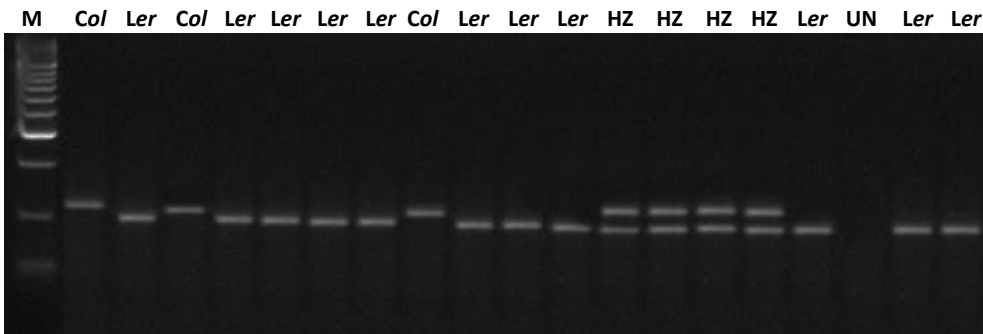
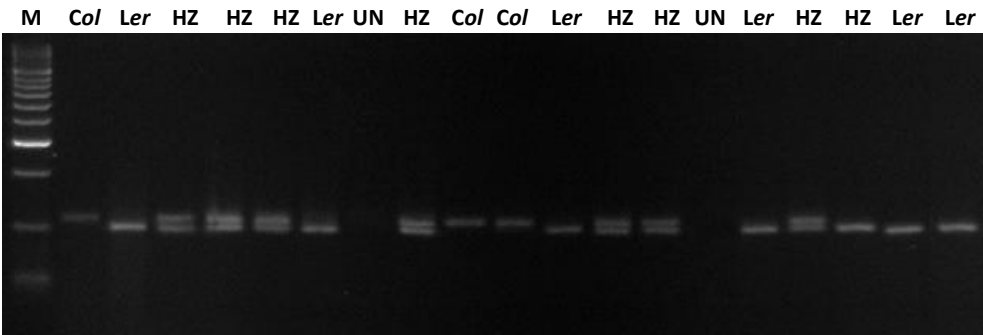
M *Col* *Ler* HZ HZ *Ler* *Ler* *Ler* *Ler* UN UN *Ler* HZ *Ler* *Col* *Ler* *Ler* *Ler* *Ler* UN



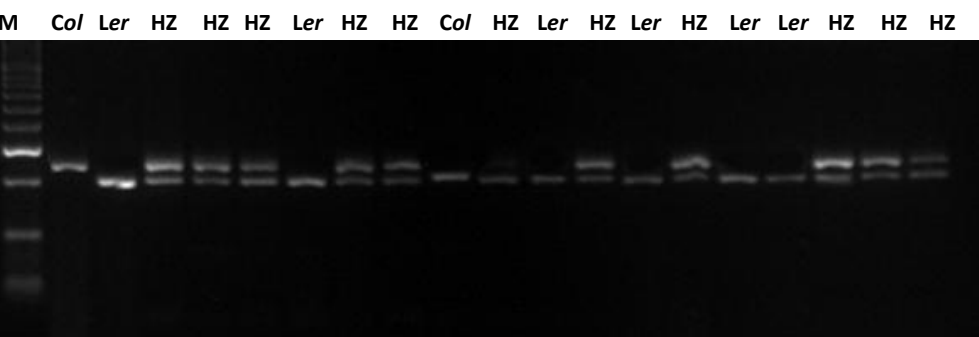
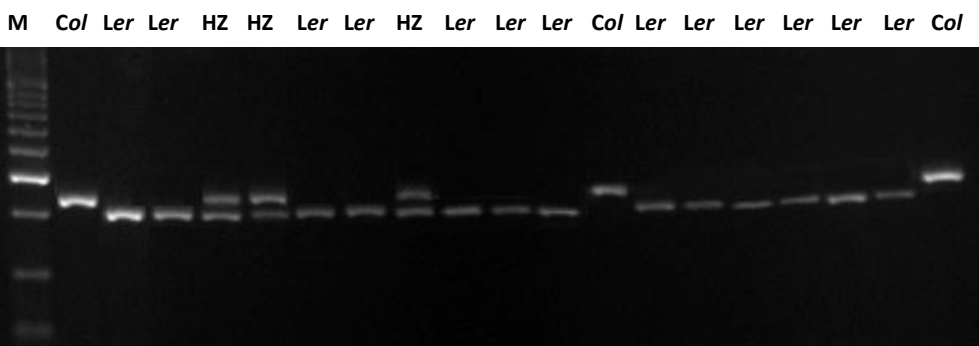
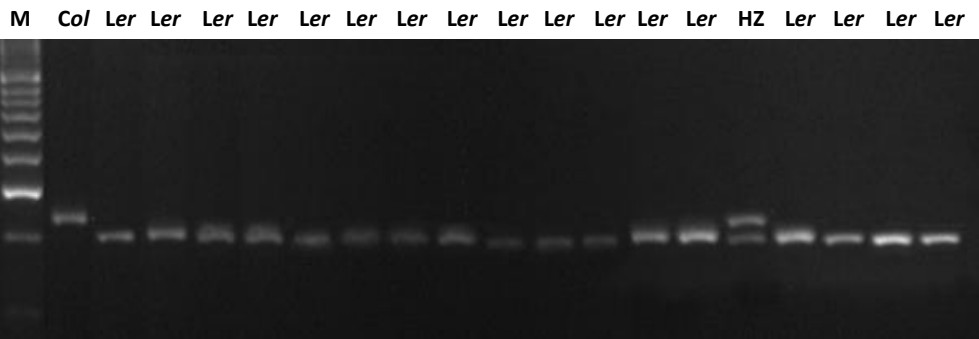
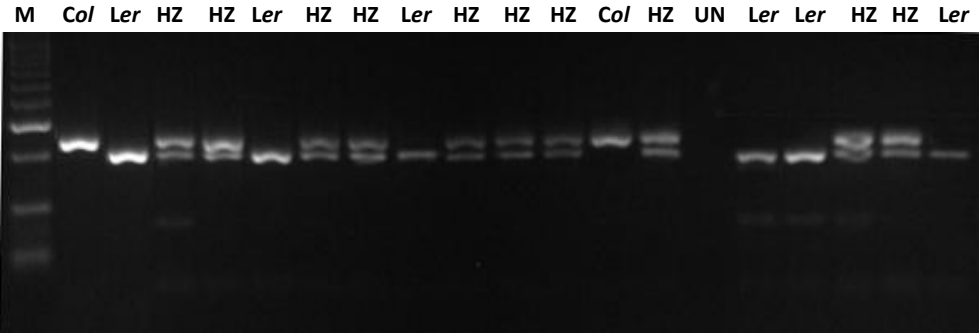
Mapping of the *msak* mutant based on SSLP marker AC026875-0804 (expected size = Col 108 bp, Ler 118 bp). UN = unknown.



Mapping of the *msak* mutant based on SSLP marker AC011438-0865 (expect size = Col 113 bp, Ler 103 bp). UN = unknown.



Mapping of the *msak* mutant based on SSLP marker AC000106-0948 (expected size = *Col* 204 bp, *Ler* 181 bp). UN = unknown.



**Mapping of the *msak* mutant based on SSLP marker
AC000132-1049 (expected size = Col 155 bp, Ler 134 bp).
UN = unknown.**

